Université catholique de Louvain (UCL)
Institute of Neuroscience (IoNS)
Alzheimer Dementia Group

Role of transmembrane GXXXG motifs in APP dimerization and β amyloid peptide oligomerization in Alzheimer's disease

Marie Decock

Supervisor: Prof. Pascal Kienlen-Campard

Thèse présentée en vue de l'obtention du grade de docteur
en sciences biomédicales et pharmaceutiques

Secteur des sciences de la santé

Février 2016

Supervisor:

Prof. Pascal Kienlen-Campard

Jury members:

President: Prof. Fadel Tissir

Steering committee members (UCL): Prof. Stefan Constantinescu

Prof. Thomas Michiels

Prof. Frederic Clotman

External members: Prof. Jochen Walter (Universität Bonn, Germany)

Prof. Nicolas Sergeant (INSERM Lilles, France)

ACKNOWLEDGEMENTS

J'aimerais tout d'abord remercier toutes les personnes qui ont participé et m'ont soutenue durant ce travail. Peu de personnes peuvent en dire autant mais j'ai l'impression d'avoir passé une bonne partie de ma jeunesse dans ce laboratoire. Tout commença lors de mon mémoire, en octobre 2008! Oui oui, il y a 7 ans et demi… J'avais déjà visité plusieurs laboratoires. A vrai dire, j'étais sur le point d'en intégrer un autre. Ayant déjà effectué mon atelier en FARL (c'était comme cela que l'unité s'appelait) et étant déjà familière avec le sujet, j'avais gardé cette visite chez Pascal pour la fin.

Evidemment, comme vous vous en doutez, **Pascal** a eu vite fait de me faire changer d'avis! Tu m'as même beaucoup émue à l'époque. Pascal, merci d'avoir cru en moi dès le début, de m'avoir prouvé que j'étais capable (lorsque je ne le pensais même pas moi-même) et de m'avoir permis de m'épanouir et évoluer comme j'ai pu le faire durant toutes ces années. Parce que à chaque petit problème et démotivation, une simple discussion avec toi éclairçissait le paysage et me remettait sur pieds pour le marathon. Pour tout cela, merci mille fois.

J'aimerais remercier tous les membres de mon **comité d'encadrement**: Le professeur **Fadel Tissir** mon président, ainsi que les professeurs **Frédéric Clotman**, **Stefan Constantinescu** et **Thomas Michiels**. Merci de votre intérêt pour mon travail, tout au long de ces 5 années. Merci professeur Constantinescu pour votre input, votre aide dans les corrections de mes articles et notre collaboration durant ces années. Merci professeur Clotman pour tous vos commentaires dans mon premier manuscrit, qui m'ont grandement aidée à l'améliorer et obtenir cette dernière version.

AKNOWLEDGEMENTS

I would like to thank the **external members** of my jury. Professors Nicolas Sergeant and Jochen Walter, thank you for your availability, your interest and your kindness. It was a great honnor for me to have the opportunity to meet you, share my work with you and attend your fantastic conferences. I wish you all the succes you deserve in your further researches.

Professeurs **Octave** et **Ilse**, je vous remercie pour votre gentillesse, bonne humeur, votre implication et vos conseils avisés lors de nos multiples réunions de laboratoire. Merci Monsieur Octave pour votre générosité et votre accueil lors des délicieux barbecues improvisés à la campagne.

Je voudrais maintenant remercier cette équipe formidable avec laquelle j'ai évolué ces 5 années (je vais essayer de le faire par ordre chronologique, certain(e)s comprendront pourquoi ☺). J'ai rencontré de très belles personnes qui sont devenues pour la plupart bien plus que des collègues…

Nathalie, pleine d'entrain et souriante, toujours prête à aider et conseiller. Tu es une scientifique et encadrante hors pair. Je te souhaite le meilleur pour ton avenir professionnel mais aussi personnel avec ta magnifique petite famille.

Laetitia, Lety, Mamy (ou ma mie, tu préfèreras), mon petit chat, on a commencé en même temps et on s'est toujours serré les coudes. Toujours souriante (enfin tu sais… la plupart du temps, en tous cas on était mis au parfum dès l'arrivée ;) /aïe) et pleine de générosité, une maitre de l'organisation (il me fallait bien ça) et une collègue hors pair… Mais je ne vais pas m'attarder sur ça, tu es devenue tellement bien plus! Parce qu'avec toi, lyser 50 puits de CHO n'est pas une corvée mais une matinée entre copines… parce que à tout moment de relâchement il y avait toujours une pause CC pour nous relancer! Tu as toujours été là pour moi, depuis le début et maintenant encore, dans les bons moments mais surtout dans les

mauvais. Tu m'as vraiment vue et fait grandir! Et on a encore plein de belles années devant nous pour continuer notre histoire…

Vincent, Vince, un des premiers hommes de ce labo, notre cobaye masculin, arrivé comme une fleur début 2009, alors que son origine était inconnue. Le moins qu'on puisse dire c'est qu'on en a passé des bons moments! Du moins dès que j'ai pu surmonter ma grande timidité de l'époque. Que ce soit au bureau, au labo, à la cafet jusqu'au P3… ta bonne humeur résonnait dans les couloirs (à partir de 10h30 évidemment). On ne voulait plus te quitter! Tellement, qu'on a investi ton bureau… On ne te remerciera jamais assez pour tous tes conseils scientifiques avisés!

Claudia, Cla, arrivée après avoir conquis tout le labo lors de son séminaire, ça en annonçait déjà la couleur! Je la voyais plus grande, mais bon… j'ai très vite compris que tout ne se mesurait pas par la taille! Une pile, toujours sur ressors, avide de connaissances et de découvertes, la personne la plus passionnée et brillante que j'ai eu l'honneur de rencontrer, tant tu m'as impressionnée toutes ses années. A côté de cela, j'ai rencontré une personne simple et adorable, à l'écoute toujours attentive, prête à se couper en 4, une voisine de bureau géniale et une compagne de voyage hors pair!

Aurélie, Aurel, Blonde, sister, la jolie petite blonde en mini short, ma folle voisine de Bench, on a parlé, chanté, dansé, pleuré… au Bench comme dans la vie, bref, je crois qu'on les a fait les 400 coups! On en a vécu des histoires folles, des crises aussi… on peut dire que notre amitié est à toutes épreuves et que quoi qu'il arrive, on s'en sort toujours main dans la main. Et il y a encore de tellement belles choses à venir! On on ne l'aurait pas parié il y a 5 ans, pas vrai? Mais on aurait signé des deux mains, et qu'est-ce qu'on se serait moins angoissées! ☺

Laurence et **Guillaume**, de très belles rencontres… on ne se voit pas souvent mais on ne s'oublie pas! On se remémorera toujours nos folles soirées, en mode barakis, en Mémé/pharma ou lors des mariages… C'est chaque fois un plaisir de pouvoir partager un moment ensemble! Je vous rejoins désormais dans le monde du privé et j'espère que nous partagerons encore longtemps toutes nos expériences autours d'un bon verre!

Serena, la Mamma, sis, Je ne sait pas par où commencer… Donc je vais commencer par ce beau jour où tu es arrivée toute timide avec ta maman à Bruxelles. Puis ta maman est repartie… et ma vie a énormément changé depuis! Tu m'as fait découvrir la vie et m'a fait m'épanouir, on a tout partagé (oui vraiment presque tout on peut le dire! ☺), et on continuera encore très longtemps. Même dans les derniers moments bien compliqués de cette thèse, tu as toujours été là. La scientifique hors pair que tu es m'as épaulée et aidée à mener ce projet à bien alors que je n'avais plus aucune ressource. Tu sais tout ce que tu représentes pour moi, ce serait impossible de tout mettre ici!

Julien, esprit scientifique dans tout ce que tu entreprends, d'une grande sensibilité et toujours de bon conseil. Je te souhaite de belles choses pour ta vie professionelle et personnelle à venir.

Cosmo et **Bruno,** la brute et le truand, les Laurel et Hardy du labo. Impossible de se concentrer dans ce bureau! Cosmo, le boucher des Carpates, toujours branché à ses sites de ventes en ligne. Véritable souris de laboratoire (bien que crainte par ses semblables), travaillant de jour comme de nuit, toujours avec une petite blague sous la main. Ta main de fer n'a d'égale que ton courage et ta générosité. Merci pour ton écoute et ton réconfort lors de ces heures tardives. Bruno, prudent et avisé, toujours à l'affut, se glissant dans les couloirs, prêt à surprendre. Je te remercie pour tous ces rires et ces bons moments dans notre bureau.

AKNOWLEDGEMENTS

Léonie, Léo, ce fut un plaisir d'être ta voisine de bureau. Toujours souriante, passionnée et toujours prête à aider. A côté de cela, tu es une très chouette personne, toujours partante pour passer de bons moments et partir pour de nouvelles aventures. Je te souhaite plein de bonheur autant dans ta vie professionnelle que personnelle ☺.

Rémi, j'ai été également enchantée de partager mon bureau avec toi. Toujours agréable, tu es également un très bon scientifique, n'en doute jamais. Intelligent et précis, tu aimes le travail bien fait et je suis sûre que tu surmonteras les difficultés de la thèse avec brio, je te souhaite beaucoup de réussite dans ta carrière!

Bernadette, last but not least (je sais que tu es tellement plus forte en anglais que tu ne le laisses paraître!). Tu as toujours été là, et pourtant, j'ai l'impression de t'avoir rencontré ces derniers mois en emménageant dans ton bureau. Tes qualités et ton expérience incroyable ne sont plus à démontrer et je te remercie pour tous tes conseils. Merci de m'avoir accueillie les bras ouverts, d'avoir fait attention à moi et de supporter encore mon désordre aujourd'hui (je vais tout ranger très vite c'est promis). Je te souhaite tout le bonheur dans ta future retraite avec tes 3 magnifiques petites filles, profites en bien.

Marie, Maria (avec l'accent bien sûr), je te remercie pour ton sourire, ta disponibilité et ta patience, et cela toutes les fois où j'ai eu besoin de ton aide. Je te souhaite le meilleur à toi et ta famille ☺

Anna, **Alexandre**, **Sabrina** et **Céline**, les « jeunes ». Eh oui j'ai été pendant de longues années LA jeune du labo mais maintenant c'est terminé! Je vous souhaite de perpétuer cette merveilleuse ambiance que nous avons eue pendant toutes ces années.

AKNOWLEDGEMENTS

Cathy et **Sarah**, toujours super sympas et de bonne humeur, je vous remercie pour votre gentillesse et votre soutien administratif durant toutes ces années.

Peng and **Matthew**, I did not have the time to know you well but I hope you enjoy your post-doc in Belgium and your project is going well. I wish you all the best in your researches and for the future.

A toute l'équipe de Manu: merci pour ces bons moments passés ensemble à la cafet ou aux drinks en tous genres. Je vous souhaite le meilleur à tous ☺

Pierre-Edouard, Pierrot, le mec d'à côté, on a commencé par se croiser dans le couloirs, par quelques sourires et quelques blagues… et une jolie amitié est née. Depuis, dans les couloirs avec Laet, au Martin V avec Jana, à l'appart avec les compères Cédric et Rémy, pour papoter boulot, sorties ou pour realiser des films, cela finit toujours en éclats de rires!

Auré, **Julie**, **Chau**, **Julien**… mes amis depuis les études, qui m'avez supportée pendant toutes ces années. Vous qui avez partagé mon quotidien, mes joies et peines, merci du fond du coeur. Chau, sans toi… c'est simple je n'aurais peut-être même jamais eu l'occasion de faire cette thèse. Merci d'avoir été là au moment décisif!

Pierre, mon poupoule d'amour, mon petit frère… Parce que malgré nos 7 années de différence tu as toujours été là pour m'écouter et me réconforter. Tu es d'une grande sensibilité, maturité ainsi que d'une générosité sans pareille. J'espère que nous partagerons toujours cette relation privilégiée, quoi qu'il arrive.

AKNOWLEDGEMENTS

Mamy, parce que tu n'oublies jamais un moment important pour moi. Tu as été ma première prof et toujours ma plus grande supportrice. Depuis le début, ton soutien sans faille et ta fierté sont mes plus grandes sources de motivation. J'ai eu les meilleures mamies que l'on puisse avoir, d'une générosité et d'un amour sans limites.

Marraine, merci d'être toujours présente, toujours volontaire et de me soutenir dans chaque étape de la vie.

Papa et **Maman**, à tout moment et toute distance, dans toutes les épreuves je peux toujours compter sur vous. Merci d'avoir supporté mon stress et mon "caractère fort" pendant toutes ces années. Parce que sans votre force et votre soutien, je n'y serais jamais parvenue. Je ne vous remercierai jamais assez de tout le mal que vous vous donnez pour que nous ne manquions jamais de rien.

François, Françis, mon koala… si on m'avait dit que je rencontrerais une espèce comme la tienne dans les derniers mois de ma thèse, je ne l'aurais jamais cru! "C'est toujours quand on ne s'y attend pas!", m'avait-on dit… Tu as été d'un soutien et d'une patience sans faille depuis notre rencontre. Ton regard me rassure et me donne la force de puiser le meilleur de moi-même au quotidien. Et en plus, qu'est-ce qu'on rigole! ☺

AKNOWLEDGEMENTS

INDEX

ABSTRACT 17

ABBREVIATIONS 19

CHAPTER I: Introduction 21

1. Alzheimer's Disease 21

1.1 The pathology 21

Generalities 21

Etiology of the disease 22

Seminal observations by Alois Alzheimer 22

1.2 Neuropathological hallmarks of Alzheimer's disease 24

Neurofibrillary tangles and tau protein 24

Senile plaques 28

1.3 The Amyloid Cascade Hypothesis 29

Update of the Amyloid Hypothesis by J.A. Hardy and D.J. Selkoe in 2002 31

Contradictions to the amyloid cascade hypothesis 34

2. The amyloid precursor protein (APP) 39

2.1 The APP protein family 39

2.2 APP structure 43

2.3 APP cellular functions 46

Neuronal and synapto-trophic function 48

Axon pruning and degeneration 48

Intracellular signaling 49

Apoptosis 50

2.4 APP Metabolism 51

The α-secretase and soluble APP α 53

The β-secretase and the amyloidogenic pathway 54

The η-secretase and Aηs 55

The γ-secretase complex and the γ-cleavage 56

AD treatments targeting the amyloidogenic processing and Aβ 66

2.5 APP cellular trafficking 69

2.6 Dimerization 71
Ectodomain dimerization 72
Dimerization of the transmembrane domain and GXXXG motifs 74
Dimerization and processing 78
2.7 FAD mutations 80
Mutations located close to the β-site 81
Mutations located at the juxtamembrane region 81
Mutations located close to the γ-site 82
3. The β amyloid peptide (Aβ) 83
3.1 Aβ heterogeneity 83
3.2 Aβ fibrils 85
Discovery and properties 85
Structure and formation of Aβ fibrils 87
Molecular structure of Aβ monomers in the fibril 91
Role of GXXXG motifs in Aβ fibrils formation 93
Differences between Aβ 40 and 42 in fibrils 95
From fibrils to oligomers hypothesis in AD 97
3.3 Aβ oligomers 99
History and properties 99
Different types of oligomeric species 101
Molecular structure of Aβ oligomers 106
GXXXG motifs in Aβ oligomerization 107
Differences between Aβ 40 and 42 oligomers 108
CHAPTER II: Aim of the thesis 109
CHAPTER III: Results 111
1. APP dimerization and Aβ production: GXXXG motifs and structural determinants 111
1.1 Analysis of the regions involved in APP dimerization and its impact on processing 111
1.2 Analysis of the structural determinants involved in APP dimerization and processing 151
Conformational changes induced by the A21G Flemish mutation 151
The LVFF motif bears a β-sheet structure able to modulate the γ-secretase processing 157
2. GXXXG/A motifs in the formation of pathogenic Aβ oligomers 165

CHAPTER IV: Discussion **211**

1. **Involvement of GXXXG motifs in full-length APP dimerization** **213**
2. **Implication of GXXXG motifs in APP CTFs dimerization** **217**
3. **Role of Glycines from GXXXG motifs in the formation of pathogenic Aβ oligomers** **221**
4. **General conclusions** **227**

BIBLIOGRAPHY **229**

ANNEX 1: List of scientific papers **271**

ANNEX 2: Collaboration paper **273**

INDEX

ABSTRACT

Alzheimer's disease (AD) is the most common neurodegenerative disorder that causes progressive cognitive decline, leading to dementia. Two types of lesions are found in AD brains: neurofibrillary tangles and senile plaques. The latter are mainly composed of the β-amyloid peptide (Aβ), a key actor in the pathogenesis. Aβ is generated by amyloidogenic processing of the amyloid precursor protein (APP), a ubiquitous type I transmembrane (TM) protein. This thesis work focuses on two features critical in the disease process: the production of Aβ and its toxic aggregation.

Several studies have suggested that dimerization of APP is closely linked to Aβ production. Nevertheless, the mechanisms controlling APP dimerization and their role in APP function are not known. We first analyzed APP dimerization and unravel the involvement of its three major domains: the ectodomain, the transmembrane domain (TMD) and the intracellular domain. Our results confirmed the pivotal role of the ectodomain in APP dimerization. We also showed that familial AD mutations in the transmembrane GXXXG/GXXXG-like motifs affect the structure and folding of the juxtamembrane/transmembrane (JM/TM) domain, which is critical for APP processing at the γ-site. Both non-familial and familial AD mutations strongly modulate Aβ production but do not consistently change dimerization of the C-terminal fragments. Finally, we found for the first time that removal of intracellular domain strongly increases APP dimerization, shifting the processing towards the non-amyloidogenic α cleavage.

Since a decade, there is a growing body of evidence that soluble Aβ oligomers precisely correlate with clinical features and symptoms associated with AD. The Aβ sequence is present in the TM region of APP, containing the $G^{25}XXXG^{33}$ and

$G^{38}XXXA^{42}$ motifs. They can be critical for both TM protein interactions and fibrillogenic properties of peptides derived from TM α-helices. In the second part of this work, we describe a highly stable assembly of Aβ oligomeric species produced in living cells. They are formed in cellular membrane compartments by direct expression of Aβ42, but not Aβ40. By a point-mutation approach, we demonstrate that glycine-to-leucine mutations in the GXXXG and GXXXA motifs dramatically affect the Aβ oligomerization process.

ABBREVIATIONS

Aβ	Amyloid β peptide
AcD	Acidic domain
AchEI	Acetylcholinesterase inhibitor
AD	Alzheimer's disease
ADAM	"A Disintegrin and metalloprotease"
ADDL	Amyloid-β derived diffusible ligands
ALID	APP-like intracellular domain
AICD	APP intracellular domain
ASPD	Amylospheroids
APH1	Anterior pharynx defective 1
APLP	Amyloid precursor-like protein
ApoE	Apolipoprotein E
APP	Amyloid precursor protein
APPs	APP soluble
BACE	Beta-site APP Cleaving Enzyme
CASK	Ca^{2+}/calmodulin-dependent serine protein kinase
CDK5	Cyclin-dependent kinase 5
CAM	Cell adhesion molecule
CSF	Cerebrospinal fluid
CTF	C-terminal fragment
CuBD	Cupper-binding domain
DNA	Deoxyribonucleic acid
EGF(R)	Epidermal growth factor (receptor)
ER	Endoplasmic reticulum
Fle	Flemish mutation
FAD/fAD	Familial forms of Alzheimer's disease
GFLD	Growth factor-like domain
GSI	Gamma-secretase inhibitor
GSK3β	Glycogen synthase kinase 3 β
HSPG	Heparan sulfate proteoglycans
JM	Juxtamembrane
KPI	Kunitz-type protease inhibitor
(d)KO	Double) Knock-out
LRRTM	Leu-rich repeat transmembrane
LTP/D	Long-term potentiation/depression
MAP(T)	Microtubule associated protein tau
MCI	Mild cognitive impairments
MW	Molecular weight
Mut/m	Mutant
NCAM	Neuronal cell-adhesion molecule
NCT	Nicastrin
FT	Neurofibrillary tangles
NICD	Notch intracellular domain
NSAID	Non-steroidal anti-inflammatory drug
PEN2	Presenilin enhancer 2
PHF	Paired helical filaments
PKA/C	Protein kinase A/C
PS	Presenilin
SAD/sAD	Sporadic forms of Alzheimer's disease
SDS	sodium dodecyl sulfate
SP	Senile plaques/Signal peptide
t/p-tau	Total/hyperphosphorylated tau protein
TGN	Trans-golgi network
TM(D)	Transmembrane (domain)

CHAPTER I: Introduction

1. Alzheimer's Disease

1.1 The pathology

Generalities

Alzheimer's disease (AD) is a severe and irreversible neurodegenerative disorder characterized by memory loss and progressive cognitive functions decline. It is affecting more than 40 million persons worldwide and this picture is supposed to increase to 115 million by 2050 according to World Alzheimer Report. Alzheimer's disease is so the most prevalent form of dementia in the elderly (Alzheimer's Association 2015). Indeed, AD represents 60-80% of all dementia and appears generally in persons older than 60 years. In Belgium, around 190 000 persons suffer from dementia, at least 150,000 of them from AD. The disease is characterized by loss of memory, reasoning and functional disabilities like language decline followed by neuropsychiatric symptoms such as depression, apathy and aggressiveness (Querfurth and LaFerla, 2010). Three stages are defined in the onset and progression of the disease. The first stage is asymptomatic; the symptoms appear generally 10 years after the onset of the disease. The second stage is called « mild cognitive impairments » (MCI). During this stage, changes in the personality occur as well as deficits in cognitive functions, although they are not severe enough to impair daily life. The last stage, also referred as dementia, is particularly invalidating for the patient. The dementia results in severe cognitive deficits affecting judgment, speech and behavior and leads to death within few years. The improvement of health care and life expectancy makes AD prevalence continuously increasing. As a

consequence, AD is a worldwide social and economic problem and lot of research efforts have been undertaken to lead to a better understanding of the disease pathway and to identify therapeutic targets. To date, medication slows down the symptoms and helps maintaining memory, but treatments are only symptomatic and there is an urgent need for specific and efficient therapeutics.

Etiology of the disease

More than 95% of AD cases are sporadic forms. Patients with sporadic AD are developing the disease without any clearly defined reason apart from aging. Only a few environmental factors like sedentary lifestyle, high fat diet or antecedents of cerebrovascular disease, type II diabetes and hypertension have been described to favor the disease occurrence (Mayeux and Stern, 2012). There are also genetic risks factors like homozygosity for the ε-4 allele of the apolipoprotein E (APOE) gene. It has been described as the major risk factor for late-onset AD. Familial forms of AD (FAD) account for 2-3 % of all cases and are responsible for early-onset and very aggressive forms of the disease. They come from autosomal dominant mutations on three known genes: the amyloid precursor protein (APP), Presenilin-1 (PS1) and Presenilin-2 (PS2) genes. These genes encode proteins of utmost importance for their role in the production of the β-amyloid peptide (Aβ). Aβ is the major component of senile plaques, a typical hallmark of the disease.

Seminal observations by Alois Alzheimer

The disease was originally described by a German neuropsychiatrist named Alois Alzheimer in 1906. He reported the case of August D., a 51 years old patient showing different symptoms of dementia. Following post-mortem examinations

of her brain, Alzheimer noticed and described two abnormal lesions present in the brain (Alzheimer et al., 1995). These lesions were further recognized as the major hallmarks of the disease, called *senile plaques* and *neurofibrillary tangles*. In November 1906, Alois Alzheimer presented his results on clinical and neuropathological characterization of the newly discovered disease at the Society of Southwest German Psychiatrists meeting in Tübingen. After that, the hallmarks were only deeper described in the 80s. In AD, the progressive diffusion of certain lesions in the brain of patients associates with the different pathological states of the disease (Braak and Braak, 1996). They start in the limbic system and are further accompanied at late stages by a general atrophy of the brain, starting from temporal and parietal lobes to frontal lobe. These regions are involved in a wide range of executive functions including memory, planning skills, orientation as well as social behavior. Affection of these regions is therefore responsible for the clinical symptoms observed throughout the disease.

1.2 Neuropathological hallmarks of Alzheimer's disease

Neurofibrillary tangles and tau protein

Neurofibrillary tangles (NFTs) are intraneuronal inclusions receiving their name from the filamentous aspect they give to neurons. At the very early stage, NFTs appear in the entorhinal cortex and spread to the limbic system. They affect regions including the hippocampus, highly associated to memory functions. At late stages, they affect the cortex and provoke a correlated impairment of the associative, sensory and motor functions. Eventually, NFTs reach the striatum and the substantia nigra (Braak and Braak, 1996;Thal et al., 2002).

From a structural point of view, NFTs are composed of aggregates made by hyperphosphorylated tau proteins (p-tau) (Mandelkow and Mandelkow, 1998). Tau protein is encoded by the MAPT gene located on chromosome 17. In adult brains, there are up to six alternative tau isoforms, derived from alternative splicing of two different domains in the protein (Fig.01) (Sergeant et al., 2005). Tau is an abundant microtubule associated protein (MAP) that acts together with α- and β-tubulin heterodimers to ensure their assembly and stability, regulating motor-driven axonal transport in neurons (Drechsel et al., 1992;Gustke et al., 1994).

Tau protein contains different domains involved in its function: some amino-terminal domains, followed by a proline-rich domain, several carboxy-terminal microtubule-binding repeats and a short tail sequence. Isoforms can count up to 2 N-ter domains (N) and 3 to 4 microtubule-binding repeats (R) (Brandt and Lee, 1993;Sergeant et al., 2005). Tau proteins possess more than 80 putative serine/threonine and five tyrosine phosphorylation sites located mainly near the R regions that are involved in microtubule binding. Phosphorylation modulates tau affinity for tubulin and regulates formation and stability of microtubules according

to cellular needs (Lindwall and Cole, 1984). Tau hyperphosphorylation during the disease process provokes its dissociation from the microtubules, leading to its own aggregation in the cytoplasm and perturbation of cellular trafficking (Alonso et al., 1996;Iqbal and Grundke-Iqbal, 2005). Some sites were described as typically phosphorylated in AD. Phosphorylation on Ser262 and Ser356 in the microtubule-binding domain induces tau detachment from the microtubules (Buee et al., 2000) and phosphorylation of Ser214 and Thr231 sites (distinct from the microtubule-binding domain) have been shown to reduce its binding ability. P301S tau mutation is responsible for inherited fronto-temporal dementia with phosphorylated filamentous tau inclusions (Allen et al., 2002). In the disease, tau hyperphosphorylation appears to result from an imbalance between the neuronal kinase and phosphatase activities.

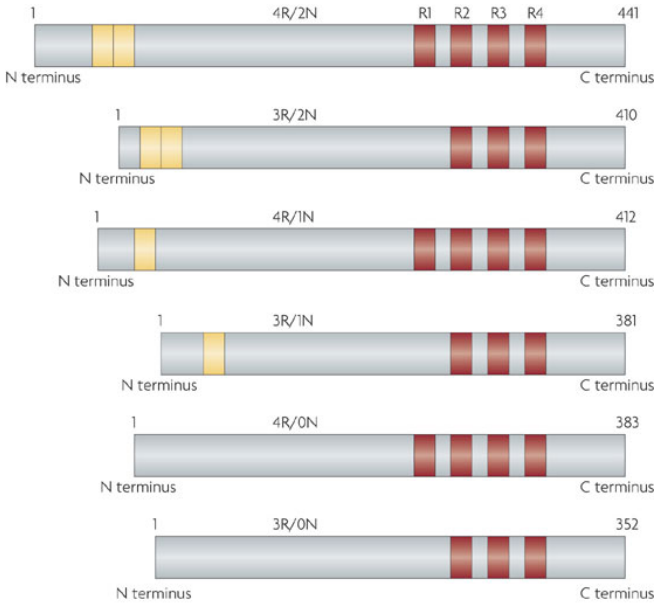

Fig.01 Different Tau isoforms derived by alternative splicing of N and R domains.

The different Tau isoforms vary by the number of N-terminal domains (N) and microtubule-binding repeats (R). N domains are depicted in yellow and R repeats in red (From Ballatore et al., 2007).

Several kinases like the protein kinase A (PKA), glycogen synthase kinase 3 β (GSK3β) and cyclin-dependent kinase 5 (Cdk5) have been demonstrated to phosphorylate tau at most of the described pathological sites (Wang et al., 1998;Liu et al., 2004). In contrast, serine/threonine phosphatase PP2A is the most effective to revert phosphorylation and aggregation of tau.

In AD, cognitive impairments correlate with the distribution of NFTs and neuronal loss (Arriagada et al., 1992). They appear in the entorhinal cortex and later in anatomically connected cortex regions (Braak and Braak, 1995). Recently, cell-to-cell transmission has emerged as a major hypothesis for Tau-dependent pathological events (Mohamed et al., 2013). It has been shown that p-Tau can also be found in extracellular compartments independently from any cell death (Chai et al., 2012) and their levels are regulated by neuronal activity *in vivo* (Yamada et al., 2014). Tau aggregation can therefore bind cellular membranes and be internalized by neighboring neurons. This way p-tau induce fibrillization of the endogenous tau proteins by a process called "seeding" (Guo and Lee, 2011). Seeding is the mechanism by which misfolded tau is able to act as a template and drive the conformational changes and aggregation of native tau proteins in a prion-like fashion. Brain extracts from mice expressing the human P301S tau induce the association of the WT protein upon injection into human WT tau transgenic mice (Clavaguera et al., 2009). Following that, injection of AD patients' brain extracts show seeding in human tau expressing mice as well as in non-transgenic mice (Clavaguera et al., 2013). However, these aggregates of murine tau formed by the human pathological protein occur to a smaller extent. Amounts of misfolded proteins are proportional to sequence similarity between the seed and the recruited soluble protein. Seeding of tau is detected prior to pathology, suggesting an important role in AD neurodegeneration (Holmes et al., 2014).

Once a small number of tau inclusions are formed they have been shown to self-propagate independently of other pathogenic mechanisms, a process called "spreading". Tau pathogenic conformations diffuse in the brain along neuronal connexions by trans-cellular propagation (Kfoury et al., 2012;Stancu et al., 2015). Studies involving seeding of pathological tau aggregates into WT mice display spreading of the pathology from the site of injection to neighboring regions (including hypothalamus) (Clavaguera et al., 2009;Clavaguera et al., 2013). Distinct tau strains can propagate indefinitely in a clonal fashion through the brain, defining different tauopathies (Sanders et al., 2014). Finally, it has been shown that these pathological mechanisms of tau seeding and spreading are potentiated by extracellular Aβ aggregation in transgenic mice (Gotz et al., 2001;Bolmont et al., 2007). Indeed, accumulating evidence *in vitro*, *in vivo* and in patients provide solid support for an Aβ-induced tau pathology (Stancu et al., 2014b). Crossing of APP/PS1 mice with 5 early-onset familial AD mutations (5xFAD) and TauP301S (PS19) transgenic mice clearly supports this idea (Stancu et al., 2014a). In this modern murine model, pathological Aβ species induce changes in tau that contribute to cognitive deficits correlating with synaptic deficits and hippocampal atrophy. In patients, earliest changes appear in cerebrospinal fluid (CSF) Aβ42, closely followed by PET imaging. Alterations in CSF t-tau and p-tau appear later in the disease process, preceding cognitive decline and brain atrophy (Jack, Jr. et al., 2013;Jack, Jr. et al., 2010).

Senile plaques

Senile plaques (SPs) were described as spherical extracellular deposits with diameters up to 200 µm. SP could be classified in 3 general types following their morphology: diffuse, neuritic and burn-out types. These 3 types of plaques represent different maturation stages of the aggregates. Diffuse plaques are amorphous non-fibrillar aggregates, they can also be found in aged persons without any cognitive problem. Diffuse plaques can further mature in neuritic plaques that are the typical lesions found in AD brains. Neuritic plaques are associated with dystrophic neurites, synaptic loss and neuroinflammation (Mott and Hulette, 2005;Pike et al., 1995). Burn-out plaques contain a condensed amyloid core without any neuritic process. These later forms are supposed to appear at very late stages of Alzheimer's disease.

The core of senile plaques is principally composed by fibrillar aggregates of the β-amyloid peptide (Aβ) cited above. Aβ is produced by the successive cleavages of the amyloid precursor protein (APP) by the β- and γ-secretases, a process called amyloidogenic processing. Gamma-secretase cleavage releases Aβ peptides ranging from 36 to 43 amino acids. Aβ40 is the most abundant isoform and Aβ42 is predominant in senile plaques (Glenner et al., 1984). They associate with many other molecules and proteins such as ApoE, aluminium, acute-phase proteins. Later, they activate microglia and reactive astrocytes. These associations lead to local inflammatory reactions involving the release of cytokines, reactive oxygen species, nitrogen intermediates and neuronal loss.

1.3 The Amyloid Cascade Hypothesis

The amyloid cascade hypothesis has been over the two last decades both a unifying model for the understanding of the core pathological molecular events, and recently, a matter of intense debate. This hypothesis was initially formulated by J. Hardy and G. Higgins in 1992.

"… deposition of amyloid β protein, the main component of the plaques, is the causative agent in Alzheimer's pathology and that the neurofibrillary tangles, cell loss, vascular damage, and dementia follow as a direct result of this deposition."

(Hardy and Higgins, 1992)

Four key events are predicted by this hypothesis to be interconnected in a hierarchical and chronological way to trigger Alzheimer's disease. AD is directly linked to β-amyloid production and clearance (event I), leading to release of the toxic Aβ species (event II). Then, Aβ accumulation initiates the formation of neurofibrillary tangles (event III) and mediate neuronal death (event IV).

The first argument advanced by the author came from trisomy 21 known as Down syndrome. This disease results from an additional copy of the chromosome 21 harboring the amyloid precursor protein gene (APP). Knowing that Trisomy 21 leads to the neuropathology of AD (Olson and Shaw, 1969), and that APP processing releases Aβ (see below), Aβ deposition related to APP gene dosage was suggested to be responsible for the AD-like neurological troubles observed in patients with Down syndrome. In addition, identification of genetic APP mutations increasing amyloidosis (Levy et al., 1990;Van et al., 1990) associated to other AD symptoms (Goate et al., 1991;Hardy, 1992;Hendrickx et al., 2013) allowed to define the biochemical consequences of APP mutations. Most of the mutations are localized near the β- and γ-secretases cleavage sites and were obviously suggested to favor APP processing and Aβ production (Citron et al., 1992)

(detailed in 2.4 FAD mutations). Furthermore, APP mutations within Aβ sequence have been described to promote the formation of fibrils (Wisniewski et al., 1991). The original hypothesis addressed several points important to understand the link between the amyloid pathology and the formation of NFTs. At that time, ideas about the mechanisms involved in Aβ mediated neurofibrillary tangles formation were merely hypothetical. However, it was known that intracellular calcium could regulate tau phosphorylation (Baudier et al., 1987) and Aβ was shown to perturb calcium homeostasis. It was therefore suggested that Aβ could trigger tau hyperphosphorylation and PHFs formation by increasing the intracellular calcium concentration (Lee et al., 1991). All the APP mutations described are responsible for only a very small proportion of all AD cases (van Duijn et al., 1991). Indeed, most of the cases occur in a sporadic manner, suggesting there must be other causes triggering Aβ deposition. Amyloid depositions and neurofibrillary tangles have been shown to also appear after brain injuries caused by trauma (Mortimer et al., 1991) and neuronal stresses (Abe et al., 1991). Although acute effects may only lead to transient disruption of APP metabolism, in some cases it could end up in initiation of AD.

Update of the Amyloid Hypothesis by J.A. Hardy and D.J. Selkoe in 2002

10 years later, with the discovery of Presenilins, the γ-secretase catalytic subunits and their FAD mutations acting on Aβ production (Scheuner et al., 1996), together with the set-up of therapeutic strategies based on this theory, the initial amyloid cascade hypothesis was critically reexamined (Hardy and Selkoe, 2002).

There were 4 new conceptually important observations strongly suggesting that cerebral accumulation of Aβ is an initial event in AD, triggering the disease progress.

1. *Mutations in the gene encoding tau protein caused frontotemporal dementia with Parkinsonism. This disease is characterized by severe neurofibrillary tangles but NO Aβ depositions, suggesting that the most severe tau alterations were not sufficient to induce amyloid plaques (Hutton et al., 1998).*
2. *Transgenic mice overexpressing mutated tau together with APP with FAD mutations undergo increased tangles formation. Aβ toxicity is tau dependent but these mice only displayed increased tangles formation whereas structure and number of plaques were unchanged (Lewis et al., 2001).*
3. *The link between ApoE and Aβ was characterized, providing strong evidence that the most severe genetic risk factor for AD is involved in Aβ metabolism (Strittmatter et al., 1993).*
4. *There was growing evidence that genetic variability in Aβ catabolism and clearance may contribute to the risk of late-onset AD (Myers et al., 2000;Bertram et al., 2000).*

A detailed pathway of events leading to Alzheimer's disease was proposed (Fig.02).

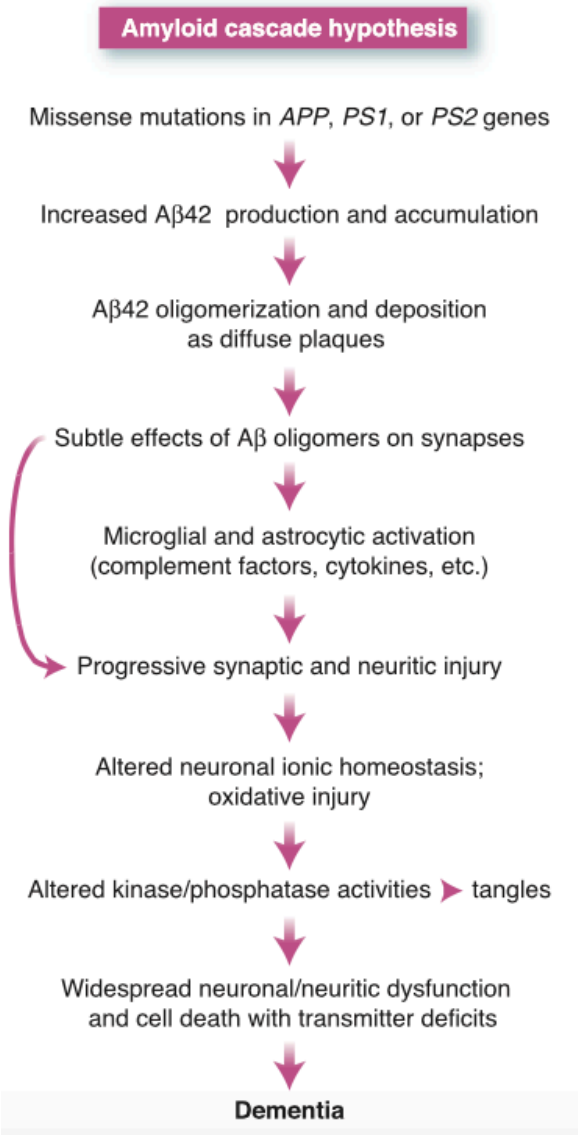

Fig.02
Schematic representation of the amyloid cascade hypothesis events leading to Alzheimer's disease (Hardy and Selkoe, 2002).

Despite all the important experimental data supporting the amyloid cascade hypothesis, some observations did not fit well with the proposed model. First, the extent of amyloid plaques does not correlate well with the degree of cognitive impairment during the progression of the disease. It has been however shown that soluble Aβ oligomeric species rather than plaques by themselves have a better correlation with disease progression (Wang et al., 1999;Lesne et al., 2006). Moreover, the degree to which FAD mutations affect Aβ production *in vitro* did not fit well with the initial idea of an increase in the amyloid load. This has been often debated, since effects of FAD mutations have been mostly addressed in cellular models that may not reflect properly the human brain complexity.

Another concern was that transgenic mice built on the amyloid cascade hypothesis (e.g. expressing FAD mutations of human APP) do not show clear-cut neuronal loss, raising in parallel the concern of rodent models to recapitulate all the array of pathological features observed in AD. The final criticisms have risen from studies showing that neurofibrillary degeneration increases with age in human. They are therefore present before amyloid plaques appearance (Braak and Braak, 1991), challenging the hypothesis that Aβ deposition plays the role of trigger in the disease onset.

Contradictions to the amyloid cascade hypothesis

As this hypothesis was stated and re-examined, at least 2 important points had to be addressed in order to validate it.

The first one was testing whether removing of the amyloid aggregates from AD brains could revert the pathology. Experimental approaches have been designed to address this point, either by targeting Aβ production (detailed in 2.2 Metabolism and trafficking) or by clearing the amyloid load in a pathological context. In mice, a variety of treatments has been set up in order to remove macroscopic senile plaques after their formation. These techniques include passive and active immunization against Aβ peptide, treatments to induce Aβ clearance and reduce inflammation. In all these cases, plaques were removed and mice recovered until 100% on behavioral tests (Cramer et al., 2012;Schenk et al., 1999), supporting the amyloid cascade hypothesis. Following these promising results in mice, clinical trials have been done in humans with early sporadic AD. Several of the participants developed antibodies against Aβ, their plaque burdens were substantially reduced but their dementia had not improved and most likely continued to worsen (Serrano-Pozo et al., 2010;Holmes et al., 2008). Two other recent reports using antibodies also failed even after 80 weeks therapy (Doody et al., 2014b;Salloway et al., 2014) (detailed in 2.2 Metabolism and trafficking). So in contrast to humans, whenever AD mice have problems in their neuronal network, these problems are reversible. None of the models involves irreversible neurodegeneration and this raises questions of interpretation. These models may reproduce some features of the disease but they lack some other biochemical deficits and fail to recapitulate the full set of AD events.

The second test challenging the hypothesis suggested introducing amyloid in healthy brains to see whether it will initiate the AD pathological cascade.

However, it has been shown that individuals can present very few or no symptoms of dementia and carry substantial amyloid burden in their brain (Villemagne et al., 2013). This is the case for a quarter to a third of all the older population that do not show impaired cognitive functions. This observation indicates that it is clearly possible to have amyloid deposits without any dementia. The simple existence of people displaying extended amyloid plaques in their brain for years without any dementia is another major challenge to the amyloid cascade hypothesis. We can assume that these persons are also oligomers-positive for an even longer period. So amyloid is not sufficient to cause dementia in humans, and it's even worse in animal models. Although mouse models overexpressing FAD APP mutants produce substantial amyloid deposits in their brain as early as 4 months, they have only modest cognitive problems. They never display any neurofibrillary tangles and show only poor or no neurodegeneration (LaFerla and Green, 2012;Gotz and Ittner, 2008). Moreover, in transgenic mice only expressing Aβ alone and no full-length APP, plaques appear but no cognitive impairments at all (Kim et al., 2013). It is true that only APP, PS but never MAPT mutation lead to FAD. But these data obtained from humans and mice models show that you cannot produce an AD-like dementia only by exposing the brain to Aβ deposits. Although Aβ is neurotoxic, it is not sufficient to recapitulate the complexity of the disease by itself.

Other elements of the pathological context need to be understood to have a clear view of the involvement of Aβ in the disease. Above all, age remains the most accepted and powerful risk factor in AD. Aging has to launch the missing elements triggering the pathology (Herrup, 2010). Progressive oxidative, metabolic or mitochondrial problems, DNA damages or senescence features accumulating with the age can be the starting point of the disease (Bucholtz and Demuth, 2013;Yao et al., 2009;Hunter et al., 2013). There is evidence that aging can also trigger

failures in autophagy (Nixon and Cataldo, 2006) and/or lysosomal function (Bezprozvanny and Mattson, 2008). It can possibly come from a loss of calcium homeostasis due to excitotoxicity occurring with aging (Yu et al., 2009;Green and LaFerla, 2008;Supnet and Bezprozvanny, 2010). AD first event can also involve neuroinflammation (Mosher and Wyss-Coray, 2014). Several groups even suggest that AD is due to a cell-cycle control failure happening in neurons (Arendt et al., 2010). Maybe the right combination of risk factors, accelerated by Aβ, is required to establish the disease.

To summarize, some findings questioned the amyloid cascade hypothesis by showing that Aβ cannot trigger the disease only by itself. It has to be a common final pathway involving Aβ and tau leading to AD, but obviously many ways to trigger those mechanisms. It has to be an event, distinct from normal aging, which establishes permanent cellular changes and alter cellular physiology. Amyloid is a great contributor to the disease process but evidence suggested that it is neither necessary nor sufficient (Fig.03) (Herrup, 2015).

Table 1 Strengths and weakness of the amyloid cascade hypothesis

	Strengths	Weaknesses
Genetics	• fAD: *APP* and *PSEN* genes are the only genes identified • sAD: *APOE* variants affect AD risk and also Aβ clearance • Rare A673T *APP* mutation lowers Aβ production and protects against AD	• fAD: No α-secretase (*ADAM10*) or *BACE* mutations yet found • sAD: *APP*, *PSEN*, *BACE* and *MAPT* (tau) polymorphisms show little association • *MAPT* mutations associate with frontotemporal dementia
Biochemistry	• Amyloid comes from APP after cleavage by γ-secretase (PSEN) • Conditions that favor γ-secretase cleavage to the longer $A\beta_{1-42}$ favor aggregation and AD • APOE4 increases risk of AD and slows clearance of Aβ	• Transgenic mice expressing only Aβ suggest amyloid alone is not sufficient[42] • Other biochemical deficits are present in AD and are sufficient to create dementia
Animal models	• Overexpression of human APP in mouse produces plaques • Mouse transgenics for human APP show memory deficits • Aβ is toxic to neurons in culture • Overexpression of human APP in fruit flies produces neurodegeneration	• Overexpression of human APP in mouse does not produce tangles, neurodegeneration or AD-like dementia • *PSEN* transgenics show neither plaques nor tangles nor neurodegeneration • Memory deficits in transgenics correct quickly and completely
Pathology	• Amyloid plaques are more frequent in AD-affected brains	• Tangles correlate better with neurodegeneration than plaques do • Individuals with substantial plaque burdens can have normal cognition
Clinical findings	• Presence of plaques on imaging associated with increased AD risk • In some subjects with amyloid burdens and early dementia, anti-amyloid therapy improves cognition[a]	• After AD begins, immunoclearing of plaques does not improve cognition[a] • By definition, there is no AD without plaques and plaque deposits without dementia is preclinical AD • No phase 3 clinical trial based on the hypothesis have been successful • Inhibition of γ-secretase increases AD symptoms
Epidemiology		• Certain nonsteroidal anti-inflammatory drugs reduce AD risk by half

Fig.03 Strengths and weaknesses of the amyloid cascade hypothesis.

Table resuming the strengths and weaknesses of the amyloid cascade hypothesis. fAD, familial AD forms; sAD, sporadic AD forms (From Herrup, 2015).

2. The amyloid precursor protein (APP)

2.1 The APP protein family

APP is a type I transmembrane protein, member of Amyloid Precursor Protein superfamily –APP and APP-like proteins, APLPs- formed by APP, APLP-1 and -2 in mammals (Goldgaber et al., 1987;Wasco et al., 1993). APLPs are very similar to APP except that they do not contain the Aβ peptide sequence (Walsh et al., 2007). APP and APLP-2 are expressed ubiquitously with particularly high expression in neurons, whereas APLP-1 is found primarily in the nervous system (Lorent et al., 1995). APLP-2 like APP contains an acidic domain called Kunitz-type protease inhibitor (KPI), while APLP-1 lacks this additional domain (Fig.04) (Aydin et al., 2012). The ectodomain E1 regions GFLD and CuBD (see in 2.1 APP structure) are

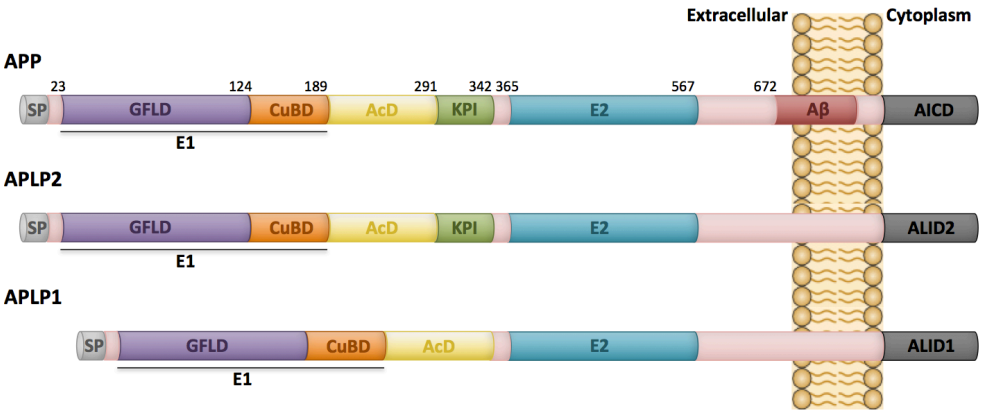

Fig.04 Differences between APP family proteins.

APP and APLP-2 possess a N-terminal signal peptide (SP). In their ectodomain, they possess a Growth factor-like domain (GFLD) and a Copper-binding domain (CuBD) together forming the E1 domain, an acidic domain (AcD) followed by a Kunitz-type protease inhibitor domain (KPI) and the E2 domain. In its extracellular domain, APLP-1 only lacks the KPI domain. APP membrane domain contains the Aβ peptide but not the APLPs but they all have an intracellular domain called either AICD (APP intracellular domain) or an APP-like intracellular domain 1 or 2 (ALID1 and 2).

present in all three proteins but are more conserved between APP and APLP-2 than APLP-1 (Dahms et al., 2010). Like APP, APP-like proteins are present in different species and undergo proteolytic processing. They produce either the AICD (APP intracellular domain) or its homologs ALID (APP-like intracellular domain). The genetic interactions of APP and APP-like genes at the level of the phenotype and the similarity in biochemical processing have generated the assumption of a functional redundancy. However, there is growing evidence that APP paralogs are not simply extra copies from the ancestral gene but have evolved to perform different neuronal events (Fig.05) (Shariati and De, 2013).

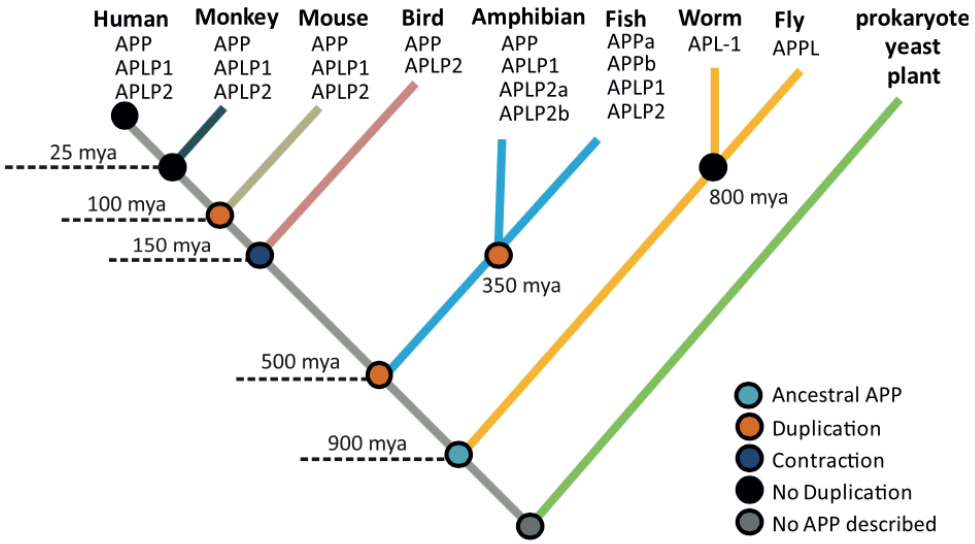

Fig.05 APP family tree.

A simplified dendrogram based on APP and its paralogs depicts the evolution events in the gene family. The duplication (orange) and contraction (deep blue) nodes are shown (lengths of the lines are not proportional to evolutionary distance between species); mya, million years ago (From Shariati et al., 2013).

Models of single and combined APP and APLP knock-out (KO) mice have been developed to study their function. Single KO for the 3 APP homologues are viable, they show only moderate but slightly different phenotypes (Heber et al., 2000;Zheng et al., 1995;Midthune et al., 2012). APP/APLP-1 double deletion is viable but deletion of APLP-2 with concomitant deletion of APP or APLP-1 displays a perinatal lethal phenotype (Heber et al., 2000;Guo et al., 2012;Aydin et al., 2011). Therefore there is a dominant function of APLP-2 but APP and APLP-1 can work together to compensate. APPsα knock-in (KI) in an APLP-2 null background but not APPsβ rescued the lethality, although they still have neuromuscular problems (Li et al., 2010;Weyer et al., 2011). This rescue is probably due to the presence of the YENPTY motif (Barbagallo et al., 2010;Matrone et al., 2011). It is clear that these 3 proteins reflect a complex evolution process that cannot be simplified by redundancies or divergences. Their neuron-specific function is preserved but innovation created divergences in their expression and interactions.

The APP gene is located on the chromosome 21 and contains 19 exons (Kang 1987). Alternative splicing of exon 2, 7, 8 and 15 expresses 10 different isoforms of 365 to 771 amino acids (Octave, 1995). The most frequent isoforms are APP 695, 751 and 770 (Fig.06). APP 695 is largely expressed in the central nervous system and is neuronal specific whereas APP 751 is ubiquitously expressed. APP 770 and 751 isoforms like APLP-2 contain an extra KPI domain, encoded by exon 7.

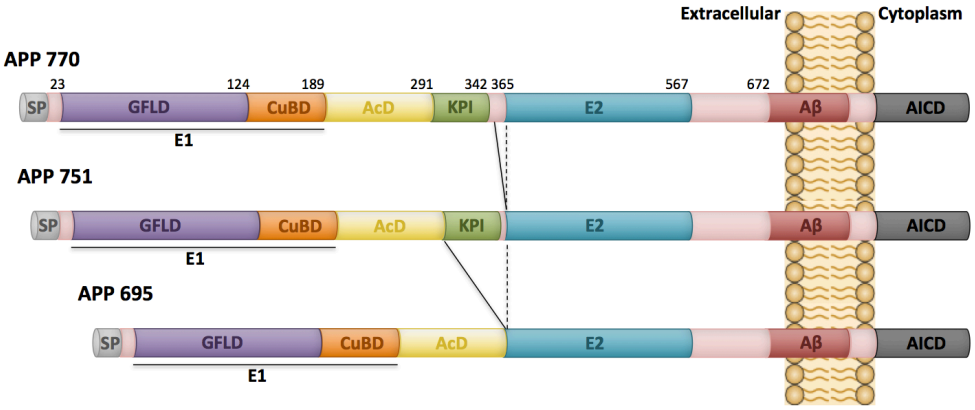

Fig.06 APP most frequent isoforms.

APP most frequent isoforms are APP 770, APP 751 and the neuronal APP 695 isoform. They are produced by alternative splicing and have similar structures. APP 770 and 751 differ from the neuronal 695 isoform by the Kunitz-type protease inhibitor domain (KPI). They all display a signal peptide (SP). They possess in their ectodomain a Growth factor-like domain (GFLD) and a Copper-binding domain (CuBD) together forming the E1 domain, an acidic domain (AcD) followed or not by a Kunitz-type protease inhibitor domain (KPI) and the E2 domain. They all also contain the Aβ peptide and the intracellular domain AICD (APP intracellular domain).

2.2 APP structure

The APP family proteins contain a large glycosylated extracellular part, a transmembrane α-helical domain and a short conserved cytoplasmic tail (Fig.07). Unstructured linker domains ensure the connexion and flexibility of these 3 domains. The extracellular part of the protein called the ectodomain possess two regions: E1 and E2. The E1 region (residues 18 to 207) structure has been completely identified by crystal structure analysis (Dahms et al., 2010). This region encompasses a growth factor-like domain (GFLD, 28-123) and a copper-binding domain (CuBD, 127-188) (Barnham et al., 2003;Rossjohn et al., 1999). These two subunits were previously suggested to be independent folding units but they rather seem to form a rigid entity (Gralle et al., 2006). The GFLD displays a highly basic surface suggested to interact with glycosaminoglycans and a hydrophobic surface important for ligand binding (Rossjohn et al., 1999). Cysteine residues 98 and 105 are part of a N-terminal flexible loop and form a disulfide bridge. The CuBD consists of a triple-stranded β-sheet packing of the α-helix (Barnham et al., 2003). This site binds Cu(II) that is reduced to Cu(I) upon the oxidation of cysteine residues 144 and 158 (Barnham et al., 2003). The E1 domain is followed by an acidic region and a Kunitz-type protease inhibitor (KPI) domain (subject to alternative splicing in both APP and APLP). The E2 region (residues 365 to 570) is the largest, its structure consists of six α-helices with double and triple stranded structures (Wang and Ha, 2004). It contains the heparan sulfate proteoglycans (HSPG) binding site and a RERMS sequence thought to promote cell growth and differentiation (Multhaup et al., 1995). APP and APLPs ectodomains are known to bind various proteins from the extracellular matrix, all influencing each other in their binding strength and probably playing a role in cellular adhesion (Beher et al., 1996;Multhaup et al., 1996).

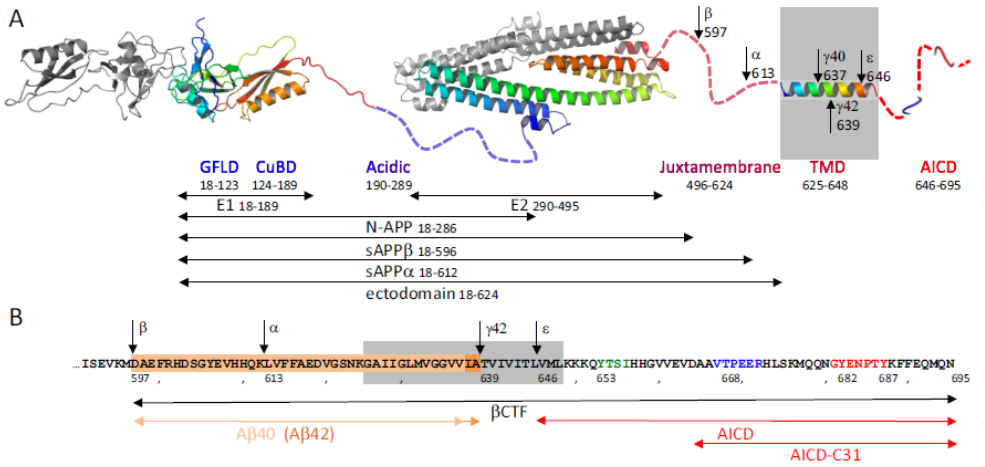

Fig.07 APP different structures and proteolytic fragments.

This represents the domains' architectures of the APP 695 isoform. The extracellular E1 and E2 domains are separated by and acidic region and linked to the juxtamembrane and transmembrane domain (TMD) and an intracellular domain (AICD). Dash lines give structurally unknown regions, proposed interactions domain within E1 and E2 are shown in grey. Arrows indicate enzymes cleavage sites and breakdown products are delimitated. The C-terminal sequence from the juxtamembrane sequence is given with the Aβ and TMD sequences underlined and AICD sequence fingerprints color-coded (From Muller and Wild, 2013).

The Aβ sequence is localized at the ectodomain and transmembrane domain boundary. The N-terminal half of the transmembrane domain contains the end of Aβ sequence (from residue 29). This region encompasses 3 consecutive GXXXG motifs and is supposed to adopt an α-helical structure (Kienlen-Campard et al., 2008). APP cytoplasmic part comprising the 47 last amino acids is called AICD for APP intracellular domain. First studies show only transiently structured regions in aqueous solution (Ramelot et al., 2000) but complete crystal structure analysis of AICD bound to Fe65 is now available (Radzimanowski et al., 2010). The C-terminal domain contains TPEE and YENPTY sequence motifs; both have threonine and/or

tyrosine phosphorylation sites (Kroenke et al., 1997;Radzimanowski et al., 2008). In the family, both APLP1 and APLP2 possess the YENPTY motifs but only APLP2 contain the TPEE motif. These two kinds of motif are binding sequences that might function as molecular switches for various binding partners (Ramelot and Nicholson, 2001;Suzuki and Nakaya, 2008). The NPXY motif is also known as a common signal for endocytosis, necessary for APP internalization (Lai et al., 1995).

The APP family proteins undergo post-translational modifications including N- and O-glycosylation, sialylation and CS GAG modification of the ectodomain and are phosphorylated at multiple sites within the intracellular domain (Suzuki and Nakaya, 2008;Jacobsen and Iverfeldt, 2009). During evolution, E1 and E2 domains together with the YENPTY motif are the most conserved sequences in APP (Coulson et al., 2000), giving clues to its hypothetical functions.

2.3 APP cellular functions

After decades of investigations, cellular functions of APP remain somehow hypothetical, due to major obstacles facing the investigations. The first issue is the complex proteolytical processing of APP that generate many fragment proteins, each showing specific interactions. The second obstacle is the partially overlapping functions of APP and APLPs, making the analysis very difficult to interpret. The assumed functions of APP are charged to either full-length APP, the AICD, Aβ or/and soluble sAPP. A large part of the admitted functions is attributed to sAPP forms. *In vivo* they constitute at least 50% of all APP forms and both sAPPα and β showed a half-life of 4-5 hours, compared to 1h for full-length APP (Morales-Corraliza et al., 2009).

Full-length membrane bound APP resembles cell surface receptors and has been shown to bind a lot of proteins trough the extracellular but also intracellular domains. APP interacts with cell-surface proteins including Alcadein (Araki et al., 2003), F-spondin (Ho and Sudhof, 2004), Reelin (Hoe et al., 2009), LRP1 (Pietrzik et al., 2004), sorL1/LR11 (Schmidt et al., 2007), Nogo-66 receptor (Park et al., 2006), Notch2 (Chen et al., 2006) and Netrin (Lourenco et al., 2009). Several of these interactions regulate APP processing but their physiological relevance is poorly understood. A lot of investigations concerning APP interactions also focused on the well-known and highly conserved YENPTY motif within the AICD region. Like lots of receptor proteins it confers clathrin-mediated endocytosis and modulates processing (Perez et al., 1999;Ring et al., 2007). Multiple intracellular binding partners of the YEPNTY motif have been identified, including kinases as well as adaptor proteins like mDab1, JIP, Shc, Grb2, Numb, X11/mint family and Fe65 family proteins. These interactions may not only modulate APP processing but also cell-signaling.

APP/APLPs proteins are upregulated during maturation and differentiation of neurons. They are present in transport vesicles and undergo anterograde transport to synaptic sites (Koo et al., 1990;Sisodia et al., 1993;Kaether et al., 2000;Szodorai et al., 2009). The protein expression and localization in neuronal cells suggest a role in synaptic adhesion and function. Although they remain elusive, the commonly admitted functions of APP are cellular and synaptic adhesion, neuronal and synapto-trophic function, axon pruning and degeneration, intracellular signaling and apoptosis. They are analyzed *in vitro* and *in vivo* with loss-of-function studies.

Cellular and synaptic adhesion

Analysis of APP and APLPs conserved domains support the adhesion property for all members of the family. First, APP extracellular domain has been shown to interact with extracellular matrix components such as heparin (Clarris et al., 1997), collagen type I (Beher et al., 1996) and laminin (Kibbey et al., 1993), indicating a role in **cell-matrix adhesion**. Independently, APP/APLPs homo- and hetero-dimerization can promote **cell-cell adhesion**. It has been reported that heparin binding to E1 or E2 domains of APP induces its homodimerization (Dahms et al., 2010;Gralle et al., 2006). *Trans*-cellular APP dimerization can mediate synaptic adhesion like neurexins/neuroligins, SynCAMs and LRRTM (leucine-rich repeat transmembrane neuronal proteins). APP extracellular sequence engages transsynaptic interactions while the intracellular domain YENPTY motif recruit pre- and post-synaptic complexes like Mint/CASK (calcium/calmodulin-dependent serine protein kinase) (Biederer et al., 2002;Wang et al., 2009). Besides a direct role, APP has also been shown to colocalize with integrins at surface adhesion sites of axons (Storey et al., 1996;Young-Pearse et al., 2008). It can also interact

with other cell adhesion molecules including NCAM (Ashley et al., 2005), NgCAM (Osterfield et al., 2008) and TAG1 (Ma et al., 2008).

Neuronal and synapto-trophic function

There are evidences that APP can also have neurotrophic activities. Deletion or reduction of APP lead to reduced neurite outgrowth, synaptic activity and impaired neuronal viability *in vivo* (Allinquant et al., 1995). This can be mediated by the full-length protein and likely involves its adhesion properties particularly through heparin-binding (Small et al., 1994). Growth promoting and trophic activities are also attributed to sAPPα. This soluble form has been shown in many experiments to promote proliferation and synaptic density (Ninomiya et al., 1993;Mucke et al., 1994;Roch et al., 1994;Meziane et al., 1998). *In vivo* sAPPα shows a role in spatial memory and LTP by neurogenesis and neurite outgrowth (Taylor et al., 2008;Turner et al., 2003). sAPPα could act as a cofactor of the epidermal growth factor (EGF) (Caille 2004), through ERK phosphorylation (Rohe et al., 2008) or downregulation of the cyclin-dependant kinase 5 (CDK5) (Han et al., 2005). The action of sAPPα is supported by APP/APLP2 dKO mice lethality fully restored by the only expression of the fragment protein (Ring et al., 2007).

Axon pruning and degeneration

Whereas sAPPα shows trophic and neuroprotective functions, sAPPβ is much less active and even described as toxic. sAPPα antagonizes dendritic degeneration and neuronal death pathway triggered by proteasome stress (Copanaki et al., 2010). In constrast, sAPPβ undergoes an additional cleavage, producing N-terminal 35 kDa derivates. Under trophic withdrawal conditions, this soluble peptide called N-APP

binds to Death receptor 6 (DR6) and mediate axon pruning and neuronal degeneration (Nikolaev et al., 2009). This mechanism could occur during normal embryonic development but also during neurodegeneration. Opposite activities between sAPPα and β are intriguing as there is only a 17 amino acids difference between the two fragments.

Intracellular signaling

AICD is highly reminiscent of the intra-cellular domain of the Notch protein NICD that triggers Notch signaling pathway and was early shown to form a similar transcriptionally active complex (Cao and Sudhof, 2001). Further studies depicted a more complex picture. AICD production may not be required for APP signaling activity but only phosphorylation of Tip60 chromatin-remodeling factor (Hass and Yankner, 2005). Finally, APP has been suggested to modulate the overall transcriptional state of a cell rather than specific genes (Giliberto et al., 2008). During the past decade, some downstream targets of APP have been proposed including KAI (Baek et al., 2002), GSK3β (Kim et al., 2003), neprilysin (Pardossi-Piquard et al., 2005), EGFR (Zhang et al., 2007), p53 (Checler et al., 2007), LRP (Liu et al., 2007), APP itself (von Rotz et al., 2004), genes involved in calcium regulation (Leissring et al., 2002), cytoskeletal dynamics (Muller et al., 2007), of genes involved in the control of cholesterol homeostasis (Pierrot et al., 2013) and several immediate early genes including EGR1 (Hendrickx et al., 2013). Despite a decade of broad investigations in this field, neither the molecular pathways nor the downstream targets have been unambiguously identified.

Apoptosis

AICD has been shown to be further cleaved by caspases and produce a 31 amino acids fragment called Jcasp or C31. This peptide is suggested to mediate cytotoxicity (Bertrand et al., 2001;Lu et al., 2003;Park et al., 2009). Despite large amyloid pathology, impaired synaptic plasticity, memory and learning are corrected in APP transgenic mice models only by mutation of the caspase cleavage site (Galvan et al., 2006). This really supports an apoptotic function of APP in the disease but needs further investigation regarding challenging results (Harris et al., 2010).

2.4 APP Metabolism

APP metabolism has been extensively studied as it generates the Aβ peptides (Fig.08). For decades, two specific pathways have been attributed to APP processing. These pathways were initially defined by their ability to produce Aβ peptide or not, so they were called amyloidogenic and non-amyloidogenic pathways. The involved endoproteolytic enzymes are commonly named secretases.

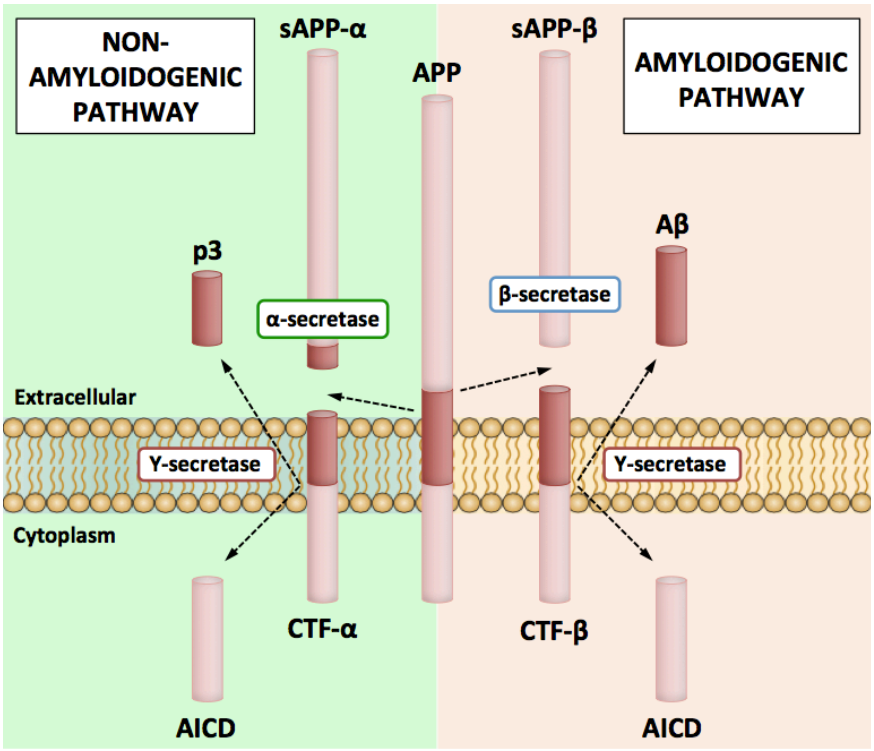

Fig.08 APP canonical processing.

Since decades, the assumed processing of APP involves two different pathways. By the non-amyloidogenic pathway, APP is cleaved by α-secretase to release sAPP-α and membrane-anchored CTF-α. Then, CTF-α is processed by the γ-secretase to produce a small p3 peptide and the AICD. The amyloidogenic pathway releases the famous Aβ peptide together with the AICD after a first β-secretase cleavage prior the γ-secretase. This β-cleavage produces a sAPP-β and a membrane-anchored CTF-β eventually cleaved by the γ-secretase.

The non-amyloidogenic pathway is the major in terms that it processes up to 80% of the APP expressed in cells. It was initially considered as the physiological processing pathway, by opposition to the amyloidogenic pathway. However, evidences rapidly came up showing that APP is processed by both pathways in all cell types under physiological conditions (Haas et al., 1995). The non-amyloidogenic pathway is initiated by the shedding of APP ectodomain by the α-secretase, releasing a soluble fragment called soluble APP α (sAPPα) and a membrane-anchored α C-terminal fragment (αCTF). In the amyloidogenic pathway leading to Aβ production, APP is instead cleaved by the β-secretase at the N-terminus of the Aβ sequence, releasing a soluble extracellular fragment (sAPPβ) and a membrane-anchored β C-terminal fragment (βCTF). The γ-secretase is a very peculiar enzyme, cleaving its substrates within their transmembrane region, a process known as Regulated Intramembrane Proteolysis or RIP. Processing of the α and β C-terminal fragments (αCTFs and βCTFs) by the γ-secretase releases the AICD in the cytoplasm in both cases (Fig.08) (Haas 1993, Zhang 2003). In the meantime, they produce either the p3 peptide from αCTF or Aβ from βCTF. However, this simple description has become much more complex over the years.

Very recently, an alternative pathway in APP processing has been characterized after the discovery of a new fragment, intermediate in size between full-length APP and CTFs (Willem et al., 2015). Indeed, before cleavage by β- or α-secretase, another enzyme called η-secretase can cut APP in its extracellular domain. This releases a sAPPη fragment in the extracellular compartment and a membrane-anchored ηCTF. The latter can be further cleaved by the α- and β-secretases to release Aη-β or Aη-α peptides (Fig.09) (Willem et al., 2015;Tyan and Koo, 2015). Apparently η-secretase processing even significantly exceeds amyloid processing in human neurons (Fig.09).

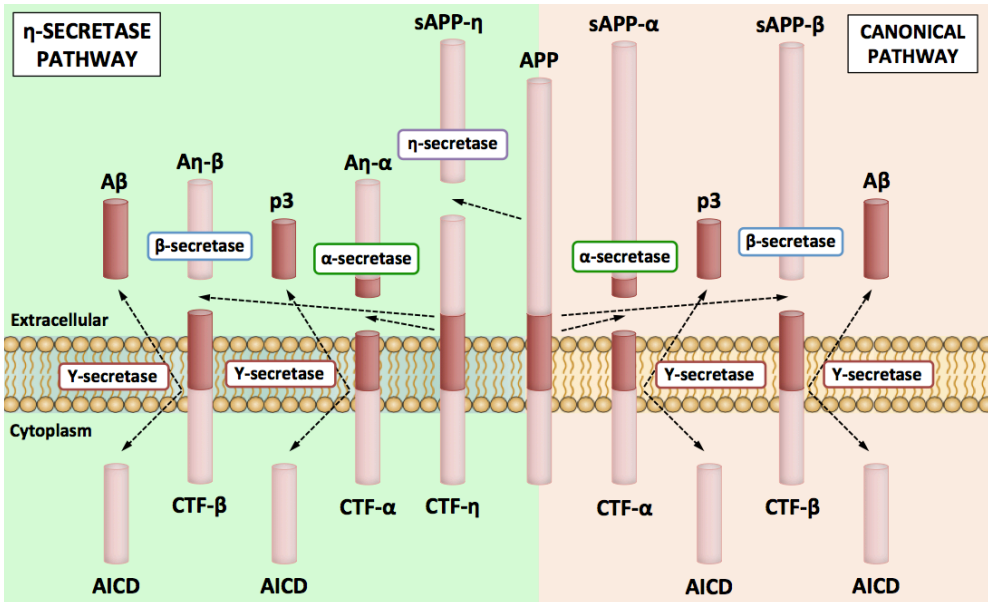

Fig.09 The η-secretase alternative pathway.

The canonical pathway involves direct cleavage of APP by α- or β-secretases, leading to further Aβ production (right side). Prior to α- or β-secretases APP can be cleaved by the η-secretase, entering the η-secretase pathway (left side).

The α-secretase and soluble APP α

The α-secretase is the key enzyme in the non-amyloidogenic pathway. The α-secretase cleaves APP between residues Lys_{16} and Leu_{17} of Aβ sequence (the α-site), precluding further formation of Aβ (Wang et al., 1991). Several proteases from the ADAM ("A disintegrin and metalloprotease") protein family have been identified under the generic umbrella of α-secretase. ADAM9, ADAM10 and ADAM17 are considered as the principal members (Asai et al., 2003). Several studies suggested that ADAM17 and ADAM10 would be responsible for the regulated α-secretase cleavage of APP (Buxbaum et al., 1998;Lammich et al., 1999). ADAM 10 can be regulated by phosphorylation through protein kinase C

(PKC) (Durairajan et al., 2011). α-cleavage of endogenous APP is inhibited by a dominant negative form of ADAM 10, with a point mutation in the zinc binding site (Lammich et al., 1999). ADAM10 is the constitutively active form of α-secretase (Kuhn et al., 2010), although its transcription and activity can be regulated by the sirtuin histone deacetylase SIRT1 (Donmez et al., 2010) for example.

Soluble APP α (sAPPα) has been attributed the axon pruning and synaptotrophic functions of APP (cf. 2.3 APP cellular functions). sAPPα has shown trophic roles during development, particularly in neuronal cells proliferation and synaptic density through its E2 RERMS motif (Baratchi et al., 2012). In addition to its neurotrophic properties, sAPPα regulates and restores memory through long-term potentiation (LTP) (Turner et al., 2003;Taylor et al., 2008). sAPPα has also neuroprotective effects against oxidative stress, ischemic injuries and antagonism of proteasome-induced cell death (Mattson et al., 1993;Smith-Swintosky et al., 1994;Copanaki et al., 2010). The most striking phenotype confirming the importance of sAPPα is its ability to restore the viability of APLP2/APP dKO mice (Ring et al., 2007).

The β-secretase and the amyloidogenic pathway

The first step of the amyloidogenic pathway involves the β-secretase also known as "β-APP cleaving enzyme" 1 or BACE1. Another member of the BACE family (BACE2) has been identified (Solans et al., 2000). BACE1 cleaves APP at the first amino acid of the Aβ sequence. Upon this cleavage, soluble APP β (sAPPβ) is released and the transmembrane APP β C-terminal fragment (βCTF) remains anchored in the membrane. BACE1 together with BACE2 are membrane-associated type I proteins containing 2 particular motifs termed D(T/S)G(T/S) in

their extracellular domain that are critical for its aspartyl protease activity (Vassar et al., 1999). They are expressed in several tissues and compete for their substrate. In the central nervous system, BACE1 is the principal active β-secretase in neurons whereas BACE2 is mostly expressed in astrocytes (Irizarry et al., 2001a). BACE1 cleaves APP at the β-site, while BACE2 cuts APP within Aβ sequence at the β'-site between residues 10 and 11 (Farzan et al., 2000;Yan et al., 2001).

Although sAPPβ share the same 83 last amino acids than sAPPα, it does not show the same neuroprotective and memory helping functions (Furukawa et al., 1996a;Furukawa et al., 1996b). sAPPβ unlike its α counterpart does not rescue APP/APLP2 knockout lethality (Li et al., 2010). Soluble APPβ has nevertheless been shown to induce axonal outgrowth and robustly drives neuronal embryonic stem cells differentiation (Freude et al., 2011). On the other hand, sAPPβ has been hypothesized to induce cell death through activation of caspase-6 (Nikolaev et al., 2009) but whether this soluble peptide is really stable *in vivo* or undergoes further cleavages to produce toxic metabolites is still under debate (Li et al., 2010).

The η-secretase and Aηs

The new APP-cleaving enzyme involves a site between amino acids 504 and 505 (APP695 numbering), N-terminal to the β-secretase cleavage site. The η-secretase involves at least the MT5 subclass of membrane-bound metalloproteinases (MT5-MMP). The η-secretase proteolysis generates a ±25 kDa CTFη ending at the APP C-terminal. ηCTF fragment protein is also further processed by β- or α-secretase, generating the Aη-β or Aη-α of 92 and 108 residues respectively with the β and α CTF. Aη peptides were identified *in vitro* as well as in mice and human brains (Willem et al., 2015). The enzyme and the ηCTF have been shown to accumulate

within dystrophic neurites in close vicinity to amyloid plaques. Aη-α has been suggested to suppress the activity of hippocampal neurons *in vivo* while Aη-β had no effect.

The γ-secretase complex and the γ-cleavage

1. *γ-secretase and regulated intramembrane proteolysis*

The γ-secretase is the enzyme involved in the last steps of both amyloidogenic and non-amyloidogenic pathway. It processes APP after ectodomain shedding by α- or β-secretase, and cleaves C-terminal fragments (α and βCTF) to release the p3 fragment or the Aβ peptide (Fig.10). In addition, cleavage of APP CTFs generates AICD a priori in both pathways.

The γ-secretase is a tetrameric high molecular weight complex with a molecular mass calculated to be ±230 kDa by scanning electron microscopy (Osenkowski et al., 2009) (Fig.10).

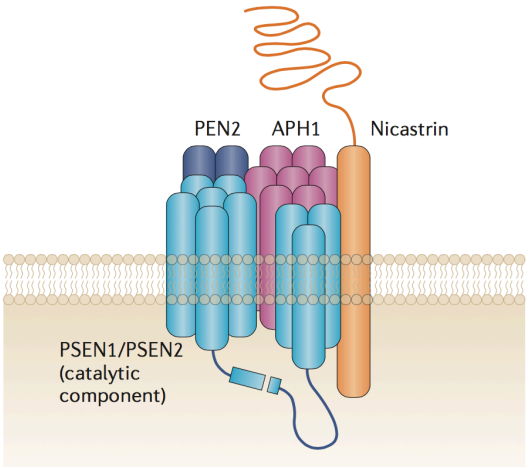

Fig.10 The γ-secretase complex subunits.

The γ-secretase is a tetrameric proteolytic complex formed by the association of PS1 or 2 (PSEN1/PSEN2), the catalytic core, with the nicastrin (NCT), presenilin enhancer 2 (PEN2) and anterior pharynx defective 1 (APH1) (From Andersson and Lendahl, 2014).

Gamma-secretase is an aspartyl protease, and it belongs to the intramembrane cleaving proteases (I-CLiPs) family. I-CliPs family proteases include S2P, the signal peptide peptidases (SPPs), the rhomboids and the Presenilins (PSs), the catalytic subunits of the γ-secretase. Among this family containing about 15 members, γ-secretase is one of the most studied. Each of these enzymes recognizes numerous substrates. At least 90 have been identified so far and are mainly type I transmembrane proteins like APP (Beel and Sanders, 2008). I-CLiPs have been implicated in a wide range of cellular responses (Annaert and De, 2002;Dillen and Annaert, 2006;Wolfe and Kopan, 2004). It is now well established that these proteases have the particularity to mediate regulated membrane proteolysis. They cleave their substrates within the hydrophobic core of their transmembrane domains.

One characteristic of the I-CLiPs is that they only accept substrates with short ectodomains. The enzyme interacts with the free amino group of substrates after the shedding of the ectodomain. This explains the sequence heterogeneity of their substrates as the targeting of the I-CLiPs relies on ectodomain shedding rather than primary sequence of the substrate. Consequently, intramembrane proteolysis is often regulated by an independent proteolytic cleavage resulting in the truncation of the substrate. This kind of proteases is often involved in intracellular signaling, by releasing intracellular domains of TM proteins (Notch), cholesterol metabolism, and can also display a proteasome-like function, removing needless transmembrane segments to prevent clogging of cellular membranes.

The active complex of the γ-secretase is composed by at least 4 core proteins: the Nicastrin (NCT), Anterior pharynx defective 1 (APH1), Presenilin enhancer 2 (PEN2) and the Presenilin 1 or 2 (PS1 or PS2). In human, there are 2 different PS and 3 different APH1 isoforms. It is thus possible to distinguish 6 different

complexes, showing distinct distributions and substrate specificity (Herreman et al., 1999;Mastrangelo et al., 2005). PSs are the catalytic core of the γ-secretase, each containing two catalytic aspartate amino acids responsible for their activity (De, 2003). PSs distinguish themselves from other I-CLiPs in their absolute requirement for their cofactors. Each of the subunits is essential to form an active γ-secretase complex (Edbauer et al., 2003). They assemble sequentially, in a 1:1:1:1 stoichiometry (Sato et al., 2007) and are superimposed on transport regulation.

2. Structure of the γ-secretase catalytic site

Recently, cryo-electromicroscopy (cryo-EM) allowed to determinate the 3D structure of the γ-secretase complex (Lazarov et al., 2006; Lu et al., 2014). The 19 TMD of the enzyme subunits are organized into a horseshoe-shaped structure with a large empty pocket in the center and two openings toward the luminal side (Fig.11). The large hydrophilic cavity contains the TMD 6 and 7 of the PS, with the catalytic aspartate residues (Sato et al., 2006). It allows the water access (mandatory for its proteolytic activity) from the intracellular but not extracellular side. NCT extracellular domain is located immediately above the hollow center of the cavity, interacting closely with its extracellular loops to cover the opening (Lazarov et al., 2006). NCT seems to contain a surface groove above the lipid membrane facing the hollow center of the horseshoe (Lu et al., 2014). This groove could be the putative substrate-binding site and is consistent with the studies involving NCT extracellular domain in substrate recognition and positioning (Dries et al., 2009;Shah et al., 2005). The two TMDs of PEN2 are likely to be inserted between PS TMD6 and 7 on the cytoplasmic side of the cavity (Lu et al., 2014).

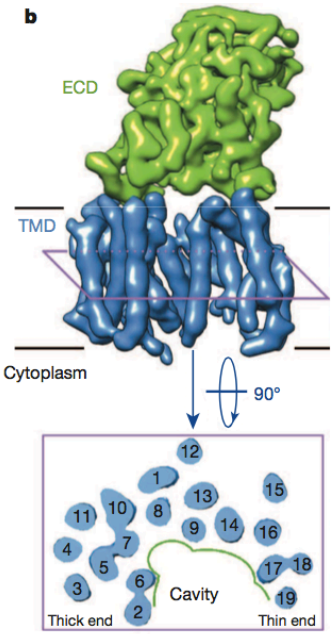

Fig.11 Cryo-EM structure of human γ-secretase complex.

3D horseshoe structure of the γ-secretase shows the transmembrane domain (TMD) in blue and the extracellular domain (ECD) in green. In the box, the lower view shows the catalytic cavity and the 19 TMDs of the γ-complex including PS, NCT, APH1 and PEN2 (Lu et al., 2014).

3. Assembly and maturation of the tetrameric complex

The correct assembly and interactions among the 19 different TMD of the γ-secretase are fundamental for its functionality. Genetic ablation of only one component of the complex is sufficient to induce mislocation, incomplete maturation and destabilization of the whole complex. The assembly is more likely to be initiated early in the endoplasmic reticulum (ER) by the interaction of APH1 with the NCT, mediated by the TMD of NCT (Fig.12). The two proteins form a stable subcomplex, to which the other components are added (LaVoie et al., 2003). Then, the NCT-APH1 subcomplex interacts with the C-ter of PS (Kaether et al., 2004;Steiner, 2008). Deletion of the last residue is sufficient to block γ-secretase assembly and NCT maturation (Kaether et al., 2004). Mutation of GXXXG motif in APH1 TMD abolishes the binding of the complex to PS, but not to

NCT (Nimura et al., 2005). In this case, PEN2 joins the trimeric intermediate and ends γ-secretase formation by initiation of the maturation. On the other hand, PEN2 may also bind PSs independently to form a second subcomplex (Fraering et al., 2004). TMD1 is known to interact with the PS N-terminal fragment (NTF) and more precisely the TMD4 (Kim and Sisodia, 2005). This interaction is independent of any other interaction with NCT-APH1 (Watanabe et al., 2005).

Association with PEN2 TMD1 leads to a major conformational rearrangement opening the putative substrate entry site. It is involved in the autocatalytic cleavage of PS in the loop between TMD6 and 7. This produces 2 fragments: NTF and CTF. They are stabilized by PEN2 and mandatory for the activation of the γ-secretase, allowing acquisition of its catalytic properties (Thinakaran et al., 1996;Takasugi et al., 2003). However, binding of PEN2 alone to PSs is not sufficient to trigger endoproteolysis, the presence of each protein is mandatory.

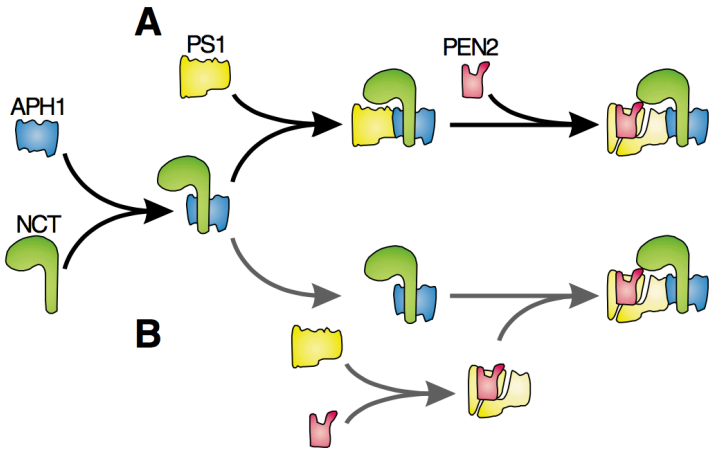

Fig.12 Sequential interactions leading to the γ-secretase complex formation.

APH1 first associates with NCT to for a stable subcomplex. (A) The subcomplex APH1-NCT further associates with PS1 and then PEN2 to form the γ-secretase. (B) PS1 and PEN2 associates to form a second subcomplex and then APH1-NCT and PS1-PEN2 associates to form the γ-secretase (From Spasic and Annaert, 2008).

The final maturation step requires extensive N-glycosylation of the NCT. It involves the whole γ-secretase assembly, leading to translocation from the ER towards the Golgi and *trans*-golgi network (TGN) where maturation is completed (Kimberly et al., 2002). Although PS expression is required for NCT glycosylation, NCT maturation is independent of PS endoproteolysis (Dries and Yu, 2008).

4. γ-secretase sequential cleavage of APP

γ-secretase processes APP in several steps. The enzymatic complex cuts the protein in a sequential manner starting from a ε-site. The ε cleavage site is located at the C-terminal part of the APP TMD. The cleavage occurs either on position 48 or 49 (Aβ numbering) (Gu et al., 2001). Cleavage at this position requires a local helix-to-coil transition of the APP helix to expose the cleavage site (Sato et al., 2009). At the intracellular membrane boundary, the helical structure is locally unraveled, allowing following amino acids of the protein to shift in the active site of the enzyme. This way, γ-secretase trims up the protein until the γ-site, producing Aβ intermediates and finally the common 38 to 42 isoforms (Fig.13) (Sato et al., 2009).

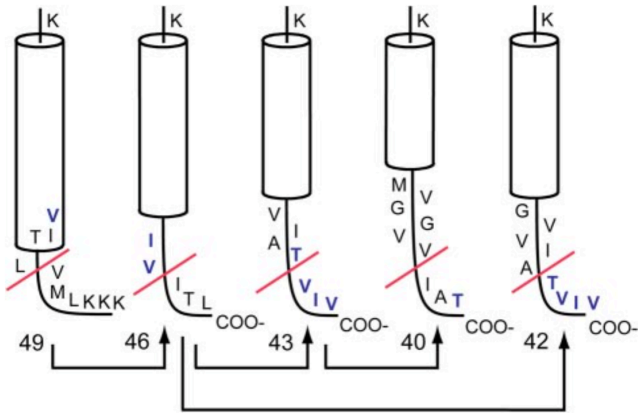

Fig.13 Unraveling of APP α-helix for γ-secretase sequential cleavage.

Cleavage of the γ-secretase at the ε-site involves unraveling of the protein to shift the following amino acids to the catalytic site. This indicates the main sequential trimming pathways leading to the production of Aβ 40 and 42 (From Sato et al., 2009).

The γ-secretase cleaves mainly every three or four residues, defining two principal cleavages consensus: Aβ49 > Aβ46 > Aβ43 > Aβ40 and Aβ48 > Aβ45 > Aβ42 > Aβ38 (Qi-Takahara et al., 2005;Takami et al., 2009). But the enzyme can also skip some more amino acids and cleave after five or six residues, making the γ-cleavage even more complex (Fig.14).

To date, no consensus motif has been identified and substrate specificity is likely to come from structural properties of the proteins. Orientation of the substrate in the catalytic pocket probably defines the Aβ production route. Thus, after ectodomain shedding, substrate docking and fitting to the catalytic site are key regulatory events for their processing by the γ-secretase (Struhl and Adachi, 2000). Trafficking of the γ-secretase and its substrates, meaning their subcellular localization in specific compartments is another key mechanism to consider for the regulation of substrate processing (Beel and Sanders, 2008). This phenomenon may also be regulated by APP homodimerization through its GXXXG motifs (2.5 Dimerization and processing). Indeed, around 25% of all the identified γ-secretase substrates, including APP, harbor the well-known dimerization motifs (Beel and Sanders, 2008).

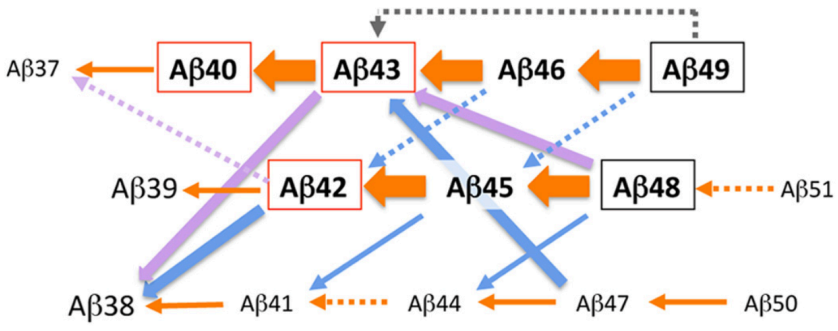

Fig.14 Scheme of the stepwise successive γ-secretase cleavages producing Aβ different isoforms.

The relative size and *thickness* of the *arrows* and *dotted lines* with *arrowheads* represent the amount of the released peptide (Matsumura et al., 2014).

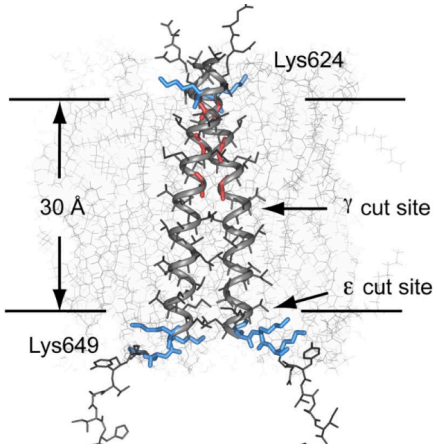

Fig.15 Structural model of APP TMD.

Proposed structural model of APP TMD dimer in synthetic membranes. ε-cleavage close to Lysine649 (APP695 numbering) would lead to local unraveling of the helix and shift of the γ-secretase binding site towards the γ-site (Sato et al., 2009).

5. The AICD

AICD is the 57 to 59 residues intracellular fragment released from APP by the γ-secretase in both amyloidogenic and non-amyloidogenic pathways. However, recent studies indicate that AICD is preferentially produced by the APP 695 isoform through the β-secretase cleavage rather than through the α-secretase (Belyaev et al., 2010). The AICD has an intrinsically disordered structure (Ramelot et al., 2000;Ando et al., 2001). This small stub can adopt different conformations explaining its versatile functions. Transient structure of APP intracellular domain is well suited to recognize a multitude of differently shaped partners, with fast rates of association/dissociation. More than 20 proteins have been reported to interact with the AICD (Muller et al., 2008). However, little is known about these interactions and their relevance *in vivo*. In the APP intracellular domain sequence, 3 interaction motifs have been identified: the ^{653}YTSI, the ^{667}VTPEER and the ^{681}GYENPTY sequences (Fig.07).

The ^{653}YTSI sequence contains the threonine^{654} and serine^{655} that are phosphorylated in the rat brain under physiological conditions (Oishi et al., 1997). This sequence is implicated in clathrin-mediated basolateral sorting of APP in epithelial cells (Lai et al., 1998). PAT1 protein is the only one demonstrated to bind directly this motif. PAT1 is associated with microtubules and mediates basolateral sorting (Kuan et al., 2006). However, no link with sorting has been identified in neurons yet (Back et al., 2007).

The second motif ^{667}VTPEER seems critically involved in pathophysiological processes. Major binders of this motif are the adaptor/scaffolding Fe65 family (Fe65, Fe65L1 and Fe65L2) (Mcloughlin et al., 2008). They can alter APP processing by interaction with AICD through their PTB2 (phosphotyrosine binding) domain. Another direct interactor of the AICD sequence is the dimeric adaptor protein 14-3-3Y (Sumioka et al., 2005). After AICD release, Fe65 can translocate to the nucleus and participate in gene transcription, with modulation by 14-3-3Y. They should imply the transcription factors CP2/LSF/LBP1 (Minopoli et al., 2001), Tip60 (Cao and Sudhof, 2001) and the nucleosome assembly factor SET (Telese et al., 2005). Possible target genes include the glycogen synthase kinase-3β (GSK3β), Neprilysin, KAI1 and the low-density lipoprotein receptor-related protein 1 (LRP1). Their physiological relevance remains controversial (Konietzko, 2012). Moreover, ^{667}VTPEER sequence contains the threonine 668 established as the major phosphorylation site of APP (Suzuki and Nakaya, 2008). In neurons, phosphorylation of this site can be mediated by the GSK3β and cyclin-dependent kinase 5 in neurons. Under thr668 phosphorylation, the prolyl isomerase Pin1 enzyme mediates isomerization of the adjacent proline 669 residue (Ando et al., 2001;Radzimanowski et al., 2008). This could have crucial consequences on AICD interacting network and APP physiological functions.

The third motif is the ^{681}GYENPTY sequence. It has been widely studied as the NPXY sequence is a well-established internalization signal for membrane proteins sorting towards endosomes and lysosomes (Chen et al., 1990;Bonifacino and Traub, 2003). The NPXY motif is well known to interact also with adaptor proteins containing a PTB or PID (phosphotyrosine interacting) domain (Uhlik et al., 2005). The binders of this motif include members of the X11/Mint, JIP (c-Jun N-terminal kinase interacting protein), Dab and Shc families as well as the Numb protein. Mints sequences reduce Aβ production, by suppression of APP translocation in lipid rafts containing the β- and γ-secretase (Wang et al., 2009;Saito et al., 2008). Interactions of the AICD with X11/Mints are also suggested to have functional roles in synapse formation and neurotransmitter release (Wang et al., 2009;Ashley et al., 2005;Weyer et al., 2011). In APP, the NPXY signal is extended by 3 N-terminal residues (GYE) containing another phosphorylated tyrosine (Tyr662) (Barbagallo et al., 2010;Perez et al., 1999). Dab1 could rather increase cell-surface localization of APP, increasing cleavage by the α-secretase (Howell et al., 1999). Tyr682 can be readily phosphorylated by the nerve growth factors TrkA and the tyrosine kinases Abl and Src (Schettini et al., 2010). Phosphorylation of Tyr682 mediates APP sorting towards the amyloidogenic processing (Barbagallo et al., 2010). Phosphorylated Tyr682 is also required for the binding of the cytoplasmic adaptor protein ShcA and Grb2 to APP CTFs. The involved cascades are known to mediate cell proliferation and gene transcription (Schettini et al., 2010).

AD treatments targeting the amyloidogenic processing and Aβ

To date, no curative treatment of AD exists. Most of therapeutic approaches only slow the symptoms and associated co-morbidities, including anxiety and depression without stopping the progression of the disease. To cope with memory loss associated with AD, lots of efforts have been undertaken to find therapeutics ameliorating memory and cognitive functions. The major -and only approved- treatments actually proposed to patients are acetylcholinesterase inhibitors (AchEI) and NMDA receptors antagonists. Degeneration of cholinergic neurons is and early event in the disease and AchEI, such as donepezil facilitating cholinergic transmission that is defective in the pathology. Treated patients show an initial improvement in cognitive functions followed by a slower decline in the next months (Hansen et al., 2008). The extracellular accumulation of glutamate induces an uncontrolled activation of NMDA receptors, inducing excitotoxicity and neurodegeneration (Dong et al., 2009). NMDA antagonists like Memantine prevent excitotoxicity without impairing the normal synaptic transmission (Lipton, 2004). Beside these neurotransmission-based therapeutic approaches, a lot of efforts have been invested to develop new specific amyloid production and accumulation on the basis of the amyloid cascade hypothesis.

Stimulating α-secretase activity is a first therapeutic strategy. Resveratrol is a well-known polyphenol particularly enriched in red wine and able to increase α-secretase activity. Increased expression of ADAM10 leads to reduction and delayed amyloid aggregation in mouse models (Postina et al., 2004). Another molecule, biostatin A, reduces Aβ levels by increased α activity linked to protein kinase C (PKC) (Etcheberrigaray et al., 2004). However, despite their potential interest, none of these candidates has been tested yet in clinical trials.

A more direct way to target the amyloid pathway was performed by evaluating molecules that inhibit β- or γ-secretase activities. β-secretase selective compounds are already under clinical investigations, some reporting encouraging results (Albert, 2009). This enzyme has a particular active site in terms of nature and size, making difficult the development of designed inhibitory compounds. Agonists of the peroxisome proliferator-activated receptor γ (PPARγ) that inhibit β-secretase failed to improve clinical biomarkers during clinical trials (Gold et al., 2010).

Targeting γ-secretase appeared as the principal but most challenging treatment perspective. γ-secretase inhibitors (GSIs) have been developed in the beginning. The first generation GSI called Semagacestat reduced Aβ levels both in plasma and cerebro-spinal fluid (CSF), but rapidly showed severe side effects that led to premature trial interruption (Bateman et al., 2009;Imbimbo and Giardina, 2011). These adverse effects, including detrimental intestinal problems, worsening cognitive functions and increased risk cancer, were attributed to parallel impairment of Notch signaling. The second generation GSI, including begacestat, avagacestat and PF-3,084,014 are specific of APP cleavage, sparing Notch (Mayer et al., 2008;Gillman et al., 2010;Lanz et al., 2010). These are currently under trial; all are well tolerated and no particular side effects are reported so far (Tong et al., 2012). Finally, γ-secretase modulators (GSMs) including non-steroidal anti-inflammatory drugs (NSAIDs) and NSAIDs-like drugs have also been discovered. Rather than blocking the enzyme, they modify the ratio of Aβ isoforms produced, increasing Aβ 38 isoform and reducing the toxic Aβ42 (Beher et al., 2004;Tomita, 2009). GSMs could have been promising but no clinical improvements were reported and trials have been halted (Green et al., 2009).

In parallel, another approach to clear Aβ peptides is the activation of the immune system, triggering its elimination by phagocytosis. Active and passive immunotherapies targeting the Aβ peptides have been evaluated in phase II (active) or phase III clinical trials. Trials based on active immunotherapy against Aβ showed an important clearance of senile plaques in patient's brain, despite no improvement of neurofibrillary tangles or cognitive functions (Vellas et al., 2009). Moreover, they have been stopped before completion due to severe adverse effect (meningoenceophalitis). Recently, a newly reported vaccine shows interesting results as it is much better tolerated than previous (Lemere, 2009). Finally, passive immunization involves administration of monoclonal or polyclonal antibodies directed against Aβ. Solanezumab and Gantenerumab are the main tested. The clinical trials investigating passive immunotherapies showed no benefit in primary outcomes (cognitive improvement and brain atrophy), despite some observations indicating a reduction of amyloid loads and complex effects on biomarkers (Doody et al., 2014b;Doody et al., 2014a).

One important consequence of these results was to call the amyloidogenic cascade hypothesis into question (Herrup, 2015). However, it is widely admitted now that therapeutic approaches simply targeting Aβ are prone to fail as long as we do not have a more complete picture of the precise nature of pathological Aβ isoforms or conformations.

2.5 APP cellular trafficking

Once produced in the endoplasmic reticulum (ER), APP undergoes a lot of post-translational modifications in its way to the plasma membrane. They include N- and O-glycosylation but also cytoplasmic and ectodomain phosphorylations. However, only a small fraction of the protein is present at the plasma membrane (±10%). Due to its ^{681}GYENPTY motif, APP is rapidly internalized by clathrin-coated pits mediated endocytosis and delivered to endosomes (Fig.16).

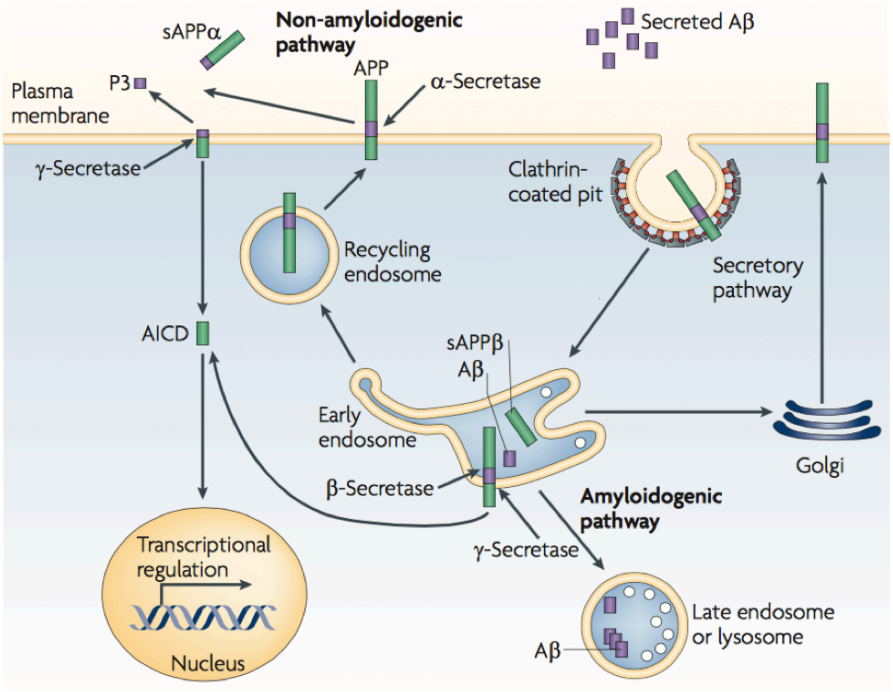

Fig.16 APP cellular trafficking.

APP traffics through the Golgi to the plasma membrane. At the membrane APP is primarily cleaved by the α-secretase and then γ-secretase to produce the P3 peptide. Membrane APP is internalized through clathrin-coated pits and delivered to endosomes where it is cleaved first by the β-secretase BACE1 to release sAPPβ. Then βCTF is processed by the γ-secretase to generate Aβ. Aβ peptides are secreted to the extracellular space but some can aggregate in the late endosomes or lysosomes (Modified from Bu, 2009).

In the endocytic pathway, only a tiny part of the precursor protein pool is recycled to the cell surface from late endosomes. Measurable amounts of APP from late endosomes are degraded in lysosomes or redirected to the trans-Golgi network (TGN). At steady state, the majority of APP localizes in the Golgi and TGN. During their stay at the plasma membrane, APP proteins can be processed by the α-secretase (Sisodia, 1992). BACE1 is predominantly active in the late Golgi/TGN and endosomes, consistent with amyloidogenic cleavage of wild-type APP during endocytic/recycling steps (Koo and Squazzo, 1994).

γ-secretase complex is present in multiple compartments including Golgi, TGN, endosomes and the plasma membrane. Studies indicate that Aβ production occurs mainly in the TGN and endocytic compartments while APP traffics through the secretory and recycling pathways (Small and Gandy, 2006). Trafficking of APP seems to highly regulate its processing. At the plasma membrane, APP is cleaved by the α-secretase and enters the non-amyloidogenic pathway. In the endosomes and TGN, the precursor protein is processed sequentially by the β- and γ-secretases to produce the Aβ peptide (Thinakaran and Koo, 2008;Zhang et al., 2012). Enzymes as well as APP trafficking in the cells can be regulated by phosphorylation (Walter et al., 2001). APP phosphorylation state of Thr668 and direct (through the ^{681}GYENPTY sequence) or indirect interactions with adaptor proteins including Fe65, Mint, Dab1 and JIP regulate its trafficking and Aβ production (Miller et al., 2006;Pietrzik et al., 2004;Ando et al., 2001;Lee et al., 2003).

2.6 Dimerization

APP has a transmembrane structure that displays a lot of similarities with cellular receptors like Notch (Brou et al., 2000) and the Epidermal Growth Factor Receptor (EGFR) (Schlessinger, 2002). These receptors associate in dimers at the plasma membrane to activate cellular pathways. Dimerization is not only required for effective ligand binding and further signaling but is also needed for maturation and transport to the plasma membrane. Interestingly, homodimerization (through determinants present in the ectodomain) has been shown to control APP trafficking to the membrane (Ben et al., 2012b). Based on structural features, there are 2 hypothetical sites controlling APP homo- and/or hetero-dimerization: the ectodomain and the transmembrane/juxtramembrane domain (TM) (Fig.17).

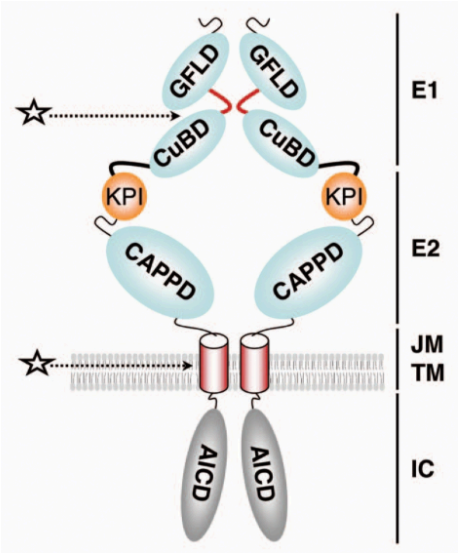

Fig.17 APP different domains suggested for its dimerization.

The APP ectodomain contains two major regions (E1 and E2). E1 possesses a copper-binding domain (CuBD), separated by a loop region (red bold line) from the Growth Factor-like Domain (GFLD). E1 and E2 are linked by and acidic region (black bold line). The E2 domain is essentially formed by the Central APP domain (CAPPD). APP770 and 751 contain a Kunitz Protease inhibitor domain (KPI). In the cytoplasmic part, APP possesses an AICD domain (APP Intracellular Domain). JM/TM, juxtamembrane and transmembrane regions. IC, intracellular region. The 2 hypothetical dimerization sites are indicated by stars (Ben Khalifa et al., 2010).

Ectodomain dimerization

The ectodomain is known to bind extracellular matrix proteins like heparin and collagen through the E1 region (Beher et al., 1996). APP has been suggested to form homodimers in a way reminiscent to EGFR. The full-length protein dimerization seems mediated by the E1 ectodomain region that contains the Growth factor-like domain (GFLD) and the Copper-binding domain (CuBD) (Soba et al., 2005). This region contains a loop formed by a disulfide bridge necessary for the conformation that stabilizes the homodimeric state (Fig.08). The E2 domain also has been shown to reversibly dimerize in solution (Wang and Ha, 2004). E2 contains the high-affinity heparan sulfate proteoglycan (HSPG) binding site. It possesses as well a RERMS sequence (Arginine^{328}-Glutamate^{329}-Arginine^{330}-Methionine^{331}-Serine^{332} amino acids sequence, APP695 numbering) that could promote cell growth and differentiation (Multhaup et al., 1995). This dimerization occurs in the longest dimension of the molecule and in an antiparallel orientation, packing the N-terminal substructure of one monomer against the C-terminal part of the other. APP and its paralogs APLPs have been shown to form *trans*-dimers in a homo- or heterotypic fashion, a process promoting cell adhesion (Soba et al., 2005). Moreover, molecular interaction of APP and APLPs was enriched in synaptic compartments. This interaction process has been described for proteins belonging to the cell adhesion molecule (CAM) family. It supports the role of APP in neuronal migration during embryogenesis (Young-Pearse et al., 2007). APP dimerization could be regulated by its binding to matrix proteins or heparin (Gralle et al., 2006;Dahms et al., 2010), Zinc (Bush et al., 1993) or sAPPα (Gralle et al., 2009). Recent studies in the team showed that the ectodomain mediates APP dimerization in the ER-Golgi intermediate compartment (ERGIC) and *trans*-Golgi network (TGN) (Ben Khalifa et al., 2012b). The KPI domain present in the APP 751

isoform (but not in APP 695) is critical for native ectodomain folding, a key regulatory mechanism for APP dimerization (Ben Khalifa et al., 2012a).

Dimerization of the transmembrane domain and GXXXG motifs

APP contains at the extracellular JM/TM boundary 3 glycine-XXX-glycine sequences called GXXXG motifs, followed by a GXXXA motif (Fig.18). It is a typical feature of APP TM domain among the APP family because APLPs do not contain any of these motifs. GXXXG motifs together with leucine zipper motifs (LXXLXXXLXX) (Eilers et al., 2002) have been shown to mediate sequence-specific dimerization in transmembrane proteins (Curran and Engelman, 2003).

GXXXG motifs are highly frequent in natural TMD sequences (12% of TM helices), suggesting their role as key dimerization motifs (Senes et al., 2000;Unterreitmeier et al., 2007). They have now been implicated in TMD interactions for more than 20 different proteins like the human leucocyte antigen (HLA) proteins, integrins, the Na/K ATPase β1 and APP (Teese and Langosch, 2015). In these GXXXG and GXXXG-like motifs, 2 glycines (G) or less frequently alanines (A) and serines (S) are separated by 3 random (X) residues: (small)XXX(small). They have been described first in the glycophorin A (GpA) protein in which they have been shown to mediate close appositions of TM α-helices (Fig.19) (Lemmon et al., 1992). The GpA LIxxGVxxGVxxT sequence allows tight dimerization by direct contact between the glycines facing each others.

Fig.18 Sequence of the APP TM and JM regions.

Sequence of the APP JM/TM part, starting from the Aβ sequence. α, β, γ (Aβ 40 and 42) and ε cleavage sites are indicated by arrows. GXXXG motifs are identified (bold) (From Sato et al., 2009).

TM-helix packing interfaces favor the small residues (G, S, A) in that (small)XXX(small) conformation (Jiang and Vakser, 2000). Insertion of these residues into other hydrophobic TMD favors dimerization (Lemmon et al., 1992;Brosig and Langosch, 1998). Structural studies suggest that GXXXG motifs can promote van der Waals interactions and hydrogen bonds through close apposition of helices. The small residues or conformation of the small side chains allow the interacting helices to be in proximity of each other (MacKenzie and Engelman, 1998;MacKenzie et al., 1997;Smith et al., 2001a;Smith and Bormann, 1995). They thus promote interactions between the main chain and hydrogen bonding residues such as serines and cysteines (Zhang et al., 2015). The glycines facing each other make hydrogen bonds (CαH•••O=C) and contribute to TMD affinity (Smith et al., 2001b;Senes et al., 2001;Hong et al., 2014;Arbely and Arkin, 2004).

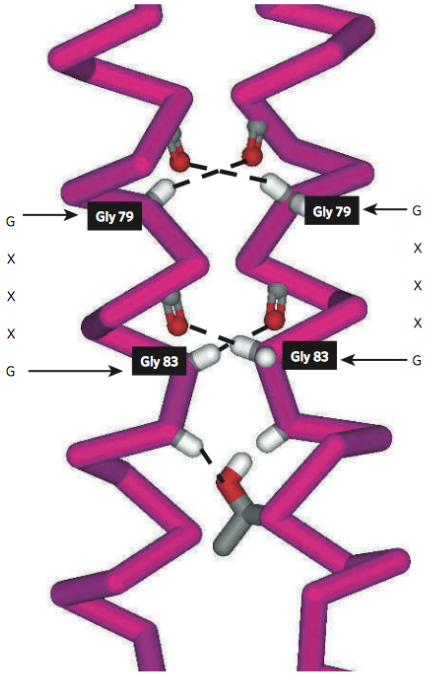

Fig.19 Structure of the glycophoryn A TM sequences dimer.

Scheme of the key packing glycines of the GXXXG motif highlighted. A Cα-H···O hydrogen bonds network between backbone carbonyls (oxygen is shown as the red atoms) and the Cα hydrogens of glycine residues (hydrogen is shown as the white atoms) are shown, along with a Cα-H···O hydrogen bond made by threonine side chain. Their hydrogen bonds are indicated by dashed lines (From Bowie et al., 2005).

It has been suggested that GXXXG neighboring β-branched residues, such as leucines, promote GXXXG-mediated dimerization by reducing the entropic cost (Russ and Engelman, 2000;Senes et al., 2000). However, recent studies could not find any specific enrichment of β-branched residues near GXXXG motifs (Dawson et al., 2002;Unterreitmeier et al., 2007). The glycines facing each other make hydrogen bonds (CαH•••O=C) and contribute to TMD affinity (Smith et al., 2001b;Senes et al., 2001;Hong et al., 2014;Arbely and Arkin, 2004). It has been suggested that GXXXG neighboring β-branched residues, such as leucines, promote GXXXG-mediated dimerization by reducing the entropic cost (Russ and Engelman, 2000;Senes et al., 2000). However, recent studies could not find any specific enrichment of β-branched residues near GXXXG motifs (Dawson et al., 2002;Unterreitmeier et al., 2007).

APP contains 3 in-register GXXXG motifs (Fig. 19) that are forming an extended interface, directly followed by a small GXXXA motif predicted to form another interface for dimerization. NMR structural analysis of APP TMD indeed revealed another parallel helix pair mediated by the association of small GXXXA interface residues (Nadezhdin et al., 2012). The GXXXA motif facilitates the close approach of the helices while bulky residues provide most of the van der Waals contacts. Recently, a modeling study has suggested that APP dimers can adopt different alternative structures in biological membranes, always through the GXXXG motifs (Dominguez et al., 2014).

Mutational studies indicated that the GXXXG/A motifs are important for C99 (CTFβ) dimerization (Kienlen-Campard et al., 2008) or dimerization of APP TM sequences measured by reporter gene assays (Munter et al., 2007). However, their influence on full-length APP dimerization has been rather debated. More recently, it has been suggested by split-fluorescent protein analysis that GXXXG motifs only play a marginal role in APP as well as in C99 dimerization (Ben Khalifa

et al., 2010;So et al., 2013). In addition to a direct role in dimerization, the GXXXG motifs present in APP have been shown to bind cholesterol (Barrett et al., 2012), acting as potential cholesterol sensors that could render dimerization sensitive to the lipid composition of the membrane bilayer. Recent publications suggest that the presence of GXXXG or (small)XXX(small) motifs within interacting sequences does not ensure that they are involved in dimerization (Li et al., 2012;Teese and Langosch, 2015).

For sure, conserved TMD residues are involved in important functional roles like helix flexibility (Li and Deber, 1994;Stelzer and Langosch, 2012), lipid interactions (Stangl and Schneider, 2015) or cellular localization (Cosson et al., 2013). But in several cases, a role in TMD interaction remains unclear.

Dimerization and processing

Homodimerization appears to play an important role in APP processing and function. An initial work reported that APP homodimers forced by disulfide bonds (K16C mutation) showed 6-8-fold increased Aβ production (Scheuermann et al., 2001). Interestingly, mutation to isoleucine (GXXXI) disrupted TMD dimerization in bacterial membranes ToxCAT system (Munter et al., 2007). This dimerization strength was likely to influence the access of γ-secretase from the ε- to γ-cleavage sites (Fig.11). Additionally, introducing mutations in GXXXG motifs of early onset Alzheimer's disease APP mutants decreased Aβ levels and rescued the disease effects (Munter et al., 2010). In contrast, our previous studies showed an enhanced dimerization of APP CTFs by mutations of GXXXG to isoleucine and leucine (GXXXL/GXXXI). Therefore, the effects observed in APP processing and Aβ production may also be dependent on the precise composition and orientation of APP dimers (Kienlen-Campard et al., 2008). In contrast, inducing dimerization of APP up to 70% of total protein levels using FKBP/rapamycin proteins led to a 50% reduction in Aβ (Eggert et al., 2009). A very recent publication showed that various covalent C99 homodimers made by cross-linking of engineered cysteines were not anymore cleaved by the γ-secretase *in vitro* (Winkler et al., 2015).

Since then, several groups gave more interest to the GXXXA motif and suggested that this motif, rather than GXXXG motifs, mediates dimerization (Gorman et al., 2008;Nadezhdin et al., 2012;Chen et al., 2014). Moreover, FAD mutation in this transmembrane region destabilized APP dimers, increasing the pool of monomeric APP and the Aβ42/40 ratio (Gorman et al., 2008). More recently, the APP TM helix appeared to be disrupted at the intracellular membrane boundary near the ε-cleavage site (Fig.20) (Sato et al., 2009). This helix-to-coil transition seems to be required for γ-secretase processing as mutations extending the α-helix inhibited ε-cleavage, led to low Aβ production and accumulation of the CTFs.

Further investigations into the TMD found that some other compounds could bind APP GXXXG motifs. Aβ lowering NSAIDs have been shown to bind the dimerization motif (Kukar et al., 2008). In particular, sulindac sulfide and its derivatives destabilized the APP TMD dimer in a concentration-dependent manner, correlating with lowered Aβ production (Richter et al., 2010). On another hand, heterodimerization with cholesterol by these same motifs could favor amyloidogenic processing (Barrett et al., 2012). Binding to cholesterol could indeed contribute to amyloidogenesis by favoring the partitioning of APP into lipid rafts that contain the β- and γ-secretases. It could therefore play a cofactor role or compete with α-secretase. These data suggest that the APP TMD dimerization through the GXXXG/GXXXA motifs can play a critical role in the generation of Aβ. One major concern here is that mutation of GXXXG/GXXXA motifs may also affect processing independently of dimerization. This makes quite complex the interpretation of GXXXG motifs' role in dimerization linked to processing.

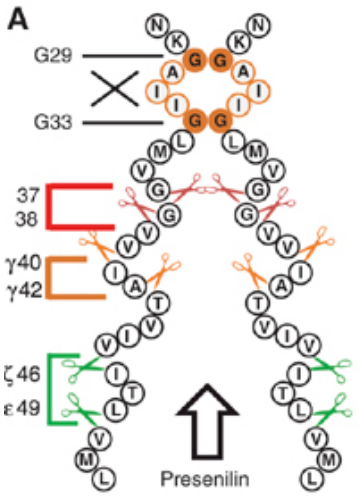

Fig.20 Model of the γ-secretase cleavage mechanism on dimeric APP TMSs.

Model of the γ-secretase cleavage mechanism on dimeric APP TMS. Sequential γ-secretase cleavages proceed from the C-terminal to the N terminal. The ε- and ζ-cleavage are suggested to occur independently of the dimeric state of the protein (green). Glycines G29 and G33 form a cross point of the two TMS helices and represent a sterical hindrance for the γ-secretase cleavage, such that the main final cleavages occur after residue 42/40 and produce Aβ42 and Aβ40 (orange). Following cleavages generating Aβ38 and Aβ37 only occur if they are not inhibited by too tight interaction of the dimer (red)
(From Munter et al., 2007).

2.7 FAD mutations

The mutations causing inherited autosomal dominant AD forms are located on 3 key genes: APP, PSEN1 and PSEN2. All these genes are involved in Aβ production. The majority of the mutations is localized in the PSEN1 gene (185 mutations identified so far) and increased the Aβ42/40 ratio (Bentahir et al., 2006). 33 mutations have been characterized in the APP gene. These mutations are clustered in 3 regions of the protein: the N-terminus of the Aβ sequence near the β-secretase cleavage site, at the juxtamembrane domain of the protein near the GXXXG/A motifs and around the γ-site (Benilova et al., 2012) (Fig.21).

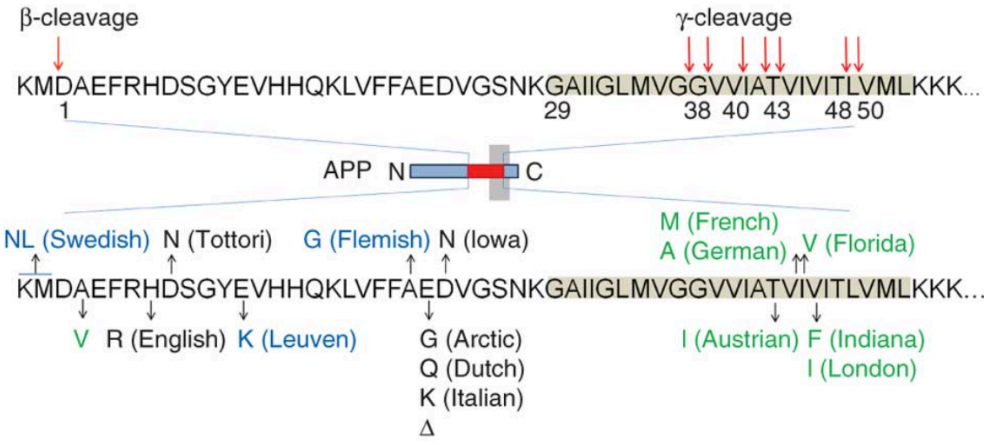

Fig.21 FAD APP mutations on the TM/JM sequence.

Sites of β-secretase and multiple γ-secretase cleavages in APP are indicated by arrows, the transmembrane domain of the protein is highlighted in gray. FAD mutations in APP TM/JM regions increase the total Aβ production (blue), alter Aβ biophysical properties (black) or affect the Aβ quantity and isoforms ratio (green) (Benilova et al., 2012).

Mutations located close to the β-site

FAD mutations clustered on the β-secretase cleavage site impact on the efficiency of the enzyme to cleave APP and initiate the amyloidogenic pathway. Among these, the Swedish mutation (KM670/671NL, APP771 numbering) affects the 2 residues ahead of the β-site and the Aβ sequence. It favors the processing of APP at this site and increases the overall production of Aβ peptides (Haas et al., 1995). Very recently, Swedish mutation has been shown to reduce Aη-α level by a strong enhancement of BACE1-mediated APP processing (Willem et al., 2015). 2 other mutations are located 2 amino acids after on the same residue (A673R and A673T, APP771 numbering; A2R and A2T, Aβ numbering), within the Aβ sequence. These showed opposites effects, increasing or decreasing Aβ levels respectively (Di et al., 2009;Jonsson et al., 2012).

Mutations located at the juxtamembrane region

JM mutations are located before the membrane boundary, a few residues before the first GXXXG motif. Among these, the effect of the Flemish mutation is striking (A692G, APP771 numbering; A21G, Aβ numbering). This FAD mutation increases the production of both Aβ 40 and 42 species, probably by disrupting the inhibition properties of an elusive inhibitory domain (Tang et al., 2014;Tian et al., 2010). Other mutations may enhance aggregation properties of the Aβ peptide. The Dutch, Italian and Arctic mutations are located on the same amino acid residue (E693Q/K/G respectively, APP numbering; E22Q/K/G, Aβ numbering). They do not appear to affect directly Aβ production but rather to induce structural changes that promote depositions in the brain, leading to cerebral hemorrhage with amyloidosis (Wilhelmus et al., 2006;Baumketner et al., 2008;Bugiani et al., 2010;Basun et al., 2008;Kalimo et al., 2013;Grant et al., 2007). Osaka mutation is a

deletion of the same residue (E693Δ; E22Δ) favoring oligomerization of Aβ (Nishitsuji et al., 2009;Tomiyama et al., 2008) and is suggested to impair the cholesterol efflux in the cells (Nomura et al., 2013).

Mutations located close to the γ-site

Many mutations are located at the APP γ-cleavage site, including London and Indiana mutations. Both mutations (V717I or V717F respectively) are situated 4 amino acids after the Aβ42 sequence (Goate et al., 1991;Murrell et al., 1991). They have the common property to increase the Aβ42/40 ratio, favoring Aβ aggregation and senile plaques formation (McGowan et al., 2005;Tanzi and Bertram, 2005).

3. The β amyloid peptide (Aβ)

3.1 Aβ heterogeneity

Monomeric Aβ is a ±4 kDa peptide. Aβ exists as a heterogeneous mixture of peptides with different properties (size, solubility, stability, biological and toxic properties). This difference comes from the alternative γ-cleavage and thus heterogeneity in the C-terminal end of the peptide. The major Aβ isoforms detected in body fluids (blood, CSF) are the Aβ 42, and 38 variants. Aβ40 is the main isoform and is continuously and abundantly produced in healthy individuals as well as in AD patients. Aβ42 was found to increase in FAD whereas Aβ 38 and smaller isoforms were decreased (Portelius et al., 2010). Increased Aβ42/Aβ40 ratio is generally considered as a hallmark of AD onset and progression.

Additional Aβ heterogeneity comes from enzymatic activities mediated by aminopeptidases, glutaminylcyclase or isomerases and kinases (De, 2010). They are responsible for post-translational modifications in the N-terminus of Aβ peptides. These modifications have critical roles in the regulation of protein activity. A variety of post-translationally modified variants have been characterized including phosphorylation (Kumar et al., 2011;Milton, 2005), truncation (Saido et al., 1996;Tekirian et al., 1998;Miravalle et al., 2005), racemization (Mori et al., 1994;Tomiyama et al., 1994), isomerization (Shimizu et al., 2000), pyroglutamination (Saido et al., 1995;Kuo et al., 1997) and oxidation (Dong et al., 2003). Aβ is phosphorylated by protein kinase A and Cdc2 *in vitro* (Milton, 2001) but also in neurons, transgenic mice and AD brains in early stages of the disease (Kumar et al., 2011). Aβ peptide is phosphorylated at residues serine 8 (Kumar et al., 2011) and serine 26 (Milton, 2001) positions. N-terminal truncated variants of Aβ beginning at positions 3, 11 and 25 have been found in

senile plaques (Tekirian et al., 1998;Miravalle et al., 2005;Guntert et al., 2006;Miller et al., 2006;Sergeant et al., 2003). Aβ Racemization at positions 7, 23 and 26 has been reported in human brains (Mori et al., 1994;Tomiyama et al., 1994) as well as isomerization on residues 1, 7 and 23 (Shimizu et al., 2000). Post-translational modifications of Aβ can promote formation of aggregates (fibrils or oligomers) as well as degradation by proteases (Fabian et al., 1994;Saito et al., 2003;Schilling et al., 2006;Kuo et al., 1998).

All these variants of Aβ result in a mix of more than 20 different forms. Qualitative changes in the spectrum of Aβ peptides rather than quantitative increases of individual species seem to define their pathological and eventual physiological properties.

3.2 Aβ fibrils

Discovery and properties

Neuritic plaques are one of the two hallmarks in Alzheimer's disease. Around 50 years ago, Cohen and Kidd revealed by electron microscopy that amyloid plaques were composed of fibrils (Cohen and CALKINS, 1959;KIDD, 1964). They were therefore described as filamentous aggregates made of β-amyloid peptide. Early works showed that Aβ can be aggregated in solution and that these high molecular weight species are responsible for specific and reversible toxicity in neuronal cultures (Pike et al., 1993;Pike et al., 1992). A link between neurodegeneration and the AD amyloid pathology was initially formulated in the so-called amyloid cascade hypothesis (Hardy, 1992). Research rapidly focused on amyloid fibrils to understand their formation, biologic properties and toxicity. *In vitro* but also *in vivo* studies regarding Aβ toxicity pointed out the neuronal cell death induced by fibrillar species, directly or indirectly (Mattson, 1997;Geula et al., 1998;McKee et al., 1998). Moreover, fibrillar intermediates showed instantaneous alteration of the electrical activity in rat cortical neurons (Walsh et al., 1999;Walsh et al., 1997). These metabolic changes mediated by Aβ fibrils were suggested to be induced by interaction with a specific cell surface receptor (Liu and Schubert, 1997;Liu et al., 1998).

These assemblies have a diameter of 10 nm and a length over the micron (Fitzpatrick et al., 2013;Knowles et al., 2007). Amyloid fibrils have high kinetics and thermodynamic stabilities (Baldwin et al., 2011) together with a huge resistance to degradation by chemical/biological agents (including detergents), temperature and pH (Hartt et al., 2011). Recently, fundamental specific properties of Aβ fibrils have been demonstrated. The first property is their ability to seed and spread in the brain. They amplify and propagate their own structures in a prion-

like manner by recruitment of additional molecules from their surroundings (Tycko, 2015). Self-propagation has already been demonstrated *in vitro* with the growth of seeded fibril. Fibril seeding only occurs when concentration of the protein overcomes its equilibrium value (Sanders et al., 2014). It implies that Aβ concentrations are saturated in the cellular or extracellular compartment where the aggregation occurs. This phenomenon is highly sequence specific and Aβ42 cannot mix with Aβ40 to seed and form fibrils (Lu et al., 2013). Fibrils can be sonicated and create a new generation of seeds able to grow into fibrils with similar structure. In agreement with this, phosphorylation of Aβ at serine 8 (pAβ) has been shown to mediate the peptide nucleation. Moreover, these pAβ nuclei were further able to promote *in vitro* aggregation of non-phosphorylated Aβ much faster than non-phosphorylated peptides (Kumar et al., 2011).

Indeed, fibrils can have different inherited structures between patients and each seed can propagate its morphology and molecular structures (Kodali et al., 2010;Petkova et al., 2005). This second property of fibrils is the polymorphism. Indeed, different fibrils appearances between AD patients have been characterized by transmission electron microscopy. Different fibril morphologies have different underlying molecular structures and their predominant structure can be controlled by subtle variations in growth conditions (Petkova et al., 2005;Paravastu et al., 2008). Some fibrils can exhibit “striated ribbon” or “twisted” morphologies and each molecular structure can propagate itself. At least 5 different polymorphisms have been observed for Aβ40 fibrils (Bertini et al., 2011;Lu et al., 2013;Fandrich et al., 2009). These different polymorphisms can lead to variations in clinical characteristics and neuropathology (Ashe and Aguzzi, 2013;Guo and Lee, 2014).

Structure and formation of Aβ fibrils

Like the other amyloid fibrils, Aβ fibrils have a cross-β structure in which individual β-strands are packed in parallel and oriented perpendicular to the fibril growth axis (Fig.22) (Kirschner et al., 1986;Ahmed et al., 2010). In each β-strand, the amino acids are in-register with one another (Benzinger et al., 1998;Antzutkin et al., 2000;Torok et al., 2002). β-strands pack in β-sheets, the latter assemble in protofilaments or protofibrils and further form fibrils (Fig.23) (Fitzpatrick et al., 2013).

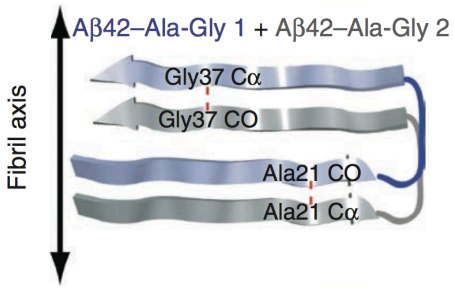

Fig.22 β-strands parallel and in-register orientation in Aβ42 fibrils.

Scheme of the parallel and in-register orientation of the N- and C-terminal β-strands in Aβ42 fibrils. The 2 Gly37 are packing to each other as well as the Ala21, with the carboxyl group (CO) facing the Carbon α (Cα). The red dashed line corresponds to the 4.7-Å distance between adjacent Ala21 residues and adjacent Gly37 residues along the fibril axis (From Ahmed et al. 2010).

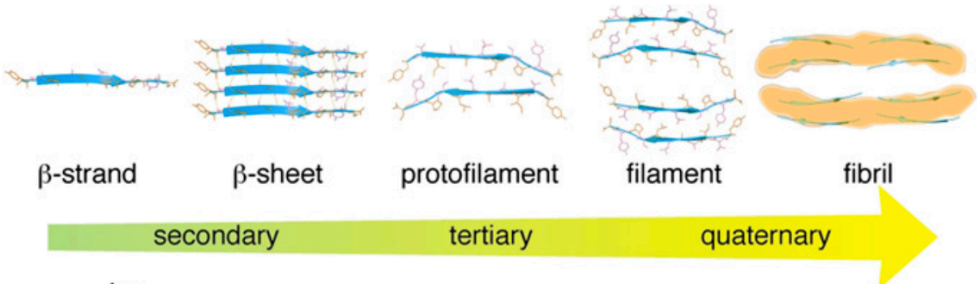

Fig.23 Packing of β-strands in fibril formation.

Hierarchy of the structures (from secondary to quaternary) for Aβ packing intermediates in self-assembly into fibrils (From Fitzpatrick et al., 2013).

Protofibrils are known as the fibril intermediates. They were identified a decade ago and described as beaded chains that have a diameter of 5 nm (Caughey and Lansbury, 2003). The length of those structures is generally under 150 nm. The basic unit of protofibrils is still under debates but lots of experiments suggest that pentameric or hexameric Aβ42 species are the basic units of protofibrils (Ahmed et al., 2010;Bitan and Teplow, 2004). These Aβ assemblies are called "paranuclei" and are likely to self-associate into protofibrils.

Fibrillization involves two separated steps (Roychaudhuri et al., 2009). First, a slow nucleation step produces a "lag phase" during assembly monitoring. This step needs the Aβ monomers to acquire a partially folded conformation and associate to form a paranucleus. Aβ exists as a mixture of many conformers (in its monomeric state) and oligomers. Only the partially folded conformation can lead to paranuclei, the "on-pathway" assemblies that make fibrils. All the other conformers and oligomeric assemblies are "off-pathway", they are not able to start the fibrillization process. After nucleation of monomers, paranuclei engage the fibril nucleation process. Fibril nucleation is unfavorable kinetically, which explains the "lag phase" of fibrillogenesis. During this process, no fibril formation is apparent and the paranuclei self-assemble into protofibrils. This nucleation is followed by a rapid fibril elongation step driving the maturation of protofibrils by a kinetically favorable process (Fig.24).

The conversion of protofibrils to fibrils involves a transition to cross-β-structure, a process called nucleated conformational conversion. Recently it has been demonstrated that the conversion involves association of the short hydrophobic LVFF sequence with the hydrophobic C-terminus of Aβ (Fu et al., 2015).

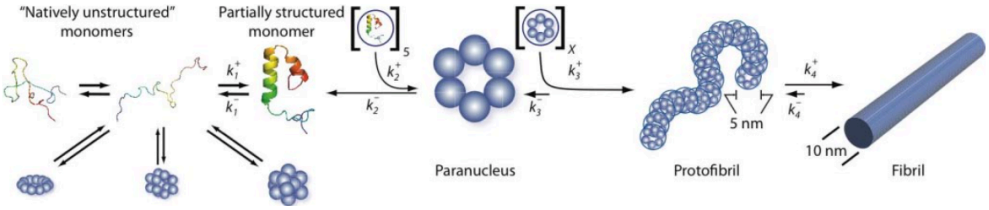

Fig.24 Aβ paranuclei formation, subunits of protofibrils forming fibrils.

Aβ is a "natively disordered" protein, existing in the monomer state as an equilibrium mixture of many conformers. Fibril assembly requires the formation of partially folded monomers able to associate in hexamers to form paranuclei. The paranuclei then self-associate and form protofibrils and further fibrils. All these steps have their proper kinetics (k). Paranucleus formation step is unfavorable kinetically (k2), which explains the lag phase of fibrillogenesis. After this critical step, paranuclei self-associate readily (k3) to form protofibrils. Protofibrils are relatively narrow (5 nm), short and flexible structures. These protofibrils comprise a significant but finite number (X) of paranuclei. Maturation of protofibrils through a kinetically favorable process (k4) yields classical amyloid-type fibrils (10-nm diameter). Other assemblies pathways produce oligomeric structures appearing to be off-pathway assemblies to fibril formation (From Roychaudhuri et al., 2009).

Fu et al. showed that under conditions of high temperatures and concentrations, Aβ and more precisely Aβ42, aggregates into unstructured low-molecular weight (low-MW) oligomers. These low-MW oligomers are able to either directly form fibrils or further stack into high-molecular weight (high-MW) oligomers that also associate in fibrils (Fig.25A). The oligomeric assemblies associate laterally to form protofibrils. During this irreversible phase, the nucleated conformational conversion occurs. It starts with the formation of an anti-parallel β-hairpin structure stabilized by intra-molecular bonds. The last step involves association of the β-hairpins into a cross β-sheet structure that contains parallel and in-register β-strands forming inter-molecular bonds (Fig.25B).

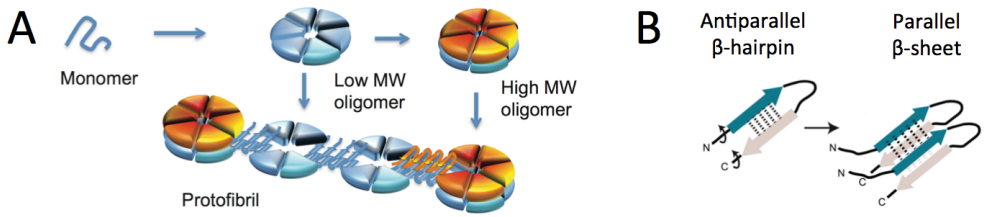

Fig.25 Nucleated conformational conversion and formation of Aβ fibrils)

(A) Unstructured Aβ42 monomers associate in low-molecular weight (low-MW) oligomers that can further combine into high-molecular weight (high-MW) oligomers. Both oligomeric forms are able to associate laterally to form fibrils. (B) Nucleated conformational conversion involves conversion of anti-parallel β-hairpin structure to β-sheet secondary structure. Intra-molecular hydrogen bonding stabilizes the anti-parallel β-strand in the β-hairpin. Rotation of these β-strands allows the formation of inter-molecular hydrogen bonds, which nucleates β-sheet secondary structure (From Fu et al., 2015

Molecular structure of Aβ monomers in the fibril

The structure of the 1-10 residues in the N-terminal part is still under debate. First Aβ was thought to be unstructured until residue 10 for Aβ40 and 17 for Aβ42 (Olofsson et al., 2006;Luhrs et al., 2005;Tycko, 2006). But Ahmed et al. observed contacts between Gln15-Gly37 and His13-Gln15 suggesting that the N-terminal β-strand starts at least at residue 13 showing that in the case of Aβ42 the first 10, rather than 17, N-terminal residues are unstructured (Ahmed et al., 2010) (Fig.26). Residues 11-40 form two β-strand regions fold into a β-strand-turn-β-strand (β-turn-β) conformation. A salt bridge between Asp23 and Lys28 is stabilizing the turn region connecting the β-strands (Finder and Glockshuber, 2007). NMR studies have suggested that the C-terminal β-strand bends at Gly37-Gly38 to allow Ala42 to contact the side chain of Met35 (Ahmed et al., 2010;Masuda et al., 2008).

There are still a lot of differences among all the studies evidencing Aβ fibril structure. They are likely resulting from examination of different peptides (Aβ40 *versus* Aβ42), experimental conditions under which the fibrils were allowed to form, post-translational modifications or oxidation of Met35 side chain. Recently, it has been shown that phosphorylation on Ser26 interferes with formation of the salt bridge between Asp23 and Lys28 (Rezaei-Ghaleh et al., 2014). Furthermore, a strong negative correlation has been shown between oxidative damage and Aβ deposition. Oxidation reduced fibril formation rate and alters fibril morphology (Butterfield, 2003). Indeed, oxidation of Met35 introduces a sulfone group and changes the polarity of Aβ subunits. Although it has no real effect on Aβ40 oligomerization, Aβ42 paranucleus formation was abolished (Bitan and Teplow, 2004;Finder and Glockshuber, 2007). It underlined the complexity of the mechanism involved in misfolding; oligomerization and further nucleation and fibrillization of Aβ.

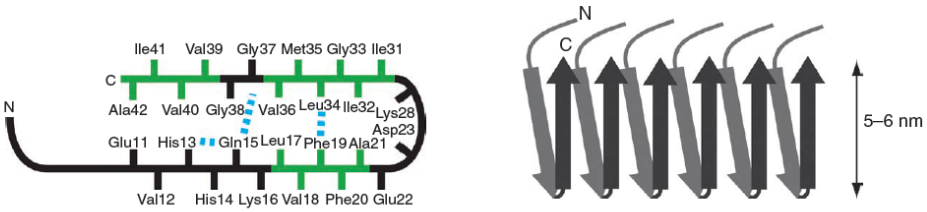

Fig.26 Molecular structure of Aβ monomers and fibrils.

Left scheme: Schematic representation of the hairpin β-strands monomer of Aβ within Aβ42 fibrils. Blue dashed lines represent molecular contacts between amino acids and green residues are implicated in hydrophobic interactions. N-terminal (N) and C-terminal (C) parts are also indicated. Right scheme: Schematic representation of a single protofilament and the parallel and in-register packing and staggering of individual β-strands. Mature fibrils may be formed by the association of two or three protofilaments (From Ahmed et al., 2010).

Role of GXXXG motifs in Aβ fibrils formation

GXXXG motifs within a hydrophobic amino-acid sequence are frequent in peptides with fibrillogenic properties derived from transmembrane α-helices (Liu et al., 2005a). Parallel orientations of individual β-strands within β-sheets together with in-register amino acids make the glycines forming notches and grooves at the surface of the β-sheet. If they face large amino acids side chains forming complementary molecular ridges, they highly stabilize sheet-to-sheet packing. β-sheets containing glycine residues are flattened due to the lack of side chain chirality. They can therefore pack all together to make large assemblies and build fibrils. The association of parallel and in-register β-strands has been observed in Aβ40 as well as in Aβ42 fibrils associated with Alzheimer's disease (Benzinger et al., 1998;Antzutkin et al., 2000;Torok et al., 2002).

Interestingly, glycine rich sequences are found in fibrillogenic regions of several proteins involved in human degenerative diseases like the Prion protein or alpha-synuclein (Fig.27). The Prion protein (PrP) is involved in the transmissible spongiform encephalopathy. This protein possesses three GXXXG motifs in an α-helical structure (Hegde et al., 1998). In the disease, the PrP adopt a pathogenic alternative folding called « scrapie » (PrP_{sc}) that converts from α-helical to β-strand structure, forming insoluble plaques in the brain (Cohen and Prusiner, 1998). A third neurodegenerative disease is Parkinson disease. It involves the α-synuclein protein, which also have a GXXXG-like motif (GXXXA) and form fibrils with β-sheet secondary structures (Kessler et al., 2003). Aβ possess three in-register GXXXG motifs. In fibrils, the first GXXXG motif is contained in a sequence of polar amino acid and is thought to be part of a β-hairpin structure. The two others are part of a long hydrophobic sequence and are therefore part of the extended β-sheet structure.

Aβ (20-42)

$F^{20}AEDVGSNKGAIIGLMVGGVVIA^{42}$

Prion (113-135)

$A^{113}GAAAAGAVVGGLGGYMLGSAMS^{135}$

α-synuclein (60-85)

$K^{60}EQVTSVGGAVVTGVTAVAQKTVEGA^{85}$

Fig.27 Aβ sequence homologies with proteins involved in neurodegenerative diseases.

GXXXG (red) and GXXXA (yellow) motifs comprises in the sequences of Aβ, the prion protein and α-synuclein (Modified from Sato et al., 2006).

Packing of Aβ peptides in fibrils involves contact of glycines from different GXXXG motifs with side chain of methionine 35 (Sato et al., 2006). When APP is cleaved, Aβ 40 and 42 are no longer stable as α-helices in the membrane. They adopt a new secondary hairpin conformation stabilized by the GXXXG motifs and then pack with other subunits to form amyloid fibrils.

Differences between Aβ 40 and 42 in fibrils

Under physiological conditions, Aβ40 is the major isoform produced in the cells. In Alzheimer's disease, the 42-residues isoform is predominant in neuritic plaques (Roher et al., 1993). The question of how a two amino-acids difference can have such a dramatic impact on toxicity and related structural properties has not been answered so far. It has been shown that Aβ42 has a higher ability to form aggregates than Aβ40 (Jarrett et al., 1993;Burdick et al., 1992). Aβ42 can in particular more easily form pentameric or hexameric paranuclei that could be the constituent of protofibrils (Bitan et al., 2003a;Bitan et al., 2003b). Aβ40 would rather associate in tetramers that eventually form fibrils, without forming paranuclei (Fig.28) (Bernstein et al., 2009). Mutation of Aβ42 two last amino acids disrupted its structure and reduces toxicity (Morimoto et al., 2004). But proline-scanning mutagenesis of Aβ40 showed no striking importance of C-terminal residues for the fibrillization process (Williams et al., 2006).

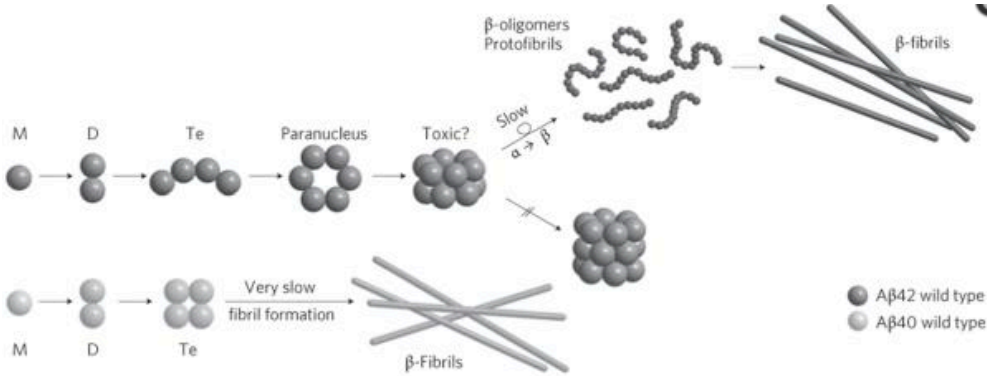

Fig.28 Model proposed by Bernstein et al. for the mechanisms regulating oligomerization and fibril formation for Aβ42 and Aβ40.

For Aβ40 (lower scheme) the key structure is tetrameric, it resists to further subunits addition. The tetramers could maybe form fibrils in very slow kinetics. In Aβ42 (upper scheme), an 'open' tetramer structure promotes the formation of planar hexamers (paranuclei) and stacked dodecamers. Then a slow transformation from α- to β-sheet may occur for the dodecamer. In a β-sheet conformation, Aβ42 dodecamers rapidly associate in protofibrils and fibrils (Bernstein et al., 2009).

Sato et al. have shown that these 2 amino acids can dramatically change fibril stabilization. They are intimately involved in subunit-subunit fibril interface as they increase hydrophobic interface between Aβ protofilaments. Moreover, although they have both parallel β-strand orientation and in-register amino acids, Aβ 40 and 42 have two different protofibril structures. Aβ40 can form protofibrils, involving alignment of Met35 with Gly33 (Sato et al., 2006). In Aβ42 protofibrils, Met35 forms contact with Gly37 and sheet-to-sheet packing between protofilament subunits is displaced by one groove in the surface (Brunelle and Rauk, 2002). This conformation strengthens amyloid fibrils packing and toxicity (Fig.29). Aβ40 assemblies are more compact than Aβ42's, due to increased conformational freedom of the Aβ42 N-terminal part. This suggests also that intermolecular interactions in Aβ42 N-ter facilitate the interactions that are mandatory for fibril formation (Urbanc et al., 2004).

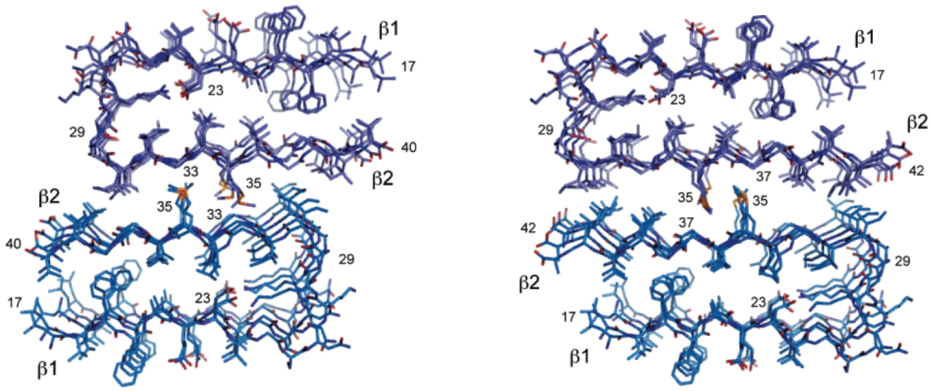

Fig.29 (A) Aβ40 fibrils **(B) Aβ42 fibrils**

Structural model proposed by Sato et al. of the Aβ fibril (only residues 17 to 40 of Aβ monomers). The protofilament subunits were docked with opposite orientations to satisfy structural and minimal energy constraints with standard methods. (A) Aβ40 fibrils. The solid-state NMR depicted contacts between Met35 and Gly33. (B) Aβ42 fibrils. Solid-state NMR depicted contacts between Met35 and Gly37 (Sato et al., 2006).

From fibrils to oligomers hypothesis in AD

Fibrils were initially considered as prime candidates to trigger neurodegeneration in Alzheimer's disease. But rapidly, a fly in the ointment appeared. More and more evidence showed that there was a poor correlation between the amounts and distribution of fibrils and the clinical status of Alzheimer's disease patients (Terry et al., 1991). If one study suggested that APP FAD transgenic mice develop the typical neuritic plaques together with neuronal loss, two other studies showed no significant loss despite extensive Aβ deposits (Irizarry et al., 2001b;Irizarry et al., 1997). Conjointly, seminal studies described transgenic mice already displaying neurological deficits prior to fibril plaques formation (Hsia et al., 1999;Mucke et al., 2000). Some authors suggested that fibrils could even be neuroprotective (Castellani et al., 2009). In all these cases and despite all information setting Aβ as first actor in the pathogenesis of AD, there is still a lack of evidence that fibrillar species trigger the disease.

At the same time, it became clear that Aβ assemblies were a more complex process. The relationship between soluble oligomers and fibrils has remained elusive. Fu et al. showed that low-MW and high-MW oligomers are both able to associate into fibrils (Fu et al., 2015). Some studies suggested that oligomers result from several aggregation events that are either « on-pathway » or « off-pathway » for fibril formation, and that these 2 come from independent pathways (Schnabel, 2011). Non-fibrillar oligomeric species were discovered, their concentration rather than fibril load correlated precisely with functional deficits in Alzheimer's disease (Lesne et al., 2006;Chen et al., 2011).

3.3 Aβ oligomers

History and properties

In APP transgenic mice, there is strong evidence for the responsibility of Aβ in age-related cognitive decline (Westerman et al., 2002;Janus et al., 2000). The role of Aβ in cognitive impairment is complex and could not be explained by fibrils. Soluble Aβ assemblies were identified in these transgenic mice corresponding with the timescale for memory decline (Lesne et al., 2006). These Aβ species disrupted memory upon administration to young rats. They were coined Aβ*56 for their 56 kDa molecular weight. In the meantime, more and more studies highlighted different Aβ oligomeric species, each disturbing neurotransmission and triggering cell death *in vitro* and *in vivo* (Lambert et al., 1998;Walsh et al., 2002). Several groups extracted soluble Aβ oligomers from patients' brains. They were intimately correlated to disease's symptoms (McDonald et al., 2010). Moreover, several APP FAD mutations increased the tendency of mutated Aβ to oligomerize (Nilsberth et al., 2001;Tomiyama et al., 2008). These oligomers range from dimers to dodecamers and higher molecular weight oligomers.

There is nevertheless no strong agreement on which oligomeric form is the most relevant for the pathology (Benilova et al., 2012). Interestingly, almost all Aβ oligomeric species showed neurotoxicity and disruption of synaptic plasticity, either by inhibition of long-term potentiation (LTP) or facilitation of long-term depression (LTD). Synthetic oligomers have been shown to alter LTP *in vitro* (Lambert et al., 1998). Afterwards, injection of purified endogenous oligomers in rats triggered similar effects (Walsh et al., 2002). Long-term depression (LTD) is enhanced upon accumulation of oligomers in the hippocampus CA1 region of mouse brain slices (Li et al., 2009). Same dimeric and trimeric Aβ species also affected behavioral tasks in rats (Cleary et al., 2005). Mechanisms are still not

known but Aβ oligomers-mediated alteration of LTP/LTD could be related to a plenty of cellular responses. Suggested mechanisms are activation of neurotransmitter receptors mGluR or NMDAR (Li et al., 2009), cellular pathways involving calcineurin (Wu et al., 2010), caspase-3 and GSK3β (Jo et al., 2011) or even action on Tau proteins (Li et al., 2009). Subtle alterations of synaptic activity associated with the early cognition problems faced by people with Alzheimer's disease. Finally, oligomeric Aβ were shown numerous times to interact directly with phospholipid bilayers. Aβ oligomers were reported to insert in cellular membranes and form β-barrels or cation channels to dysregulate calcium levels and mitochondrial function (Arispe et al., 2007;Arispe et al., 1993;Caughey and Lansbury, 2003;Laganowsky et al., 2012).

Different types of oligomeric species

In the brain, Aβ can be present as a mix of different oligomeric forms. Assignments are complex but there are two kinds of commonly used classifications. Oligomers can be separated in two groups: *ex vivo* and *in vitro* oligomers. There are several *ex vivo* brain-derived oligomeric species, the most relevant being the Aβ dimers/trimers, Aβ*56 (Lesne et al., 2006;Shankar et al., 2009) and amylospheroids (Hoshi et al., 2003). The other described oligomeric forms were aggregated *in vitro*, the most widely studied being ADDLs (Lambert et al., 1998), globulomers (Barghorn et al., 2005) and annular protofibrils (Lashuel et al., 2002a). Oligomers can also be separated according to their structure. Conformation-dependent antibodies were developed. They specifically distinguish amyloid fibrils and prefibrillar oligomers. These antibodies bind general epitopes associated with specific aggregation states, regardless of the amino acids sequence. A11 antibody recognizes prefibrillar oligomers. They are soluble oligomers that did not display any fibrillar structure (Glabe, 2008). On the opposite, the OC antibody recognizes specifically fibrils and fibrillar structured oligomers (fibrillar oligomers). Aβ soluble assemblies can therefore be classified in two other groups: fibrillar oligomers (OC+/A11-) and prefibrillar oligomers (A11+/OC-).

1. *Dimers and trimers*

   These low molecular weight species were discovered from brain extracts fractionation by non-denaturating size exclusion chromatography and correlated well with synaptotoxicity (Shankar et al., 2009). They were described as the minimal toxic species *in vivo* but a grey zone remained as whether the toxicity was directly caused by the dimers themselves

(Benilova et al., 2012). The conformation of these species is not clear yet but the A11 antibody did not recognize them. Despite, they were shown to rapidly aggregate into stable fibrils (O'Nuallain et al., 2010).

2. *Aβ*56*

   These assemblies have an apparent molecular weight of 56 kDa corresponding to dodecamers. They were found in transgenic mice and patient brains, where they correlated with cognitive decline (Lesne et al., 2006). They are prefibrillar assemblies recognized by the A11 antibody. An important point to note is that detergents used in the extraction buffer (SDS) could promote non-physiological aggregation (Bitan et al., 2005). Whether these oligomers form as such *in vivo* has thus to be firmly established. Aβ*56 induced concentration-dependent cognitive impairment whereas trimers from Tg2576 mouse brain did not (Reed et al., 2011).

3. *Amylospheroids (ASPDs)*

   Larger Aβ structures have been isolated from AD brain tissue. They are highly toxic spherical Aβ assemblies of 10-15 nm (Noguchi et al., 2009;Matsumura et al., 2011). Interestingly, they were not recognized by the A11 antibody and were described to be a parallel off-pathway to fibrils (Lacor et al., 2007;Matsumura et al., 2011). Studies revealed that the most toxic ASPDs must be 128 kDa 32-mers. Their concentration correlated with the pathological severity of AD (Noguchi et al., 2009). They showed high toxicity and activated tau protein kinase I/GSK3β (Hoshi et al., 2003).

4. *ADDLs*

Amyloid-β derived diffusible ligands (ADDLs) are assemblies ranging from trimers, tetramers to dodecamers (Lambert et al., 2001). They are formed *in vitro* by 24 hours incubation of synthetic Aβ42 in culture medium (Lambert et al., 1998). They are A11 positive and were described off-pathway, classified with prefibrillar oligomers. They are formed at low doses, inhibited LTP and specifically fixed neurons synaptic terminals (Lacor et al., 2004;Wang et al., 2004). Similar oligomers were found in cerebrospinal fluid and AD brain, showing equivalent properties to synthetic oligomers (Georganopoulou et al., 2005;Gong et al., 2003). They showed the ability to attach dendritic surfaces in small clusters with ligand-like specificity (Gong et al., 2003).

5. *Globulomers*

These assemblies are highly stable dodecamers, the synthetic counterpart of Aβ*56. They were formed *in vitro* after dilution and incubation in specific solvents containing SDS or fatty acids (Barghorn et al., 2005). Globulomers migrate at 38-48 kDa on SDS gels. They were shown to alter synaptic activity by inhibition of calcium current through binding to neurons in an age-dependent fashion (Nimmrich et al., 2008). Finally they were detected in AD brains and demonstrated off-pathway by specific antibodies (Barghorn et al., 2005;Gellermann et al., 2008).

6. *Annular protofibrils (APFs)*

They are composed by hexamers (maybe paranuclei). APFs are stable, A11 positives and generated in a completely independent pathway from Aβ fibril formation (off-pathway) (Lasagna-Reeves et al., 2011;Kayed et al., 2009). During *in vitro* incubation, Aβ starts forming oligomers at early times. After a while, it forms protofibrils and ring-shaped pore-like

structures referred as the annular protofibrils (Lashuel et al., 2002b). They were formed by circularization of prefibrillar oligomeric species. APFs were consistent with similar species observed in many amyloid diseases although their proper contribution to pathogenesis was not clear (Lashuel and Lansbury, Jr., 2006). They were also proposed to act like β-barrel pore-forming toxins that permeabilize membranes (The amyloid pore hypothesis). Recently they were described in human brain tissues (Lasagna-Reeves et al., 2011). This have been supported by the model from Shafrir et al. describing a 155 kDa 36-stranded β-barrel forming transmembrane cation-selective channel (Shafrir et al., 2010).

It is important to consider whether the oligomers formed *in vitro* are relevant to the pathology. *In vitro* assemblies do not produce homogenous preparations but rather mixtures of different oligomeric species in equilibrium (Hayden and Teplow, 2013). Moreover, synthetic oligomers did not show the same potency than physiologically produced oligomers (Finder, 2010), they only caused toxicity at much higher levels. Aβ oligomers may structure and assemble differently in cellular environments than in solution and maybe undergo further post-translational modifications. However, the asset of studying synthetic oligomers is their purity. The consequent effects are directly attributable to the oligomers described and not to contaminating factors present in the cellular, tissue or body fluids samples.

To conclude, we would like to point out the attention to the fact that intriguingly, lots of Aβ assemblies described to date are hexamers or multiples (Aβ*56, ADDLs, globulomers…) (Fig.30). The idea of an hexamer building block or paranucleus becomes more and more relevant in Aβ oligomerization during the pathogenesis of Alzheimer's disease (Bernstein et al., 2009;Bitan et al., 2003b;Roychaudhuri et al., 2009). Moreover, FAD mutations including the Flemish mutation (A21G) were

shown to favor hexameric and dodecameric species (Gessel et al., 2012). It appeared to be a real correlation between hexamers distribution and the disease.

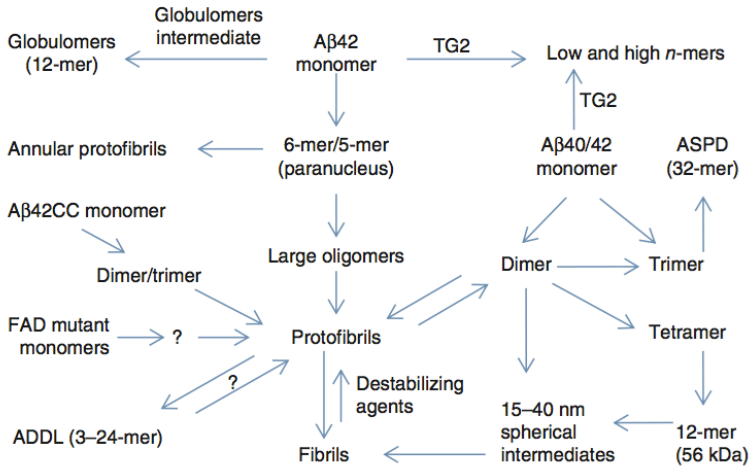

Fig.30 Scheme of interconversion between different cellular or synthetic Aβ oligomers.

All the different Aβ species exist in a complex equilibrium, influenced by environmental factors. They can coexist in the brain. Despite their different structure, stability and concentration, they may contribute to the pathogenicity of AD (From Benilova and De Strooper, 2012).

Molecular structure of Aβ oligomers

Structural heterogeneity of Aβ oligomers has been a major hindrance to obtain high-resolution structural data and establish precisely their molecular structure. Some Aβ oligomers display the same parallel in-register β-sheets than the fibrils. Other oligomeric forms adopt distinct structures (Cerf et al., 2009;Ahmed et al., 2010;Morgado et al., 2012;Stroud et al., 2012;Eckert et al., 2008).

The most relevant model for molecular structure of prefibrillar oligomers up to date is the triple-strand model, characterized by Gu et al. in 2014 (Fig.31) (Gu et al., 2014). The model depicted prefibrillar oligomers with β-sheet structures containing 3 β-strands in an antiparallel arrangement. The β-strands are described on residues 1-9, 13–23 and 28–42 with 2 turn regions connecting them (Ma and Nussinov, 2011;Gu et al., 2014). This triple-strand antiparallel model converts to fibrils by reorganization of its structure into fibril β-sheets by a nucleated conformational conversion named « strand rotation ». β-strands undergo a 90° rotation along the strand direction to form parallel in-register β-sheets.

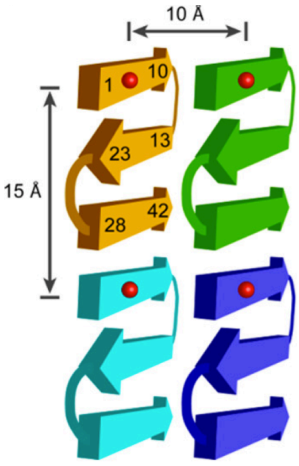

Fig.31 Triple-strand model of prefibrillar Aβ42 oligomers.

Scheme illustrating the triple-stand model of oligomers. Each Aβ42 subunit consists of three β-strands interacting through backbone hydrogen bonds. The numbers represent residue positions and red balls represent spin labels used to probe the side chain mobility (Gu et al., 2014).

GXXXG motifs in Aβ oligomerization

For oligomerization, GXXXG motifs have a packing mode distinct from symmetrical α-helices dimerization of transmembrane proteins like the Glycophorin A (MacKenzie et al., 1997). GXXXG motifs implicated in oligomerization are called glycine zipper motifs. In glycine zipper packing, the motif packs against a different face of the associate helix. These motifs have been found in a lot of homooligomeric channel proteins and are strongly conserved between species (Kim and Sisodia, 2005). In human diseases, one of these proteins is the well-known VacA toxin from Helicobacter Pylori, the agent causing almost all stomach ulcers (Covacci et al., 1999). Mutation of the glycines involved in the zipper motif abolished channel activity of the toxin (McClain et al., 2003). In Aβ peptide, such motifs have a critical impact on aggregation, helping β-sheets packing and eventually formation of fibrils in solution (Liu et al., 2005b;Sato et al., 2006). In cellular membranes, the presence of glycine zipper motifs was suggested to mediate α-helices packing and homo-oligomerization of channel proteins, ranging from tetrameric to hexameric complexes (Kim and Hecht, 2006;McClain et al., 2003;Cross et al., 2001;Shapiro et al., 1996). To support the idea that glycine zipper motif drives the formation of Aβ oligomers, synthetic Aβ containing gly-to-leu mutations were used in vitro (Kim and Sisodia, 2005;Hung et al., 2008). They showed a reduction of toxicity compared to WT peptides. This reduced toxicity correlated with reduction of small oligomeric species and increased rates of fibril formation in solution (Hung et al., 2008). Harmeier et al. highlighted the G33 residue as critical for Aβ42 assembly (Harmeier et al., 2009). Its mutation in Aβ promoted rapid oligomerization through conformational changes favoring high molecular weight oligomers. The synthetic G33L peptide was unable to impair LTP in hippocampal slices. In contrast, Aβ G37L was less toxic after endogenous expression did not show any detectable amyloid *in vivo* (Fonte et al., 2011).

Differences between Aβ 40 and 42 oligomers

Structure and composition of Aβ42 oligomers are markedly different from Aβ40 assemblies (Ahmed et al., 2010), although it is still matter of debates. A first hypothesis is that Aβ40 oligomers are large spherical aggregates containing β-sheets that rapidly convert to protofibrils and fibrils. This may reflect the lower toxic effects observed with Aβ40. Indeed, if Aβ40 have parallel and in-register β-sheet structures in both oligomers and fibrils (Chimon et al., 2007), it is not the case for Aβ42 oligomers. They were shown to form β-sheet secondary structures in fibrils but not in oligomers (Ahmed et al., 2010).

Another study using ion motility coupled to mass spectrometry revealed differences in primary oligomers formed by Aβ 40 and 42. Aβ40 rather formed tetramers whereas Aβ42 formed hexamers and dodecamers (Bernstein et al., 2009). Moreover, FAD mutations in Aβ40 gave rise to high order oligomers, ranging from hexamers to dodecamers (Gessel et al., 2012). Similarly, mutation of Glu22 and Asp23 are able to make Aβ40 producing higher order assemblies without affecting Aβ42 oligomers (Grant et al., 2007).

CHAPTER II: Aim of the thesis

The amyloid β peptide is one of the key players in Alzheimer's disease. Increase in Aβ production or aggregation are key features in the pathogenesis. APP amyloidogenic processing has been widely studied to understand these phenomena. This work focuses on two features that are critical in the disease process: Aβ production and its toxic aggregation.

Several studies have suggested that dimerization of APP is closely linked to Aβ production. APP mutations responsible for inherited AD cases are mainly clustered in the JM/TM regions at the α-, β- and γ-cleavage sites. Each of them modulates APP processing differently and the precise mechanisms behind their effects on amyloidogenesis are not known. Understanding these mechanisms represent a fundamental challenge in Alzheimer research. APP has been shown to dimerize in living cells and dimerization is thought to regulate its amyloidogenic processing. Association of the ectodomain and/or TMD is supposed to mediate APP dimerization.

The **first aim** of this work was to decipher APP homodimerization with a novel sensitive method and unravel the involvement of its three major domains: the ectodomain, the transmembrane domain (TMD) and the intracellular domain. We also addressed the role of both familial and non-familial AD mutations of the GXXXG motifs in APP TMD dimerization and processing. The results are described in the first paper.

We also collaborated to the work of Steven O. Smith and colleagues bringing new insights on the extracellular structure of APP CTFs and the impact of structural determinants on processing. This led to the submission/publication of two papers. The first one was aimed at studying the impact of the Flemish A21G mutation on

CTFs structure and Aβ production. The second one was aimed at scanning the determinants of the C99 extracellular region and their impact on cleavage by the γ-secretase. The data obtained identified the influence of the LVFFA motif, critical determinant in the processing of amyloidogenic C-terminal fragments by formation of a β-sheet structure. We contributed to these works by analyzing the amyloidogenic processing of the different mutants generated.

Since a decade, there is a growing body of evidence that soluble Aβ oligomers precisely correlate with the clinical features and symptoms associated with AD. The Aβ sequence is present in the TM region of APP, containing the $G^{25}XXXG^{33}$ and $G^{38}XXXA^{42}$ motifs. They can be critical for both TM protein interactions and fibrillogenic properties of peptides derived from TM α-helices. We discovered a highly stable assembly of Aβ42. They are formed in cellular membrane-bound compartments, and can be generated by direct expression of Aβ42, but not Aβ40. The **second aim** of the thesis was to characterize the role of the TM $G^{25}XXXG^{33}$ and $G^{38}XXXA^{42}$ motifs in the formation of Aβ assemblies by introducing point mutations. We also measured the effect of such soluble oligomeric species on neuronal maturation and differentiation. The results of this study are represented in a fourth paper.

CHAPTER III: Results

1. APP dimerization and Aβ production: GXXXG motifs and structural determinants

1.1 Analysis of the regions involved in APP dimerization and its impact on processing

In this study, we focused on the regions involved in full-length APP dimerization and the controversial role of the GXXXG motifs. APP dimerization has already been studied but the precise role of the different domains and the link with Aβ production are still controversial. We analyzed the role of the ectodomain previously suggested to mediate APP dimerization, the transmembrane domain containing the well-known GXXXG dimerization motifs, and exclusively the intracellular domain.

To clearly define the role of the different domains in dimerization, we used a novel approach: the split-luciferase. This approach allows a sensitive detection of proteins dimerization in living cells. APP is fused to the N- or C-terminal part of the Gaussia luciferase enzyme. Association of the two constructs reconstitutes the enzyme, giving a strong luminescent signal upon addition of its substrate.

To study the involvement of the ectodomain in dimerization, we built constructs expressing full-length APP and truncated forms representing APP cleaved by the β-secretase (C99) or α-secretase (C83). By site-directed mutagenesis, we constructed two mutants affecting the role of the transmembrane GXXXG motifs. The first construct contains the FAD Flemish (Fle) mutation (A617G, APP695 numbering) known to dramatically increase Aβ production. The second mutant is

called mut5 and disrupts the central GXXXG motif by replacement with leucine residues (GG625/629LL). Ectodomain's involvement was studied using APP constructs lacking the intracellular domain (APPΔC).

Comparison between the C-terminal fragments C99 and C83 with full-length APP showed a strong reduction of dimerization upon removal of the ectodomain, confirming its implication in the association. Despite the drastic increase (Fle) and decrease (m5) in processing observed with the GXXXG mutants, we could not measure such differences in terms of C-terminal fragments dimerization. Finally, we found a drastic increase in APP dimerization and α-secretase cleavage when the intracellular domain is removed (APPΔC). For the first time, we showed that APP intracellular domain has a strong role in dimerization and that full-length APP dimerization can regulate the non-amyloidogenic processing.

This work has been published in the following paper.

Analysis by a highly sensitive split luciferase assay of the regions involved in APP dimerization and its impact on processing

Marie Decock[a], Laetitia El Haylani[a], Serena Stanga[a], Ilse Dewachter[a], Jean-Noël Octave[a], Steven O. Smith[b], Stefan N. Constantinescu[c], Pascal Kienlen-Campard[a,*]

[a]Institute of Neuroscience, Université catholique de Louvain, Brussels 1200, Belgium
[b]Department of Biochemistry and Cell Biology, Stony Brook University, Stony Brook, NY 11794-5215, USA
[c]Ludwig Institute for Cancer Research and Université catholique de Louvain, de Duve Institute, Brussels 1200, Belgium

Running title: *Evaluating APP dimerization using a split luciferase assay*

Published in FEBS Open Bio. 2015 Sep 6;5:763-73.

doi: 10.1016/j.fob.2015.09.002.

*Correspondance to:

Pascal Kienlen-Campard

Université catholique de Louvain

Institute of Neuroscience IoNS/CEMO

Avenue Mounier 53 box B1.53.02

B-1200 Brussels BelgiumPhone.: +32 2 764 93 35 Fax: +32 2 764 54 60

E-mail: pascal.kienlen-campard@uclouvain.be

ABSTRACT

Alzheimer's disease (AD) is a neurodegenerative disease that causes progressive loss of cognitive functions, leading to dementia. Two types of lesions are found in AD brains: neurofibrillary tangles and senile plaques. The latter are mainly composed by the β-amyloid peptide (Aβ) generated by amyloidogenic processing of the amyloid precursor protein (APP). Several studies have suggested that dimerization of APP is closely linked to Aβ production. Nevertheless, the mechanisms controlling APP dimerization and their role in APP function are not known. Here we used a new luciferase complementation assay to analyze APP dimerization and unravel the involvement of its three major domains: the ectodomain, the transmembrane domain and the intracellular domain. Our results indicate that within cells full-length APP dimerizes more than its α and β C-terminal fragments, confirming the pivotal role of the ectodomain in this process. Dimerization of the APP transmembrane (TM) domain has been reported to regulate processing at the γ-cleavage site. We show that both non-familial and familial AD mutations in the TM GXXXG motifs strongly modulate Aβ production, but do not consistently change dimerization of the C-terminal fragments. Finally, we found for the first time that removal of intracellular domain strongly increases APP dimerization. Increased APP dimerization is linked to increased non-amyloidogenic processing.

Keywords: Alzheimer's disease, APP, Dimerization, GXXXG motifs, Amyloid beta peptide, Split luciferase

INTRODUCTION

The amyloid precursor protein (APP) is a ubiquitously expressed type 1 transmembrane protein [1,2]. APP undergoes proteolysis via two distinct pathways known as the amyloidogenic and the non-amyloidogenic pathways. APP processing is initiated by the shedding of the large ectodomain by either an α-secretase (non-amyloidogenic pathway) or the β-secretase BACE1 (amyloidogenic pathway). APP β-cleavage generates a membrane-anchored β C-terminal fragment (βCTF or C99), which is further cleaved by the c-secretase complex to generate the Aβ peptides. The 40 and 42 amino acids Aβ isoforms (Aβ40 and Aβ42, respectively) are the major constituents of the senile plaques, a typical lesion found in the brain of patients with Alzheimer's disease (AD) [4]. Mutations responsible for inherited or familial AD cases (FAD) are located in the APP or presenilin genes (PS1 and PS2). The presenilin proteins are the catalytic subunits of the γ-secretase. AD mutations typically result in an increased Aβ42/Aβ40 ratio [2]. Imbalanced production of Aβ, along with its aggregation and accumulation in the brain, may therefore play a critical role in the onset and progression of AD [5].

Although Aβ involvement in the pathology has been extensively studied over the past decades, our knowledge of the physiological function of APP and the cellular mechanism regulating its processing remain remarkably incomplete. APP belongs with its two paralogs APLP1 and APLP2 to the APP-like protein family. Unique features in each member of the family could account for its specialized and specific function [6]. Ten APP isoforms generated by alternative splicing of the APP transcript have been identified [3]. The major ones (APP695, APP751 and APP770) differ in their extracellular domain by a Kunitz-type protease inhibitor

(KPI) domain present in non-neuronal isoforms (APP751 and APP770), but absent in the neuronal one (APP695).

APP has been proposed to mediate dendritic spine arrangement, neural cell migration and synapse formation, including neuromuscular junctions formation [7] that could underlie the neuromuscular phenotype observed in APP knock-out mice [8]. The possible physiological role of APP can be related to its structural properties. APP resembles a transmembrane receptor with an extracellular region displaying features of a cell surface receptor or an adhesion molecule [9,10]. These different functional regions include copper binding and growth factor-like domains and are required for homo- and heterophilic interactions [11,12]. For instance, APP has been shown to interact with Notch [11,13], another major γ-secretase substrate, and even with the Aβ peptide generated by its processing [14]. APP dimerization is therefore likely to play a pivotal role in its processing and function. Recent studies have indicated that APP dimerization involves both the E1 and KPI regions of the ectodomain [11,15–17] and GXXXG motifs of the transmembrane (TM) domain [18,19]. GXXXG motifs are structural determinants favoring close apposition of TM helices and formation of TM dimers [20,21,38]. The TM region of APP contains three consecutive GXXXG motifs. The FAD A21G mutation (Aβ numbering) known as the Flemish mutation [24] extends the GXXXG interface by adding a fourth GXXXG motif and triggers Aβ production. This strongly suggests that TM interactions are involved in pathophysiological processing of APP [19,23,25,26,33]. It is of particular interest to clearly establish the relation between APP dimerization and its processing, especially its cleavage at the γ site. Studies on APP dimerization have largely been carried out using bio-chemical approaches (crosslinking, co-immunoprecipitation) [27] focused on TM domain interactions in reconstituted micelles or membrane bilayers [22] or have used purified peptides for structural approaches [27–30]. Very few studies have

addressed APP dimerization in living cells. Although split fluorescent proteins assays [13,31,32] have revealed a positive role of the KPI domain in APP dimerization, the role of TM dimerization has appeared much more controversial. It has even been suggested that the TM domain plays only a marginal role in full-length APP dimerization [9,27].

Indeed, the extent of APP and CTFs dimerization in living cells is poorly known. There is no information about the respective contribution of its 3 major domains, and especially of its intracellular domain in this process. The link between APP dimerization and processing is controversial [27,36]. Here we use a new dynamic and highly sensitive split protein assay, the split luciferase assay [37] to define the role and the contribution of the different APP regions to dimerization and clarify the correlation between its dimerization and processing. Our major findings are that full-length APP forms more dimers than APP β and αCTFs. Mutations in the GXXXG motifs, including FAD mutants (Flemish), do not consistently alter dimerization. Strikingly, deletion of intracellular domain strongly favors dimerization. Finally, we found that the extent of dimerization is not correlated to Aβ production, but that increased dimerization observed with APP lacking its intracellular region is linked to increased non-amyloidogenic processing.

MATERIAL AND METHODS

Chemicals and reagents

Restriction enzymes, Taq DNA polymerase, all culture media, penicillin-streptomycin solution and Lipofectamine® transfection reagent, Nu-Page® Novex® 4–12% Bis-Tris gels and buffers were from Life Technology Corporation (Carlsbad, CA). Fetal bovine serum (FBS) for culture media was purchased from Thermo Scien- tific (Rockford, IL). Transfection reagent Trans-IT2020 was from Mirus Bio Corporation (Madison, WI). Analytical grade solvents, salts and poly-L-lysine were from Sigma-Aldrich (St Louis, MO). N-[N-(3,5-difluorophenacetyl)-L-alanyl]-S-phenylglycine-butyl ester (DAPT) was from Calbiochem (Camarillo, CA). Protease inhibitor cocktail was purchased from Roche (Basel, Switzerland). BCA protein assay kit was from Pierce (Rockford, IL, USA). Nitrocellulose membranes were obtained from GE Healthcare (Fairfield, CT). ECL reagents were obtained from Perkin Elmer Inc. (Waltham, MA). Gaussia luciferase substrate Coelenterazine native was purchased from Prolume® Ltd. (Pinetop, AZ). The luciferase cell lysis buffer was from New England Biolabs (Ipswich, MA). The following primary antibodies were used: anti-amyloid β antibody, clone W0-2 (EMD Millipore, Billerica, MA), anti-amyloid precursor protein, C-terminal antibody (Sigma-Aldrich, St Louis, MO), anti-GLuc antibody (New England Biolabs, Ipswich, MA). Fluorescent nucleic acid stain DAPI was obtained from Sigma–Aldrich (St Louis, MO). Secondary antibodies coupled to HRP were obtained from Amersham Bioscience (Uppsala, Sweden) and fluorescent secondary antibodies coupled to Alexa fluorochromes were from Life Technology Corporation (Carlsbad, CA).

Fluorescent mounting medium was from DAKO (Agilent Technologies, Santa Clara, CA, USA).

Cells lines and cell culture

Chinese hamster ovary (CHO) cell lines were grown in Ham's F-12 medium. The medium was supplemented with 10% of fetal bovine serum (FBS) and penicillin–streptomycin solution (10 units-10 µg). All cell cultures were maintained at 37°C in a humidified atmosphere (5% CO2).

Plasmids, site-directed mutagenesis and cloning

GCN4 leucine zipper split-luciferase constructs Zip-hGLuc1 and Zip-hGLuc2 in pcDNA3.1 vectors were obtained from the group of S.W. Michnick [37]. All the constructs expressing APP and APP fragments fused to humanized Gaussia luciferase (hGluc) halves. They were obtained by PCR amplification of APP sequences encoded by expression vectors previously described [19] with forward and reverse primers harboring the NotI and ClaI restriction sites, respectively. PCR products were digested and further inserted in the NotI/ClaI restrictions sites of the Zip-hGLuc1 and Zip-hGLuc2 constructs, removing the GCN4 leucine zipper sequence of the backbone. All constructs were verified by full sequencing (Macrogen Europe, Amsterdam, The Netherlands). C83 mutants were obtained by Quick-change site-specific mutagenesis (Stratagene, La Jolla, CA) as previously described [31].

Cell transfection and treatment

CHO cells were transfected with Lipofectamin reagent 24 h after seeding following manufacturer's instructions. Plasmids expressing the split-luciferase proteins were cotransfected in a 1:1 ratio. The control plasmid (Mock) was the corresponding empty vector. MEF cells (PS+/+ and PS-/-) were transfected using Trans-IT2020 according to the manufacturer's instructions. CHO cells were treated with DAPT for 15 h at a final concentration of 1 µM. 48 h after transfection, medium was collected, treated with protease inhibitors cocktail (Roche) and stored at 20°C for ECLIA assay. Cells were harvested and lysed in Luciferase Cell Lysis Buffer (New England Biolab) and pelleted by quick centrifugation at 4°C for 1 min. Protein concentrations of cell lysates were measured by the BCA protein assay kit (Pierce). Cell lysates were further used for Gaussia luciferase assay and Western blotting. Samples were aliquoted in 5ml polystyrene round-bottom tubes at a final concentration of 10 µg of proteins in 20 µl in Luciferase Cell Lysis Buffer. Native coelenterazine was reconstituted as a stock solution of 1 mg/ml in methanol (stored frozen), diluted 30 min prior reading in DMEM without phenol red and used at a final concentration of 20 µM. 50 µl of coelenterazine was added to tubes and luminescence directly measured on a Sirius Luminometer (Berthold, Pforzheim, Germany).

Western blotting

Ten µg of protein of cell lysates were heated for 10 min at 70°C in loading buffer (Luciferase Cell Lysis Buffer with 0.5 M DTT and staining Nupage blueTM), loaded and separated onto 4–12% NupageTM bis-Tris gel, and then transferred for 2 h at 30 V onto nitrocellulose membranes. Ponceau Red staining was used to check gel

loading and transfer accuracy. After blocking with 5% non-fat milk in PBS, membranes were incubated overnight at 4°C with one of the primary antibodies: anti-amyloid β antibody, clone W0-2 (1/2500), anti-amyloid precursor protein, C-terminal antibody (1/2000), anti-hGLuc antibody (1/2000). Membranes were washed with PBS-Tween (0.005%) and incubated with the secondary antibodies anti-mouse (1:10,000) or anti-rabbit (1:10,000) coupled to peroxidase prior to ECL detection (GE Healthcare). Signals were quantified with a Gel Doc 2000 imaging system coupled to a Quantity One™ software (Bio-Rad).

Immunocytochemistry

Cells were seeded on coverslips previously incubated with poly-L-lysine (10 mg/ml). Prior to staining, cells were rinsed twice with Opti-MEM® (Life Technology Corporation) and fixed with 4% paraformaldehyde (PFA) for 15 min. After 3 washes in PBS, cells were permeabilized with PBS1X/0.3% Triton100X for 30 min and blocked in PBS1X/fetal bovine serum 5%/0.1% Triton100X for 30 min. Primary antibodies were prepared in the blocking solution and incubated O/N at 4°C. Primary antibodies used were anti-human amyloid β antibody, clone W0-2 (1:2500), anti-amyloid precursor protein, C-terminal antibody (1:2000), anti-hGLuc antibody (1:2000). After 3 washes in PBS, cells were incubated with secondary antibodies (goat anti-mouse Alexa 465 and goat anti-rabbit Alexa 488 and 465, 1:500 in blocking solution) and DAPI (1:2000) for 1 h at 4°C. After 3 washes in PBS, cells were stored in PBS-azide 0.1% at 4°C or mounted with fluorescent mounting medium for coverslips. Pictures were acquired with an Evos fluorescence microscope (Advanced Microscopy Group, Mill Creek, Washington, USA) or with an Olympus Fluoview confocal microscope (Olympus America Inc., Center Valley, Pennsylvania, USA).

Aβ and sAPP measurements

Aβ38, Aβ40 and Aβ42 peptides were quantified in the cell medium as previously described [39] by the Aβ multiplex electrochemiluminescence immunoassay (ECLIA) (Meso Scale Discovery, Gaithersburg, MD). sAPPα and β were quantified using a sAPPα/sAPPβ multiplex ECLIA (Meso Scale Discovery). Cells were conditioned in serum-free medium for 16 h before harvesting. Cell medium was then collected and Aβ or sAPP were quantified according to the manufacturer's instructions. Aβ produced from split-luciferase constructs was quantified with the human Aβ specific 6E10 multiplex assay.

The number of samples (n) in each experimental condition is indicated in figure legends. The data were analyzed using GraphPad Prism software by analysis of variance (ANOVA) followed by unpaired t test (2 experimental conditions) or by Bonferroni's Multiple Comparison tests (more than 2 experimental conditions).

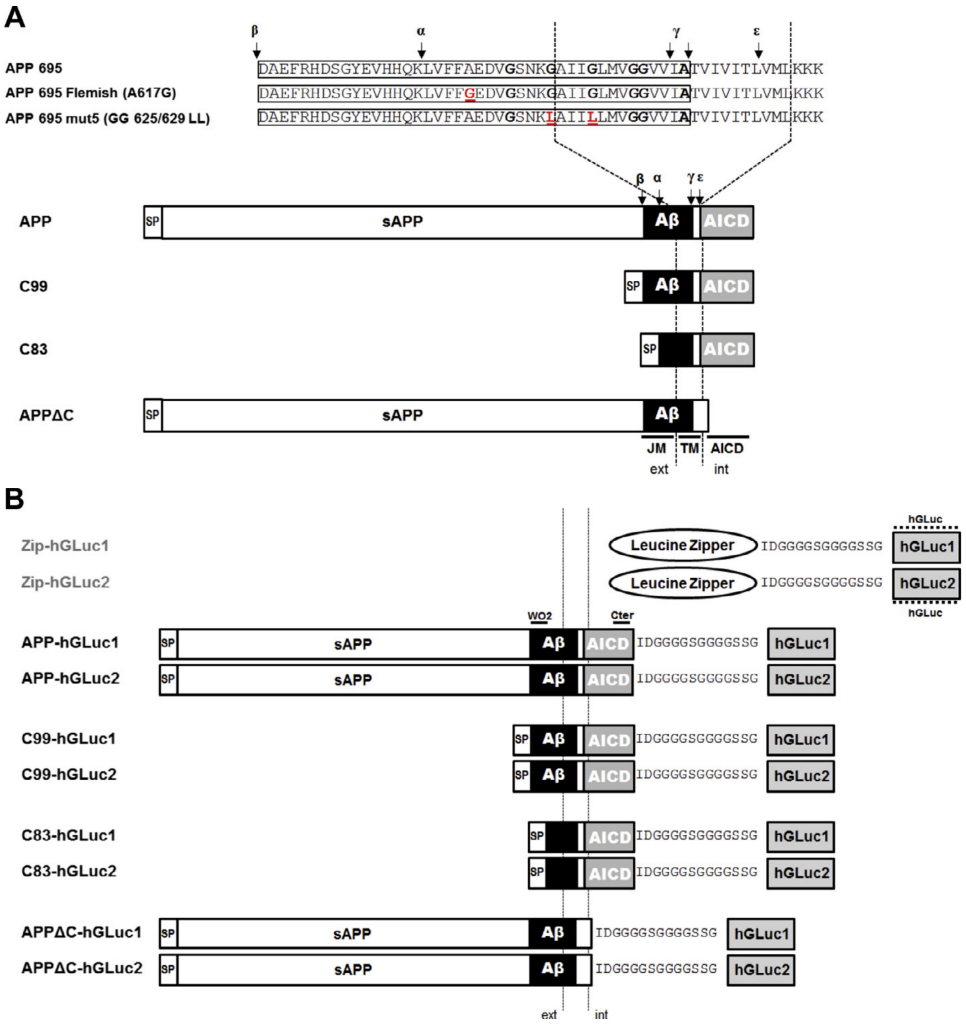

Fig. 1. Schematic representation of the different APP split-luciferase constructs.

(A) Schematic representation of the different human APP and APP C-terminal fragments generated for fusion to the humanized Gaussia luciferase moieties (hGLuc). APPΔC corresponds to APP695 deleted from its intracellular C-terminal domain (stop after the KKKQY intracellular sequence). C99 and C83 correspond to the APP α and β C-terminal fragments, respectively. All the N-terminally truncated CTFs are fused to the APP signal peptide (SP). Abbreviations are as follows: TM, transmembrane; JM, juxtamembrane; AICD, APP intracellular domain; ext, extracellular; int, intracellular. The positions of Flemish and mutant 5 (mut5) mutations are underlined and amino acid substitutions are in red. The cleavage sites of α (α)-, β (β)- and γ (γ and ε)-secretases are indicated by arrows. (B) Schematic representation of APP constructs fused to hGLuc moieties (hGLuc1 and hGLuc2). The epitopes of the human-specific W0-2 antibody, the APP C-terminal and hGLuc antibodies are indicated.

RESULTS

APP and APP C-terminal fragments dimerization in cells analyzed by luciferase complementation assays

To analyze human APP dimerization and the contribution of its extracellular, juxtamembrane/transmembrane (JM/TM) and intracellular (AICD) domains to this process, we generated vectors expressing the full-length and truncated APP proteins (Fig. 1A) fused to complementary humanized Gaussia luciferase (hGluc) fragments referred to as hGluc1 and hGluc2 corresponding to N-terminal and C-terminal moieties, respectively. C99 and C83 correspond to β- and α-secretase cleavage products fused to the APP signal peptide. APPDC corresponds to the APP protein truncated after the KKKYQ sequence at the TM/intracellular interface. To analyze the role of membrane GXXXG motifs in dimerization, we generated 2 mutants modifying the interactive properties of the GXXXG interface [19,24]. The first mutation corresponds to the FAD Flemish mutation (A617G, APP695 numbering or A21G, Aβ numbering). It extends the GXXXG interface and helical structure of the surrounding residues [29]. The double GG625/629LL mutant (GG29/33LL, Aβ numbering) hereafter referred as mutant 5 (mut5) carries glycine to leucine mutations of the central GXXXG motif. These mutations have been previously reported to affect interaction of APP TM helices and strongly impair amyloidogenic processing [19]. As a positive control, we used yeast transcription factor GCN4 leucine zipper fusion proteins (Zip-hGLuc1 and Zip- hGLuc2) [37]. The leucine zipper of GCN4 is a strong dimerization domain. All the constructs generated for this study are represented in Fig. 1A and B.

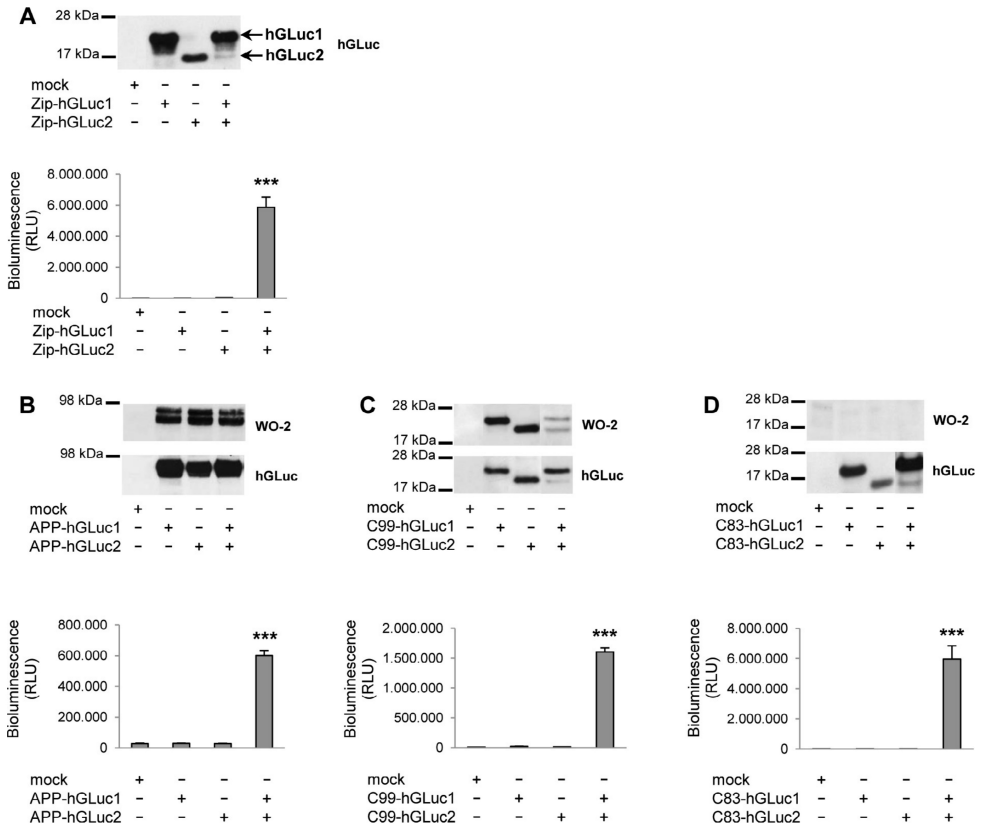

Fig. 2. Dimerization of APP and APP C-terminal fragments in living cells measured by the split-luciferase complementation assay.

(A) Validation of the luciferase complementation assay for measuring protein dimerization in CHO cells. Cells were transfected with the control empty vector (mock) or the GCN4 leucine zipper–coding sequences fused to hGLuc moieties (Zip-hGluc1 and 2). Expression of the fusion proteins was checked in cell lysates by Western blotting with the hGLuc antibody (top). Luciferase activity (bioluminescence) was measured and expressed as RLU (bottom). Values (means ± SEM) are representative of 3 independent experiments (n = 4 in each experiment). ***$p < 0.0001$, as compared to control (mock). APP-hGLuc1 and 2 (B), C99-hGLuc1 and 2 (C) or C83-hGLuc1 and 2 proteins (D) were transfected in CHO cells. Protein expression was monitored in cell lysates by Western blotting with the W0-2 and hGluc antibodies (top panels). Luciferase activity was measured and expressed as RLU (bottom). Values (means ± SEM) are representative of 3 independent experiments (n = 4 in each experiment). ***$p < 0.0001$, as compared to control (mock).

We first validated the luciferase complementation approach as a tool to measure protein dimerization in living CHO cells by measuring bioluminescence upon transfection with the GCN4 leucine zipper hGLuc constructs. Western blotting of cell lysates indicated that Zip-hGLuc1 and Zip-hGLuc2 were detected as 17 and 18 kDa bands recognized by the polyclonal anti-hGLuc antibody (Fig. 2A). Transfection of Zip-hGLuc1 and Zip-hGLuc2 alone did not generate any bioluminescent signal whereas co-transfection of both generated high levels of luciferase activity (Fig. 2A). Co-expression of the hGLuc1 and hGLuc2 moieties alone (not fused to any APP protein sequence) did not generate luciferase activity (data not shown). This clearly validated the luciferase complementation approach as a very sensitive tool to measure dimerization in cells.

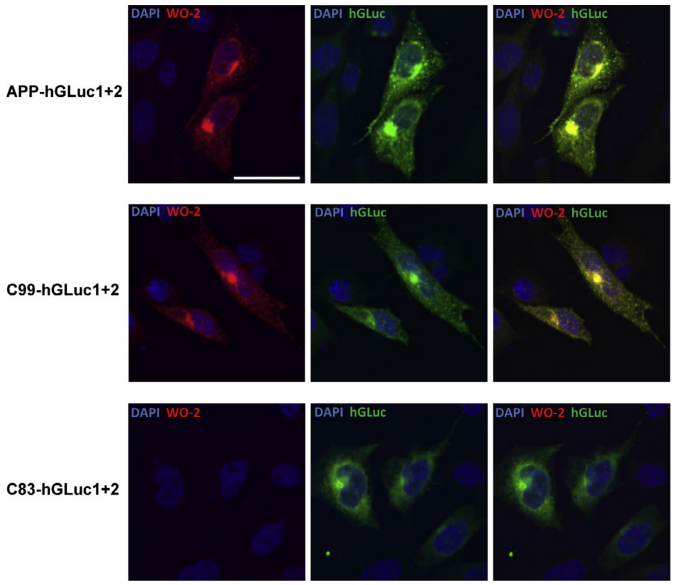

Fig. 3. Localization of split-luciferase constructs in CHO cells. Cells were co-transfected with the two split-luciferase constructs expressing either APP C99 or C83. Nuclei were stained with DAPI, and APP fusion constructs were stained by the W0-2 and/or hGLuc antibodies. Scale bar: 5 µm.

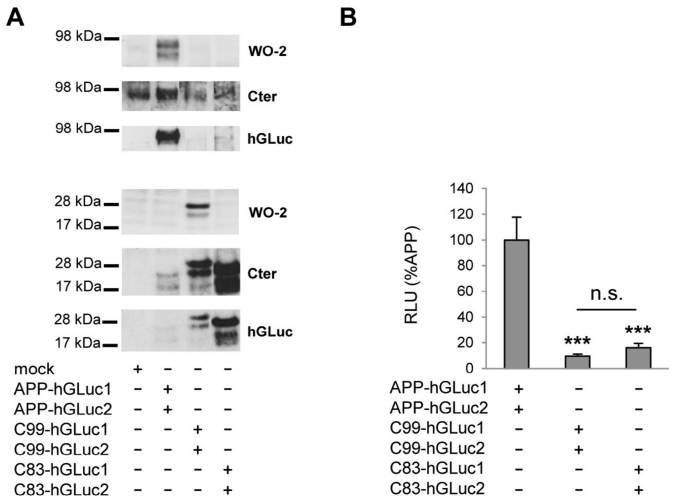

Fig. 4. Comparison of APP and APP C-terminal fragment dimerization. Cells were transfected with the control empty vector (mock), the APP-hGLuc1 and 2, C99-hGLuc1 and 2 or C83-hGLuc1 and 2 constructs. (A) Protein expression was monitored in cell lysates by Western blotting with the W0-2, Cter or hGLuc antibodies. (B) Luciferase activity was measured and expressed as RLU normalized to APP (set to 100%). Values (means ± SEM) are representative of 3 independent experiments (n = 4 in each experiment). ***p < 0.001, n.s. (non-significant), as compared to APP-hGLuc1 and 2.

We next compared dimerization of the APP, C99 and C83 constructs (Fig. 2B-D). Immunoblots performed with the W0-2 antibody, the hGLuc antibody or the APP C-terminal antibody (Cter) showed that all constructs were expressed at readily detectable levels. Immunolabelling of the double transfected cells indicated a vesicular localization of the APP fusion proteins (Fig. 3), particularly in the perinuclear region. APP hGLuc fusion proteins had a subcellular distribution consistent with a post-ER/cis-Golgi localization previously reported for endogenous APP and APP fragments, but also for fusion constructs used in split protein assays [27,31,40]. Signals of antibodies directed against human APP epitopes (W0-2) or hGLuc epitopes completely co-localized, excluding the hypothesis that spurious cleavage or degradation products could be responsible for bioluminescent signals.

After normalization to expression levels of the fusion proteins (Fig. 4A), our results indicated that APP dimerizes significantly more (± 5 times) than its α and β C-terminal fragments (Fig. 4B). Similar results were obtained with all the antibodies used for cell lysate quantifications (W0-2, Cter or hGLuc). These observations suggest that C-terminal fragments of APP (β or αCTFs) form dimers to a smaller extent than full-length APP. We further investigated this hypothesis by treating transfected cells with DAPT, a γ-secretase allosteric inhibitor, inducing the accumulation of γ-secretase substrates in cells. DAPT effects were consistent with those observed on non-tagged human APP in the same cells (Fig. 5A) [19]. DAPT treatment resulted mainly in the accumulation of αCTFs (Fig. 5A and B). Bioluminescence measured after DAPT treatment indicated a small -although significant- decrease in APP dimerization, but importantly no increase in αCTF or βCTF dimerization was measured under the same conditions (Fig. 5C). Similar results were observed in PSdKO mouse embryonic fibroblasts (MEFs) that are devoid of γ-secretase activity (data not shown). Together, these data indicate that

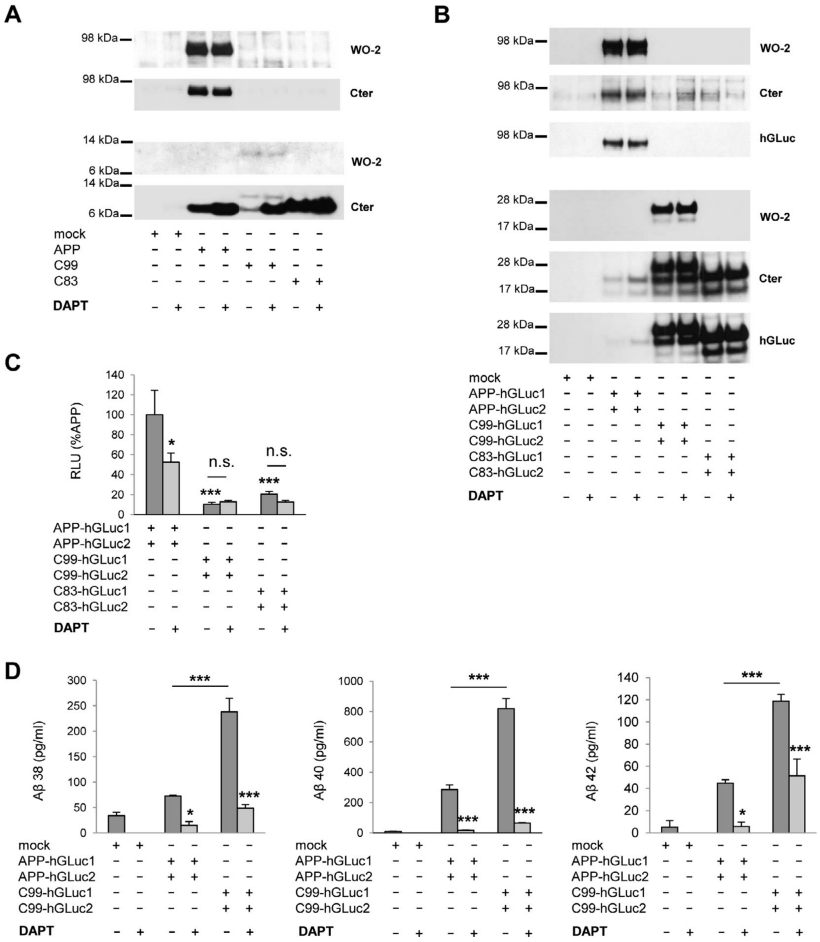

Fig. 6. Involvement of GXXXG motifs in CTF dimerization and Aβ production. CHO cells were transfected with C99-hGLuc1 and 2 or C83-hGLuc1 and 2 and their Flemish (Fle) and mutant 5 (mut5) corresponding mutants. (A) Cells transfected with the control empty vector (mock), the C99-hGLuc1 and 2, C99Fle-hGLuc1 and 2 or C99mut5-hGLuc1 and 2 proteins. Protein expression was monitored in cell lysates by Western blotting with the W0-2 or hGluc antibodies (top panels). Luciferase activity was measured and expressed as RLU normalized to non-mutated C99 (bottom). Values (means ± SEM) are representative of 5 independent experiments (n = 4 in each experiment). *p < 0.05, **p < 0.01 and ***p < 0.001, as compared to C99-hGLuc1 and 2. (B) Cells transfected with the control empty vector (mock), the C83-hGLuc1 and 2, C83Fle-hGLuc1 and 2 or C83mut5-hGLuc1 and 2 proteins. Protein expression was monitored in cell lysates by Western blotting with the Cter or hGLuc antibodies (top panels). Luciferase activity was measured and expressed as RLU normalized to non-mutated C83 (bottom). Values (means ± SEM) are representative of 3 independent experiments (n = 4 in each experiment). *p < 0.05, **p < 0.01 and n.s. (non significant), as compared to C83-hGLuc1 and 2. (C) Aβ 38, 40 and 42 production for C99-hGLuc1 and 2, C99Fle-hGLuc1 and 2 or C99mut5-hGLuc1 and 2 was measured by ECLIA in the culture media and given in pg/ml. Values (means ± SEM) are representative of 3 independent experiment (n = 4 in each experiment). ***p < 0.001, as compared to non-mutated C99.

APP CTFs dimerize much less than full-length APP. Their accumulation by a γ-secretase inhibitor did not increase dimerization, suggesting that only a pool of CTFs are forming dimers, which are not accessible to cleavage by γ-secretase. DAPT treatment efficiently inhibited the γ-cleavage of APP split luciferase constructs, as evidenced by the strong inhibition of Aβ release (Fig. 5D).

GXXXG motifs are not critical for CTFs dimerization

Our recent work showed that mutation of the GXXXG motifs modifies TM interactions of the APP CTFs [19]. To determine whether GXXXG motifs are involved in CTFs homo-dimerization by a quantitative approach, we compared dimerization of C99 (corresponding to the βCTF of APP), C99 with the Flemish mutation or C99 mut5 (Fig. 1A). Both C99 mutants exhibited the same dimerization profile as wild-type C99 (Fig. 6A). Similar experiments were carried out with C83 constructs, corresponding to the APP αCTF. C99 and C83 constructs had similar expression profiles (Fig. 6B). Both the Flemish mutant and mut5 showed a slight but significant decrease in dimerization of C99. For C83, dimerization of the Flemish mutant was slightly but significantly increased, whereas dimerization of mut5 was not affected. Mutation of the GXXXG motifs was reported to dramatically impact Aβ production (Fig. 6C). We previously showed [19,29] that the Flemish FAD mutation increased Aβ production whereas mutant 5 strongly decreased it. Our data (Fig. 6) indicate that mutations of GXXXG motifs strongly affect APP γ-cleavage without a corresponding change in dimerization of the APP CTFs.

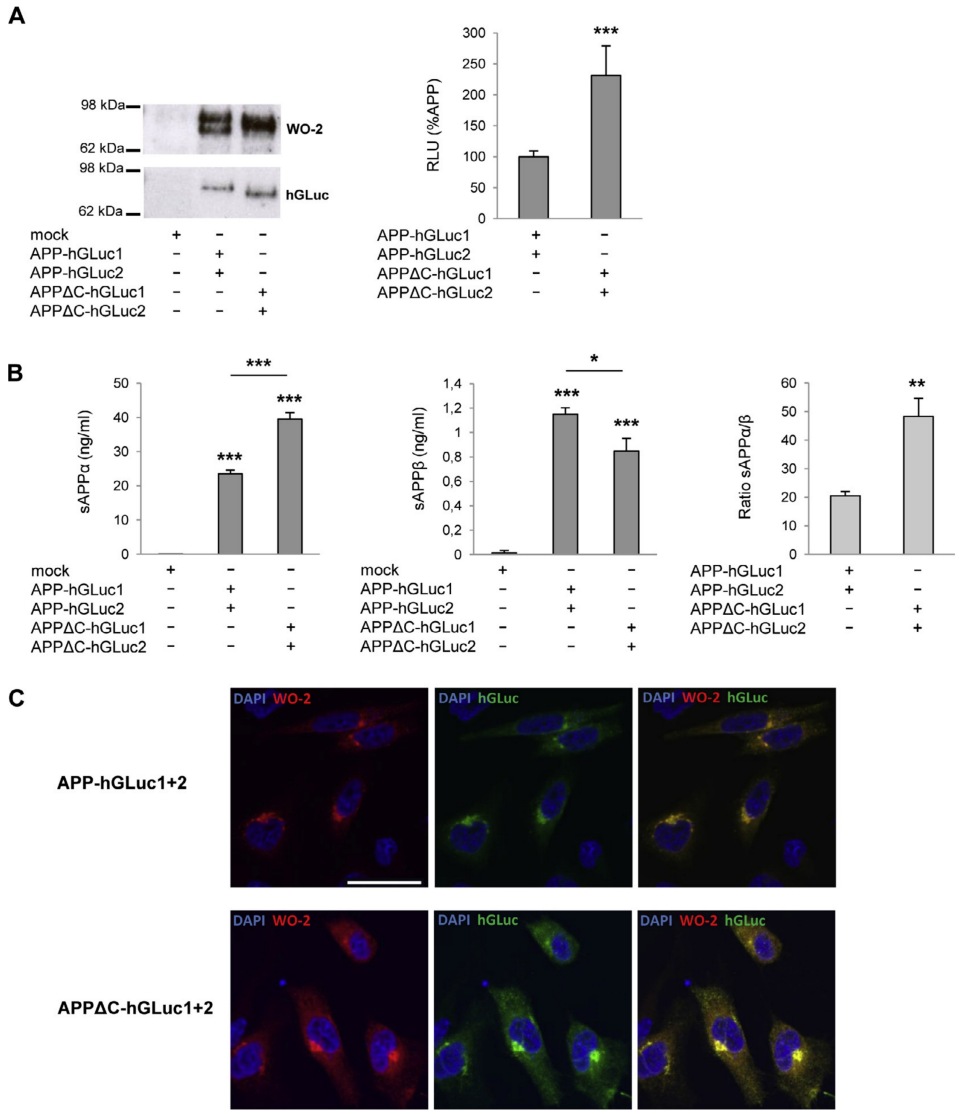

Fig. 7. Influence of the intracellular in APP dimerization. (A) Protein expression was monitored in cell lysates by Western blotting with the W0-2 or hGluc antibodies (left panel). Luciferase activity was measured and expressed as RLU normalized to APP (set to 100%, right panel). Values (means ± SEM) are representative of 2 independent experiments (n = 4 in each experiment). ***p < 0.001, as compared to APP-hGLuc1 and 2. (B) sAPPα and β production of APP-hGLuc1 and 2 and APPΔC-hGLuc1 and 2 constructs were monitored by ECLIA in the culture media of cells and are given in ng/ml. *p < 0.05 and ***p < 0.001, as compared to non-transfected cells or as indicated. Ratio of sAPPα on sAPPβ produced was calculated in the same experiments. **p < 0.01, as compared to APP-hGLuc1 and 2 (C) Immunostaining of cells co-expressing APP or APPΔC constructs of either. Nuclei were stained with DAPI, and APP fusion constructs were stained by the W0-2 and/or hGLuc antibodies. Scale bar: 5 µm.

APP C-terminal region regulates APP dimerization and non-amyloidogenic processing

We finally examined the role of the APP intracellular C-terminal domain in dimerization. We generated APPΔC split-luciferase constructs, corresponding to APP deleted from its intracellular region (Fig. 1). Indeed, much attention has been given so far to the contribution of the extracellular and TM domains to APP dimerization, but nothing is known about the role of its intracellular region. Both APP and APPΔC were recognized by the W0-2 and hGLuc antibodies, and both constructs were expressed at similar levels (Fig. 7A). Immunostaining (Fig. 7C) indicated that APP and APPΔC displayed similar subcellular distribution profiles. Results in Fig. 7A clearly showed that APPΔC formed more dimers than APP in cells. Expression of C99 constructs identically lacking their intracellular domains (C55) led to the same increased dimerization (data not shown). To know whether this drastic change in dimerization is related to APP metabolism, we measured sAPPα and sAPPβ levels produced by those cells. Soluble APPα and sAPPβ production are indicators of the ectodomain shedding occurring as a first step of the non-amyloidogenic and amyloidogenic processing, respectively. Cells expressing APPΔC-hGLuc showed increased sAPPα levels and reduced sAPPβ production. The ratio between sAPPα and sAPPβ significantly increased, indicating that APPΔC metabolism is shifted towards non-amyloidogenic processing.

DISCUSSION

Dimerization appears to be a key modulator of APP processing and function. APP shares many features with cell adhesion molecules and TM receptors [9]. APP homo- and hetero-association are involved in transcellular interactions [11]. Homodimerization was proposed to directly correlate to amyloidogenic processing and Aβ production. We and others found that disruption of TM interaction motifs leads to impaired Aβ production [18,19], suggesting that the formation of dimeric amyloidogenic CTFs is a control mechanism of APP γ-cleavage. However, whether dimerization promotes or inhibits processing itself has been a matter of debate [25,26]. Recent studies indicated that, in contrast to Aβ production, dimerization is not altered in FAD mutants [27], challenging the hypothesis that dimerization is involved in amyloidogenic processing. Indeed, the extent of APP and APP CTFs dimerization in cells, its relation to amyloidogenic processing and the contribution of the different APP domains in this process remain unclear and poorly known.

APP homo- and/or hetero-dimerization have been reported so far using different approaches, including co-immunopreciptation and non-denaturing electrophoresis, FRET-based assays and split-protein assays [19,27,41]. We recently used the bimolecular fluorescence complementation (BiFC) method, or split-YFP, to analyze dimerization of APP695 and APP751 isoforms [17,31]. This method has gained popularity in the field to study protein–protein interactions in living cells [13,42]. Its major advantage is to allow direct visualization of protein interactions without the use of biochemical reagents or antibodies that might themselves modify the dimerization properties of the proteins investigated. The major drawbacks of BiFC are that the fluorescent protein halves are prone to self-

assembly independent of a protein–protein interaction event, and that the split position promotes irreversible self-interaction of the two non-fluorescent fragments, which may result in the detection of false positive signals [43]. Here we used the split Gaussia luciferase assay, a more recent, quantitative and dynamic complementation method to circumvent drawbacks of previous split protein approaches [37]. The humanized Gaussia princeps luciferase (hGLuc) can generate over 100-fold higher bioluminescent signal than other luciferases and is the smallest known coelenterazine-using luciferase, making it an ideal candidate for protein complementation assays.

APP and the various APP C-terminal fragments fused to the split-protein used in our study were readily expressed in CHO cells and detectable by Western blotting by different antibodies, thus allowing normalization of the bioluminescence to the bioluminescent protein content. This is an important asset when compared to the split YFP approach [31], in which quantitative comparison of protein dimerization is more difficult to achieve. We also checked that the co-expression of the hGLuc halves alone do not generate a bioluminescent signal (data not shown), excluding the possibility that the luciferase protein halves self-assemble independently of a protein–protein interaction event, a critical possible bias in split protein assays [43]. Grafting hGLuc halves at the C-terminus does not impair APP subcellular localization or processing. The split luciferase assays we developed appeared therefore as a very sensitive and reliable tool to decipher the mechanisms of APP dimerization in cells.

We first observed that full length APP dimerizes more than its C-terminal fragments. At similar expression levels, the extent of APP dimerization is at least 5 times higher than for C99 or C83. C99 and C83 seem to have only poor and restricted dimerization properties [30]. Their accumulation upon cell treatment

with a γ-secretase inhibitor (DAPT) does not increase the bioluminescent signal. This observation strongly argues that CTF dimers are not substrates of the γ-secretase. Under the same conditions (DAPT treatment), APP dimerization was slightly but significantly reduced although cellular levels of the protein were unchanged. One possible interpretation to this unexpected observation is that the accumulation of CTFs (endogenous or hGLuc tagged) upon DAPT treatment could interfere with full-length APP dimerization. This seems to be indeed the case since co-transfection of APP-hGLuc and C83-hGLuc formed dimers to a lesser extent than APP homodimers (see Supplementary Fig. S1).

Previous studies have shown that APP dimers can be readily observed in cells and that dimers are formed in the early secretory pathway [31]. Our results are in line with these observations, and confirm that determinants playing a major role in APP dimerization (E1 and KPI domains) are located in its extracellular region [15,31]. Dimerization driven by ectodomain regions appears as a key mechanism for APP trafficking to the cell surface [15,16]. Much more attention has been recently given to dimerization of the APP JM/TM regions and the role of these regions in amyloidogenic processing and Aβ production. APP contains 3 in-register GXXXG motifs that start in the extracellular JM sequence and continue into the TM domain. These motifs are well known to stabilize TM protein interactions by close apposition of TM α-helices [44,45].

Structural approaches have established that APP JM/TM sequences interact through GXXXG motifs interfaces [28–30]. Mutations of these motifs strongly modulate their interaction and impair Aβ production [18,19]. We found in a previous study [17] that mutation of GXXXG motifs did not affect dimerization of full length APP. We confirmed by the split luciferase system that mutation in a critical GXXXG motif (mut5) has no effect on full-length APP dimerization (see

Supplementary Fig. S2). In addition, GXXXG mutations did no modify the sAPPα/sAPPβ ratio, excluding the hypothesis that they indirectly contribute to the production of Aβ by facilitating the shedding of the of APP ectodomain through the α- or β-secretase pathways. This strongly suggested that GXXXG motifs might play a critical role in APP CTF dimerization, after the removal of the bulky ectodomain by α- or β-secretase. We directly addressed this point by mutating the GXXXG motifs in C99 and C83 (corresponding to β and αCTF, respectively) and measuring the effect on dimerization by the split luciferase assay. We analyzed 2 different mutants: mut5 with mutations of the central GXXXG motif (GG29/33LL) disrupting the GXXXG interface and the FAD Flemish mutant (A21G) adding a fourth in register GXXXG motif extending the GXXXG interface. These mutations had only a very moderate effect on C83 and C99 dimerization. No consistent effect was measured with C83 mut5 and A21G constructs. Decreased dimerization was measured for both mutated C99 constructs, although the effect was moderate. These observations first indicate that C99 and C83 dimerization might be different, due to determinants located between the α- and β-cleavage sites. Contrary to what was previously suggested, mutation of GXXXG motifs do not trigger the formation of stable TM dimers through the GXXXA motif located downstream [19]. Importantly, there was no direct relationship between the effects of the mutation on dimerization and Aβ production. The Flemish mutation significantly increased Aβ release, whereas mut5 blocked it. This is consistent with very recent results showing an independent relationship between APP dimerization and γ-secretase processivity [26,27,36]. Rather than changing dimerization, mutation of glycine residues in the GXXXG motifs might induce a conformational change increasing the fitness of the substrate for γ-secretase activity, and thus Aβ production [29]. In fact, the GXXXG motif has been shown to interact with NSAIDs and cholesterol, playing the role of a cholesterol sensor

pocket [30,35]. JM/TM regions are sensitive to the membrane lipid context and are targeted by drugs acting as γ-secretase modulators, but probably independent of their dimerization properties. It would be of interest to evaluate with the split luciferase assay how these compounds impact dimerization, if GXXXG mutants show different sensitivities, and how they can be related to their modulatory effect on Aβ production.

One major finding in this study is that deletion of APP intracellular domain importantly increased its dimerization. So far, the intracellular domain has never been shown to influence APP dimerization. We built AICD split-luciferase constructs and found that AICD does not dimerize by itself (data not shown). One possible explanation could be that the interaction of the APP intracellular region with proteins like G0 protein or Fe65 [46,47] favors dimerization. Indeed, APP has been shown to interact with adaptor proteins like Fe65 by its YENPTY intracellular motif [48,49] and this association could impair or compete with dimerization. When we expressed Fe65 together with APP in CHO cells we did not modify APP dimerization measured by split-luciferase (see Supplemen- tary Fig. S3). This does not exclude the possibility that other unknown interacting protein modulate dimerization. An alternative hypothesis could be that dimerization is related to trafficking, which in turn impacts processing. APPΔC is directed to the secretory pathway but cannot be internalized properly due to loss of the NPTY internalization motif [31,50]. At this stage, we cannot define whether increased dimerization of APPΔC is the cause or a consequence of the reduced endocytosis, but we can propose that the amount of APPΔC stays high in cells because they fail to be endocytosed in compartments where they are further processed. This would in turn favor its non-amyloidogenic processing, known to occur close to the cell surface. This is consistent with our observations, indicating that increased dimerization of APPΔC is linked to increased cleavage by α-secretase, inducing a

shift towards non-amyloidogenic pathway. Interestingly, compounds that have been shown to destabilize dimerization of the APP ectodomain indeed regulate cleavage by α-secretase [34]. However, the question of whether α-secretase cleaves APP dimers, or whether dimerization favors trafficking to compartments where a-cleavage occurs, remains totally open.

CONCLUSION

We used the recent split luciferase assay to study APP dimerization in cells. In contrast to what was suggested in previous studies, we found that the APP CTFs (C99 and C83) dimerized at a low level when compared to full-length APP. Mutation of the TM interaction GXXXG motifs did not significantly affect CTF dimerization. Combining dimerization studies and measurement of Aβ production, we found that there is no direct relationship between APP dimerization and γ-cleavage. In fact, major determinants controlling APP dimerization appear to be its intracellular domain. Increasing APP dimerization favors its non-amyloidogenic processing. This brings new and important insights on the different regions driving APP dimerization, and the relationship between dimerization and processing.

CONTRIBUTIONS

M.D. and P.K.C. designed research; M.D., L.E.H. and S.S. con- ducted experiments, M.D. and P.K-C. analyzed data and wrote the paper with fundamental input of S.O.S., S.C., I.D., and J-N.O.

ACKNOWLEDGEMENTS

This work was supported by a grant of the Belgian F.N.R.S FRIA (Fonds National pour la Recherche Scientifique) to M.D., Founda- tion for Research on Alzheimer's disease (P.K-C.), by the Interuni- versity Attraction Poles Programme-Belgian Sate-Belgian Science Policy (IAP-P7/16 and IAP-P7/13) to J-N.O. and P.K-C, and by the NIH (AG027317) to S.O.S. We are grateful to J-F. Paradis and S.W. Michnick (UMontreal) for the leucine zipper split-luciferase plasmids. We greatly acknowledge B. Tasiaux for her excellent technical support.

REFERENCES

[1]Kang,J.,Lemaire,H.G.,Unterbeck,A.,Salbaum,J.M.,Masters,C.L.,Grzeschik,K. H.,Multhaup, G., Beyreuther, K. and Muller-Hill, B. (1987) The precursor of Alzheimer's disease amyloid A4 protein resembles a cell-surface receptor. Nature 325, 733–736.

[2] Selkoe, D.J. (2004) Alzheimer disease: mechanistic understanding predicts novel therapies. Ann. Intern. Med. 140, 627–638.

[3] Octave, J.N. (1995) The amyloid peptide and its precursor in Alzheimer's disease. Rev. Neurosci. 6, 287–316.

[4] Glenner, G.G. and Wong, C.W. (1984) Alzheimer's disease: initial report of the purification and characterization of a novel cerebrovascular amyloid protein. Biochem. Biophys. Res. Commun. 120, 885–890.

[5] Hardy, J. and Selkoe, D.J. (2002) The amyloid hypothesis of Alzheimer's disease: progress and problems on the road to therapeutics. Science 297, 353– 356.

[6] Shariati, S.A. and De, S.B. (2013) Redundancy and divergence in the amyloid precursor protein family. FEBS Lett. 587, 2036–2045.

[7] Weyer,S.W.,Klevanski,M.,Delekate,A.,Voikar,V.,Aydin,D.,Hick,M.,Filippov, M., Drost, N., Schaller, K.L., Saar, M., Vogt, M.A., Gass, P., Samanta, A., Jaschke, A., Korte, M., Wolfer, D.P., Caldwell, J.H. and Muller, U.C. (2011) APP and APLP2 are essential at PNS and CNS synapses for transmission, spatial learning and LTP. EMBO J. 30, 2266–2280.

[8] Klevanski, M., Saar, M., Baumkotter, F., Weyer, S.W., Kins, S. and Muller, U.C. (2014) Differential role of APP and APLPs for neuromuscular synaptic morphology and function. Mol. Cell Neurosci. 61, 201–210.

[9] Khalifa,N.B.,Van,H.J.,Tasiaux,B.,Huysseune,S.,Smith,S.O.,Constantinescu,S. N., Octave, J.N. and Kienlen-Campard, P. (2010) What is the role of amyloid precursor protein dimerization? Cell Adh. Migr. 4, 268–272.

[10] Coulson, E.J., Paliga, K., Beyreuther, K. and Masters, C.L. (2000) What the evolution of the amyloid protein precursor supergene family tells us about its function. Neurochem. Int. 36, 175–184.

[11] Soba, P., Eggert, S., Wagner, K., Zentgraf, H., Siehl, K., Kreger, S., Lower, A., Langer, A., Merdes, G., Paro, R., Masters, C.L., Muller, U., Kins, S. and Beyreuther, K. () Homo- and heterodimerization of APP family members promotes intercellular adhesion. EMBO J. 24, 3624–3634.

[12] Kaden, D., Voigt, P., Munter, L.M., Bobowski, K.D., Schaefer, M. and Multhaup, G. (2009) Subcellular localization and dimerization of APLP1 are strikingly different from APP and APLP2. J. Cell Sci. 122, 368–377.

[13] Chen, C.D., Oh, S.Y., Hinman, J.D. and Abraham, C.R. (2006) Visualization of APP dimerization and APP-Notch2 heterodimerization in living cells using bimolecular fluorescence complementation. J. Neurochem. 97, 30–43.

[14] Shaked, G.M., Kummer, M.P., Lu, D.C., Galvan, V., Bredesen, D.E. and Koo, E.H. (2006) Abeta induces cell death by direct interaction with its cognate extracellular domain on APP (APP 597–624). FASEB J. 20, 1254–1256.

[15] Kaden, D., Munter, L.M., Joshi, M., Treiber, C., Weise, C., Bethge, T., Voigt, P., Schaefer, M., Beyermann, M., Reif, B. and Multhaup, G. (2008) Homophilic interactions of the amyloid precursor protein (APP) ectodomain are regulated by the loop region and affect beta-secretase cleavage of APP. J. Biol. Chem. 283, 7271–7279.

[16] Isbert, S., Wagner, K., Eggert, S., Schweitzer, A., Multhaup, G., Weggen, S., Kins, S. and Pietrzik, C.U. (2012) APP dimer formation is initiated in the endoplasmic reticulum and differs between APP isoforms. Cell Mol. Life Sci. 69, 1353–1375.

[17] Ben, K.N., Tyteca, D., Courtoy, P.J., Renauld, J.C., Constantinescu, S.N., Octave, J. N. and Kienlen-Campard, P. (2012) Contribution of Kunitz protease inhibitor and transmembrane domains to amyloid precursor protein homodimerization. Neurodegener. Dis. 10, 92–95.

[18] Munter, L.M., Voigt, P., Harmeier, A., Kaden, D., Gottschalk, K.E., Weise, C., Pipkorn, R., Schaefer, M., Langosch, D. and Multhaup, G. (2007) GxxxG motifs within the amyloid precursor protein transmembrane sequence are critical for the etiology of Abeta42. EMBO J. 26, 1702–1712.

[19] Kienlen-Campard, P., Tasiaux, B., Van, H.J., Li, M., Huysseune, S., Sato, T., Fei, J. Z., Aimoto, S., Courtoy, P.J., Smith, S.O., Constantinescu, S.N. and Octave, J.N. (2008) Amyloidogenic processing but not amyloid precursor protein (APP) intracellular C-terminal domain production requires a precisely oriented APP dimer assembled by transmembrane GXXXG motifs. J. Biol. Chem. 283, 7733– 7744.

[20] Russ, W.P. and Engelman, D.M. (2000) The GxxxG motif: a framework for transmembrane helix-helix association. J. Mol. Biol. 296, 911–919.

[21] Brosig, B. and Langosch, D. (1998) The dimerization motif of the glycophorin A transmembrane segment in membranes: importance of glycine residues. Protein Sci. 7, 1052–1056.

[22] Gorman, P.M., Kim, S., Guo, M., Melnyk, R.A., McLaurin, J., Fraser, P.E., Bowie, J. U. and Chakrabartty, A. (2008) Dimerization of the transmembrane domain of amyloid precursor proteins and familial Alzheimer's disease mutants. BMC Neurosci. 9, 17.

[23] Munter, L.M., Botev, A., Richter, L., Hildebrand, P.W., Althoff, V., Weise, C., Kaden, D. and Multhaup, G. (2010) Aberrant amyloid precursor protein (APP) processing in hereditary forms of Alzheimer disease caused by APP familial Alzheimer disease mutations can be rescued by mutations in the APP GxxxG motif. J. Biol. Chem. 285, 21636–21643.

[24] Hendriks, L., van Duijn, C.M., Cras, P., Cruts, M., Van, H.W., van, H.F., Warren, A., McInnis, M.G., Antonarakis, S.E. and Martin, J.J. (1992) Presenile dementia and cerebral haemorrhage linked to a mutation at codon 692 of the beta-amyloid precursor protein gene. Nat. Genet. 1, 218–221.

[25] Scheuermann, S., Hambsch, B., Hesse, L., Stumm, J., Schmidt, C., Beher, D., Bayer, T.A., Beyreuther, K. and Multhaup, G. (2001) Homodimerization of amyloid precursor protein and its implication in the amyloidogenic pathway of Alzheimer's disease. J. Biol. Chem. 276, 33923–33929.

[26] Eggert, S., Midthune, B., Cottrell, B. and Koo, E.H. (2009) Induced dimerization of the amyloid precursor protein leads to decreased amyloid-beta protein production. J. Biol. Chem. 284, 28943–28952.

[27] So, P.P., Khodr, C.E., Chen, C.D. and Abraham, C.R. (2013) Comparable dimerization found in wildtype and familial Alzheimer's disease amyloid precursor protein mutants. Am. J. Neurodegener. Dis. 2, 15–28.

[28] Sato, T., Tang, T.C., Reubins, G., Fei, J.Z., Fujimoto, T., Kienlen-Campard, P., Constantinescu, S.N., Octave, J.N., Aimoto, S. and Smith, S.O. (2009) A helix-to- coil transition at the epsilon-cut site in the transmembrane dimer of the amyloid precursor protein is required for proteolysis. Proc. Natl. Acad. Sci. USA 106, 1421–1426.

[29] Tang, T.C., Hu, Y., Kienlen-Campard, P., El, H.L., Decock, M., Van, H.J., Fu, Z., Octave, J.N., Constantinescu, S.N. and Smith, S.O. (2014) Conformational changes induced by the A21G Flemish mutation in the amyloid precursor protein lead to increased Abeta production. Structure 22, 387–396.

[30] Song, Y., Hustedt, E.J., Brandon, S. and Sanders, C.R. (2013) Competition between homodimerization and cholesterol binding to the C99 domain of the amyloid precursor protein. Biochemistry 52, 5051–5064.

[31] Ben, K.N., Tyteca, D., Marinangeli, C., Depuydt, M., Collet, J.F., Courtoy, P.J., Renauld, J.C., Constantinescu, S., Octave, J.N. and Kienlen-Campard, P. (2012) Structural features of the KPI domain control APP dimerization, trafficking, and processing. FASEB J. 26, 855–867.

[32] So, P.P., Zeldich, E., Seyb, K.I., Huang, M.M., Concannon, J.B., King, G.D., Chen, C. D., Cuny, G.D., Glicksman, M.A. and Abraham, C.R. (2012) Lowering of amyloid beta peptide production with a small molecule inhibitor of amyloid-beta precursor protein dimerization. Am. J. Neurodegener. Dis. 1, 75–87.

[33] Asada-Utsugi, M., Uemura, K., Noda, Y., Kuzuya, A., Maesako, M., Ando, K., Kubota, M., Watanabe, K., Takahashi, M., Kihara, T., Shimohama, S., Takahashi, R., Berezovska, O. and Kinoshita, A. (2011) N-cadherin enhances APP dimerization at the extracellular domain and modulates Abeta production. J. Neurochem. 119, 354–363.

[34] Libeu, C.A., Descamps, O., Zhang, Q., John, V. and Bredesen, D.E. (2012) Altering APP proteolysis: increasing sAPPalpha production by targeting dimerization of the APP ectodomain. PLoS One 7, e40027.

[35] Richter, L., Munter, L.M., Ness, J., Hildebrand, P.W., Dasari, M., Unterreitmeier, S., Bulic, B., Beyermann, M., Gust, R., Reif, B., Weggen, S., Langosch, D. and Multhaup, G. (2010) Amyloid beta 42 peptide (Abeta42)-lowering compounds directly bind to Abeta and interfere with amyloid precursor protein (APP) transmembrane dimerization. Proc. Natl. Acad. Sci. USA 107, 14597–14602.

[36] Jung, J.I., Premraj, S., Cruz, P.E., Ladd, T.B., Kwak, Y., Koo, E.H., Felsenstein, K.M., Golde, T.E. and Ran, Y. (2014) Independent relationship between amyloid precursor protein (APP) dimerization and gamma-secretase processivity. PLoS One 9, e111553.

[37] Remy, I. and Michnick, S.W. (2006) A highly sensitive protein-protein interaction assay based on Gaussia luciferase. Nat. Methods 3, 977–979. [38] Marinangeli, C., Tasiaux, B., Opsomer, R., Hage, S., Sodero, A.O., Dewachter, I.,

[38] Octave, J.N., Smith, S.O., Constantinescu, S.N. and Kienlen-Campard, P. (2015) Presenilin transmembrane domain 8 conserved AXXXAXXXG motifs are required for the activity of the gamma-secretase complex. J. Biol. Chem. 290, 7169–7184.

[39] Hage, S., Stanga, S., Marinangeli, C., Octave, J.N., Dewachter, I., Quetin-Leclercq, J. and Kienlen-Campard, P. (2015) Characterization of Pterocarpus erinaceus kino extract and its gamma-secretase inhibitory properties. J. Ethnopharmacol. 163, 192–202.

[40] Annaert, W.G., Levesque, L., Craessaerts, K., Dierinck, I., Snellings, G., Westaway, D., George-Hyslop, P.S., Cordell, B., Fraser, P. and De, S.B. (1999) Presenilin 1 controls gamma-secretase processing of amyloid precursor protein in pre-golgi compartments of hippocampal neurons. J. Cell Biol. 147, 277–294.

[41] Devauges, V., Marquer, C., Lecart, S., Cossec, J.C., Potier, M.C., Fort, E., Suhling, K. and Leveque-Fort, S. (2012) Homodimerization of amyloid precursor protein at the plasma membrane: a homoFRET study by time-resolved fluorescence anisotropy imaging. PLoS One 7, e44434.

[42] Kerppola, T.K. (2006) Complementary methods for studies of protein interactions in living cells. Nat. Methods 3, 969–971.

[43] Horstman, A., Tonaco, I.A., Boutilier, K. and Immink, R.G. (2014) A cautionary note on the use of split-YFP/BiFC in plant protein-protein interaction studies. Int. J. Mol. Sci. 15, 9628–9643.

[44] Smith, S.O., Song, D., Shekar, S., Groesbeek, M., Ziliox, M. and Aimoto, S. (2001) Structure of the transmembrane dimer interface of glycophorin A in membrane bilayers. Biochemistry 40, 6553–6558.

[45] Lemmon, M.A., Flanagan, J.M., Treutlein, H.R., Zhang, J. and Engelman, D.M. (1992) Sequence specificity in the dimerization of transmembrane alpha- helices. Biochemistry 31, 12719–12725.

[46] Nishimoto, I., Okamoto, T., Matsuura, Y., Takahashi, S., Okamoto, T., Murayama, Y. and Ogata, E. (1993) Alzheimer amyloid protein precursor complexes with brain GTP-binding protein G(o). Nature 362, 75–79.

[47] Fiore, F., Zambrano, N., Minopoli, G., Donini, V., Duilio, A. and Russo, T. (1995) The regions of the Fe65 protein homologous to the phosphotyrosine interaction/phosphotyrosine binding domain of Shc bind the intracellular domain of the Alzheimer's amyloid precursor protein. J. Biol. Chem. 270, 30853–30856.

[48] Guenette, S.Y., Chen, J., Jondro, P.D. and Tanzi, R.E. (1996) Association of a novel human FE65-like protein with the cytoplasmic domain of the beta- amyloid precursor protein. Proc. Natl. Acad. Sci. USA 93, 10832–10837.

[49] Borg, J.P., Ooi, J., Levy, E. and Margolis, B. (1996) The phosphotyrosine interaction domains of X11 and FE65 bind to distinct sites on the YENPTY motif of amyloid precursor protein. Mol. Cell Biol. 16, 6229–6241.

[50] Selkoe, D.J., Yamazaki, T., Citron, M., Podlisny, M.B., Koo, E.H., Teplow, D.B. and Haass, C. (1996) The role of APP processing and trafficking pathways in the formation of amyloid beta-protein. Ann. N. Y. Acad. Sci. 777, 57–64.

SUPPLEMENTARY DATA

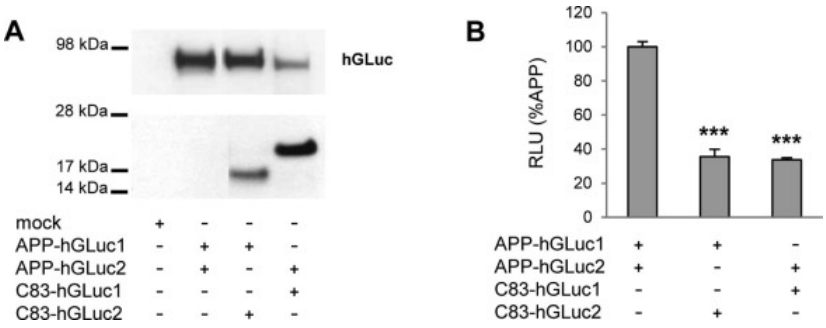

Supplementary Fig. 1. Dimerization of APP and C83 heterodimers.

Cells were transfected with the control empty vector (mock), the APP-hGLuc1 and 2, APP-hGLuc1 together with C83-hGluc2 or C83-hGLuc1 with APP-hGLuc2 constructs. (A) Protein expression was monitored in cell lysates by Western blotting with the hGLuc antibody. (B) Luciferase activity was measured and expressed as RLU normalized to APP (set to 100%). Values (means ± SEM) are representative of 3 independent experiments (n=4 in each experiment).*** $p<0.001$ as compared to APP-hGLuc1 and 2.

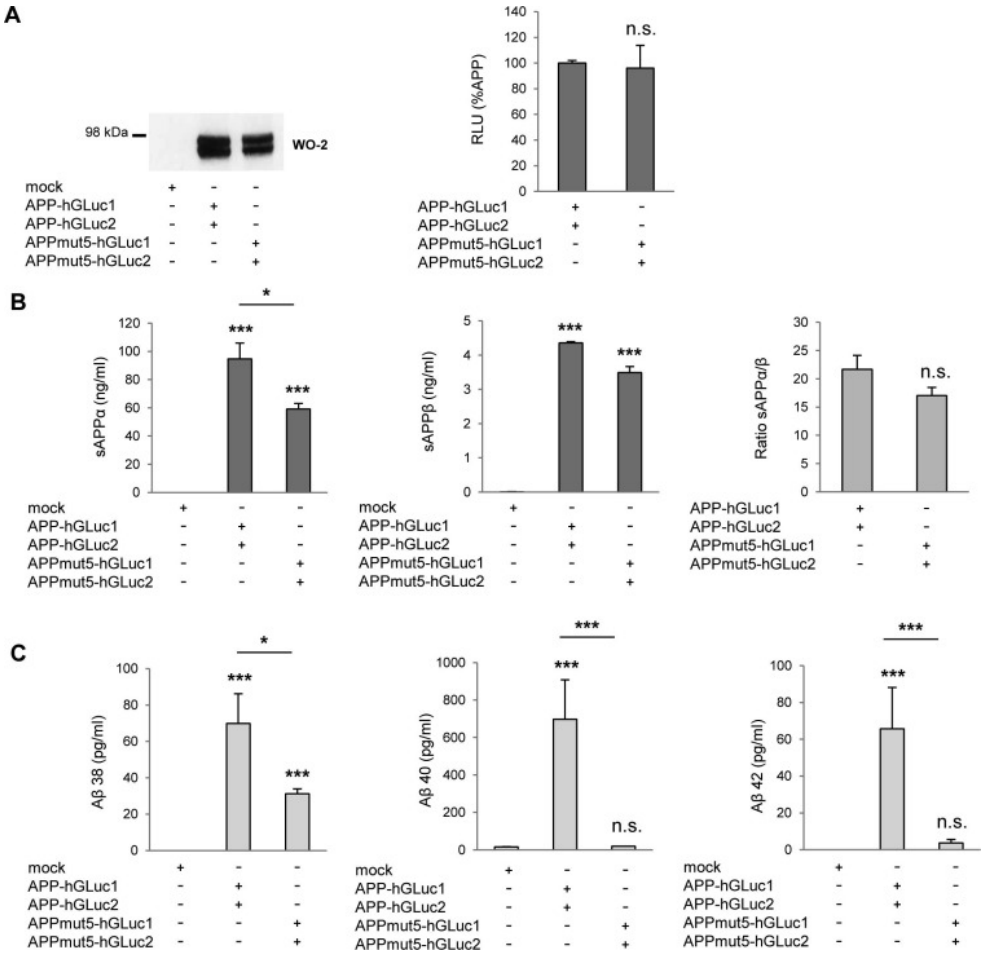

Supplementary Fig. 2. Dimerization and metabolism of APP GXXXG mutant 5.

CHO cells were transfected with APP-hGLuc1 and 2 and the corresponding GXXXG mutant 5 (mut5). (A) Protein expression in cells transfected with the control empty vector (mock), the APP-hGLuc1 or APPmut5-hGLuc1 and 2 proteins was monitored by Western blotting with the W0-2 antibody (left panel). Luciferase activity was measured and expressed as RLU normalized to non-mutated APP (right panel). Values (means ± SEM) are representative of 2 independent experiments (n=4 in each experiment). n.s. (non-significant), as compared to APP-hGLuc1 and 2. (B) sAPPα and β production of APP-hGLuc1 and 2 and APPmut5-hGLuc1 and 2 constructs were monitored by ECLIA in the culture media of cells and are given in ng/ml. * $p<0.05$, *** $p<0.001$, n.s. (non-significant), as compared to non-transfected cells or as indicated. Ratio of sAPPα to sAPPβ was calculated in the same experiments. n.s. (non-significant), as compared to APP-hGLuc1 and 2. (C) Aβ38, 40 and 42 production from APP-hGLuc1 and 2 or APPmut5-hGLuc1 and 2 was measured by ECLIA in the culture media and given in pg/ml. Values (means _ SEM) are representative of 3 independent experiments (n=4 in each experiment). * $p<0.05$, *** $p<0.001$, as compared to non-mutated APP.

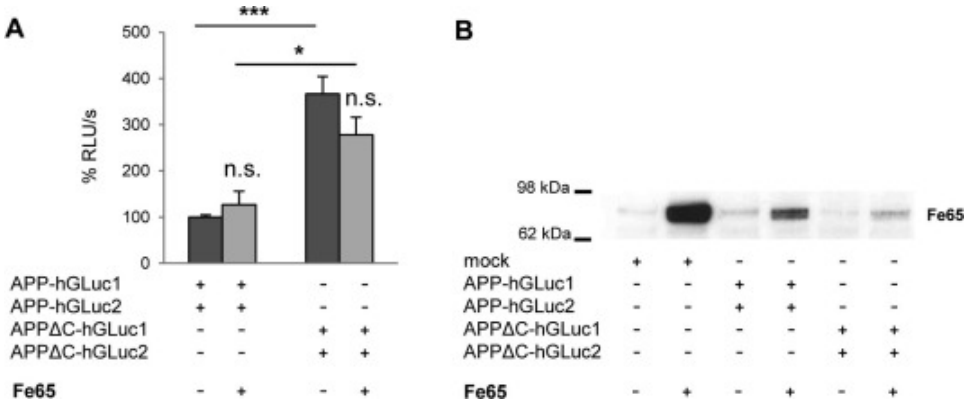

Supplementary Fig. 3. Influence of Fe65 overexpression on APP dimerization.

CHO cells were transfected with APP-hGLuc1 and 2 or APPΔC-hGLuc1 and 2 together with Fe65. (A) Luciferase activity was measured and expressed as RLU normalized to APP-hGLuc1 and 2 without Fe65 overexpression. Values (means ± SEM) are representative of 2 independent experiments (n=4 in each experiment). * $p<0.05$ and *** $p < 0.001$, as compared to APP- hGLuc1 and 2. (B) Expression of Fe65 in the different conditions was monitored by Western blotting using Fe65 antibody (Cell Signaling, Danvers, MA).

1.2 Analysis of the structural determinants involved in APP dimerization and processing

Together, the two following papers derived from the collaboration with Steven O. Smith and colleagues analyzed the role of the alanine 21 and the LVFF motif and depicted the structure of the C99 extracellular domain. These works explained how structural determinants present in APP C-terminal fragments modulate γ-secretase processing independently of dimerization.

Conformational changes induced by the A21G Flemish mutation

Author's contribution: Measure of the Aβ production by the C99 and C55 constructs with the Flemish (A21G, Aβ numbering) and LVFF/AAAA mutations.

These results have been published in Structure by Tang et al. in 2014 (Annex 2).

Our aim was to define the structural determinants involved in APP dimerization and processing; we contributed to the work of Tang and colleagues with the analysis of conformational changes induced in APP by the Flemish mutation.

There are several clusters of FAD mutations in APP, located close to the α-, β- and γ-secretase cleavage sites. These specific mutations impact Aβ production by increasing the total amounts of Aβ or favoring Aβ42 over the shorter isoforms. The Flemish mutation cluster is located below the α-cleavage site. The removal of a single methyl group in the Flemish mutant (A21G position) increased Aβ levels by approximately 2- to 4-fold, without interfering with the α-secretase (De et al., 1998;Tian et al., 2010). This work focuses on the impact of the Flemish mutation A21G on the structure of APP and its processing.

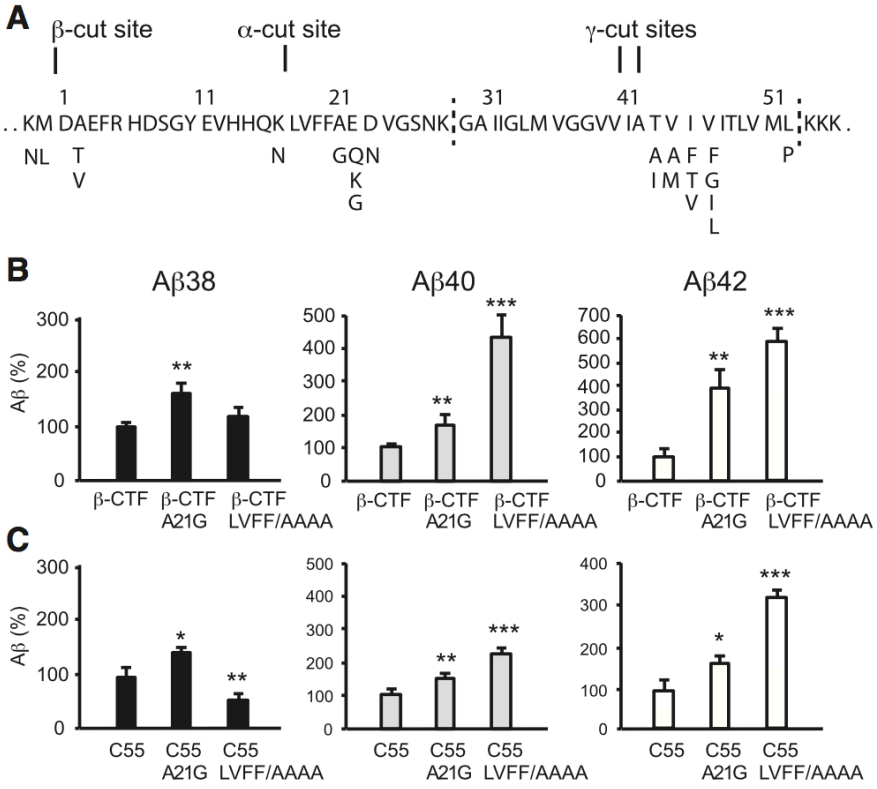

Fig. R1. Increase of Aβ Secretion in the A21G and LVFF to AAAA Mutations

(A) Sequence of the extracellular and TM regions of the βCTF. The βCTF is produced by β-secretase cleavage of APP. The first 28 amino acids form the extracellular region of the βCTF and contain the α-secretase cleavage site. The TM domain (denoted by vertical dashed lines) contains the site of γ-secretase cleavage. Both the extracellular and TM regions contain sites of familial AD mutations, shown as the single-letter amino acids below the sequence. **(B)** Comparison of the levels of Aβ38, Aβ40, and Aβ42 produced by γ-secretase cleavage of the WT βCTF, A21G, and LVFF to AAAA mutants. **(C)** Comparison of the levels of Aβ38, Aβ40, and Aβ42 produced by γ-secretase cleavage of WT C55 and the corresponding A21G and LVFF to AAAA mutants. Statistical significance was evaluated by one-way ANOVA followed by Dunnett's post hoc test. Values are the means ± SE, n > 5; *p < 0.05; **p < 0.01; ***p < 0.001, compared to control.

The precise structure of the APP JM/TM region has already been shown to have substantial effect on γ-secretase processing. The $L^{17}VFFA^{21}$ motif, containing the alanine 21 is an inhibitory motif. Its deletion increased γ-secretase efficiency about 25-fold (Fig.R1A) (Tian et al., 2010). A21G mutation has been suggested to disrupt the LVFFA effect and to alter APP interaction with the γ-secretase. On the opposite, the $G^{25}SNK^{28}$ motif located few residues below the LVFFA had the opposite effect (Ren et al.,2007). Structural analysis of the C99 structure has shown helical structures for the LVFF sequence and the TM domain containing the GXXXG motifs. The Flemish mutation can therefore increase the helical structure and influence TM helices dimerization and processing.

In this paper, we first confirmed that the A21G mutation and the LVFF-to-alanine (LVFF/AAAA) mutation increase the Aβ production from C99 (Fig.R1B) but also from C55 (Fig.R1C). C55 represents the minimal sequence containing the entire TM domain of the βCTF needed for γ-secretase processing.

Measurements of C55 structure in synthetic bilayers provided evidence that the extracellular sequence comprising the LVFF motif has a β-strand secondary structure. The Ala21 is at the edge of the β-sheet folding and its mutation to glycine influences the upstream sequence. The A21G mutation resulted in large chemical changes in the $F^{19}F^{20}$ and Gly25 residues, inducing structural modifications in the LVFF as well as GSNK structures and favoring Aβ production.

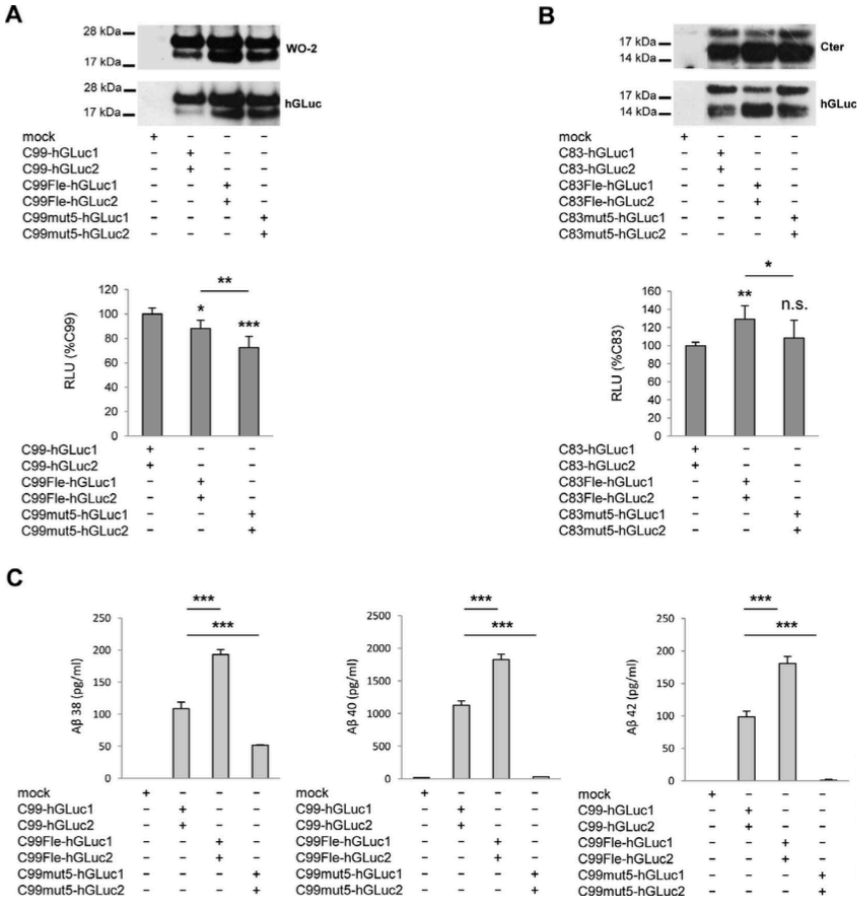

Fig. R2. Involvement of GXXXG motifs in CTF dimerization and Ab production. CHO cells were transfected with C99-hGLuc1 and 2 or C83-hGLuc1 and 2 and their GXXXG Flemish (Fle) and mutant 5 (mut5) corresponding mutants.

(A) Cells transfected with the control empty vector (mock), the C99-hGLuc1 and 2, C99Fle-hGLuc1 and 2 or C99mut5-hGLuc1 and 2 proteins. Protein expression was monitored in cell lysates by Western blotting with the W0-2 or hGluc antibodies (top panels). Luciferase activity was measured and expressed as RLU normalized to non-mutated C99 (bottom). Values (means ± SEM) are representative of 5 independent experiments (n = 4 in each experiment).*p < 0.05, **p < 0.01 and ***p < 0.001, as compared to C99-hGLuc1 and 2. **(B)** Cells transfected with the control empty vector (mock), the C83-hGLuc1 and 2, C83Fle-hGLuc1 and 2 or C83mut5-hGLuc1 and 2 proteins. Protein expression was monitored in cell lysates by Western blotting with the Cter or hGLuc antibodies (top panels). Luciferase activity was measured and expressed as RLU normalized to non-mutated C83 (bottom). Values (means ± SEM) are representative of 3 independent experiments (n = 4 in each experiment). *p < 0.05, **p < 0.01 and n.s. (non significant), as compared to C83-hGLuc1 and 2. **(C)** Aβ 38, 40 and 42 production for C99-hGLuc1 and 2, C99Fle-hGLuc1 and 2 or C99mut5-hGLuc1 and 2 was measured by ECLIA in the culture media and given in pg/ml. Values (means ± SEM) are representative of 3 independent experiment (n = 4 in each experiment). ***p < 0.001, as compared to non-mutated C99.

Structural measurements showed unambiguously that the A21G dimer is mediated by the GXXXG interface. However, they also observed that the Flemish mutation only had a small impact on dimerization. It implies that the large influence of the mutation on γ-secretase processing is associated with the structural changes in the JM domain rather than with dimerization. These results are consistent with our data published in FEBS Open Bio showing that Flemish and mut5 mutations have strong influences on processing (Fig.R2C) but only slight impacts on dimerization of CTFs measured by split-luciferase (Fig.R2A and B from Fig.6 Decock et al., 2015).

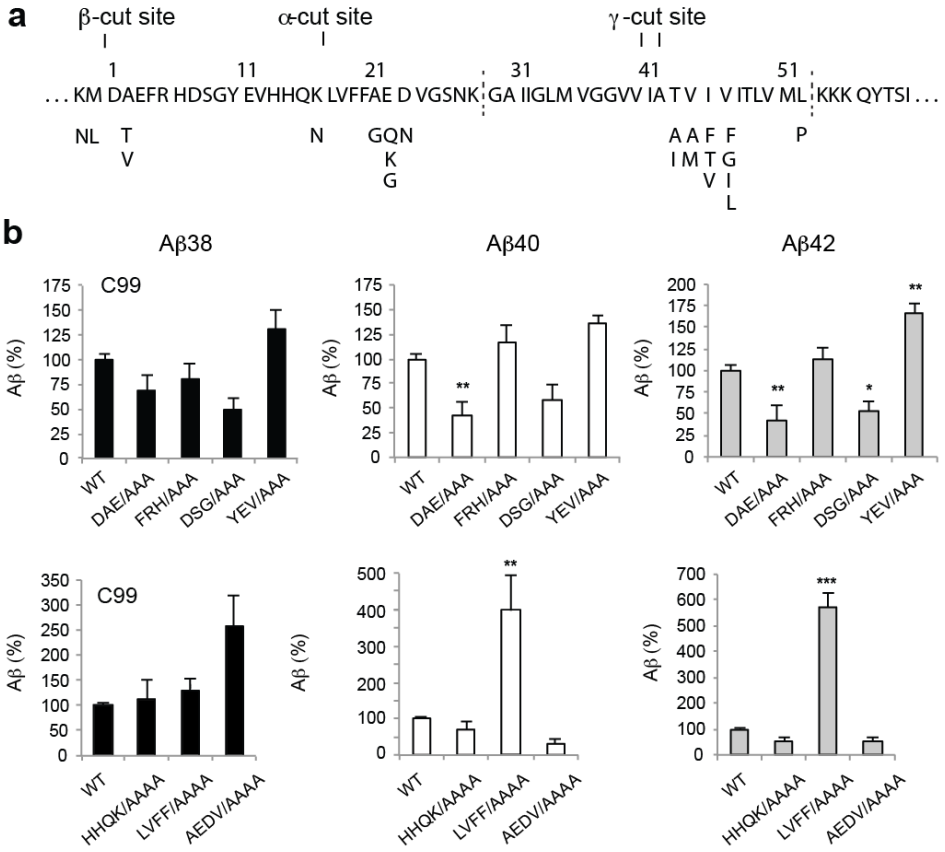

Fig. R3. Sequence and processing of C99

(a) Sequence of the extracellular and transmembrane domains of C99. The α-, β- and γ-cleavage sites are shown. The substrate numbering is based on the APP695 isoform of APP, where Asp597 corresponds to the first residue (*i.e.* Asp1) of the βCTF. In the following, we use the βCTF numbering, which coincides with the numbering of the Aβ peptides. **(b)** Alanine scanning mutagenesis of the extracellular domain of C99 reveals increased Aβ production. Comparison of the levels of Aβ38, Aβ40 and Aβ42 produced by γ-secretase cleavage of wild-type βCTF and the corresponding N terminal alanine mutants. Values are the means ± S.E., n > 5; *, p < 0.05; **, p < 0.01; ***, p < 0.001, compared with control.

The LVFF motif bears a β-sheet structure able to modulate the γ-secretase processing

Author's contribution: Measure of the Aβ production by the C99 and C55 constructs comprising the alanine-scanning mutations.

These results are in submission by Hu Y et al.

It has already been suggested that the $L^{17}VFFA^{21}$ sequence is part of an inhibitory motif modulating γ-secretase processing (Tian et al., 2010;Tang et al., 2014). Upon deletion of this motif in the C99, the catalytic efficiency of γ-secretase increases dramatically. It was demonstrated that this LVFFA sequence folds into an anti-parallel β-sheet secondary structure. The Flemish A21G mutation severely impaired the inhibitory effect of this region, implying that the interaction between APP and γ-secretase is altered upon mutation. The conclusions from the first collaboration were that the C99 extracellular domain has a β-sheet conformation, and that transition region between the extracellular and TM domain has a substantial effect on the position of γ-cleavage. This new paper focused deeper on the role of each motif and residue comprised in the extracellular/juxtamembranaire domain of APP C-terminal fragments and more precisely on the so-called LVFFA motif.

To analyze the impact of each part of the extracellular domain on the structure and processing of C99, here, alanine-scanning mutations were performed along the whole domain and more precisely in the LVFFA motif (Fig.R3a). The β-conformation of each mutant was assessed by structural analyses of the C55 (the 55-first amino acids of the C99 including its extracellular and TM domain). We measured the Aβ levels of every mutant, monitoring the interaction with the γ-

secretase. Finally, the location of the LVFF sequence was measured relatively to the membrane bilayer.

Structural analysis on C55 confirmed a β-sheet secondary structure in the YEV and LVFF sequences, roughly correlated with the increased processing upon their mutation. The FF residues of the LVFF sequence and more particularly the F19 position are critical to the formation of the β structure in C99 extracellular domain. FF are part of an inhibitory motif (LVFFA) termed ASID (APP substrate inhibitory motif), negatively modulating γ-secretase activity (Tian et al., 2010). The very 16 N-terminal amino acids were shown to have a specific role in the regulation of the ASID inhibitory potency. Mutation within the intervening HHQK sequence did not influence the β-sheet band, suggesting that this region forms a loop connecting the YEV and LVFF β-strands. The LVFF sequence is inserted into the bilayer region of the membrane. The GYEV motif, comprised in the 16 N-terminal amino acids, is deleted upon cleavage by the α-secretase, leading to loss of the β-sheet structure. Together, these data suggested that the N-terminal part of βCTF plays a role in the down-regulation of APP and γ-secretase interaction. Importantly, mutation to alanine of YEV and of LVFF stretches led to higher levels of amyloidogenic processing (Fig.R3), further supporting the notion that these sequences cooperate.

1. Role of the extracellular sequence in C99 processing

Analyses of Aβ levels from C99 with alanine mutation of the $D^{1}A^{2}E^{3}$ and $D^{7}S^{8}G^{9}$ sequences showed a reduction in the levels of Aβ38, Aβ40, significant for the Aβ42 (Fig.R3b). The highest effect of alanine mutation within the N-terminal part of C99 laid in the $Y^{10}E^{11}V^{12}$ sequence. Mutation of YEV to AAA led to a slight increase in Aβ38 and Aβ40, concomitant with a significant increase in Aβ42. These

results indicate that the structure or interactions of the N-terminal residues of C99 also influence γ-secretase processing.

Within the second 12 residues of the C99 sequence, mutation of the $H^{13}H^{14}Q^{15}K^{16}$ and $A^{21}E^{22}D^{23}V^{24}$ sequences to alanine resulted in slightly decreased Aβ40 and Aβ42 production (Fig.R3b). However, mutation of the intervening $L^{17}V^{18}F^{19}F^{20}$ sequence resulted in a significant increase in secreted Aβ40 and Aβ42. Comparison of the mutational results in the C99 ectodomain clearly showed the largest influence in Aβ production derives from the LVFF motif.

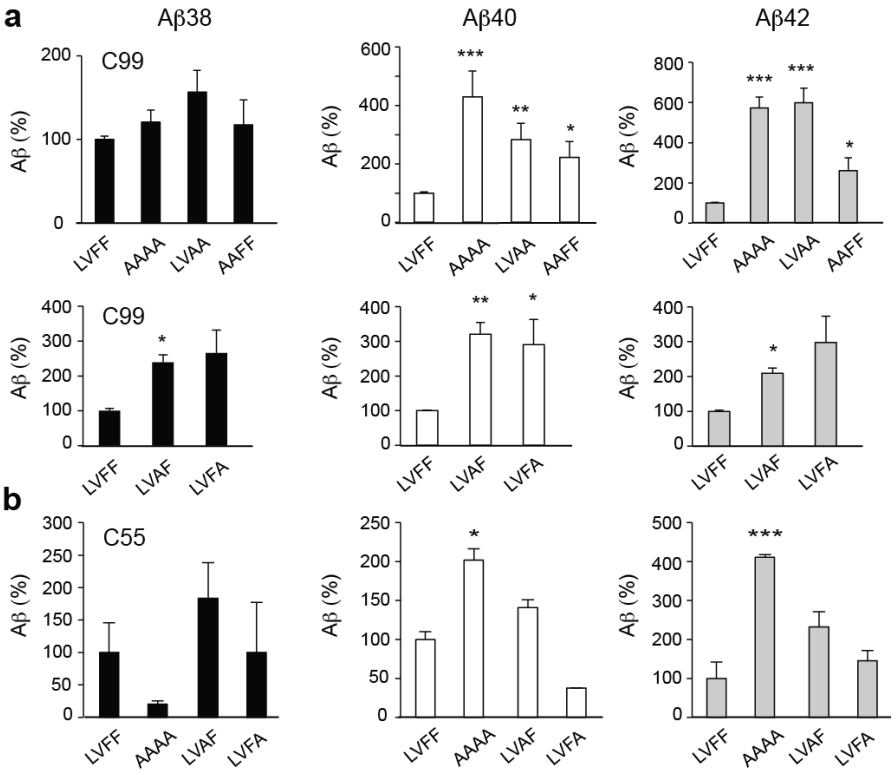

Fig. R4. Processing data on double and single mutants within the LVFF sequence of C99

Alanine scanning mutagenesis of the C99 LVFF motif reveals the critical role of F19 and F20. Comparison of the levels of Aβ38, Aβ40 and Aβ42 produced by γ-secretase cleavage of wild-type motif (LVFF) and the corresponding N terminal alanine mutants.C99 **(a)** and C55 **(b)**. Values are the means ± S.E., n > 5; *, p < 0.05; **, p < 0.01; ***, p < 0.001, compared with control.

2. Phe19 and Phe20 are critical determinants for C99 and C55 processing

To better define the LVFFA residues involved in the control of the extracellular domain structure of APP, single/double amino acids replacements were performed in the LVFF motif of C99 and C55. In the C99, $F^{19}F^{20}$ sequence contributes to a higher production of Aβ40 and Aβ42 than the $L^{17}V^{18}$ sequence (Fig.R4a). The individual mutation of FA and AF resulted in comparable effects. Mutation of LVFF to AAAA in the C55 resulted in significant increase in Aβ40 and Aβ42 (Fig.R4b). However, the individual amino acid changes on F19 led to higher levels of secreted Aβ40 and Aβ42 than for the F20A mutant.

We also investigated the dimerization of the C99 LVFF mutant by split-luciferase assay (unpublished data). On the contrary to the Flemish mutant A21G, we observed a strong dimerization upon mutation of the LVFF inhibitory motif (Fig.R5). This suggests that disruption of the LVFF inhibitory motif allows stronger interaction of the TM helices. The cleavage of CTFs dimers by the γ-secretase is still controversial and needs further understanding (Scheuermann et al., 2001;Eggert et al., 2009;Winkler et al., 2015).

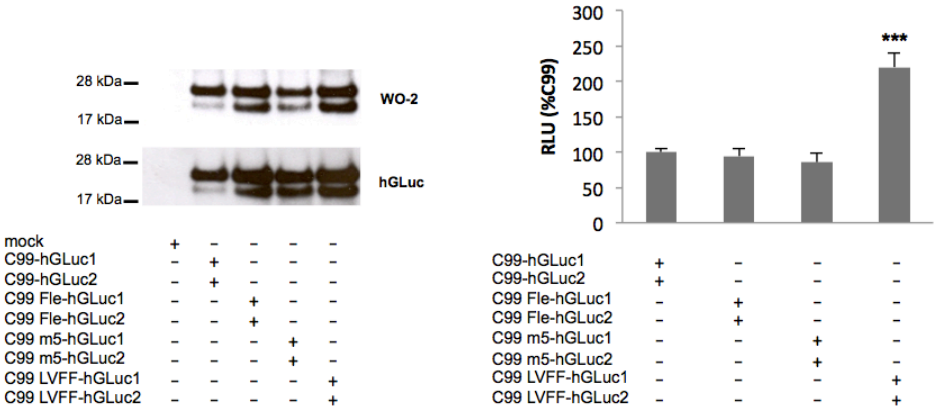

Fig. R5. Dimerization of C99 Flemish (Fle), mut5 (m5) and LVFF mutants (unpublished data)

Cells transfected with the control empty vector (mock), the C99-hGLuc1 and 2, C99Fle-hGLuc1 and 2, C99m5-hGLuc1 and 2 or C99LVFF-hGLuc1 and 2 proteins. Protein expression was monitored in cell lysates by Western blotting with the W0-2 or hGluc antibodies (left panels). Luciferase activity was measured and expressed as RLU normalized to non-mutated C99 (bottom). Values (means ± SEM) are representative of 5 independent experiments (n = 4 in each experiment). ***$p < 0.001$, as compared to C99-hGLuc1 and 2.

β-Sheet Structure within the Extracellular Domain of C99 Regulates Processing

Yi Hu[1], Pascal Kienlen-Campard[3], Tzu-Chun Tang[1], Xiaoshu Pan[1], Marie Decock[3], Joanne Van Hees[2], Ziao Fu[1], Jean-Noel Octave[3], Stefan N. Constantinescu[2] and Steven O. Smith[1*]

[1]Department of Biochemistry and Cell Biology, Stony Brook University, Stony Brook, NY 11794-5215.
[2]Ludwig Institute for Cancer Research and de Duve Institute, Université catholique de Louvain, Brussels 1200, Belgium

[3]Institute of Neuroscience, Université catholique de Louvain, Brussels 1200, Belgium.

Running title: *Structure of Extracellular Region of C55*

In submission

2. GXXXG/A motifs in the formation of pathogenic Aβ oligomers

We studied the role of TM GXXXG and GXXXA motifs in the formation of pathogenic oligomers in living cells. Since a decade, there is growing evidence that oligomeric Aβ triggers the toxicity in AD pathogenesis. We observed a unique ±25-30 kDa Aβ oligomeric form produced in CHO cells cellular compartments upon expression of C99 and C42 (corresponding to Aβ42). These oligomers are highly stable and could correspond to hexamers.

The Aβ comprises the JM/TM domain of APP. GXXXG TM motifs has been investigated in full-length APP and CTFs but it remains controversial whether they mediate or not dimerization. Here we analyzed the role of $G^{29}XXXG^{33}$ and $G^{38}XXXA^{42}$ motifs in the formation of Aβ oligomers. We performed alanine mutation in the central $G^{29}XXXG^{33}$ motif (mutant 5/m5) and in the $G^{38}XXXA^{42}$ motif (mutant A/mA) to analyze their oligomerization in cells.

GXXXG motifs and above all the GXXXA motif were critical for the oligomerization process. Interestingly, the GXXXA Ala42 is the last residue of the Aβ42 peptide, deleted in the Aβ40 isoform. Mutations affecting both GXXXG and GXXXA motifs showed intermediate oligomers production. The Gly38 showed a dominant effect and reduced importantly the formation of Aβ oligomers. Finally, these assemblies did not show any toxicity in survival assay but highly affected neuronal differentiation in a model of cholinergic neurons (NG108-15). NG108-15 cells treated with medium from C42 and C42m5 enriched in oligomers, showed impaired differentiation and reduced neurite outgrowth. On the contrary, the maturation of cells treated with media of C42mA-expressing cells, in which no

oligomeric Aβ is detected, had an appropriate differentiation pattern similar to control-treated cells.

Together, our data suggested that differentiation and neurite outgrowth of neuronal cells are impaired by the presence of the Aβ oligomers produced by living cells. These oligomers are highly stable and the GXXXG/A motifs present in their sequence are critical for their association.

This work has been submitted for reviewing on February 22nd, 2016 in Frontiers in Aging Neuroscience in the format of the following paper.

Glycines from the APP GXXXG/GXXXA transmembrane motifs promote formation of pathogenic Aβ oligomers in cells

Marie Decock[1], Serena Stanga[1], Jean Noël Octave[1], Ilse Dewachter[1], Steven O. Smith[2], Stefan N. Constantinescu[3#], Pascal Kienlen-Campard[1#*]

[1]Institute of Neuroscience, Université catholique de Louvain, Brussels 1200, Belgium
[2]Department of Biochemistry and Cell Biology, Stony Brook University, Stony Brook, NY 11794-5215, USA
[3]Ludwig Institute for Cancer Research and Université catholique de Louvain, de Duve Institute, Brussels 1200, Belgium
[#] These authors contributed equally

Running title: *GXXXG motifs and Aβ oligomers*

Submitted to Frontiers in Aging Neuroscience on February 22, 2016.

*Correspondance to:

Pascal Kienlen-Campard

Université catholique de Louvain

Institute of Neuroscience IoNS/CEMO

Avenue Mounier 53 box B1.53.02

B-1200 Brussels BelgiumPhone.: +32 2 764 93 35 Fax: +32 2 764 54 60

E-mail: pascal.kienlen-campard@uclouvain.be

ABSTRACT

Alzheimer's disease (AD) is the most common neurodegenerative disorder characterized by progressive cognitive decline leading to dementia. The amyloid precursor protein (APP) is a ubiquitous type I transmembrane (TM) protein sequentially processed to generate the β-amyloid peptide (Aβ), the major constituent of senile plaques that are typical AD lesions. There is a growing body of evidence that soluble Aβ oligomers correlate with clinical symptoms associated with the disease. The Aβ sequence begins in the extracellular juxtamembrane region of APP and includes roughly half of the TM domain. This region contains GXXXG and GXXXA motifs, which are critical for both TM protein interactions and fibrillogenic properties of peptides derived from TM α-helices. Glycine-to-leucine mutations of these motifs were previously shown to affect APP processing and Aβ production in cells. However, the detailed contribution of these motifs to APP dimerization, their relation to processing, and the conformational changes they can induce within Aβ species remains undefined. Here, we describe highly resistant Aβ42 oligomers that are produced in cellular membrane compartments. They are formed in cells by processing of the APP amyloidogenic C-terminal fragment (C99), or by direct expression of a peptide corresponding to Aβ42, but not to Aβ40. By a point-mutation approach, we demonstrate that glycine-to-leucine mutations in the $G^{29}XXXG^{33}$ and $G^{38}XXXA^{42}$ motifs dramatically affect the Aβ oligomerization process. G33 and G38 in these motifs are specifically involved in Aβ oligomerization; the G33L mutation strongly promotes oligomerization, while G38L blocks it with a dominant effect on G33 residue modification. Finally, we report that the secreted Aβ42 oligomers display pathological properties consistent with their suggested role in AD, but do not induce toxicity in survival

assays with neuronal cells. Exposure of neurons to these Aβ42 oligomers dramatically affects neuronal differentiation and, consequently, neuronal network maturation.

Keywords: Alzheimer's disease, amyloid precursor protein, beta-amyloid peptide, oligomers, GXXXG motifs, neuronal differentiation

INTRODUCTION

The amyloid precursor protein (APP) is a ubiquitously expressed type 1 transmembrane protein (Kang et al., 1987;Selkoe, 2004) whose processing in the amyloidogenic pathway leads to the production of the β-amyloid peptides (Aβ). Aβ peptides are the major constituent of the senile plaques, a hallmark of AD (Glenner and Wong, 1984). Mutations responsible for inherited AD cases (early-onset or familial AD) are located in the genes coding for APP or the presenilins. The presenilins (PS1 and PS2) are the catalytic subunits of γ-secretase, a multiprotein complex that cleaves the APP β-C-terminal fragment (βCTF or C99) to generate Aβ in the last step of the amyloidogenic pathway. APP or PS mutations typically result in imbalanced Aβ production and an increased Aβ42/Aβ40 ratio (Selkoe, 2004). These observations led to the amyloid cascade hypothesis, predicting that the initial steps of AD, which initiate a cascade of pathogenic events, are related to Aβ production and clearance, (Hardy and Allsop, 1991). Although this hypothesis remains a matter of debate (Herrup, 2015), experimental lines of evidence from cellular models, transgenic animals and patient brain samples has been overwhelming (Hardy, 2009).

AD onset and progression appears to be directly linked to the accumulation of abnormally folded Aβ assemblies. Although fibrillogenic species were first suggested to be responsible for AD-induced neurotoxic events, growing evidence shows that soluble Aβ oligomers are more strongly correlated with clinical symptoms associated with the disease (Lesne et al., 2006;McDonald et al., 2010). Different Aβ oligomers have been described, ranging from dimers to dodecamers and high molecular weight assemblies. These assemblies can be classified between an “off-pathway” or an “on-pathway” with respect to fibrillization.

Soluble oligomers have been characterized in transgenic mouse brains (Kawarabayashi et al., 2001;Lesne et al., 2006;Shankar et al., 2009;Pham et al., 2010), and to some extent in brains of AD patients (Hayden and Teplow, 2013). Still, the key toxic Aβ species remain poorly defined in terms of both molecular structure and relevance to the mechanisms underlying long term potentiation defects and neuronal cell death.

Structural studies on Aβ assemblies have largely come from *in vitro* measurements of synthetic peptides corresponding to Aβ40 and Aβ42. Aβ40 is the predominant isoform (~90%) generated by γ-secretase cleavage, while Aβ42 (10%) is the major component of amyloid plaques. Monomeric Aβ has predominantly a random coil structure. Monomers associate into small MW oligomers (dimers – hexamers) which are able to associate into larger MW oligomers that laterally associate into protofibrils. The conversion of protofibrils to fibrils involves a transition to cross-β-structure. The conversion involves association of the short hydrophobic LVFF sequence with the hydrophobic C-terminus of Aβ (Fu et al., 2015).

Glycines appear to be important in both the turn region between β-strands and in the C-terminal β-sheet. Glycines have a critical impact on peptide aggregation, facilitating the association of β-sheets during fibril formation *in vitro* (Sato et al., 2006;Liu et al., 2005). Fibrillization of synthetic Aβ peptides containing glycine-to-leucine (G to L) mutations has been monitored *in vitro* (Kim and Hecht, 2006;Hung et al., 2008). Treatment of neuronal cells showed a reduction of toxicity for mutated peptides when compared to non-mutated Aβ. Reduced toxicity correlated with a reduction of small oligomeric species in solution and increased rates of fibril formation (Hung et al., 2008). Harmeier and colleagues highlighted G33 as critical for the generation of Aβ42 assemblies (Harmeier et al., 2009). Mutation of G33 promoted rapid Aβ oligomerization by conformational changes

that favored the formation of high molecular weight oligomers. In contrast, a G37L substitution dramatically reduced Aβ toxicity as measured by cell dysfunction, cell death, synaptic alteration in primary neurons and transgenic *C. elegans* models (Fonte et al., 2011). Important limitations in studies using synthetic Aβ peptides to generate oligomers *in vitro* are their exact relevance to AD pathology. The soluble oligomers are formed *in vitro* at relatively high concentrations. At lower concentrations, which may be more representative of physiological conditions, the monomer – oligomer equilibrium shifts toward the monomeric state, which is non-toxic and presumably is more easily cleared from the brain. The structure and stability of soluble oligomers that are produced physiologically have consequently been of considerable interest.

G33 and G37 lie within the hydrophobic C-terminus of the Aβ peptide and represent a GXXXG motif. This motif occurs abundantly in the TM helices of membrane proteins where it facilitates TM helix dimerization. Strikingly, C99 has three consecutive GXXXG motifs, followed by a GXXXA motif, all of which have been implicated in dimerization and regulation of C99 processing by the γ-secretase (Kienlen-Campard et al., 2008;Munter et al., 2007).. The structural role that the GXXXG motif plays critically depends on the structural element in which it occurs and the exposure to water. In aqueous environments, glycine is able to adopt multiple conformations due to the lack of a side chain and the ability of the backbone NH to hydrogen bond to water (glycine is known as a helix breaker in soluble proteins and often occurs in turn sequences.) In hydrophobic TM helices, glycines in a GXXXG motif fall on one face of a TM α-helix and facilitate helix-helix dimerization. The TM helices are energetically favored due to intrahelical backbone hydrogen bonding in the absence of water and helix association is favored due to interhelical van der Waals and hydrogen bonding interactions. Interestingly, in β-sheet the glycines in a GXXXG motif lie on one face of the β-

sheet and when the β-strands are parallel and in-register, they form long surface grooves that facilitate sheet-to-sheet packing that excludes water (Sato et al., 2006). This multifaceted nature of glycine is highlighted in its role at each stage of the process from TM helix to soluble oligomer to fibril. The same multifaceted nature of glycine may underlie the aggregation of the human prion protein, which also contains three consecutive GXXXG motifs.

We have further investigated the role of the GXXXG/GXXXA motifs in dimerization of C99 and oligomerization of Aβ produced by living cells. We found that mutation of the critical G33 and G38 residues, respectively, in the $G^{29}XXXG^{33}$ and $G^{38}XXXA^{42}$ motifs did not affect dimerization of C99. In contrast, mutations in these motifs triggered the assembly of Aβ42 into ~28 kDa oligomers corresponding to the expected molecular weight of Aβ hexamers. Similar oligomers are not detected with constructs producing only Aβ40. The Aβ42 oligomers generated by living cells are resistant to temperature and denaturing conditions. They are enriched in membrane-bounded compartments, and released in the extracellular medium. Finally, we showed that Aβ42 oligomers generated by living cells did not display neurotoxic effects, but greatly affected neuronal differentiation and the formation of neuronal networks.

MATERIAL AND METHODS

Chemicals and reagents

Restriction enzymes, Taq DNA polymerase, all culture media, penicillin-streptomycin solution, HAT and Lipofectamine® transfection reagents, Nu-Page® Novex® 4-12% Bis-Tris gels and buffers were from Life Technology Corporation (Carlsbad, CA). Fetal bovine serum (FBS) for culture media was purchased from Thermo Scientific (Rockford, IL). Analytical grade solvents, salts and poly-L-lysine were from Sigma-Aldrich (St Louis, MO). Protease inhibitor cocktail was purchased from Roche (Basel, Switzerland). BCA protein assay kit was from Pierce (Rockford, IL, USA). Nitrocellulose membranes were obtained from GE Healthcare (Fairfield, CT). ECL reagents were obtained from Perkin Elmer Inc. (Waltham, MA). The following primary antibodies were used: anti-Amyloid β Antibody, clone W0-2 (EMD Millipore, Billerica, MA), Anti-Amyloid Precursor Protein C-terminal, anti-MAP2 and anti-actine antibody (Sigma-Aldrich, St Louis, MO), and anti-GLuc antibody (New England Biolabs, Ipswich, MA).. Fluorescent nucleic acid stain DAPI was obtained from Sigma-Aldrich (St Louis, MO). Secondary antibodies coupled to HRP were obtained from Amersham Bioscience (Uppsala, Sweden) and fluorescent secondary antibody coupled to Alexa fluorochromes from Life Technology Corporation (Carlsbad, CA).

Cells lines and cell culture

Chinese hamster ovary (CHO) cell lines were grown in Ham's F-12 medium. The media was supplemented with 10% of fetal bovine serum (FBS) and penicillin-

streptomycin solution (10 units-10 µg). All cell cultures were maintained at 37 °C in a humidified atmosphere (5% CO_2). Mouse neuroblastoma x Rat glioma hybrid cell lines (NG108-15) were grown in DMEM supplemented with 10% FBS, 2% HAT, a mixture of hypoxanthine, aminopterin and thymidine, and antibiotics. Differentiation of NG108-15 cells was induced by switching from regular medium to 1% FBS medium (Stanga et al., 2015).

Plasmids, cloning and site-directed mutagenesis

C99, C42 mutants and various C-terminally truncated constructs of C99 were obtained by Quick-change site-specific mutagenesis (Stratagene, La Jolla, CA) as previously described (Ben et al., 2012b). The plasmids expressing APP fragments fused to humanized *Gaussia* luciferase (hGluc) halves were obtained by PCR amplification of APP sequences encoded by expression vectors previously described (Decock et al., 2015). All constructs were verified by full sequencing (Macrogen Europe, Amsterdam, The Netherlands).

Cell transfection and conditioning

CHO cells were transfected with Lipofectamin reagent 24 hours after seeding following manufacturer's instructions. Plasmids expressing the split-luciferase proteins were cotransfected in a 1:1 ratio. The control plasmid (mock) used was the corresponding empty vector. 48 hours after transfection, media were collected, treated with protease inhibitors cocktail (Roche) and stored at -20°C for ECLIA assay. Cells were harvested and lysed in sample buffer (125 mM TrisHCl pH 6.8, glycerol 20% and SDS 4%) supplemented with protease inhibitor cocktail.

Protein concentrations were measured by the BCA protein assay kit from Pierce (Rockford, IL, USA) prior to Western blotting.

Transfected CHO cell culture media have been used as source of oligomers to treat NG108-15 cells at day 1 and day 3 of differentiation. One day after transfection, CHO cells were maintained in medium without FBS. The CHO conditioned media enriched in oligomers were mixed (1:1 ratio) to NG108-15 cells differentiation medium (1% FBS). Treated NG108-15 cells were fixed and processed for immunocytochemistry (day 5).

Western blotting

Proteins (10 µg) from cell lysates or culture media (20 µl) were heated for 10 minutes at 70 °C in loading buffer (lysis buffer supplemented with 0.5 M DTT and staining Nupage blue™), separated in 4–12% Nupage™ bis-Tris gel and transferred for 2 hours at 30 V onto nitrocellulose membranes. Ponceau Red staining was used to check gel loading and transfer accuracy. After blocking (5% non-fat milk in PBS), membranes were incubated overnight at 4 °C with the primary antibodies: anti-Amyloid β Antibody, clone W0-2 (1/2,500), Anti-Amyloid Precursor Protein, C-terminal antibody (1/2,000), anti-GLuc antibody (1/2,000). Membranes were washed with PBS-Tween (0.005%) and incubated with the secondary antibodies anti-mouse (1:10,000) or anti-rabbit (1:10,000) coupled to peroxidase prior to ECL detection from GE Healthcare (Little Chalfont, UK). Signals were quantified with a Gel Doc 2000 imaging system coupled to Quantity one™ software from Bio-Rad (Hercules, CA, USA).

Gaussia luciferase assay

Samples were aliquoted in 5 ml polystyrene round-bottom tubes at a final concentration of 10 µg of protein in 20 µl in Luciferase Cell Lysis Buffer (Promega, Madison, WI). Native coelenterazine was reconstituted as a stock solution of 1 mg/ml in methanol (stored frozen), diluted 30 minutes prior reading in DMEM without phenol red and used at a final concentration of 20 µM. 50 µl of coelenterazine was added to tubes and luminescence directly measured on a Sirius Luminometer (Berthold, Pforzheim, Germany).

Aβ quantification

Aβ38, Aβ40 and Aβ42 peptides were quantified in the cell medium as previously described (Hage et al., 2015a) using the Aβ multiplex electro-chemiluminescence immunoassay (ECLIA) (Meso Scale Discovery, Gaithersburg, MD). Cells were conditioned in serum-free medium for 16 hours; cell medium was collected and Aβ were quantified according to the manufacturer's instructions with the human Aβ specific 6E10 multiplex assay.

Cell survival assay

Cell viability (NG108-15 cells) was assessed with a MTS assay after 24 hours of treatment, according to manufacturer's instruction (Promega, Madison, WI). Plates were measured at 490 nm using a microplate spectrophotometer Victor X3 Multilabel Plate Reader (PerkinElmer, Waltham, MA).

Immunocytochemistry

Cells were seeded on 12-well plates previously incubated with poly-L-lysine (10 mg/ml). Prior to staining, cells were rinsed twice with Opti-MEM® (Life Technology Corporation) and fixed with 4% paraformaldehyde (PFA) for 15 min. After 3 washes in PBS, cells were permeabilized with PBS1X/0.3% Triton100X for 30 min and blocked in PBS1X/fetal bovine serum 5%/0.1% Triton100X for 30 min. Primary antibody MAP2 (1:500) was prepared in the blocking solution and incubated O/N at 4 °C. After 3 washes in PBS, cells were incubated with secondary antibody (Goat anti-mouse Alexa 488, 1:500 in blocking solution) and DAPI (1:2000) for 1 hour at 4 °C. After 3 washes in PBS, cells were stored in PBS-azide 0.1% at 4 °C. Pictures were acquired with an Evos fluorescence microscope (Advanced Microscopy Group, Mill Creek, Washington, USA).

Statistical analysis

The number of samples (n) in each experimental condition is indicated in figure legends. The data were analyzed using GraphPad Prism software by analysis of variance (ANOVA) followed by unpaired t test (2 experimental conditions) or by Bonferroni's Multiple Comparison tests (more than 2 experimental conditions).

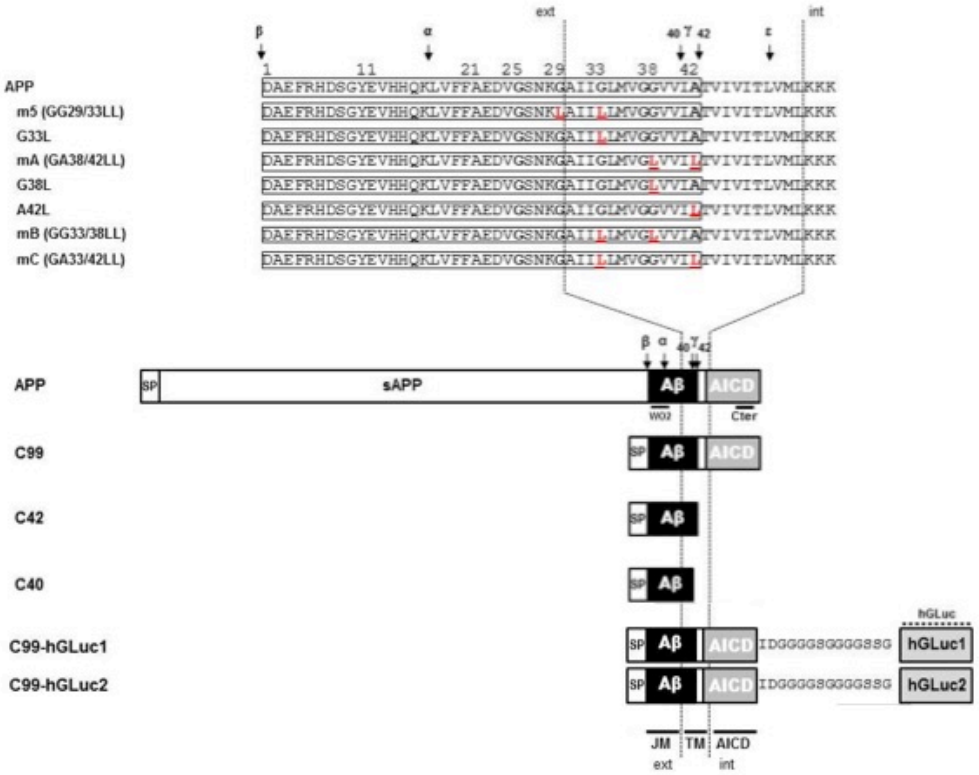

Figure 1. Schematic representation of the different APP mutants and APP constructs used for the study.

(A) Schematic representation of human APP and APP C-terminal fragments including the different mutatants generated. Numbering corresponds to aminoacid position in the Aβ sequence. C99 correspond to the APP β C-terminal fragment, C42 to the Aβ42 peptide and C40 to the Aβ40 petide. All C-terminal contructs are fused to the human APP signal peptide (SP). TM: Transmembrane region; JM: Juxtamembrane region; AICD: APP IntraCellular Domain; ext: extracellular; int: intracellular. The aminoacid substitutions generated by site-directed mutagenesis are in red. The cleavage sites of α (α)-, β (β)- and γ (γ and ε)-secretases are indicated by arrows. C99-hGLuc1 and C99-hGLuc2 correspond to C99 constructs fused to hGLuc moieties used for the analyzis of C99 dimerization in split luciferase assays. The epitopes recognized by the human-specific W0-2 antibody, the APP C-terminal and hGLuc antibodies are indicated.

RESULTS

Expression of APP C-terminal fragments leads to the accumulation of oligomeric Aβ peptides

In our previous work we reported that expression of C99 (corresponding to the β-CTF of APP) leads to the formation of an oligomer, which is detected in denaturating gels as a higher molecular weight band (around 25 kDa). These bands were thought to contain dimers of C99 (Kienlen-Campard et al., 2008), but also -possibly- oligomers of Aβ or other peptides, as well as a mix of C99 and truncated C99 peptides.

In order to characterize the nature of this higher molecular weight band, we expressed in CHO cells different APP constructs: human APP695 (neuronal isoform of APP), C99 (the amyloidogenic β C-terminal stub) and C42, which corresponds to the sequence of human Aβ42, that we engineered by adding a stop codon after residue 42 of Aβ. Both C99 and C42 are fused to the APP signal peptide to ensure proper targeting to the secretory pathway. Similar constructs were generated by introducing a stop codon after residue 40 of Aβ to generate C40, or by fusing gaussia luciferase moieties to the C-terminus of C99 to measure its dimerization by a split protein assay (Decock et al., 2015). All these constructs are depicted in **Figure 1**.

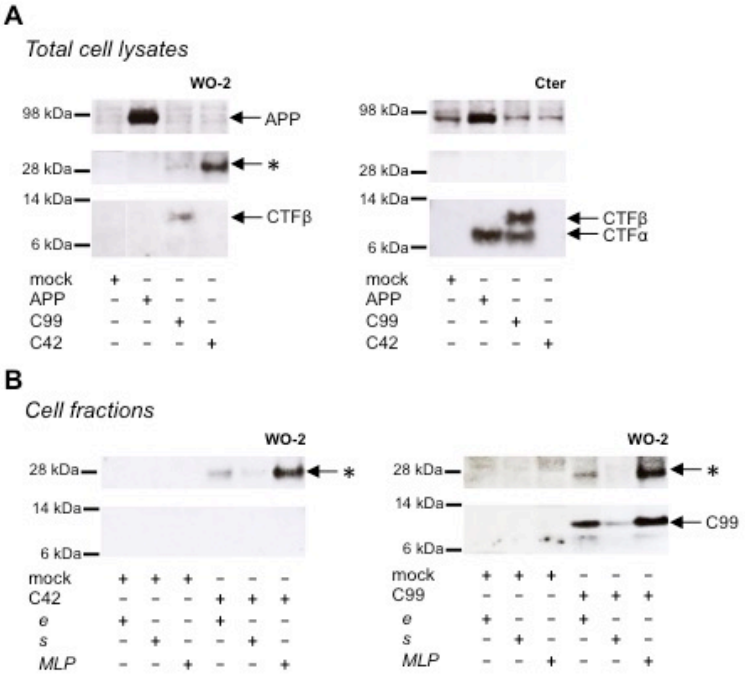

Figure 2. Detection of oligomeric bands in cells expressing C99 and C42.

(A) Expression of APP, C99 and C42 in CHO cells analyzed in total cel lysates by Western blotting with the W0-2 antibody (left panel) and the APP C-terminal antibody (right panel). The presence of APP, βCTF (C99) and and αCTF are indicated by arrows. The star (*) indicates the presence of an unexpected band around 30 kDa. (B) Cells fractions of C42- (left panel) and C99- (right panel) transfected cells were analyzed by Western blotting with the W0-2 antibody. Total cell lysates (e) were fractionated into soluble (s) and membrane-enriched vesicular fractions (MLP). The presence of the higher molecular weight band (*) is indicated by arrows.

As previously reported, βCTFs are barely detectable upon APP expression (**Figure 2**), the vast majority of APP being processed by the non-amyloidogenic pathway in cells (Haas et al., 1995). C99 expression (corresponding to βCTF) led to the detection of a monomeric band and the previously reported higher molecular weight band (**Figure 2A**). Strikingly, C42 expression produced a similar high molecular weight band, whereas no band corresponding to monomeric C42 was detected under these conditions. To note, this higher molecular weight band was not detected in APP-expressing cell lysates. We previously suggested (Kienlen-Campard et al., 2008) that this band could correspond to C99 dimers, but the molecular weight (~25-30 kDa) observed here is not consistent with this idea (**Figure 2A**). Importantly, the oligomeric band detected was not recognized by an antibody directed against the APP C-terminus that recognizes C99 and APP CTFs (**Figure 2A**). Sub-cellular fractionation experiments showed that the oligomeric band is enriched in vesicular compartments (MLP) but barely absent from the soluble fractions (**Figure 2B**), strongly suggesting that the oligomers -like C99- are either membrane associated, or present in a cell membrane-bounded compartment but not in the cytosol.

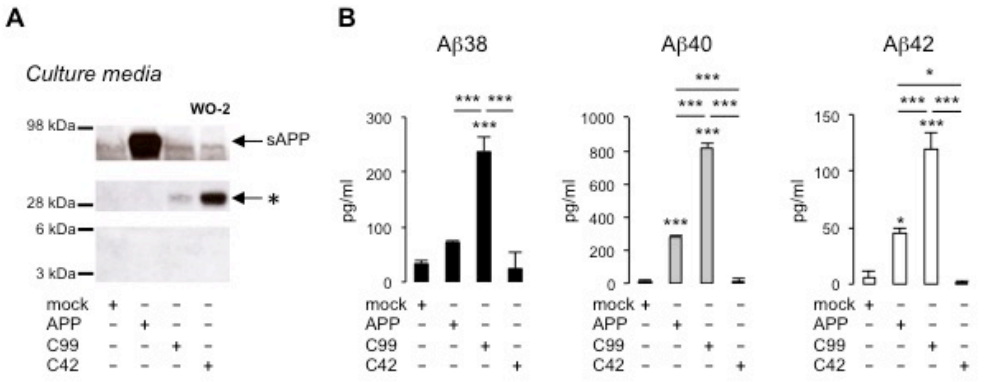

Figure 3. Detection of oligomeric bands and measurement of Aβ in the extracellular medium of cells expressing C99 and C42.

(A) Culture media of CHO cells expressing APP, C99 and C42 were analyzed by Western blotting using the W0-2 antibody. The ~ 30 kDa (*) detected in culture media -similar to the one observed in cell lysates- is indicated by an arrow. (B) Soluble monomeric Aβ 38, 40 and 42 were quantified by ECLIA in the culture media of transfected cells. Values (means ± SEM) given in pg/ml are representative of 3 independent experiments (n=3 in each experiment). *** p<0.001, * p<0.05, as compared to control (mock-transfected cells).

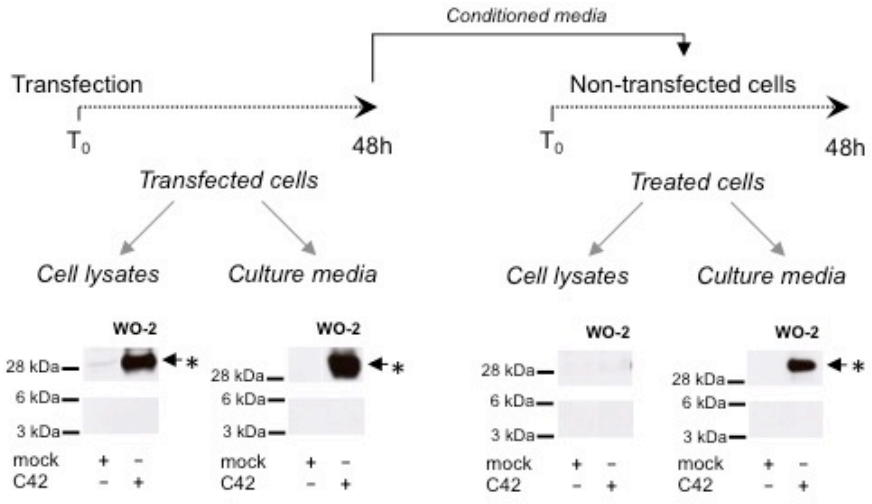

Figure 4. Oligomers detected in cells and not re-captured from the culture medium.

CHO cells were either transfected by the C42 construct (transfected cells) or treated (treated cells) for 48 h with the conditioned culture medium of C42-transfected cells (mock, non-transfected), as depicted on the top of the figure. The cell lysates and culture media of transfected and treated cells were recovered and analyzed by Western blotting with the W0-2 antibody. The ~ 30 kDa oligomeric band (*) detected in cell lysates and culture media is indicated by an arrow.

The same oligomeric bands were revealed by Western blotting in the culture medium of cells expressing either C99 or C42 (**Figure 3A**), but they were not detectable in the medium of cells expressing full-length APP. We measured the production of soluble Aβ in the culture media by the highly sensitive ECLIA multiplex Aβ assay, which detects soluble Aβ38/Aβ40/Aβ42 monomeric isoforms in the same sample (Hage et al., 2013;Hage et al., 2015b). As previously shown, soluble monomeric Aβ was readily detected in culture media of APP- and C99-expressing cells, with Aβ40 being the most abundant isoform. C99 constructs produced 3-5 times more Aβ than full length APP (**Figure 3B**). Strikingly, the C42 construct did not produce detectable Aβ, excepted very low amounts of Aβ38. Due to the specificity of the assay (soluble monomeric Aβ isoforms), this suggested that only oligomeric Aβ isoforms were generated by C42-expressing cells, in line with the higher molecular weight bands detected by an anti-human Aβ antibody in the same media (**Figure 3A**).

We next investigated whether the oligomeric bands detected in cells could correspond to oligomeric Aβ recaptured from the culture medium. We used conditioned media of C42-expressing cells to treat non-transfected cells for 48 hours. Media and cells were collected and analyzed after treatment (**Figure 4**). The ~30 kDa band was still present in the culture medium after treatment, indicating its stability. No similar signal was found in the lysates of treated cells, in contrast to those of C42-expressing cells. This indicated the oligomers detected were primarily produced in cells and not recaptured from the culture medium where they are also present.

Together, results obtained strongly suggested that the high MW band could correspond to oligomeric Aβ42 peptides, but did not formally exclude that they are formed by the assembly of other Aβ isoforms (e.g. the major Aβ40 isoform) or truncated APP C-terminal fragments. To test this hypothesis we expressed C40

constructs in cells, which correspond to the Aβ40 sequence. C40-expressing cells did not produce the oligomers found in C42-expressing cells (Supplementary Figure 1). This indicates that the oligomeric bands observed are produced by Aβ42- but not Aβ40-expressing constructs. To further confirm this hypothesis, bands around 30 kDa were excised from gels and subjected to nano liquid chromatography (nano-LC) coupled to tandem mass spectrometry (MS/MS). The peptides identified correspond to human Aβ sequences (Supplementary Figure 2). No other APP fragments (e.g. from the C-terminus) were identified in these gel samples, even in C99-expressing cells. Thus, we can conclude that the oligomers detected in transfected cells are indeed Aβ oligomers, and more precisely Aβ42 oligomers.

Figure 5. Impact of GXXXG/GXXXA mutations on C99 dimerization and Aβ oligomerization.

(A) Schematic representation of human the C99 and C42 contructs used. Numbering corresponds to aminoacid position in the C99 sequence. The aminoacid substitutions generated by site-directed mutagenesis are in red. Glycine and alanine residues of GXXXG/GXXA sequences are underlined. TM: Transmembrane region; ext: extracellular; int: intracellular. (B) Expression of C99 and Aβ oligomers analyzed in cell lysates by Western blotting with the APP C-terminal antibody and the W0-2 antibody, respectively. Oligomers (*) and C99 are indicated by arrows. (C) Expression of C99 and Aβ oligomers analyzed in lysates of cells expressing the different C99 mutants by Western blotting with the W0-2 antibody. Oligomers (*) and C99 are indicated by an arrow. (D,E) Dimerization of C99 and C99 mutants (m5, mA) was measured in living cells by the split-luciferase complementation assay. Cells were transfected with C99-coding sequences fused to two hGLuc moieties (hGluc1 and 2, see Figure 1). Bioluminescence (luciferase activity) was measured as RLU and given as percentage of bioluminescence detected in cells co-expressing C99-hGLuc1 and C99-hGLuc2. Values (means ± SEM) are representative of 3 independent experiments (n = 4 in each experiment). ***$p < 0.001$, n.s. (non-significant), as compared to control (mock-transfected cells). Expression of the fusion proteins was checked in cell lysates by Western blotting with the hGLuc antibody and the W0-2 antibody. (F) Analysis of Aβ oligomerization was monitored by Western blotting with the W0-2 antibody in cell lysates or culture media of cells expressing C42 or C42 mutants. Actin was used as loading probe (cell lysates). Oligomers (*) are indicated by an arrow.

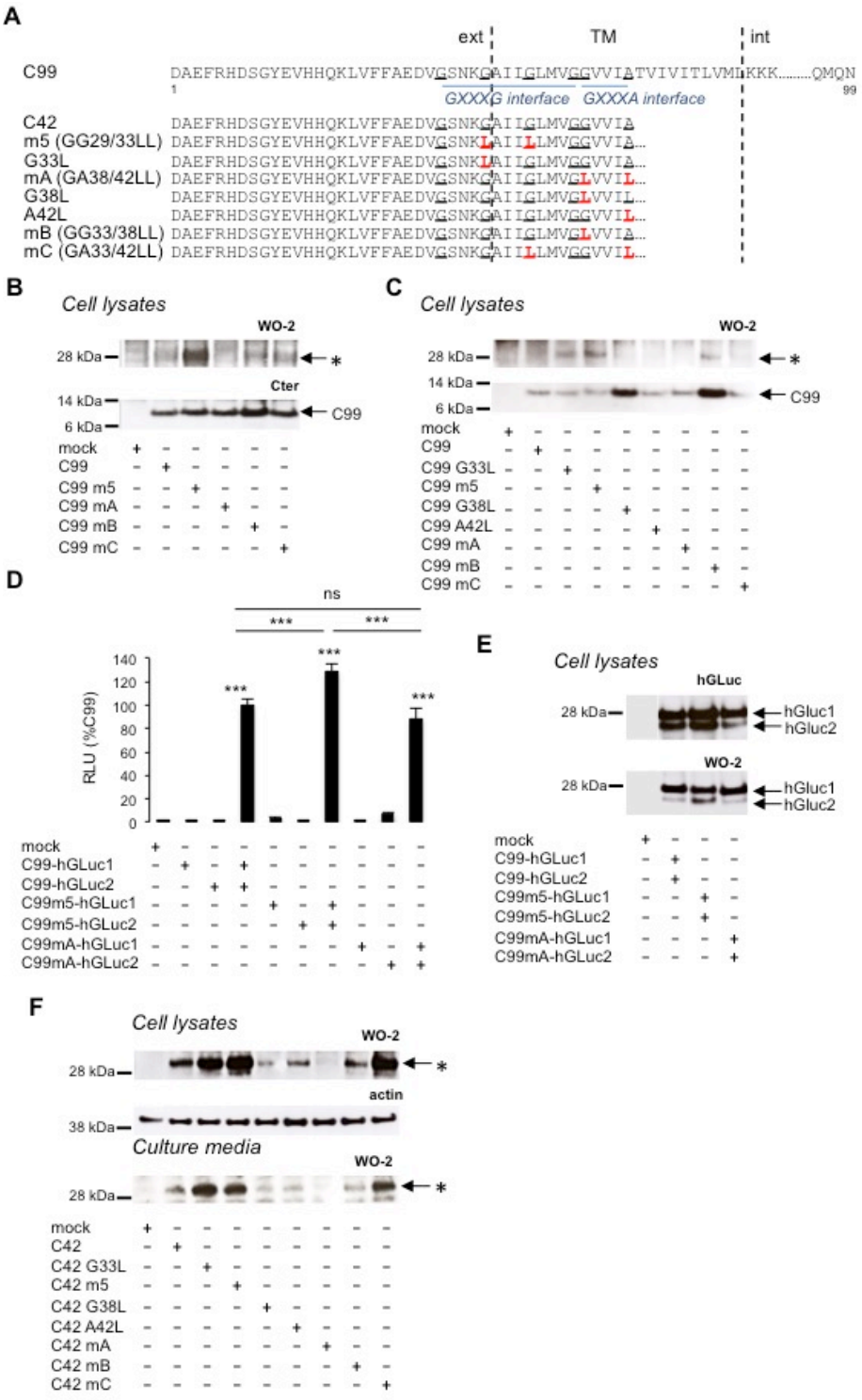
A
ext
TM
int
C99
DAEFRHDSGYEVHHQKLVFFAEDVGSNKGAIIGLMVGGVVIATVIVITLVMLKKK.....QMQN
GXXXG interface
GXXXA interface
C42
m5 (GG29/33LL)
G33L
mA (GA38/42LL)
G38L
A42L
mB (GG33/38LL)
mC (GA33/42LL)
B
Cell lysates
WO-2
28 kDa
Cter
14 kDa
6 kDa
C99
mock
C99 m5
C99 mA
C99 mB
C99 mC
C
Cell lysates
WO-2
28 kDa
14 kDa
6 kDa
C99
mock
C99
C99 G33L
C99 m5
C99 G38L
C99 A42L
C99 mA
C99 mB
C99 mC
D
ns
***
RLU (%C99)
mock
C99-hGLuc1
C99-hGLuc2
C99m5-hGLuc1
C99m5-hGLuc2
C99mA-hGLuc1
C99mA-hGLuc2
E
Cell lysates
hGLuc
28 kDa
hGluc1
hGluc2
WO-2
mock
C99-hGLuc1
C99-hGLuc2
C99m5-hGLuc1
C99m5-hGLuc2
C99mA-hGLuc1
C99mA-hGLuc2
F
Cell lysates
WO-2
28 kDa
actin
38 kDa
Culture media
mock
C42
C42 G33L
C42 m5
C42 G38L
C42 A42L
C42 mA
C42 mB
C42 mC

Mutations of glycine residues present in GXXXG on GXXXA motifs are critical for the Aβ oligomerization process

We previously reported that oligomeric bands identified here as Aβ42 oligomers were more abundant with C99 constructs mutated in GXXXG motifs (Kienlen-Campard et al., 2008). In our initial hypothesis, GXXXG mutations induced rotations in the TM helical regions that form stable associations through the GXXXA interface, strengthening dimerization of APP transmembrane domains (TMD). We mutated the glycine and alanine residues within the $G^{29}XXXG^{33}/G^{38}XXXA^{42}$ motifs (**Figure 5A**) to study their contribution to C99 dimerization and Aβ oligomerization.. The levels of the Aβ oligomeric band was highly increased in cells expressing C99 mutated in the central GXXXG motif (GG29/33LL, referred to as m5) with respect to cells expressing non-mutated C99, but the size of the oligomers remained the same (**Figure 5B**). Strikingly, the GA38/42LL mutation (referred to as mA) abolished Aβ oligomer production, and mutations affecting $G^{29}XXXG^{33}$, $G^{33}XXXG^{37}$ and $G^{38}XXXA^{42}$ motifs (referred to as mB and mC) produced intermediate levels of oligomers. We analyzed the contribution of key G/A residue of the $G^{29}XXXG^{33}/G^{38}XXXA^{42}$ motif to oligomer formation. The single G33L mutation was sufficient to induce the oligomerization profile observed with m5 (GG23/33LL). In that context (G33L), mutation of small residues from the $G^{38}XXXA^{42}$ interface (mB = GG33/38LL and mC = GA33/42LL) reduced the oligomerization promoted by the mutation of the critical G33 residue (**Figure 5C**). We found that these oligomeric bands did not result from changes in C99 dimerization (Kienlen-Campard et al., 2008;Ben Khalifa et al., 2012a;Munter et al., 2007). Dimerization measured by a highly sensitive split protein assay (Decock et al., 2015) was found to be equivalent for C99, C99 m5 and C99 mA (**Figure 5D, 5E**), whereas oligomeric bands are abundant in C99 m5 but not in C99 mA cell lysates (**Figure 5B**). Altogether, this indicated that mutations of glycine residues could

play a critical but dual role in Aβ production, without major changes in overall dimerization of C99. This was further addressed by expressing mutants of C42 in cells. Identical mutations to those studied in the C99 were introduced in C42 (**Figure 5A**). Mutation of glycine residues from $G^{29}XXXG^{33}$ and $G^{33}XXXG^{37}$ motifs, especially the G33L mutation, strongly increased the production of Aβ oligomers, that migrated at the same size as C99-derived oligomers (**Figure 5F**). Mutation of small residues (G/A) of the $G^{38}XXXA^{42}$ motif abolished oligomerization. Strikingly, the single G38L mutation decreased oligomerization of C42, and the G38L mutation in the context of G33L (mB) strongly impaired oligomerization of G33L mutants. On the other hand, the A42L mutation had moderate effects and was not able to counteract the increased oligomerization induced by G33L mutation (mC). The oligomers detected had the same electrophoretic profile in cell lysates and culture media, confirming the idea that oligomers are formed in cells and released into the culture medium. The critical residues for Aβ oligomerization are G33 and G38. G33L mutation strongly promotes oligomerization; G38L blocks it with a dominant effect on G33 residue modification.

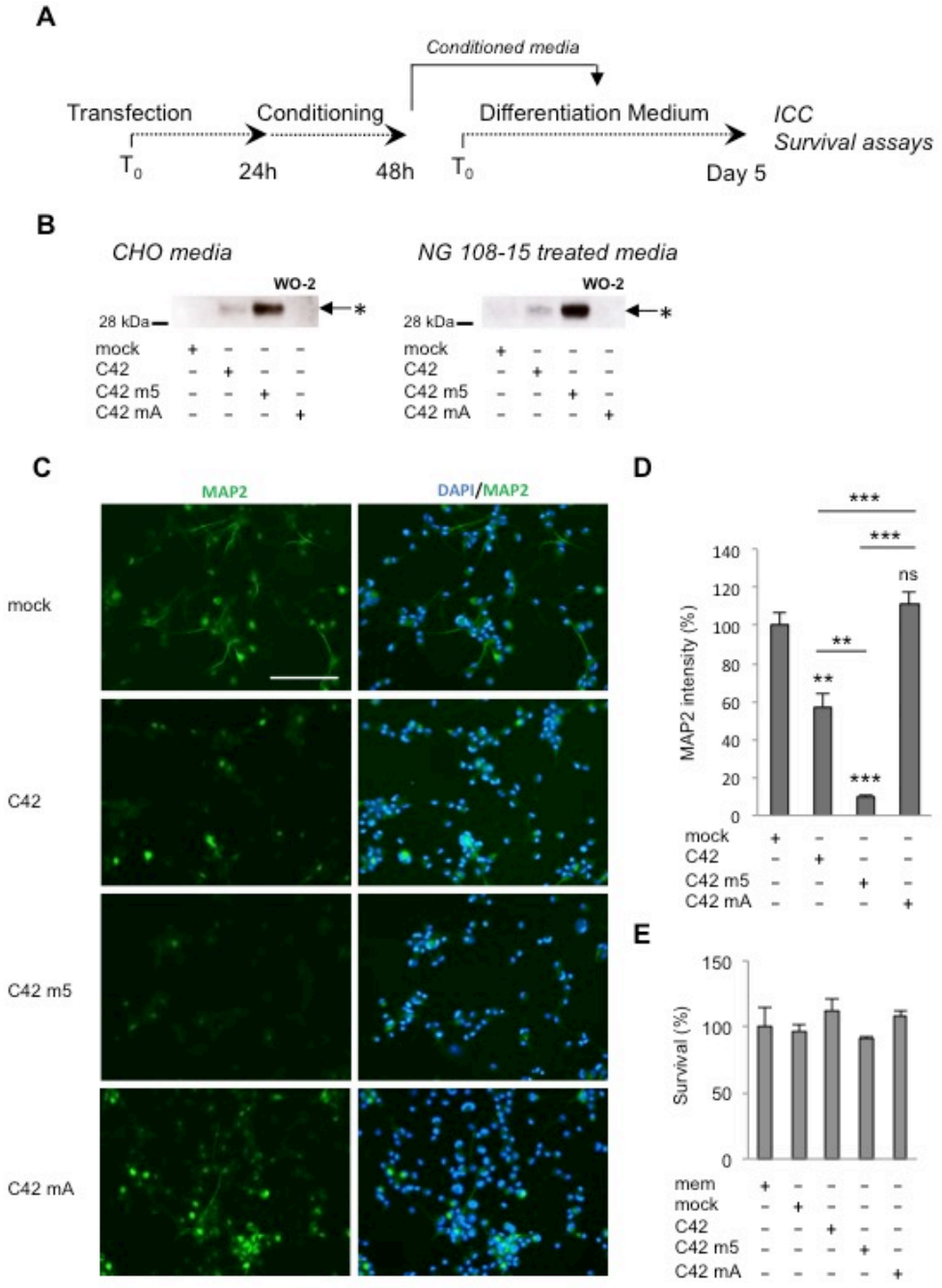
A
Conditioned media
Transfection
Conditioning
Differentiation Medium
ICC
Survival assays
T0
24h
48h
T0
Day 5
B
CHO media
NG 108-15 treated media
WO-2
28 kDa
mock
C42
C42 m5
C42 mA
C
MAP2
DAPI/MAP2
mock
C42
C42 m5
C42 mA
D
MAP2 intensity (%)
ns
E
Survival (%)
mem
mock
C42
C42 m5
C42 mA

Oligomeric Aβ42 peptides affect neuronal differentiation

One important question was to understand whether the oligomers we found to be produced in cells and released in the extracellular medium displayed pathological properties. A growing number of studies indicate that the pathological properties of Aβ are directly related to the formation of particular oligomeric assemblies (Benilova et al., 2012). We used the culture medium of CHO cells transfected with C42, C42m5 and C42mA to treat neuronal NG108-15 cells when differentiation is induced (**Figure 6A**). Culture media recovered from transfected CHO cells (after 24 hours of conditioning) showed the Aβ oligomeric profile detailed above: oligomeric Aβ was found in C42-expressing cells, at higher levels in cells expressing C42m5 but not in those expressing C42mA. All had the same electrophoretic profile. NG108-15 cells were treated for 5 days with CHO cell medium, renewed every 48 h. At the end of the treatment, oligomeric bands of Aβ were readily detectable in medium of treated NG108-15 cells (**Figure 6B**).

Figure 6. Effects of Aβ oligomers on neuronal cell differentiation and survival.

(A). Neuronal NG108-15 cells were treated with media of control CHO cells (mock) or CHO cells transfected with C42, C42 mutant 5 (m5) or C42 mutant A (mA) during the differentiation process. (B) The presence of Aβ oligomers in the media of CHO producing cells and NG108-15 cells (at day 5) was assessed by Western blotting with the W0-2 antibody. (C) Neuronal differentiation was assessed by immunostaining of NG108-15 treated cells with the MAP2 antibody. Nuclei were stained with the DAPI. Scale: 200µm. (D) Quantification of MAP2 immunostaining was performed and expressed as percentage of intensity measured in NG108-15 cells treated with the control medium (mock). Values (means ± SEM) are representative of 3 independent experiments (n = 2 in each experiment). ***p < 0.0001, **p<0.001, ns (non-significant) as compared to cells treated with the control medium. (D) Survival of the NG108-15 cells was assessed by MTS assay and given as percentage of survival measured in cells treated with the control medium. Values (means ± SEM) are representative of 3 independent experiments (n = 3 in each experiment). Statistical analysis showed non-significant differences between the conditions.

Five days after treatment, control cells showed the typical neurite outgrowth of differentiated NG108-15 cells (Stanga et al., 2015) measured by MAP2 staining (**Figure 6C**). NG108-15 cells treated with medium from C42- and C42m5-expressing CHO cells showed altered differentiation and reduced neurite outgrowth. The intensity of MAP2 staining was particularly reduced in cells treated with media from C42m5-expressing cells (**Figure 6D**), in which the highest concentration of Aβ oligomers was detected. In contrast, the differentiation pattern of cells treated with media of C42mA-expressing cells, in which no oligomeric Aβ is detected, was comparable to the one of non-treated cells. Thus, differentiation and neurite outgrowth of NG108-15 cells is impaired by the presence of Aβ oligomers. Importantly, this is not simply linked to cytotoxicity of these oligomers since the treatments did not affect NG108-15 cell survival in all the conditions tested (**Figure 6E**). Together, these data highlight an intrinsic property of specific Aβ oligomers to disrupt the formation of a neuronal network, which might be a very early event in β-amyloid pathologies.

DISCUSSION

Our major findings are that: i) expression of a construct coding for a peptide corresponding to Aβ42 leads to the formation of oligomers of 28-30 kDa that are resistant to denaturation and SDS, with no detection of monomeric Aβ42. These oligomers display neuropathological properties; ii) the same size oligomer can be detected when C99 (βCTF) is expressed, but in this case also a monomeric form can be detected, suggesting that the location of processing in the cell can influence the extent of oligomerization; iii) Aβ40 does not induce the formation of such oligomeric species; iv) the oligomers induced by Aβ42 and C99 are similar, and their size remains identical upon mutation; v) the formation of oligomers is regulated by the $G^{29}XXXG^{33}$ and $G^{38}XXXA^{42}$ transmembrane motifs – Gly33 of the $G^{29}XXXG^{33}$ motifs exerts a negative effect and Gly38 of the GXXXA motif exerts a stimulatory effect on oligomer formation; and vi) the same motifs also regulate processing of C99 (Kienlen-Campard et al., 2008) without affecting the extent of C99 dimerization in cells.

Aβ42 oligomers are formed in cells

The oligomeric peptides revealed by Western blotting that were initially thought to be C99 dimers (Kienlen-Campard et al., 2008) correspond indeed to Aβ42 oligomers. These Aβ oligomers are produced in cells either by the processing of APP amyloidogenic fragment (C99) to Aβ, or when a peptide corresponding to Aβ42 is expressed in cells. Strikingly, soluble Aβ monomeric forms are only detected in C99-expressing cells and not when Aβ42 is expressed. Thus, the maintenance of soluble Aβ42 might depend on intracellular compartments where

C99 fragments are processed. C42 fragments generate Aβ42 without being processed by the γ-secretase. We found that C55 fragments containing the KKK capping motifs at the TM/intracellular junction become substrates for γ-secretase (Supplementary Figure 4). This is quite intriguing and needs to be further investigated, but it suggests that monomeric Aβ can only be produced by specific substrates and in specific compartments. As soon as these requirements are met, Aβ shows a high propensity to aggregate, both in cells and in the supernatant. When Aβ42 is directly produced in cellular compartments (C42 constructs), it spontaneously aggregates to form oligomers and soluble monomeric Aβ is no more detectable. It remains in that regard to be determined whether co-expression of Aβ42 and C99 would allow the detection of soluble Aβ42, would increase the levels of Aβ42 oligomers or promote formation of a higher molecular weight oligomer. Aβ oligomers we detected are enriched in membrane-bound compartments and found in cell culture medium in conditions where no cytotoxicity is readily measured in CHO cells. They are thus secreted rather than simply released in the extracellular space upon cell death and subsequent leaking of intracellular components. In addition, we found that intracellular oligomers are not recaptured from the culture medium, or at least at very low levels that cannot be detected in our experimental conditions. This strongly supports the conclusion that Aβ oligomers are readily formed in cells and further secreted in the extracellular medium. Intriguingly, only Aβ assemblies of ~25/30kDa, corresponding to the expected molecular weight of Aβ hexamers, can be detected under our experimental conditions. It does not exclude that other Aβ oligomers are produced by the cells, but their conformation should in this case not be stable enough to withstand the denaturing conditions (SDS) we used to run Western blots. The Aβ oligomers we identified are very stable, resistant to SDS, temperature (Supplemental Figure 3) and formic acid denaturation (not shown).

Oligomers were detected only with constructs expressing Aβ42, and not Aβ40. Aβ42, unlike Aβ40, can form stable trimeric and tetrameric complexes (Chen and Glabe, 2006) as well as globulomer structures (dodecamers) in the presence of SDS (Barghorn et al., 2005), and can form pentamers and hexamers in solution (Bitan et al., 2003;Bernstein et al., 2009). SDS was suggested to artificially produce stable Aβ assemblies. We found Aβ oligomers in the culture media that were not isolated by SDS-based extraction, suggesting that they are not generated by a spurious effect of the detergent. One obvious question is to understand how such Aβ42 oligomers can assemble in cells. Previous studies showed that low-temperature and low-salt conditions can stabilize disc-shaped oligomers (Ahmed et al., 2010). They do not have the β-sheet structure characteristic of fibrils, but are rather composed of loosely aggregated strands. Importantly, it has recently been shown that at physiological temperature (37°C) and at high concentration, Aβ42 rapidly aggregates into unstructured specific oligomers (Fu et al., 2015). The high concentrations achieved here by direct expression of Aβ42 could indeed mimic pathological situation in which Aβ accumulates in specific cellular compartments.

G33 and G38 residues from $G^{29}XXXG^{33}$ and $G^{38}XXXA^{42}$ motifs dramatically affect the Aβ oligomerization process.

Small aminoacid residues (G/A) present in GXXXG or GXXXA motifs are known to promote TM helix association. Their mutation was shown to strongly affect the processing of β-CTF (Munter et al., 2007;Kienlen-Campard et al., 2008). Using a protein fragment complementation assay based on *Gaussia princeps* luciferase, we show that the effects on C99 dimerization of the $G^{29}XXXG^{33}$ and $G^{38}XXXA^{42}$ motifs mutation are not major and that these motifs might change the precise

interface of dimers, but do not mediate on - off effects on dimerization events, at least when measured by the proximity of the C-terminal ends. These results are totally in line with our recently published work (Decock et al., 2015). GXXXG motifs present in APP TM region might regulate processing of amyloidogenic CTFs either independently of dimerization or by controlling precise dimeric conformations.

We showed that mutation of these glycine residues indeed dramatically affects the formation of Aβ oligomers. G33 and G38 play a predominant role in this process by promoting or blocking oligomerization, respectively. Importantly, identical Aβ oligomers are detected in cells expressing mutated or non-mutated C99 or C42. For the GXXXG mutants, high amounts of oligomers are detected, but no soluble monomeric Aβ is measured by ECLIA. Soluble monomeric Aβ was not detected for the different GXXXA mutants, but the mutations in these constructs are at positions preventing detection by the C-terminal ECLIA capture antibody. Our results would suggest that soluble monomeric Aβ is produced by the different mutants, but the mutations either shift the monomeric-oligomeric Aβ equilibrium toward the formation of oligomeric forms (G33 mutants) or block the conversion from monomers to oligomers (G38 mutants). The turn in the Aβ structure at G38 is a characteristic of Aβ42 oligomers and molecular contacts have been reported in the monomeric unit of Aβ42 fibrils between G38 and F19 (Luhrs et al., 2005) and between M35 and A42 (Masuda et al., 2008). The particular roles of G38 and A42 could first explain the low oligomerization profile of Aβ produced from C99mA and C42mA in which both G38 and A42 are mutated, and the absence of oligomer formation with Aβ40 lacking the A42 position. G38 is important to form a solvent accessible turn in the β-hairpin structure of the Aβ42 building blocks assembled in oligomers. G38 to L mutation could thus break the conformation of Aβ monomers which promotes the formation of oligomers as proposed by Ahmed

et al (Ahmed et al., 2010). G33 residue is part of the $G^{33}LMVG^{37}$ hydrophobic sequence forming a β-strand which is critical for the Aβ monomers to adopt an antiparallel β-hairpin structure present in Aβ oligomers prior to conversion to β-sheet structure. Mutation at G33 position is thus very likely to modify Aβ conformation in a way that favors oligomerization. Our results are in line with previous studies highlighting G33 as critical for the generation of Aβ42 assemblies (Harmeier et al., 2009). Mutation of G33 was suggested to promote rapid Aβ oligomerization by conformational changes favoring the formation of high molecular weight oligomers. However, these observations await further structural studies in order to clearly understand how G33 and G38 can control in an opposite way the Aβ oligomerization we observed in cells.

Aβ42 oligomers produced by cells display neuropathological properties.

Emerging evidence indicates that Aβ oligomers, and not Aβ fibrils have neuropathological properties. Aβ oligomers can rapidly interact with cell membranes and display neurotoxic effects, before a further possible conversion to protofibrils or fibrils (Ahmed et al., 2010). Apart from cytotoxic effects, Aβ oligomers have been shown to cause various neuronal dysfunctions. Accumulation of soluble (non-fibrilar) Aβ forms is correlated with the progression of AD (McLean et al., 1999) and is a predictor of synaptic changes and disruption of neuronal circuits occurring in the pathology (Lue et al., 1999;Hsia et al., 1999). We showed here that Aβ oligomers released in the cell medium strongly impair neuronal differentiation and neurite outgrowth, but did not display significant neurotoxic effects. The neurotoxic effect of Aβ42 were reported to depend on its intraneuronal accumulation (Bayer and Wirths, 2010; Kienlen-Campard and Octave, 2002), but this is restricted to neurons or primary neuron cultures and

does not occur in cell lines (Kienlen-Campard et al., 2002). It would be of particular interest to further address Aβ 42 oligomers formation, distribution and cytotoxic effects in neurons or neuronal cultures. This could be highly relevant for sporadic Alzheimer's disease where with age the capacity to maintain Aβ soluble decreases and Aβ42 accumulates in neurons as an early event. Previous studies have shown that Aβ concentrated by more than 2 order of magnitude to reach micromolar concentrations in acidic vesicular compartments (Hu et al., 2009). This local high increase in Aβ concentration could initiate oligomerization in these compartments. This gives strong impetus to address the formation and precise subcellular localization of Aβ oligomers in neurons, and to analyze whether and how they are related to neuronal dysfunction.

However, the fact that Aβ oligomers did not induce cytotoxic effects but strongly impaired neurite outgrowth and maturation of the neuronal network is in line with previous observations. The extracellular accumulation of a 56-kDa soluble Aβ oligomer, isolated from brain of AD transgenic mice, impaired memory independently of any neuronal loss (Lesne et al., 2006). It would be of particular interest to investigate if oligomers identical to the one we identified here could be isolated from AD mice models or brains of AD patients. Important to note, neuronal-specific mechanisms like post-translational modifications participate to Aβ oligomerization. For instance, phosphorylation at different positions including Ser8 and Ser26 has been shown to enhance or block the formation of Aβ oligomers in brains (Kumar et al., 2011;Kumar et al., 2013). Whether these neuronal mechanisms could regulate Aβ assemblies we identified here should be further understood. Up to now, a puzzling list of Aβ oligomer species supposed to be multimers of a fundamental Aβ trimer assembly (hexamers, nonamers, dodecamers) have been identified from various experimental models (including human AD brains and brains of AD transgenic mice), isolated under different

experimental conditions (Benilova et al., 2012). Still, i) they provide no clear evidence as to which are pathologically relevant; ii) the molecular mechanisms underlying their precise assembly is poorly understood.

In conclusion, we reported here that specific Aβ oligomeric forms can be produced in living cells, and secreted in the extracellular medium. Such Aβ assemblies are stable, resistant to temperature and SDS, and impair neuronal maturation and differentiation. They are detected when Aβ is generated upon C99 processing, and at high levels when Aβ42 but not Aβ40 is directly expressed in cells. We found two glycine residues to be critical in Aβ assembly: G33 and G38. Mutation of G33 dramatically increases Aβ oligomerization, whereas mutation of G38 impairs it. This suggests a protective and triggering role of G33 and G38 in the Aβ oligomerization process, respectively. These observations are in line with previous ones, pointing the important role of the G38 in the Aβ strand-turn-strand conformation specifically observed in oligomers. In conclusion, our data provide experimental evidence that Aβ oligomers observed *in vitro* are readily produced in living cells, and prompts further investigation into their precise structure, how they assemble, and their pathological relevance to human disease.

ACKNOWLEDGEMENTS

This work was supported by a grant of the Belgian F.N.R.S FRIA (Fonds National pour la Recherche Scientifique) to M.D. Foundation for Research on Alzheimer's disease (P.K-C.), by the Interuniversity Attraction Pole Programme-Belgian Sate-Belgian Science Policy (IAP-P7/16 and IAP-P7/13) to J-N.O. and P.K-C, by the Fondation Médicale Reine Elisabeth (FMRE) to JNO, ID and PKC, by the Action de Recherche Concertée (ARC 14/19-059) to P.K-C and a grant from the NIH (AG29317) to S.O.S. Support to S.N.C. was from the Ludwig Institute for Cancer Research, FRS-FNRS, Salus Sanguinis Foundation, the Action de Recherche Concertée project ARC10/15–027 of the University catholique de Louvain, the Fondation contre le Cancer, the PAI Programs BCHM61B5 and Belgian Medical Genetics Initiative. We are grateful to J-F. Paradis and S.W. Michnick (UMontreal) for the leucine zipper split-luciferase plasmids.

AUTHORS CONTRIBUTIONS

M.D. and P.K.C. designed research; M.D. and S.S. conducted experiments, M.D., S.S., S.N.C. and P.K.C. analyzed data and wrote the paper with fundamental input of S.O.S., I.D., and J-N.O.

SUPPLEMENTARY DATA

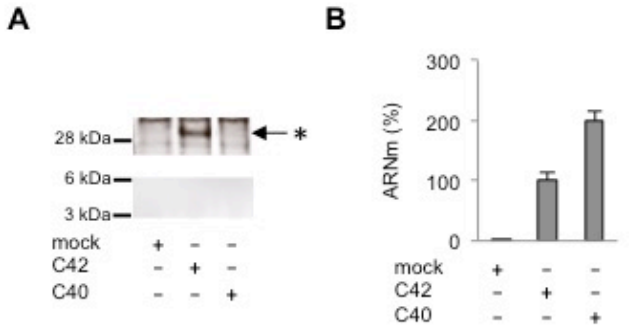

Supplementary Figure 1. Expression of C40 and C42 mA do not lead to Aβ oligomers formation.

Cells were transfected with the control empty vector (mock), or constructs expressing C42 or C40. (A) Analysis of C42/C40 expression and Aβ oligomerization was monitored in cell lysates by Western blotting with the W0-2 antibody. Oligomers (*) are indicated by arrows. (B) Expression of C42 and C40 mRNA levels were measured by RTqPCR with the same primers and given as percentage of mRNA levels measured in C42-expressing cells.

Confidence	Sequence	Activation Type	XCorr	Δ Score	Charge	m/z [Da]	MH+ [Da]	ΔM [ppm]
High	HDSGYEVHHQK	CID	3,05	1,00	2	668,805	1336,604	0,67
High	HDSGYEVHHQK	CID	2,67	1,00	3	446,206	1336,605	1,55
High	LEDAEFR	CID	1,85	1,00	2	440,212	879,418	-2,87

Summary

Sample	Confident identification	Coverage	MW [kDa]	calc. pI	Score	Description
mock	No					
C42	C42	40,91	4,8	5,14	7,57	> C42

Supplementary Figure 2. Mass spectrometry analysis of the oligomeric bands produced in C42-expressing cells.

Cell lysates from non-transfected (mock) and C42 transfected cell were separated on NuPage gradient gels in denaturating conditions. Gel bands around 30 kDa were excised and proteins were extracted and digested with trypsin. Following digestion, purified peptide samples were analyzed by nanoLC coupled to tandem mass spectrometry (MS/MS). The raw MS file were analyzed and searched against the APP protein sequence database. The results summarized showed the high confidence identification of two peptide sequences contained in the C42/Aβ42 peptides. C42 and Aβ42 sequences are given on the top of the tables. Peptide sequences identified are in bold. Signal peptide sequence is in blue.

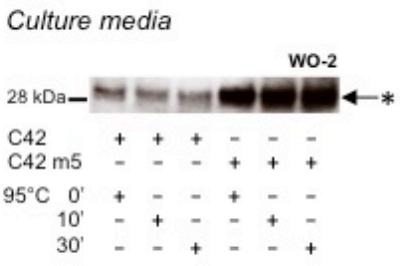

Supplementary Figure 3. Resistance of Aβ oligomers to temperature.

Media of cells expressing C42 or C42m5 were collected and heated at 95°C for 0, 10 to 30 minutes prior to Western blotting revealed with the W0-2 antibody. Oligomers (*) are indicated by an arrow.

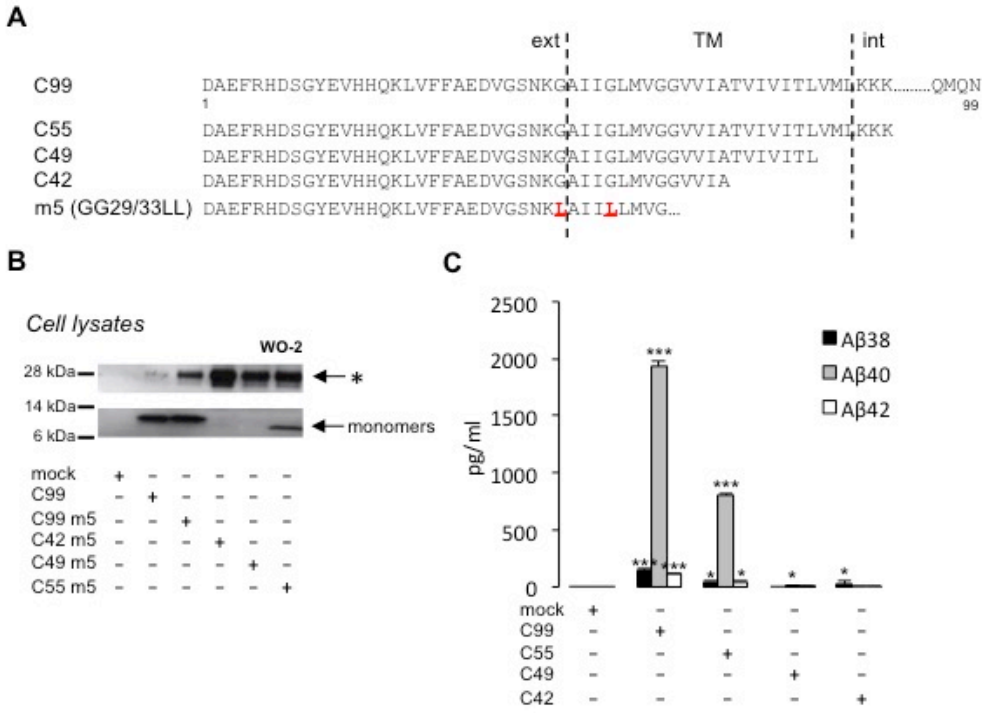

Supplementary Figure 4. Aβ oligomers formation in cells expressing different C-terminal truncations of C99.

(A) Schematic representation of the different constructs. C99 corresponds to the APP β C-terminal fragment. Numbering corresponds to aminoacid position in the C99 sequence. C55, C49 and C42 have been generated by entering a stop codon at positions 55, 49 and 42 of C99, respectively. TM: Transmembrane region; ext: extracellular; int: intracellular. The aminoacid substitution (referred to as m5) generated for each construct appears in bold and red. (B) Expression of C99, C99 m5, C45 m5, C49 m5 and C55 m5 in CHO cells analyzed by Western blotting with the W0-2 antibody. Oligomers (*) and monomers are indicated by arrows. (C) Aβ 38, 40 and 42 were quantified by ECLIA in the culture media of transfected cells. Values (means ± SEM) given in pg/ml are representative of 3 independent experiments (n=3 in each experiment). * $p<0.05$, *** $p<0.001$, as compared to control cells (mock-transfected cells).

REFERENCES

Ahmed M, Davis J, Aucoin D, Sato T, Ahuja S, Aimoto S, Elliott JI, Van Nostrand WE, Smith SO (2010) Structural conversion of neurotoxic amyloid-beta(1-42) oligomers to fibrils. Nat Struct Mol Biol 17:561-567.

Barghorn S, Nimmrich V, Striebinger A, Krantz C, Keller P, Janson B, Bahr M, Schmidt M, Bitner RS, Harlan J, Barlow E, Ebert U, Hillen H (2005) Globular amyloid beta-peptide oligomer - a homogenous and stable neuropathological protein in Alzheimer's disease. J Neurochem 95:834-847.

Bayer TA, Wirths O (2010) Intracellular accumulation of amyloid-Beta - a predictor for synaptic dysfunction and neuron loss in Alzheimer's disease. Front Aging Neurosci 2:8.

Ben Khalifa N, Tyteca D, Courtoy PJ, Renauld JC, Constantinescu SN, Octave JN, Kienlen-Campard P (2012a) Contribution of Kunitz protease inhibitor and transmembrane domains to amyloid precursor protein homodimerization. Neurodegener Dis 10:92-95.

Ben Khalifa N, Tyteca D, Marinangeli C, Depuydt M, Collet JF, Courtoy PJ, Renauld JC, Constantinescu S, Octave JN, Kienlen-Campard P (2012b) Structural features of the KPI domain control APP dimerization, trafficking, and processing. FASEB J 26:855-867.

Benilova I, Karran E, De SB (2012) The toxic Abeta oligomer and Alzheimer's disease: an emperor in need of clothes. Nat Neurosci 15:349-357.

Bernstein SL, Dupuis NF, Lazo ND, Wyttenbach T, Condron MM, Bitan G, Teplow DB, Shea JE, Ruotolo BT, Robinson CV, Bowers MT (2009) Amyloid-beta protein oligomerization and the importance of tetramers and dodecamers in the aetiology of Alzheimer's disease. Nat Chem 1:326-331.

Bitan G, Kirkitadze MD, Lomakin A, Vollers SS, Benedek GB, Teplow DB (2003) Amyloid beta -protein (Abeta) assembly: Abeta 40 and Abeta 42 oligomerize through distinct pathways. Proc Natl Acad Sci U S A 100:330-335.

Chen YR, Glabe CG (2006) Distinct early folding and aggregation properties of Alzheimer amyloid-beta peptides Abeta40 and Abeta42: stable trimer or tetramer formation by Abeta42. J Biol Chem 281:24414-24422.

Decock M, El HL, Stanga S, Dewachter I, Octave JN, Smith SO, Constantinescu SN, Kienlen-Campard P (2015) Analysis by a highly sensitive split luciferase assay of the regions involved in APP dimerization and its impact on processing. FEBS Open Bio 5:763-773.

Fonte V, Dostal V, Roberts CM, Gonzales P, Lacor PN, Velasco PT, Magrane J, Dingwell N, Fan EY, Silverman MA, Stein GH, Link CD (2011) A glycine zipper motif mediates the formation of toxic beta-amyloid oligomers in vitro and in vivo. Mol Neurodegener 6:61.

Fu Z, Aucoin D, Davis J, Van Nostrand WE, Smith SO (2015) Mechanism of Nucleated Conformational Conversion of Abeta42. Biochemistry 54:4197-4207.

Glenner GG, Wong CW (1984) Alzheimer's disease: initial report of the purification and characterization of a novel cerebrovascular amyloid protein. Biochem Biophys Res Commun 120:885-890.

Haas C, Hung AY, Citron M, Teplow DB, Selkoe DJ (1995) beta-Amyloid, protein processing and Alzheimer's disease. Arzneimittelforschung 45:398-402.

Hage S, Marinangeli C, Stanga S, Octave JN, Quetin-Leclercq J, Kienlen-Campard P (2013) Gamma-Secretase Inhibitor Activity of a Pterocarpus erinaceus Extract. Neurodegener Dis.

Hage S, Stanga S, Marinangeli C, Octave JN, Dewachter I, Quetin-Leclercq J, Kienlen-Campard P (2015a) Characterization of Pterocarpus erinaceus kino extract and its gamma-secretase inhibitory properties. J Ethnopharmacol 163:192-202.

Hage S, Stanga S, Marinangeli C, Octave JN, Dewachter I, Quetin-Leclercq J, Kienlen-Campard P (2015b) Characterization of Pterocarpus erinaceus kino extract and its gamma-secretase inhibitory properties. J Ethnopharmacol 163:192-202.

Hardy J (2009) The amyloid hypothesis for Alzheimer's disease: a critical reappraisal. J Neurochem 110:1129-1134.

Hardy J, Allsop D (1991) Amyloid deposition as the central event in the aetiology of Alzheimer's disease. Trends Pharmacol Sci 12:383-388.

Harmeier A, Wozny C, Rost BR, Munter LM, Hua H, Georgiev O, Beyermann M, Hildebrand PW, Weise C, Schaffner W, Schmitz D, Multhaup G (2009) Role of amyloid-beta glycine 33 in oligomerization, toxicity, and neuronal plasticity. J Neurosci 29:7582-7590.

Hayden EY, Teplow DB (2013) Amyloid beta-protein oligomers and Alzheimer's disease. Alzheimers Res Ther 5:60.

Herrup K (2015) The case for rejecting the amyloid cascade hypothesis. Nat Neurosci 18:794-799.

Hsia AY, Masliah E, McConlogue L, Yu GQ, Tatsuno G, Hu K, Kholodenko D, Malenka RC, Nicoll RA, Mucke L (1999) Plaque-independent disruption of neural circuits in Alzheimer's disease mouse models. Proc Natl Acad Sci U S A 96:3228-3233.

Hu X, Crick SL, Bu G, Frieden C, Pappu RV, Lee JM (2009) Amyloid seeds formed by cellular uptake, concentration, and aggregation of the amyloid-beta peptide. Proc Natl Acad Sci U S A 106:20324-20329.

Hung LW, Ciccotosto GD, Giannakis E, Tew DJ, Perez K, Masters CL, Cappai R, Wade JD, Barnham KJ (2008) Amyloid-beta peptide (Abeta) neurotoxicity is modulated by the rate of peptide aggregation: Abeta dimers and trimers correlate with neurotoxicity. J Neurosci 28:11950-11958.

Kang J, Lemaire HG, Unterbeck A, Salbaum JM, Masters CL, Grzeschik KH, Multhaup G, Beyreuther K, Muller-Hill B (1987) The precursor of Alzheimer's disease amyloid A4 protein resembles a cell-surface receptor. Nature 325:733-736.

Kawarabayashi T, Younkin LH, Saido TC, Shoji M, Ashe KH, Younkin SG (2001) Age-dependent changes in brain, CSF, and plasma amyloid (beta) protein in the Tg2576 transgenic mouse model of Alzheimer's disease. J Neurosci 21:372-381.

Kienlen-Campard P, Miolet S, Tasiaux B, Octave JN (2002) Intracellular amyloid-beta 1-42, but not extracellular soluble amyloid-beta peptides, induces neuronal apoptosis. J Biol Chem 277:15666-15670.

Kienlen-Campard P, Octave JN (2002) Correlation between beta-amyloid peptide production and human APP-induced neuronal death. Peptides 23:1199-1204.

Kienlen-Campard P, Tasiaux B, Van HJ, Li M, Huysseune S, Sato T, Fei JZ, Aimoto S, Courtoy PJ, Smith SO, Constantinescu SN, Octave JN (2008) Amyloidogenic processing but not amyloid precursor protein (APP) intracellular C-terminal domain production requires a precisely oriented APP dimer assembled by transmembrane GXXXG motifs. J Biol Chem 283:7733-7744.

Kim W, Hecht MH (2006) Generic hydrophobic residues are sufficient to promote aggregation of the Alzheimer's Abeta42 peptide. Proc Natl Acad Sci U S A 103:15824-15829.

Kumar S, Rezaei-Ghaleh N, Terwel D, Thal DR, Richard M, Hoch M, Mc Donald JM, Wullner U, Glebov K, Heneka MT, Walsh DM, Zweckstetter M, Walter J (2011) Extracellular phosphorylation of the amyloid beta-peptide promotes formation of toxic aggregates during the pathogenesis of Alzheimer's disease. EMBO J 30:2255-2265.

Kumar S, Wirths O, Theil S, Gerth J, Bayer TA, Walter J (2013) Early intraneuronal accumulation and increased aggregation of phosphorylated Abeta in a mouse model of Alzheimer's disease. Acta Neuropathol 125:699-709.

Lesne S, Koh MT, Kotilinek L, Kayed R, Glabe CG, Yang A, Gallagher M, Ashe KH (2006) A specific amyloid-beta protein assembly in the brain impairs memory. Nature 440:352-357.

Liu W, Crocker E, Zhang W, Elliott JI, Luy B, Li H, Aimoto S, Smith SO (2005) Structural role of glycine in amyloid fibrils formed from transmembrane alpha-helices. Biochemistry 44:3591-3597.

Lue LF, Kuo YM, Roher AE, Brachova L, Shen Y, Sue L, Beach T, Kurth JH, Rydel RE, Rogers J (1999) Soluble amyloid beta peptide concentration as a predictor of synaptic change in Alzheimer's disease. Am J Pathol 155:853-862.

Luhrs T, Ritter C, Adrian M, Riek-Loher D, Bohrmann B, Dobeli H, Schubert D, Riek R (2005) 3D structure of Alzheimer's amyloid-beta(1-42) fibrils. Proc Natl Acad Sci U S A 102:17342-17347.

Masuda Y, Uemura S, Nakanishi A, Ohashi R, Takegoshi K, Shimizu T, Shirasawa T, Irie K (2008) Verification of the C-terminal intramolecular beta-sheet in Abeta42 aggregates using solid-state NMR: implications for potent neurotoxicity through the formation of radicals. Bioorg Med Chem Lett 18:3206-3210.

McDonald RJ, Craig LA, Hong NS (2010) The etiology of age-related dementia is more complicated than we think. Behav Brain Res 214:3-11.

McLean CA, Cherny RA, Fraser FW, Fuller SJ, Smith MJ, Beyreuther K, Bush AI, Masters CL (1999) Soluble pool of Abeta amyloid as a determinant of severity of neurodegeneration in Alzheimer's disease. Ann Neurol 46:860-866.

Munter LM, Voigt P, Harmeier A, Kaden D, Gottschalk KE, Weise C, Pipkorn R, Schaefer M, Langosch D, Multhaup G (2007) GxxxG motifs within the amyloid precursor protein transmembrane sequence are critical for the etiology of Abeta42. EMBO J 26:1702-1712.

Pham E, Crews L, Ubhi K, Hansen L, Adame A, Cartier A, Salmon D, Galasko D, Michael S, Savas JN, Yates JR, Glabe C, Masliah E (2010) Progressive accumulation of amyloid-beta oligomers in Alzheimer's disease and in amyloid precursor protein transgenic mice is accompanied by selective alterations in synaptic scaffold proteins. FEBS J 277:3051-3067.

Sato T, Kienlen-Campard P, Ahmed M, Liu W, Li H, Elliott JI, Aimoto S, Constantinescu SN, Octave JN, Smith SO (2006) Inhibitors of amyloid toxicity based on beta-sheet packing of Abeta40 and Abeta42. Biochemistry 45:5503-5516.

Selkoe DJ (2004) Alzheimer disease: mechanistic understanding predicts novel therapies. Ann Intern Med 140:627-638.

Shankar GM, Leissring MA, Adame A, Sun X, Spooner E, Masliah E, Selkoe DJ, Lemere CA, Walsh DM (2009) Biochemical and immunohistochemical analysis of an Alzheimer's disease mouse model reveals the presence of multiple cerebral Abeta assembly forms throughout life. Neurobiol Dis 36:293-302.

Stanga S, Zanou N, Audouard E, Tasiaux B, Contino S, Vandermeulen G, Rene F, Loeffler JP, Clotman F, Gailly P, Dewachter I, Octave JN, Kienlen-Campard P (2015) APP-dependent glial cell line-derived neurotrophic factor gene expression drives neuromuscular junction formation. FASEB J.

CHAPTER IV: Discussion

The initial aim of our project was to depict precisely the contribution of APP GXXXG and GXXXA motifs in its dimerization, and more precisely in dimerization of the amyloidogenic β C-terminal fragment (βCTF or C99). This was elaborated -at that time- on recently published work indicating that mutation in the APP GXXXG motifs altered its dimerization properties (Munter et al., 2007;Kienlen-Campard et al., 2008). Two different interpretations resulted from these studies. The first one was that glycine residues at position 29 and 33 (C99/Aβ numbering) form a cross-point in APP TM dimers. This cross-point is loosened upon substitution of Gly with Leu or Ile, hydrophobic amino acids with bulky lateral chains (Munter et al., 2007). The second interpretation was that Gly-to-Leu mutation of GXXXG motifs rotates the TM dimers, favoring dimerization through the alternative GXXXA interface. It leads in turns to the formation of stable (SDS-resistant) C99 dimers that cannot be cleaved by the γ-secretase.

We addressed the importance of GXXXG membrane motifs in APP self-assembly on 2 critical aspects of Alzheimer's disease pathogenicity: dimerization of APP (full-length/CTFs) with the consequences on the amyloidogenic processing and Aβ oligomerization, which is directly linked to pathogenicity.

We first addressed the possible involvement of GXXXG motifs in dimerization of full-length APP. Then, we assessed their importance in APP CTFs dimerization and the possible link with processing by the γ-secretase. In the last part, we studied the involvement of glycines residues from GXXXG and GXXXA motifs in the formation of Aβ oligomers. Our major findings are that dimerization of APP and APP CTFs is not impaired by mutations of the critical glycines residues. Thus, dimerization that readily occurs in living cell might involve hitherto unknown

determinants and mechanisms, which require further investigations. Although they do not affect dimerization per se, mutation of GXXXG motifs dramatically affects Aβ production. This brings new insight in recent work to which we contributed, showing that the GXXXG determinants shape the JM/TM region of APP in a way that is critical for processing by the γ-secretase. Finally, we discovered that glycines residues were also critical for Aβ42 oligomerization. Gly33 and Gly38 positions have opposite effect by promoting or preventing the formation of Aβ42 oligomers displaying pathological properties.

In 2016, despite no efficient therapeutic outcome, Alzheimer's disease is still the most studied neurodegenerative disease worldwide. This infatuation is due to its constantly increasing rate and prevalence in developed countries, making it a so important social and economic issue. The 25 years old amyloid cascade hypothesis, stating that the imbalance between Aβ production and clearance is the first event in AD, has often been rephrased, debated, reappraised and challenged. It remains a core hypothesis that requires always clarification and ultimate validation by the development of efficient therapies targeting the amyloid side of the pathology. We hope that the findings we reported and discuss here will contribute to a better understanding of the pathogenesis, and give clues for therapeutic development.

1. Involvement of GXXXG motifs in full-length APP dimerization

First, we confirmed by a novel and highly sensitive method that **full-length APP dimerization is mostly driven by the ectodomain**. APP has been shown in many studies to homo- and heterodimerize (Scheuermann et al., 2001;Soba et al., 2005), a feature reminiscent of other single pass transmembrane proteins (Schlessinger, 2002). Several recent studies have been addressing the mechanisms involved in APP dimerization. The reported results suggest that this process can involve either the extracellular or transmembrane domain of APP. It has been first proposed that APP dimerization involves the E1 region of the ectodomain (Soba et al., 2005), by a process controlling APP transdimerization implicated in cellular adhesion properties. Structural studies also suggested that the E2 region could mediate APP dimerization (Wang and Ha, 2004). Our team as well as other groups identified the high occurrence of GXXXG and GXXXG-like motifs in APP JM/TM regions, and found that mutation of these motifs altered APP dimerization properties (Kienlen-Campard et al., 2008;Munter et al., 2007). However, the approach used (ToxR system, co-immunoprecipitation) failed to firmly conclude about the existence of APP dimers in living cells, and the roles of GXXXG motifs in this context. Naouel Ben Khalifa, during her PhD in the team, investigated APP dimerization by fluorescence complementation (BiFC) and gave the first clues on APP dimerization in living cells (Ben Khalifa et al., 2012b). She has already addressed the role of GXXXG motifs and has showed that disruption of the central motif by mutation of the 2 glycines has no significant effect on full-length APP dimerization. APP homodimerization is essentially mediated by the ectodomain, and the presence of a Kunitz-like Protein Inhibitor domain (KPI) in the APP 751

isoform favors this association. We confirmed these results in our project (see paper 1), first by showing that APP dimerizes more than its C-terminal fragments in cells. Secondly, GXXXG mutations we introduced in the full-length APP did not show any differences in dimerization (Ben Khalifa et al., 2012a). Although dimers of APP CTFs can be readily detected in living cells by our method, when compared to APP, CTFs dimerization appears as a marginal event.

We showed here for the first time that **APP dimerization is enhanced by removal of the intracellular domain**. This appeared to us as an unexpected result, since APP intracellular domain is short, displays an intrinsically disordered structure (Ramelot et al., 2000;Ando et al., 2001) and does not present any determinant clearly involved in protein dimerization (Ramelot and Nicholson, 2001). A simple interpretation is that presence of the AICD within APP sequence forces a conformation restraining dimerization. This finding adds another argument to the idea that different domains of the protein, apart from GXXXG motifs and TM/JM regions, influence APP intrinsic dimerization properties. This has been addressed so far for the ectodomain, but not for the intracellular region, leading to hypothesis awaiting further experimental support. APP intracellular domain contains at least 3 sequences known to interact with more than 20 proteins including Fe65, X11/Mint and JIP. Fe65 have been identified to interact with the AICD. This association is involved in AICD-dependent transcription and form complexes with other cell surface proteins like lipoproteins receptors LRP and ApoEr2 (Cao and Sudhof, 2001;Pietrzik et al., 2004;Guenette et al., 1996). Fe65 as well as other AICD partners like X11α and X11β have already been shown to alter APP processing (Lee et al., 2003;Ando et al., 2001). We tested the potential role of AICD in APP dimerization when Fe65 is overexpressed but did not measure any effect on dimerization in CHO cells (data not shown). Nevertheless, the association of such proteins with the AICD might play a role in APP dimerization

and should be further investigated. A second hypothesis explaining the increased dimerization of APP lacking the intracellular domain is the removal of the GYENPTY internalization sequence. It is well known that retention of APP at the plasma membrane inhibits its degradation (Lichtenthaler, 2012). The resulting accumulation of APP at the plasma membrane could increase dimerization rate. This would suggest that dimerization occurs in specific compartments, like the plasma membrane, and prompts to investigate the precise sub-cellular localization of APP dimers. We showed that the **removal of the intracellular domain, enhancing dimerization, favors APP processing towards the non-amyloidogenic pathway**. Only ±10% of total APP protein resides at the cell surface where it can be rapidly cleaved by the α-secretase (Sisodia, 1992). At steady state, the majority of APP resides in the Golgi region, where the active β- and γ-secretases are present. Subcellular trafficking is well known to be a critical process in APP processing. Dimerization seems to favor APP trafficking towards non-amyloidogenic rather than amyloidogenic compartments. This is consistent with the increased α-secretase processing observed with compounds targeting of APP ectodomain dimerization (Libeu et al., 2012), and also with the Aβ decrease/sAPPα increase resulting from forced APP dimerization (Eggert et al., 2009). In our previous works, we found that dimers are generated along the secretory pathway and are probably enriched in the intermediate/cis-Golgi compartments. Increased dimerization of APP751 favors the non-amyloidogenic processing (Ben Khalifa et al., 2012b). We suggest that APP dimerization, which occurs early in the secretory pathway, could act as a signal that favors sorting from the *trans*-Golgi network (TGN) to the plasma membrane. APP in its dimeric form could escape from the Golgi compartments without being cleaved by the β- and γ-secretases. APP dimers could also be less internalized, due to masking of the internalization sequence. In any case, the result would be an increased

localization of APP at the plasma membrane where it is processed by the α-secretase. It is still difficult to know the percentage of APP under dimeric form at the plasma membrane, and the techniques we used here are not suitable to address this point. Another important question in this respect is to know whether APP can be cleaved by α-secretase in a dimeric state. A better comprehension of the mechanisms regulating APP trafficking towards the different pathways, and the contribution of dimerization we propose here, could be of interest to find novel solutions to struggle pathogenic Aβ production.

2. Implication of GXXXG motifs in APP CTFs dimerization

We demonstrate that **GXXXG motifs mutations do not readily impair dimerization of APP C-terminal fragments**. Although CTFs dimerize less than full-length APP, they have already been shown to form contacts between GXXXG motifs within the lipid bilayer (Sato et al., 2009). The orientation of APP TM helices in the dimers has been determined and is mediated by the GXXXG motifs rather than the GXXXA (Sato et al., 2009). Still, other publications using similar structural approaches found that APP TM interactions involve the GXXXA interface (Nadezhdin et al., 2012). The precise contribution of GXXXG and GXXXA interfaces in APP dimerization appear here as a matter of debate. Important to know, most of the studies addressing this question have been up to now carried out by structural approaches using synthetic or recombinant peptides reconstituted in micelles or lipid bilayers.

Our initial hypothesis was that the contribution of GXXXG and GXXXA motifs to APP dimerization was masked in full length protein, and unraveled by the shedding of the bulky ectodomain by α- or β-secretase. Our results do not show any consistent effect of GXXXG mutations on αCTF dimerization and only weak effects on βCTF dimerization. First the relevance and the extent of C99 dimerization has be recently questioned. Studies have shown that βCTF homodimerization is weak and maybe irrelevant *in vivo* (Song et al., 2013). Our work indicates that C99 dimers can be readily detected in living cells, but to a smaller extent than APP dimers. This initial view of the mechanisms involved in C99 dimerization, driven by GXXXG interfaces, is getting more complex. Recently, motifs present in the extracellular region of C99 have been depicted as a key determinant in dimerization (Tang et al., 2014; Hu et al. to be submitted).

Structural changes (by alanine mutations) in the $L^{17}VFFAEDVGSNK^{28}$ extracellular sequence lead to a disruption of the LVFF motif, and increases dimerization. A strong $L^{17}V^{18}F^{19}F^{20}$ inhibitory sequence is located at the α-site in APP CTFs and is folded in a hairpin anti-parallel β-sheet secondary structure. The LVFF β-sheet is linked to the TM α-helix, containing the $G^{25}S^{26}N^{27}K^{28}$ sequence, with the critical A^{21} position appearing to be at a breakpoint between the 2 secondary structures (Tang et al., 2014). These structural motifs strongly influence the conformation of APP CTFs and their ability to dimerize, although contacts in dimers might in any case be formed through the GXXXG and GXXXA interfaces.

Environmental factors like the membrane composition have also been found to influence C99 structure (Lu et al., 2011). Cholesterol has been suggested to bind GXXXG motifs and to stabilize the dimeric state of βCTF (Song et al., 2013). Thus, dimerization of the WT APP TM sequence is weak but can be modulated by structural motifs, protein concentration, mutations and membrane environment.

Another important point that is rising from our results is that **dimerization cannot be directly correlated to APP γ-cleavage and Aβ production**. GXXXG mutations as well as FAD mutations are known to modulate APP processing at the γ-site. Moreover, mutations of the GXXXG glycines rescue the effects of early onset FAD mutations on Aβ production (Munter et al., 2010). To note, FAD mutations do not affect APP dimerization and thereby APP dimerization does not appear to be responsible for the changes in Aβ production linked to early onset FAD (So et al., 2013). With a sensitive method to assay dimerization in living cells, we are not able to see any striking differences in dimerization of mutants that produce very different amounts of Aβ. We can suggest that, apart from their known role in TM dimerization, GXXXG motifs do not regulate processing by modifying the strength of the association. It is in line with recent results showing an independent relationship between APP dimerization and γ-secretase processivity (Eggert et al.,

2009;So et al., 2013; Jung et al., 2014). Rather than changing dimerization, mutation of glycines comprised in the GXXXG motifs might induce conformational changes increasing or decreasing the fitness of the substrate for the γ-secretase complex. Following this hypothesis, the large influence of the A21G mutation on processing might be associated with structural changes in the extracellular domain rather than dimerization. To summarize, GXXXG and GXXXG-like motifs are likely to regulate the ability of APP to be efficiently processed by the γ-secretase, by controlling the helical structure of the JM/TM regions (Tang et al., 2014).

Apart from dimerization, many cellular factors appear to influence the overall production of Aβ peptides and the Aβ42/Aβ40 ratio, including the presence of cholesterol (Beel and Sanders, 2008;Simons et al., 1998;Wahrle et al., 2002). γ-secretase modulators, NSAIDs and cholesterol are also known to interact with the TM domain of APP. Using these compounds and the split-luciferase approach, we could further investigate whether they act on APP processing by impacting dimerization of the amyloidogenic C-terminal fragments. To conclude here, both structural and environmental factors can induce conformational changes in APP resulting in modification of processivity at the γ-site. This is an important point to keep in mind for the development of therapeutics targeting Aβ production.

3. Role of Glycines from GXXXG motifs in the formation of pathogenic Aβ oligomers

Lot of recent evidences propose the non-fibrillar Aβ oligomeric forms as the key actors in the neurodegeneration occurring in Alzheimer's disease. They correlate precisely with the deficits (cognitive deficits, synaptic function impairments) observed during the pathogenesis (Lesne et al., 2006;Chen and Glabe, 2006). Amyloidogenic protein oligomers are often metastable and various sizes of oligomers coexist in heterogeneous mixtures. A broad array of Aβ oligomers has been described, isolated or produced in different models (Fig.30). The process of Aβ oligomerization has been widely studied *in vitro*, with synthetic Aβ peptides. A clear advantage of this approach is to work on pure Aβ material, and to track each step of the oligomerization process. On the other hand, Aβ assemblies have been isolated from brain tissues of AD transgenic mice (Lesne et al., 2006). The precise conformation of potentially pathogenic Aβ oligomers, or the relevance of *in vitro*-generated oligomers is an intense matter of debate (for a review, see Benilova et al., 2012). We discovered **a highly stable oligomeric specie that self-assembles in living cells**. We don't know here whether the oligomeric species produced in our experimental set up include other assemblies or intermediates that are less stable under the same conditions and thus not detected. However, they did not show significant toxicity in living cells but **obvious pathogenic properties on treated neuronal cells**. This is consistent with previous publications on Aβ oligomeric species depicting a disruption of the neuronal function, and particularly synaptic transmission (Lambert et al., 1998;Li et al., 2009). Lesne et al. have shown similar unique SDS-stable oligomeric assemblies correlating to memory deficits and displaying a concentration-dependent effect, independently of any neuronal loss

(Lesne et al., 2006;Reed et al., 2011). These species were termed Aβ*56 (±56 kDa), corresponding to soluble dodecamers. Aβ*56 assemblies were identified *ex vivo* from transgenic mice and AD patients brains. Further investigation of the formation the oligomeric assemblies we observe in mice models or AD brains are needed to confirm their relevance *in vivo*.

Nevertheless, the first set of results proves that oligomers are produced naturally by expression in mammalian cells and can be secreted in the extracellular media with a similar profile (conformation). We don't know exactly if Aβ oligomers form into the lipid bilayer immediately after production by the γ-secretase, or in the lumen of intracellular compartments. Our data indicate that they are enriched in membrane fractions. This is consistent with previous studies showing that oligomerization occurs when Aβ concentrate in vesicular compartments, reaching micromolar concentrations (Hu et al., 2009). At physiological temperature (37°C) and at high concentration, Aβ42 has been shown to rapidly aggregates into unstructured specific oligomers (Fu et al., 2015). The high concentrations achieved here by direct expression of Aβ42 could indeed mimic pathological situation in which Aβ accumulates in specific cellular compartments.

The oligomers we identified are produced in cells either by the processing of APP amyloidogenic fragment (C99) or by direct expression of Aβ42. Strikingly, soluble Aβ monomeric forms are only detected upon expression of constructs including the TM/intracellular junction (C99 and C55) but not when Aβ42 is directly expressed. This needs further investigation as it suggests that monomeric Aβ could only be produced by specific substrates in specific cellular compartments. In this case, the direct expression of Aβ42 in cellular compartments will always lead to spontaneously massive aggregation in oligomers, without any chance of monomeric detection.

The apparent molecular weight of oligomers, reflecting the number of monomers assembled, can also vary between cell-types and environmental conditions. The oligomers we observed were about 25-30 kDa and can correspond to hexamers, or less probably heptamers. It has been reported that the pathological assemblies of Aβ (Aβ*56, ADDLs, globulomers…) are multiples of hexameric basal units. Interestingly, the oligomers we evidenced are likely to be hexamers and the pathogenic Aβ*56 assemblies are described as dodecamers. Aβ hexamers can serve as building blocks for the formation of high-molecular weight oligomers or fibrils (Bernstein et al., 2009;Bitan et al., 2003;Roychaudhuri et al., 2009;Ahmed et al., 2010). Pentameric or hexameric Aβ species can also correspond to paranuclei, the described basic units of protofibrils (Ahmed et al., 2010;Bitan et al., 2004). A stable Aβ SDS-resistant hexamer has been studied, that undergoes interconversion to form fibrils (Gu et al., 2014). Hexameric species have also been described in pore-like oligomers. Some Aβ oligomeric forms have been reported to insert in cellular membranes and form β-barrels or cation channels (Arispe et al., 1992). Charles Glabe's team also demonstrated that their annular protofibrils species (Lashuel et al., 2002) are made of six Aβ hexamers subunits (Kayed et al., 2009;Lasagna-Reeves et al., 2011). Whether the Aβ species we observe are "on-pathway" for fibril formation has not been investigated. They can be prefibrillar or fibrillar assemblies. To answer that question, the structure of these oligomers has to be analyzed more precisely. Post-translational modifications have been shown to influence Aβ oligomerization in AD (Kumar et al., 2011). The presence of phosphorylated sites in these assemblies is interesting to investigate for further characterization.

The oligomeric forms we observe are **highly dependent of the TM glycines present in the GXXXG/A motifs**. Introduction of single and double mutations in glycines of the GXXXG and GXXXA motifs changes drastically the ability of Aβ to

form the oligomers. Several FAD mutations in APP have already been shown to increase the tendency of Aβ to oligomerize (Nilsberth et al., 2001;Tomiyama et al., 2008). More specifically, it has been shown that FAD mutations including Flemish mutation (A21G) increase formation of hexameric and dodecameric species (Gessel et al., 2012). Here again, a real correlation seems to exist between the formation of hexamers and the pathology.

Mutation of Aβ42 $G^{25}XXXG^{29}$ motifs strongly increases the oligomerization. In contrast, mutation of the $G^{38}XXXA^{42}$ and particularly the Gly38 abolishes the assembly. Mutation of these glycine residues indeed dramatically affects the formation of Aβ oligomers. Gly33 and Gly38 play a predominant role in this process by shifting the monomeric-oligomeric Aβ equilibrium toward the formation of oligomers (Gly33 mutants) or blocking the conversion from monomers to oligomers (Gly38 mutants). It can be explained by structural functions of these residues. The turn in the Aβ structure at Gly38 is a characteristic of Aβ42 oligomers but not Aβ40 and is very important for the β-hairpin structure (Ahmed et al., 2010). Molecular contacts have been reported between G38 and F19 (Luhrs et al., 2005) and between M35 and A42 (Masuda et al., 2008) in Aβ42 fibrils. Indeed, expression here of Aβ40, lacking the complete GXXXA motif, did not show any oligomerization in cells. Gly33 residue is part of the $G^{33}LMVG^{37}$ hydrophobic sequence forming a β-strand and is also critical for the conversion of antiparallel β-hairpin to β-sheet structure. Moreover, Gly33 mutation has been suggested to promote rapid Aβ oligomerization in high molecular weight oligomers (Harmeier et al., 2009). Mutation at Gly33 position is thus very likely to modify Aβ conformation in a way that favors oligomerization. The mutated glycines/alanine are parts of structural determinants involved in the formation and/or stability of the oligomerization. However, these observations await further structural studies in order to clearly understand how glycines 33 and

38 can control in an opposite way Aβ oligomerization in cells. Our results bring insight to the idea that intrinsic properties of Aβ40 and Aβ42 govern their different involvement in pathogeny.

4. General conclusions

My thesis work aimed at bringing novel insights in the role of GXXXG motifs present in APP TM region. These motifs were suggested to mediate dimerization of APP, despite recurrent and growing debate. We adapted and used a very recent approach (split luciferase) to confirm that APP ectodomain plays a major role in its dimerization. APP dimerization is influenced by structural determinant present in the intracellular part of the protein and probably also by interactions with contributors. Dimerization may not modulate directly the processing of APP at the γ-secretase cleavage site, but more likely shifting the processing toward the non-amyloidogenic pathway. GXXXG motifs are present in a region where many FAD mutations are clustered. Mutation of APP GXXXG motifs critically impairs APP processing by the γ-secretase. GXXXG motifs were therefore suggested to mediate dimerization of APP, regulating Aβ production. According to our results, mutations of APP GXXXG and GXXXG-like motifs do not critically affect dimerization of APP CTFs.

However, we show for the first time that GXXXG and GXXXG-like motifs are critical for an other important aspect of Alzheimer's disease: the formation of highly stable and pathogenic Aβ oligomers in the cells. The mutation of the glycine 38 residue (from the GXXXA motif) strongly inhibits Aβ oligomerization and rescue the pathogenic effects of the oligomers observed on neurons. The better characterization of these oligomeric species and their role in Alzheimer's disease could lead to a better understanding of Alzheimer's disease and eventually effective therapeutic outcomes.

BIBLIOGRAPHY

Abe K, Tanzi RE, Kogure K (1991) Selective induction of Kunitz-type protease inhibitor domain-containing amyloid precursor protein mRNA after persistent focal ischemia in rat cerebral cortex. Neurosci Lett 125:172-174.

Ahmed M, Davis J, Aucoin D, Sato T, Ahuja S, Aimoto S, Elliott JI, Van Nostrand WE, Smith SO (2010) Structural conversion of neurotoxic amyloid-beta(1-42) oligomers to fibrils. Nat Struct Mol Biol 17:561-567.

Albert JS (2009) Progress in the development of beta-secretase inhibitors for Alzheimer's disease. Prog Med Chem 48:133-161.

Allen B, Ingram E, Takao M, Smith MJ, Jakes R, Virdee K, Yoshida H, Holzer M, Craxton M, Emson PC, Atzori C, Migheli A, Crowther RA, Ghetti B, Spillantini MG, Goedert M (2002) Abundant tau filaments and nonapoptotic neurodegeneration in transgenic mice expressing human P301S tau protein. J Neurosci 22:9340-9351.

Allinquant B, Hantraye P, Mailleux P, Moya K, Bouillot C, Prochiantz A (1995) Downregulation of amyloid precursor protein inhibits neurite outgrowth in vitro. J Cell Biol 128:919-927.

Alonso AC, Grundke-Iqbal I, Iqbal K (1996) Alzheimer's disease hyperphosphorylated tau sequesters normal tau into tangles of filaments and disassembles microtubules. Nat Med 2:783-787.

Alzheimer A, Stelzmann RA, Schnitzlein HN, Murtagh FR (1995) An English translation of Alzheimer's 1907 paper, "Uber eine eigenartige Erkankung der Hirnrinde". Clin Anat 8:429-431.

Andersson ER, Lendahl U (2014) Therapeutic modulation of Notch signalling--are we there yet? Nat Rev Drug Discov 13:357-378.

Ando K, Iijima KI, Elliott JI, Kirino Y, Suzuki T (2001) Phosphorylation-dependent regulation of the interaction of amyloid precursor protein with Fe65 affects the production of beta-amyloid. J Biol Chem 276:40353-40361.

Annaert W, De SB (2002) A cell biological perspective on Alzheimer's disease. Annu Rev Cell Dev Biol 18:25-51.

Antzutkin ON, Balbach JJ, Leapman RD, Rizzo NW, Reed J, Tycko R (2000) Multiple quantum solid-state NMR indicates a parallel, not antiparallel, organization of beta-sheets in Alzheimer's beta-amyloid fibrils. Proc Natl Acad Sci U S A 97:13045-13050.

Araki Y, Tomita S, Yamaguchi H, Miyagi N, Sumioka A, Kirino Y, Suzuki T (2003) Novel cadherin-related membrane proteins, Alcadeins, enhance the X11-like protein-mediated stabilization of amyloid beta-protein precursor metabolism. J Biol Chem 278:49448-49458.

Arbely E, Arkin IT (2004) Experimental measurement of the strength of a C alpha-H...O bond in a lipid bilayer. J Am Chem Soc 126:5362-5363.

Arendt T, Bruckner MK, Mosch B, Losche A (2010) Selective cell death of hyperploid neurons in Alzheimer's disease. Am J Pathol 177:15-20.

Arispe N, Diaz JC, Simakova O (2007) Abeta ion channels. Prospects for treating Alzheimer's disease with Abeta channel blockers. Biochim Biophys Acta 1768:1952-1965.

Arispe N, Pollard HB, Rojas E (1993) Giant multilevel cation channels formed by Alzheimer disease amyloid beta-protein [A beta P-(1-40)] in bilayer membranes. Proc Natl Acad Sci U S A 90:10573-10577.

Arriagada PV, Growdon JH, Hedley-Whyte ET, Hyman BT (1992) Neurofibrillary tangles but not senile plaques parallel duration and severity of Alzheimer's disease. Neurology 42:631-639.

Asai M, Hattori C, Szabo B, Sasagawa N, Maruyama K, Tanuma S, Ishiura S (2003) Putative function of ADAM9, ADAM10, and ADAM17 as APP alpha-secretase. Biochem Biophys Res Commun 301:231-235.

Ashe KH, Aguzzi A (2013) Prions, prionoids and pathogenic proteins in Alzheimer disease. Prion 7:55-59.

Ashley J, Packard M, Ataman B, Budnik V (2005) Fasciclin II signals new synapse formation through amyloid precursor protein and the scaffolding protein dX11/Mint. J Neurosci 25:5943-5955.

Aydin D, Filippov MA, Tschape JA, Gretz N, Prinz M, Eils R, Brors B, Muller UC (2011) Comparative transcriptome profiling of amyloid precursor protein family members in the adult cortex. BMC Genomics 12:160.

Aydin D, Weyer SW, Muller UC (2012) Functions of the APP gene family in the nervous system: insights from mouse models. Exp Brain Res 217:423-434.

Back S, Haas P, Tschape JA, Gruebl T, Kirsch J, Muller U, Beyreuther K, Kins S (2007) beta-amyloid precursor protein can be transported independent of any sorting signal to the axonal and dendritic compartment. J Neurosci Res 85:2580-2590.

Baek SH, Ohgi KA, Rose DW, Koo EH, Glass CK, Rosenfeld MG (2002) Exchange of N-CoR corepressor and Tip60 coactivator complexes links gene expression by NF-kappaB and beta-amyloid precursor protein. Cell 110:55-67.

Baldwin AJ, Knowles TP, Tartaglia GG, Fitzpatrick AW, Devlin GL, Shammas SL, Waudby CA, Mossuto MF, Meehan S, Gras SL, Christodoulou J, Anthony-Cahill SJ, Barker PD, Vendruscolo M, Dobson CM (2011) Metastability of native proteins and the phenomenon of amyloid formation. J Am Chem Soc 133:14160-14163.

Ballatore C, Lee VM, Trojanowski JQ (2007) Tau-mediated neurodegeneration in Alzheimer's disease and related disorders. Nat Rev Neurosci 8:663-672.

Baratchi S, Evans J, Tate WP, Abraham WC, Connor B (2012) Secreted amyloid precursor proteins promote proliferation and glial differentiation of adult hippocampal neural progenitor cells. Hippocampus 22:1517-1527.

Barbagallo AP, Weldon R, Tamayev R, Zhou D, Giliberto L, Foreman O, D'Adamio L (2010) Tyr(682) in the intracellular domain of APP regulates amyloidogenic APP processing in vivo. PLoS One 5:e15503.

Barghorn S, Nimmrich V, Striebinger A, Krantz C, Keller P, Janson B, Bahr M, Schmidt M, Bitner RS, Harlan J, Barlow E, Ebert U, Hillen H (2005) Globular amyloid beta-peptide oligomer - a homogenous and stable neuropathological protein in Alzheimer's disease. J Neurochem 95:834-847.

Barnham KJ, McKinstry WJ, Multhaup G, Galatis D, Morton CJ, Curtain CC, Williamson NA, White AR, Hinds MG, Norton RS, Beyreuther K, Masters CL, Parker MW, Cappai R (2003) Structure of the Alzheimer's disease amyloid precursor protein copper binding domain. A regulator of neuronal copper homeostasis. J Biol Chem 278:17401-17407.

Barrett PJ, Song Y, Van Horn WD, Hustedt EJ, Schafer JM, Hadziselimovic A, Beel AJ, Sanders CR (2012) The amyloid precursor protein has a flexible transmembrane domain and binds cholesterol. Science 336:1168-1171.

Basun H, Bogdanovic N, Ingelsson M, Almkvist O, Naslund J, Axelman K, Bird TD, Nochlin D, Schellenberg GD, Wahlund LO, Lannfelt L (2008) Clinical and neuropathological features of the arctic APP gene mutation causing early-onset Alzheimer disease. Arch Neurol 65:499-505.

Bateman RJ, Siemers ER, Mawuenyega KG, Wen G, Browning KR, Sigurdson WC, Yarasheski KE, Friedrich SW, Demattos RB, May PC, Paul SM, Holtzman DM (2009) A gamma-secretase inhibitor decreases amyloid-beta production in the central nervous system. Ann Neurol 66:48-54.

Baudier J, Lee SH, Cole RD (1987) Separation of the different microtubule-associated tau protein species from bovine brain and their mode II phosphorylation by Ca2+/phospholipid-dependent protein kinase C. J Biol Chem 262:17584-17590.

Baumketner A, Krone MG, Shea JE (2008) Role of the familial Dutch mutation E22Q in the folding and aggregation of the 15-28 fragment of the Alzheimer amyloid-beta protein. Proc Natl Acad Sci U S A 105:6027-6032.

Beel AJ, Sanders CR (2008) Substrate specificity of gamma-secretase and other intramembrane proteases. Cell Mol Life Sci 65:1311-1334.

Beher D, Clarke EE, Wrigley JD, Martin AC, Nadin A, Churcher I, Shearman MS (2004) Selected non-steroidal anti-inflammatory drugs and their derivatives target gamma-secretase at a novel site. Evidence for an allosteric mechanism. J Biol Chem 279:43419-43426.

Beher D, Hesse L, Masters CL, Multhaup G (1996) Regulation of amyloid protein precursor (APP) binding to collagen and mapping of the binding sites on APP and collagen type I. J Biol Chem 271:1613-1620.

Belyaev ND, Kellett KA, Beckett C, Makova NZ, Revett TJ, Nalivaeva NN, Hooper NM, Turner AJ (2010) The transcriptionally active amyloid precursor protein (APP) intracellular domain is preferentially produced from the 695 isoform of APP in a {beta}-secretase-dependent pathway. J Biol Chem 285:41443-41454.

Ben Khalifa N, Van HJ, Tasiaux B, Huysseune S, Smith SO, Constantinescu SN, Octave JN, Kienlen-Campard P (2010) What is the role of amyloid precursor protein dimerization? Cell Adh Migr 4:268-272.

Ben Khalifa N, Tyteca D, Courtoy PJ, Renauld JC, Constantinescu SN, Octave JN, Kienlen-Campard P (2012a) Contribution of Kunitz protease inhibitor and transmembrane domains to amyloid precursor protein homodimerization. Neurodegener Dis 10:92-95.

Ben Khalifa N, Tyteca D, Marinangeli C, Depuydt M, Collet JF, Courtoy PJ, Renauld JC, Constantinescu S, Octave JN, Kienlen-Campard P (2012b) Structural features of the KPI domain control APP dimerization, trafficking, and processing. FASEB J 26:855-867.

Benilova I, Karran E, De SB (2012) The toxic Abeta oligomer and Alzheimer's disease: an emperor in need of clothes. Nat Neurosci 15:349-357.

Bentahir M, Nyabi O, Verhamme J, Tolia A, Horre K, Wiltfang J, Esselmann H, De SB (2006) Presenilin clinical mutations can affect gamma-secretase activity by different mechanisms. J Neurochem 96:732-742.

Benzinger TL, Gregory DM, Burkoth TS, Miller-Auer H, Lynn DG, Botto RE, Meredith SC (1998) Propagating structure of Alzheimer's beta-amyloid(10-35) is parallel beta-sheet with residues in exact register. Proc Natl Acad Sci U S A 95:13407-13412.

Bernstein SL, Dupuis NF, Lazo ND, Wyttenbach T, Condron MM, Bitan G, Teplow DB, Shea JE, Ruotolo BT, Robinson CV, Bowers MT (2009) Amyloid-beta protein oligomerization and the importance of tetramers and dodecamers in the aetiology of Alzheimer's disease. Nat Chem 1:326-331.

Bertini I, Gonnelli L, Luchinat C, Mao J, Nesi A (2011) A new structural model of Abeta40 fibrils. J Am Chem Soc 133:16013-16022.

Bertram L, Blacker D, Mullin K, Keeney D, Jones J, Basu S, Yhu S, McInnis MG, Go RC, Vekrellis K, Selkoe DJ, Saunders AJ, Tanzi RE (2000) Evidence for genetic linkage of Alzheimer's disease to chromosome 10q. Science 290:2302-2303.

Bertrand E, Brouillet E, Caille I, Bouillot C, Cole GM, Prochiantz A, Allinquant B (2001) A short cytoplasmic domain of the amyloid precursor protein induces apoptosis in vitro and in vivo. Mol Cell Neurosci 18:503-511.

Bezprozvanny I, Mattson MP (2008) Neuronal calcium mishandling and the pathogenesis of Alzheimer's disease. Trends Neurosci 31:454-463.

Biederer T, Cao X, Sudhof TC, Liu X (2002) Regulation of APP-dependent transcription complexes by Mint/X11s: differential functions of Mint isoforms. J Neurosci 22:7340-7351.

Bitan G, Fradinger EA, Spring SM, Teplow DB (2005) Neurotoxic protein oligomers--what you see is not always what you get. Amyloid 12:88-95.

Bitan G, Kirkitadze MD, Lomakin A, Vollers SS, Benedek GB, Teplow DB (2003a) Amyloid beta -protein (Abeta) assembly: Abeta 40 and Abeta 42 oligomerize through distinct pathways. Proc Natl Acad Sci U S A 100:330-335.

Bitan G, Teplow DB (2004) Rapid photochemical cross-linking--a new tool for studies of metastable, amyloidogenic protein assemblies. Acc Chem Res 37:357-364.

Bitan G, Vollers SS, Teplow DB (2003b) Elucidation of primary structure elements controlling early amyloid beta-protein oligomerization. J Biol Chem 278:34882-34889.

Bolmont T, Clavaguera F, Meyer-Luehmann M, Herzig MC, Radde R, Staufenbiel M, Lewis J, Hutton M, Tolnay M, Jucker M (2007) Induction of tau pathology by intracerebral infusion of amyloid-beta -containing brain extract and by amyloid-beta deposition in APP x Tau transgenic mice. Am J Pathol 171:2012-2020.

Bonifacino JS, Traub LM (2003) Signals for sorting of transmembrane proteins to endosomes and lysosomes. Annu Rev Biochem 72:395-447.

Bowie JU (2005) Solving the membrane protein folding problem. Nature 438:581-589.

Braak H, Braak E (1991) Neuropathological stageing of Alzheimer-related changes. Acta Neuropathol 82:239-259.

Braak H, Braak E (1995) Staging of Alzheimer's disease-related neurofibrillary changes. Neurobiol Aging 16:271-278.

Braak H, Braak E (1996) Evolution of the neuropathology of Alzheimer's disease. Acta Neurol Scand Suppl 165:3-12.

Brandt R, Lee G (1993) Functional organization of microtubule-associated protein tau. Identification of regions which affect microtubule growth, nucleation, and bundle formation in vitro. J Biol Chem 268:3414-3419.

Brosig B, Langosch D (1998) The dimerization motif of the glycophorin A transmembrane segment in membranes: importance of glycine residues. Protein Sci 7:1052-1056.

Brou C, Logeat F, Gupta N, Bessia C, LeBail O, Doedens JR, Cumano A, Roux P, Black RA, Israel A (2000) A novel proteolytic cleavage involved in Notch signaling: the role of the disintegrin-metalloprotease TACE. Mol Cell 5:207-216.

Brunelle P, Rauk A (2002) The radical model of Alzheimer's disease: specific recognition of Gly29 and Gly33 by Met35 in a beta-sheet model of Abeta: an ONIOM study. J Alzheimers Dis 4:283-289.

Bu G (2009) Apolipoprotein E and its receptors in Alzheimer's disease: pathways, pathogenesis and therapy. Nat Rev Neurosci 10:333-344.

Bucholtz N, Demuth I (2013) DNA-repair in mild cognitive impairment and Alzheimer's disease. DNA Repair (Amst) 12:811-816.

Buee L, Bussiere T, Buee-Scherrer V, Delacourte A, Hof PR (2000) Tau protein isoforms, phosphorylation and role in neurodegenerative disorders. Brain Res Brain Res Rev 33:95-130.

Bugiani O, Giaccone G, Rossi G, Mangieri M, Capobianco R, Morbin M, Mazzoleni G, Cupidi C, Marcon G, Giovagnoli A, Bizzi A, Di FG, Puoti G, Carella F, Salmaggi A, Romorini A, Patruno GM, Magoni M, Padovani A, Tagliavini F (2010) Hereditary cerebral hemorrhage with amyloidosis associated with the E693K mutation of APP. Arch Neurol 67:987-995.

Burdick D, Soreghan B, Kwon M, Kosmoski J, Knauer M, Henschen A, Yates J, Cotman C, Glabe C (1992) Assembly and aggregation properties of synthetic Alzheimer's A4/beta amyloid peptide analogs. J Biol Chem 267:546-554.

Bush AI, Multhaup G, Moir RD, Williamson TG, Small DH, Rumble B, Pollwein P, Beyreuther K, Masters CL (1993) A novel zinc(II) binding site modulates the function of the beta A4 amyloid protein precursor of Alzheimer's disease. J Biol Chem 268:16109-16112.

Butterfield DA (2003) Amyloid beta-peptide [1-42]-associated free radical-induced oxidative stress and neurodegeneration in Alzheimer's disease brain: mechanisms and consequences. Curr Med Chem 10:2651-2659.

Buxbaum JD, Liu KN, Luo Y, Slack JL, Stocking KL, Peschon JJ, Johnson RS, Castner BJ, Cerretti DP, Black RA (1998) Evidence that tumor necrosis factor alpha converting enzyme is involved in regulated alpha-secretase cleavage of the Alzheimer amyloid protein precursor. J Biol Chem 273:27765-27767.

Cao X, Sudhof TC (2001) A transcriptionally [correction of transcriptively] active complex of APP with Fe65 and histone acetyltransferase Tip60. Science 293:115-120.

Castellani RJ, Lee HG, Siedlak SL, Nunomura A, Hayashi T, Nakamura M, Zhu X, Perry G, Smith MA (2009) Reexamining Alzheimer's disease: evidence for a protective role for amyloid-beta protein precursor and amyloid-beta. J Alzheimers Dis 18:447-452.

Caughey B, Lansbury PT (2003) Protofibrils, pores, fibrils, and neurodegeneration: separating the responsible protein aggregates from the innocent bystanders. Annu Rev Neurosci 26:267-298.

Cerf E, Sarroukh R, Tamamizu-Kato S, Breydo L, Derclaye S, Dufrene YF, Narayanaswami V, Goormaghtigh E, Ruysschaert JM, Raussens V (2009) Antiparallel beta-sheet: a signature structure of the oligomeric amyloid beta-peptide. Biochem J 421:415-423.

Chai X, Dage JL, Citron M (2012) Constitutive secretion of tau protein by an unconventional mechanism. Neurobiol Dis 48:356-366.

Checler F, Sunyach C, Pardossi-Piquard R, Sevalle J, Vincent B, Kawarai T, Girardot N, St George-Hyslop P, da Costa CA (2007) The gamma/epsilon-secretase-derived APP intracellular domain fragments regulate p53. Curr Alzheimer Res 4:423-426.

Chen CD, Oh SY, Hinman JD, Abraham CR (2006) Visualization of APP dimerization and APP-Notch2 heterodimerization in living cells using bimolecular fluorescence complementation. J Neurochem 97:30-43.

Chen IH, Hu JH, Jow GM, Chuang CC, Lee TT, Liu DC, Jeng CJ (2011) Distal end of carboxyl terminus is not essential for the assembly of rat Eag1 potassium channels. J Biol Chem 286:27183-27196.

Chen W, Gamache E, Rosenman DJ, Xie J, Lopez MM, Li YM, Wang C (2014) Familial Alzheimer's mutations within APPTM increase Abeta42 production by enhancing accessibility of epsilon-cleavage site. Nat Commun 5:3037.

Chen WJ, Goldstein JL, Brown MS (1990) NPXY, a sequence often found in cytoplasmic tails, is required for coated pit-mediated internalization of the low density lipoprotein receptor. J Biol Chem 265:3116-3123.

Chen YR, Glabe CG (2006) Distinct early folding and aggregation properties of Alzheimer amyloid-beta peptides Abeta40 and Abeta42: stable trimer or tetramer formation by Abeta42. J Biol Chem 281:24414-24422.

Chimon S, Shaibat MA, Jones CR, Calero DC, Aizezi B, Ishii Y (2007) Evidence of fibril-like beta-sheet structures in a neurotoxic amyloid intermediate of Alzheimer's beta-amyloid. Nat Struct Mol Biol 14:1157-1164.

Citron M, Oltersdorf T, Haass C, McConlogue L, Hung AY, Seubert P, Vigo-Pelfrey C, Lieberburg I, Selkoe DJ (1992) Mutation of the beta-amyloid precursor protein in familial Alzheimer's disease increases beta-protein production. Nature 360:672-674.

Clarris HJ, Cappai R, Heffernan D, Beyreuther K, Masters CL, Small DH (1997) Identification of heparin-binding domains in the amyloid precursor protein of Alzheimer's disease by deletion mutagenesis and peptide mapping. J Neurochem 68:1164-1172.

Clavaguera F, Akatsu H, Fraser G, Crowther RA, Frank S, Hench J, Probst A, Winkler DT, Reichwald J, Staufenbiel M, Ghetti B, Goedert M, Tolnay M (2013) Brain homogenates from human tauopathies induce tau inclusions in mouse brain. Proc Natl Acad Sci U S A 110:9535-9540.

Clavaguera F, Bolmont T, Crowther RA, Abramowski D, Frank S, Probst A, Fraser G, Stalder AK, Beibel M, Staufenbiel M, Jucker M, Goedert M, Tolnay M (2009) Transmission and spreading of tauopathy in transgenic mouse brain. Nat Cell Biol 11:909-913.

Cleary JP, Walsh DM, Hofmeister JJ, Shankar GM, Kuskowski MA, Selkoe DJ, Ashe KH (2005) Natural oligomers of the amyloid-beta protein specifically disrupt cognitive function. Nat Neurosci 8:79-84.

Cohen AS, CALKINS E (1959) Electron microscopic observations on a fibrous component in amyloid of diverse origins. Nature 183:1202-1203.

Cohen FE, Prusiner SB (1998) Pathologic conformations of prion proteins. Annu Rev Biochem 67:793-819.

Copanaki E, Chang S, Vlachos A, Tschape JA, Muller UC, Kogel D, Deller T (2010) sAPPalpha antagonizes dendritic degeneration and neuron death triggered by proteasomal stress. Mol Cell Neurosci 44:386-393.

Cosson P, Perrin J, Bonifacino JS (2013) Anchors aweigh: protein localization and transport mediated by transmembrane domains. Trends Cell Biol 23:511-517.

Coulson EJ, Paliga K, Beyreuther K, Masters CL (2000) What the evolution of the amyloid protein precursor supergene family tells us about its function. Neurochem Int 36:175-184.

Covacci A, Telford JL, Del GG, Parsonnet J, Rappuoli R (1999) Helicobacter pylori virulence and genetic geography. Science 284:1328-1333.

Cramer PE, Cirrito JR, Wesson DW, Lee CY, Karlo JC, Zinn AE, Casali BT, Restivo JL, Goebel WD, James MJ, Brunden KR, Wilson DA, Landreth GE (2012) ApoE-directed therapeutics rapidly clear beta-amyloid and reverse deficits in AD mouse models. Science 335:1503-1506.

Cross KJ, Wharton SA, Skehel JJ, Wiley DC, Steinhauer DA (2001) Studies on influenza haemagglutinin fusion peptide mutants generated by reverse genetics. EMBO J 20:4432-4442.

Curran AR, Engelman DM (2003) Sequence motifs, polar interactions and conformational changes in helical membrane proteins. Curr Opin Struct Biol 13:412-417.

Dahms SO, Hoefgen S, Roeser D, Schlott B, Guhrs KH, Than ME (2010) Structure and biochemical analysis of the heparin-induced E1 dimer of the amyloid precursor protein. Proc Natl Acad Sci U S A 107:5381-5386.

Dawson JP, Weinger JS, Engelman DM (2002) Motifs of serine and threonine can drive association of transmembrane helices. J Mol Biol 316:799-805.

De JC, Zehr C, Yager D, Prada CM, Younkin S, Hendriks L, Van BC, Eckman CB (1998) Flemish and Dutch mutations in amyloid beta precursor protein have different effects on amyloid beta secretion. Neurobiol Dis 5:281-286.

De SB (2003) Aph-1, Pen-2, and Nicastrin with Presenilin generate an active gamma-Secretase complex. Neuron 38:9-12.

De SB (2010) Proteases and proteolysis in Alzheimer disease: a multifactorial view on the disease process. Physiol Rev 90:465-494.

Di FG, et al. (2009) A recessive mutation in the APP gene with dominant-negative effect on amyloidogenesis. Science 323:1473-1477.

Dillen K, Annaert W (2006) A two decade contribution of molecular cell biology to the centennial of Alzheimer's disease: are we progressing toward therapy? Int Rev Cytol 254:215-300.

Dominguez L, Foster L, Meredith SC, Straub JE, Thirumalai D (2014) Structural heterogeneity in transmembrane amyloid precursor protein homodimer is a consequence of environmental selection. J Am Chem Soc 136:9619-9626.

Dong J, Atwood CS, Anderson VE, Siedlak SL, Smith MA, Perry G, Carey PR (2003) Metal binding and oxidation of amyloid-beta within isolated senile plaque cores: Raman microscopic evidence. Biochemistry 42:2768-2773.

Dong W, Vuletic S, Albers JJ (2009) Differential effects of simvastatin and pravastatin on expression of Alzheimer's disease-related genes in human astrocytes and neuronal cells. J Lipid Res 50:2095-2102.

Donmez G, Wang D, Cohen DE, Guarente L (2010) SIRT1 suppresses beta-amyloid production by activating the alpha-secretase gene ADAM10. Cell 142:320-332.

Doody RS, Farlow M, Aisen PS (2014a) Phase 3 trials of solanezumab and bapineuzumab for Alzheimer's disease. N Engl J Med 370:1460.

Doody RS, Thomas RG, Farlow M, Iwatsubo T, Vellas B, Joffe S, Kieburtz K, Raman R, Sun X, Aisen PS, Siemers E, Liu-Seifert H, Mohs R (2014b) Phase 3 trials of solanezumab for mild-to-moderate Alzheimer's disease. N Engl J Med 370:311-321.

Drechsel DN, Hyman AA, Cobb MH, Kirschner MW (1992) Modulation of the dynamic instability of tubulin assembly by the microtubule-associated protein tau. Mol Biol Cell 3:1141-1154.

Dries DR, Shah S, Han YH, Yu C, Yu S, Shearman MS, Yu G (2009) Glu-333 of nicastrin directly participates in gamma-secretase activity. J Biol Chem 284:29714-29724.

Dries DR, Yu G (2008) Assembly, maturation, and trafficking of the gamma-secretase complex in Alzheimer's disease. Curr Alzheimer Res 5:132-146.

Durairajan SS, Liu LF, Lu JH, Koo I, Maruyama K, Chung SK, Huang JD, Li M (2011) Stimulation of non-amyloidogenic processing of amyloid-beta protein precursor by cryptotanshinone involves activation and translocation of ADAM10 and PKC-alpha. J Alzheimers Dis 25:245-262.

Eckert A, Hauptmann S, Scherping I, Meinhardt J, Rhein V, Drose S, Brandt U, Fandrich M, Muller WE, Gotz J (2008) Oligomeric and fibrillar species of beta-amyloid (A beta 42) both impair mitochondrial function in P301L tau transgenic mice. J Mol Med (Berl) 86:1255-1267.

Edbauer D, Winkler E, Regula JT, Pesold B, Steiner H, Haass C (2003) Reconstitution of gamma-secretase activity. Nat Cell Biol 5:486-488.

Eggert S, Midthune B, Cottrell B, Koo EH (2009) Induced dimerization of the amyloid precursor protein leads to decreased amyloid-beta protein production. J Biol Chem 284:28943-28952.

Eilers M, Patel AB, Liu W, Smith SO (2002) Comparison of helix interactions in membrane and soluble alpha-bundle proteins. Biophys J 82:2720-2736.

Etcheberrigaray R, Tan M, Dewachter I, Kuiperi C, Van dA, I, Wera S, Qiao L, Bank B, Nelson TJ, Kozikowski AP, Van LF, Alkon DL (2004) Therapeutic effects of PKC activators in Alzheimer's disease transgenic mice. Proc Natl Acad Sci U S A 101:11141-11146.

Fabian H, Szendrei GI, Mantsch HH, Greenberg BD, Otvos L, Jr. (1994) Synthetic post-translationally modified human A beta peptide exhibits a markedly increased tendency to form beta-pleated sheets in vitro. Eur J Biochem 221:959-964.

Fandrich M, Meinhardt J, Grigorieff N (2009) Structural polymorphism of Alzheimer Abeta and other amyloid fibrils. Prion 3:89-93.

Farzan M, Schnitzler CE, Vasilieva N, Leung D, Choe H (2000) BACE2, a beta -secretase homolog, cleaves at the beta site and within the amyloid-beta region of the amyloid-beta precursor protein. Proc Natl Acad Sci U S A 97:9712-9717.

Finder VH (2010) Alzheimer's disease: a general introduction and pathomechanism. J Alzheimers Dis 22 Suppl 3:5-19.

Finder VH, Glockshuber R (2007) Amyloid-beta aggregation. Neurodegener Dis 4:13-27.

Fitzpatrick AW, Debelouchina GT, Bayro MJ, Clare DK, Caporini MA, Bajaj VS, Jaroniec CP, Wang L, Ladizhansky V, Muller SA, MacPhee CE, Waudby CA, Mott HR, De SA, Knowles TP, Saibil HR, Vendruscolo M, Orlova EV, Griffin RG, Dobson CM (2013) Atomic structure and hierarchical assembly of a cross-beta amyloid fibril. Proc Natl Acad Sci U S A 110:5468-5473.

Fonte V, Dostal V, Roberts CM, Gonzales P, Lacor PN, Velasco PT, Magrane J, Dingwell N, Fan EY, Silverman MA, Stein GH, Link CD (2011) A glycine zipper motif mediates the formation of toxic beta-amyloid oligomers in vitro and in vivo. Mol Neurodegener 6:61.

Fraering PC, LaVoie MJ, Ye W, Ostaszewski BL, Kimberly WT, Selkoe DJ, Wolfe MS (2004) Detergent-dependent dissociation of active gamma-secretase reveals an interaction between Pen-2 and PS1-NTF and offers a model for subunit organization within the complex. Biochemistry 43:323-333.

Freude KK, Penjwini M, Davis JL, LaFerla FM, Blurton-Jones M (2011) Soluble amyloid precursor protein induces rapid neural differentiation of human embryonic stem cells. J Biol Chem 286:24264-24274.

Fu Z, Aucoin D, Davis J, Van Nostrand WE, Smith SO (2015) Mechanism of Nucleated Conformational Conversion of Aβ42. Biochemistry 54:4197-4207.

Furukawa K, Barger SW, Blalock EM, Mattson MP (1996a) Activation of K+ channels and suppression of neuronal activity by secreted beta-amyloid-precursor protein. Nature 379:74-78.

Furukawa K, Sopher BL, Rydel RE, Begley JG, Pham DG, Martin GM, Fox M, Mattson MP (1996b) Increased activity-regulating and neuroprotective efficacy of alpha-secretase-derived secreted amyloid precursor protein conferred by a C-terminal heparin-binding domain. J Neurochem 67:1882-1896.

Galvan V, Gorostiza OF, Banwait S, Ataie M, Logvinova AV, Sitaraman S, Carlson E, Sagi SA, Chevallier N, Jin K, Greenberg DA, Bredesen DE (2006) Reversal of Alzheimer's-like pathology and behavior in human APP transgenic mice by mutation of Asp664. Proc Natl Acad Sci U S A 103:7130-7135.

Gellermann GP, Byrnes H, Striebinger A, Ullrich K, Mueller R, Hillen H, Barghorn S (2008) Abeta-globulomers are formed independently of the fibril pathway. Neurobiol Dis 30:212-220.

Georganopoulou DG, Chang L, Nam JM, Thaxton CS, Mufson EJ, Klein WL, Mirkin CA (2005) Nanoparticle-based detection in cerebral spinal fluid of a soluble pathogenic biomarker for Alzheimer's disease. Proc Natl Acad Sci U S A 102:2273-2276.

Gessel MM, Bernstein S, Kemper M, Teplow DB, Bowers MT (2012) Familial Alzheimer's disease mutations differentially alter amyloid beta-protein oligomerization. ACS Chem Neurosci 3:909-918.

Geula C, Wu CK, Saroff D, Lorenzo A, Yuan M, Yankner BA (1998) Aging renders the brain vulnerable to amyloid beta-protein neurotoxicity. Nat Med 4:827-831.

Giliberto L, Zhou D, Weldon R, Tamagno E, De LP, Tabaton M, D'Adamio L (2008) Evidence that the Amyloid beta Precursor Protein-intracellular domain lowers the stress threshold of neurons and has a "regulated" transcriptional role. Mol Neurodegener 3:12.

Gillman KW, et al. (2010) Discovery and Evaluation of BMS-708163, a Potent, Selective and Orally Bioavailable gamma-Secretase Inhibitor. ACS Med Chem Lett 1:120-124.

Glabe CG (2008) Structural classification of toxic amyloid oligomers. J Biol Chem 283:29639-29643.

Glenner GG, Wong CW, Quaranta V, Eanes ED (1984) The amyloid deposits in Alzheimer's disease: their nature and pathogenesis. Appl Pathol 2:357-369.

Goate A, Chartier-Harlin MC, Mullan M, Brown J, Crawford F, Fidani L, Giuffra L, Haynes A, Irving N, James L, . (1991) Segregation of a missense mutation in the amyloid precursor protein gene with familial Alzheimer's disease. Nature 349:704-706.

Gold M, Alderton C, Zvartau-Hind M, Egginton S, Saunders AM, Irizarry M, Craft S, Landreth G, Linnamagi U, Sawchak S (2010) Rosiglitazone monotherapy in mild-to-moderate Alzheimer's disease: results from a randomized, double-blind, placebo-controlled phase III study. Dement Geriatr Cogn Disord 30:131-146.

Goldgaber D, Lerman MI, McBride OW, Saffiotti U, Gajdusek DC (1987) Characterization and chromosomal localization of a cDNA encoding brain amyloid of Alzheimer's disease. Science 235:877-880.

Gong Y, Chang L, Viola KL, Lacor PN, Lambert MP, Finch CE, Krafft GA, Klein WL (2003) Alzheimer's disease-affected brain: presence of oligomeric A beta ligands (ADDLs) suggests a molecular basis for reversible memory loss. Proc Natl Acad Sci U S A 100:10417-10422.

Gorman PM, Kim S, Guo M, Melnyk RA, McLaurin J, Fraser PE, Bowie JU, Chakrabartty A (2008) Dimerization of the transmembrane domain of amyloid precursor proteins and familial Alzheimer's disease mutants. BMC Neurosci 9:17.

Gotz J, Chen F, van DJ, Nitsch RM (2001) Formation of neurofibrillary tangles in P301l tau transgenic mice induced by Abeta 42 fibrils. Science 293:1491-1495.

Gotz J, Ittner LM (2008) Animal models of Alzheimer's disease and frontotemporal dementia. Nat Rev Neurosci 9:532-544.

Gralle M, Botelho MG, Wouters FS (2009) Neuroprotective secreted amyloid precursor protein acts by disrupting amyloid precursor protein dimers. J Biol Chem 284:15016-15025.

Gralle M, Oliveira CL, Guerreiro LH, McKinstry WJ, Galatis D, Masters CL, Cappai R, Parker MW, Ramos CH, Torriani I, Ferreira ST (2006) Solution conformation and heparin-induced dimerization of the full-length extracellular domain of the human amyloid precursor protein. J Mol Biol 357:493-508.

Grant MA, Lazo ND, Lomakin A, Condron MM, Arai H, Yamin G, Rigby AC, Teplow DB (2007) Familial Alzheimer's disease mutations alter the stability of the amyloid beta-protein monomer folding nucleus. Proc Natl Acad Sci U S A 104:16522-16527.

Green KN, LaFerla FM (2008) Linking calcium to Abeta and Alzheimer's disease. Neuron 59:190-194.

Green RC, Schneider LS, Amato DA, Beelen AP, Wilcock G, Swabb EA, Zavitz KH (2009) Effect of tarenflurbil on cognitive decline and activities of daily living in patients with mild Alzheimer disease: a randomized controlled trial. JAMA 302:2557-2564.

Gu L, Liu C, Stroud JC, Ngo S, Jiang L, Guo Z (2014) Antiparallel triple-strand architecture for prefibrillar Abeta42 oligomers. J Biol Chem 289:27300-27313.

Gu Y, Misonou H, Sato T, Dohmae N, Takio K, Ihara Y (2001) Distinct intramembrane cleavage of the beta-amyloid precursor protein family resembling gamma-secretase-like cleavage of Notch. J Biol Chem 276:35235-35238.

Guenette SY, Chen J, Jondro PD, Tanzi RE (1996) Association of a novel human FE65-like protein with the cytoplasmic domain of the beta-amyloid precursor protein. Proc Natl Acad Sci U S A 93:10832-10837.

Guntert A, Dobeli H, Bohrmann B (2006) High sensitivity analysis of amyloid-beta peptide composition in amyloid deposits from human and PS2APP mouse brain. Neuroscience 143:461-475.

Guo JL, Lee VM (2011) Seeding of normal Tau by pathological Tau conformers drives pathogenesis of Alzheimer-like tangles. J Biol Chem 286:15317-15331.

Guo JL, Lee VM (2014) Cell-to-cell transmission of pathogenic proteins in neurodegenerative diseases. Nat Med 20:130-138.

Guo Q, Wang Z, Li H, Wiese M, Zheng H (2012) APP physiological and pathophysiological functions: insights from animal models. Cell Res 22:78-89.

Gustke N, Trinczek B, Biernat J, Mandelkow EM, Mandelkow E (1994) Domains of tau protein and interactions with microtubules. Biochemistry 33:9511-9522.

Haas C, Hung AY, Citron M, Teplow DB, Selkoe DJ (1995) beta-Amyloid, protein processing and Alzheimer's disease. Arzneimittelforschung 45:398-402.

Han P, Dou F, Li F, Zhang X, Zhang YW, Zheng H, Lipton SA, Xu H, Liao FF (2005) Suppression of cyclin-dependent kinase 5 activation by amyloid precursor protein: a novel excitoprotective mechanism involving modulation of tau phosphorylation. J Neurosci 25:11542-11552.

Hansen RA, Gartlehner G, Webb AP, Morgan LC, Moore CG, Jonas DE (2008) Efficacy and safety of donepezil, galantamine, and rivastigmine for the treatment of Alzheimer's disease: a systematic review and meta-analysis. Clin Interv Aging 3:211-225.

Hardy J (1992) Framing beta-amyloid. Nat Genet 1:233-234.

Hardy J, Selkoe DJ (2002) The amyloid hypothesis of Alzheimer's disease: progress and problems on the road to therapeutics. Science 297:353-356.

Hardy JA, Higgins GA (1992) Alzheimer's disease: the amyloid cascade hypothesis. Science 256:184-185.

Harmeier A, Wozny C, Rost BR, Munter LM, Hua H, Georgiev O, Beyermann M, Hildebrand PW, Weise C, Schaffner W, Schmitz D, Multhaup G (2009) Role of amyloid-beta glycine 33 in oligomerization, toxicity, and neuronal plasticity. J Neurosci 29:7582-7590.

Harris JA, Devidze N, Halabisky B, Lo I, Thwin MT, Yu GQ, Bredesen DE, Masliah E, Mucke L (2010) Many neuronal and behavioral impairments in transgenic mouse models of Alzheimer's disease are independent of caspase cleavage of the amyloid precursor protein. J Neurosci 30:372-381.

Hass MR, Yankner BA (2005) A {gamma}-secretase-independent mechanism of signal transduction by the amyloid precursor protein. J Biol Chem 280:36895-36904.

Hayden EY, Teplow DB (2013) Amyloid beta-protein oligomers and Alzheimer's disease. Alzheimers Res Ther 5:60.

Heber S, Herms J, Gajic V, Hainfellner J, Aguzzi A, Rulicke T, von KH, von KC, Sisodia S, Tremml P, Lipp HP, Wolfer DP, Muller U (2000) Mice with combined gene knock-outs reveal essential and partially redundant functions of amyloid precursor protein family members. J Neurosci 20:7951-7963.

Hegde RS, Mastrianni JA, Scott MR, DeFea KA, Tremblay P, Torchia M, DeArmond SJ, Prusiner SB, Lingappa VR (1998) A transmembrane form of the prion protein in neurodegenerative disease. Science 279:827-834.

Hendrickx A, Pierrot N, Tasiaux B, Schakman O, Brion JP, Kienlen-Campard P, De SC, Octave JN (2013) Epigenetic induction of EGR-1 expression by the amyloid precursor protein during exposure to novelty. PLoS One 8:e74305.

Herreman A, Hartmann D, Annaert W, Saftig P, Craessaerts K, Serneels L, Umans L, Schrijvers V, Checler F, Vanderstichele H, Baekelandt V, Dressel R, Cupers P, Huylebroeck D, Zwijsen A, Van LF, De SB (1999) Presenilin 2 deficiency causes a mild pulmonary phenotype and no changes in amyloid precursor protein processing but enhances the

embryonic lethal phenotype of presenilin 1 deficiency. Proc Natl Acad Sci U S A 96:11872-11877.

Herrup K (2010) Reimagining Alzheimer's disease--an age-based hypothesis. J Neurosci 30:16755-16762.

Herrup K (2015) The case for rejecting the amyloid cascade hypothesis. Nat Neurosci 18:794-799.

Ho A, Sudhof TC (2004) Binding of F-spondin to amyloid-beta precursor protein: a candidate amyloid-beta precursor protein ligand that modulates amyloid-beta precursor protein cleavage. Proc Natl Acad Sci U S A 101:2548-2553.

Hoe HS, Lee KJ, Carney RS, Lee J, Markova A, Lee JY, Howell BW, Hyman BT, Pak DT, Bu G, Rebeck GW (2009) Interaction of reelin with amyloid precursor protein promotes neurite outgrowth. J Neurosci 29:7459-7473.

Holmes BB, Furman JL, Mahan TE, Yamasaki TR, Mirbaha H, Eades WC, Belaygorod L, Cairns NJ, Holtzman DM, Diamond MI (2014) Proteopathic tau seeding predicts tauopathy in vivo. Proc Natl Acad Sci U S A 111:E4376-E4385.

Holmes C, Boche D, Wilkinson D, Yadegarfar G, Hopkins V, Bayer A, Jones RW, Bullock R, Love S, Neal JW, Zotova E, Nicoll JA (2008) Long-term effects of Abeta42 immunisation in Alzheimer's disease: follow-up of a randomised, placebo-controlled phase I trial. Lancet 372:216-223.

Hong C, Oksanen HM, Liu X, Jakana J, Bamford DH, Chiu W (2014) A structural model of the genome packaging process in a membrane-containing double stranded DNA virus. PLoS Biol 12:e1002024.

Hoshi M, Sato M, Matsumoto S, Noguchi A, Yasutake K, Yoshida N, Sato K (2003) Spherical aggregates of beta-amyloid (amylospheroid) show high neurotoxicity and activate tau protein kinase I/glycogen synthase kinase-3beta. Proc Natl Acad Sci U S A 100:6370-6375.

Howell BW, Lanier LM, Frank R, Gertler FB, Cooper JA (1999) The disabled 1 phosphotyrosine-binding domain binds to the internalization signals of transmembrane glycoproteins and to phospholipids. Mol Cell Biol 19:5179-5188.

Hsia AY, Masliah E, McConlogue L, Yu GQ, Tatsuno G, Hu K, Kholodenko D, Malenka RC, Nicoll RA, Mucke L (1999) Plaque-independent disruption of neural circuits in Alzheimer's disease mouse models. Proc Natl Acad Sci U S A 96:3228-3233.

Hu X, Crick SL, Bu G, Frieden C, Pappu RV, Lee JM (2009) Amyloid seeds formed by cellular uptake, concentration, and aggregation of the amyloid-beta peptide. Proc Natl Acad Sci U S A 106:20324-20329.

Hung LW, Ciccotosto GD, Giannakis E, Tew DJ, Perez K, Masters CL, Cappai R, Wade JD, Barnham KJ (2008) Amyloid-beta peptide (Abeta) neurotoxicity is modulated by the rate of peptide aggregation: Abeta dimers and trimers correlate with neurotoxicity. J Neurosci 28:11950-11958.

Hunter S, Arendt T, Brayne C (2013) The senescence hypothesis of disease progression in Alzheimer disease: an integrated matrix of disease pathways for FAD and SAD. Mol Neurobiol 48:556-570.

Hutton M, et al. (1998) Association of missense and 5'-splice-site mutations in tau with the inherited dementia FTDP-17. Nature 393:702-705.

Imbimbo BP, Giardina GA (2011) gamma-secretase inhibitors and modulators for the treatment of Alzheimer's disease: disappointments and hopes. Curr Top Med Chem 11:1555-1570.

Iqbal K, Grundke-Iqbal I (2005) Metabolic/signal transduction hypothesis of Alzheimer's disease and other tauopathies. Acta Neuropathol 109:25-31.

Irizarry MC, Locascio JJ, Hyman BT (2001a) beta-site APP cleaving enzyme mRNA expression in APP transgenic mice: anatomical overlap with transgene expression and static levels with aging. Am J Pathol 158:173-177.

Irizarry MC, Locascio JJ, Hyman BT (2001b) beta-site APP cleaving enzyme mRNA expression in APP transgenic mice: anatomical overlap with transgene expression and static levels with aging. Am J Pathol 158:173-177.

Irizarry MC, McNamara M, Fedorchak K, Hsiao K, Hyman BT (1997) APPSw transgenic mice develop age-related A beta deposits and neuropil abnormalities, but no neuronal loss in CA1. J Neuropathol Exp Neurol 56:965-973.

Jack CR, Jr., Knopman DS, Jagust WJ, Petersen RC, Weiner MW, Aisen PS, Shaw LM, Vemuri P, Wiste HJ, Weigand SD, Lesnick TG, Pankratz VS, Donohue MC, Trojanowski JQ (2013) Tracking pathophysiological processes in Alzheimer's disease: an updated hypothetical model of dynamic biomarkers. Lancet Neurol 12:207-216.

Jack CR, Jr., Knopman DS, Jagust WJ, Shaw LM, Aisen PS, Weiner MW, Petersen RC, Trojanowski JQ (2010) Hypothetical model of dynamic biomarkers of the Alzheimer's pathological cascade. Lancet Neurol 9:119-128.

Jacobsen KT, Iverfeldt K (2009) Amyloid precursor protein and its homologues: a family of proteolysis-dependent receptors. Cell Mol Life Sci 66:2299-2318.

Janus C, Pearson J, McLaurin J, Mathews PM, Jiang Y, Schmidt SD, Chishti MA, Horne P, Heslin D, French J, Mount HT, Nixon RA, Mercken M, Bergeron C, Fraser PE, St George-

Hyslop P, Westaway D (2000) A beta peptide immunization reduces behavioural impairment and plaques in a model of Alzheimer's disease. Nature 408:979-982.

Jarrett JT, Berger EP, Lansbury PT, Jr. (1993) The carboxy terminus of the beta amyloid protein is critical for the seeding of amyloid formation: implications for the pathogenesis of Alzheimer's disease. Biochemistry 32:4693-4697.

Jiang S, Vakser IA (2000) Side chains in transmembrane helices are shorter at helix-helix interfaces. Proteins 40:429-435.

Jo J, Whitcomb DJ, Olsen KM, Kerrigan TL, Lo SC, Bru-Mercier G, Dickinson B, Scullion S, Sheng M, Collingridge G, Cho K (2011) Abeta(1-42) inhibition of LTP is mediated by a signaling pathway involving caspase-3, Akt1 and GSK-3beta. Nat Neurosci 14:545-547.

Jonsson T, et al. (2012) A mutation in APP protects against Alzheimer's disease and age-related cognitive decline. Nature 488:96-99.

Kaether C, Capell A, Edbauer D, Winkler E, Novak B, Steiner H, Haass C (2004) The presenilin C-terminus is required for ER-retention, nicastrin-binding and gamma-secretase activity. EMBO J 23:4738-4748.

Kaether C, Skehel P, Dotti CG (2000) Axonal membrane proteins are transported in distinct carriers: a two-color video microscopy study in cultured hippocampal neurons. Mol Biol Cell 11:1213-1224.

Kalimo H, Lalowski M, Bogdanovic N, Philipson O, Bird TD, Nochlin D, Schellenberg GD, Brundin R, Olofsson T, Soliymani R, Baumann M, Wirths O, Bayer TA, Nilsson LN, Basun H, Lannfelt L, Ingelsson M (2013) The Arctic AbetaPP mutation leads to Alzheimer's disease pathology with highly variable topographic deposition of differentially truncated Abeta. Acta Neuropathol Commun 1:60.

Kayed R, Pensalfini A, Margol L, Sokolov Y, Sarsoza F, Head E, Hall J, Glabe C (2009) Annular protofibrils are a structurally and functionally distinct type of amyloid oligomer. J Biol Chem 284:4230-4237.

Kessler JC, Rochet JC, Lansbury PT, Jr. (2003) The N-terminal repeat domain of alpha-synuclein inhibits beta-sheet and amyloid fibril formation. Biochemistry 42:672-678.

Kfoury N, Holmes BB, Jiang H, Holtzman DM, Diamond MI (2012) Trans-cellular propagation of Tau aggregation by fibrillar species. J Biol Chem 287:19440-19451.

Kibbey MC, Jucker M, Weeks BS, Neve RL, Van Nostrand WE, Kleinman HK (1993) beta-Amyloid precursor protein binds to the neurite-promoting IKVAV site of laminin. Proc Natl Acad Sci U S A 90:10150-10153.

KIDD M (1964) ALZHEIMER'S DISEASE - AN ELECTRON MICROSCOPICAL STUDY. Brain 87:307-320.

Kienlen-Campard P, Tasiaux B, Van HJ, Li M, Huysseune S, Sato T, Fei JZ, Aimoto S, Courtoy PJ, Smith SO, Constantinescu SN, Octave JN (2008) Amyloidogenic processing but not amyloid precursor protein (APP) intracellular C-terminal domain production requires a precisely oriented APP dimer assembled by transmembrane GXXXG motifs. J Biol Chem 283:7733-7744.

Kim HS, Kim EM, Lee JP, Park CH, Kim S, Seo JH, Chang KA, Yu E, Jeong SJ, Chong YH, Suh YH (2003) C-terminal fragments of amyloid precursor protein exert neurotoxicity by inducing glycogen synthase kinase-3beta expression. FASEB J 17:1951-1953.

Kim J, Chakrabarty P, Hanna A, March A, Dickson DW, Borchelt DR, Golde T, Janus C (2013) Normal cognition in transgenic BRI2-Abeta mice. Mol Neurodegener 8:15.

Kim SH, Sisodia SS (2005) Evidence that the "NF" motif in transmembrane domain 4 of presenilin 1 is critical for binding with PEN-2. J Biol Chem 280:41953-41966.

Kim W, Hecht MH (2006) Generic hydrophobic residues are sufficient to promote aggregation of the Alzheimer's Abeta42 peptide. Proc Natl Acad Sci U S A 103:15824-15829.

Kimberly WT, LaVoie MJ, Ostaszewski BL, Ye W, Wolfe MS, Selkoe DJ (2002) Complex N-linked glycosylated nicastrin associates with active gamma-secretase and undergoes tight cellular regulation. J Biol Chem 277:35113-35117.

Kirschner DA, Abraham C, Selkoe DJ (1986) X-ray diffraction from intraneuronal paired helical filaments and extraneuronal amyloid fibers in Alzheimer disease indicates cross-beta conformation. Proc Natl Acad Sci U S A 83:503-507.

Knowles TP, Fitzpatrick AW, Meehan S, Mott HR, Vendruscolo M, Dobson CM, Welland ME (2007) Role of intermolecular forces in defining material properties of protein nanofibrils. Science 318:1900-1903.

Kodali R, Williams AD, Chemuru S, Wetzel R (2010) Abeta(1-40) forms five distinct amyloid structures whose beta-sheet contents and fibril stabilities are correlated. J Mol Biol 401:503-517.

Konietzko U (2012) AICD nuclear signaling and its possible contribution to Alzheimer's disease. Curr Alzheimer Res 9:200-216.

Koo EH, Sisodia SS, Archer DR, Martin LJ, Weidemann A, Beyreuther K, Fischer P, Masters CL, Price DL (1990) Precursor of amyloid protein in Alzheimer disease undergoes fast anterograde axonal transport. Proc Natl Acad Sci U S A 87:1561-1565.

Koo EH, Squazzo SL (1994) Evidence that production and release of amyloid beta-protein involves the endocytic pathway. J Biol Chem 269:17386-17389.

Kroenke CD, Ziemnicka-Kotula D, Xu J, Kotula L, Palmer AG, III (1997) Solution conformations of a peptide containing the cytoplasmic domain sequence of the beta amyloid precursor protein. Biochemistry 36:8145-8152.

Kuan YH, Gruebl T, Soba P, Eggert S, Nesic I, Back S, Kirsch J, Beyreuther K, Kins S (2006) PAT1a modulates intracellular transport and processing of amyloid precursor protein (APP), APLP1, and APLP2. J Biol Chem 281:40114-40123.

Kuhn PH, Wang H, Dislich B, Colombo A, Zeitschel U, Ellwart JW, Kremmer E, Rossner S, Lichtenthaler SF (2010) ADAM10 is the physiologically relevant, constitutive alpha-secretase of the amyloid precursor protein in primary neurons. EMBO J 29:3020-3032.

Kukar TL, et al. (2008) Substrate-targeting gamma-secretase modulators. Nature 453:925-929.

Kumar S, Rezaei-Ghaleh N, Terwel D, Thal DR, Richard M, Hoch M, Mc Donald JM, Wullner U, Glebov K, Heneka MT, Walsh DM, Zweckstetter M, Walter J (2011) Extracellular phosphorylation of the amyloid beta-peptide promotes formation of toxic aggregates during the pathogenesis of Alzheimer's disease. EMBO J 30:2255-2265.

Kuo YM, Emmerling MR, Woods AS, Cotter RJ, Roher AE (1997) Isolation, chemical characterization, and quantitation of A beta 3-pyroglutamyl peptide from neuritic plaques and vascular amyloid deposits. Biochem Biophys Res Commun 237:188-191.

Kuo YM, Webster S, Emmerling MR, De LN, Roher AE (1998) Irreversible dimerization/tetramerization and post-translational modifications inhibit proteolytic degradation of A beta peptides of Alzheimer's disease. Biochim Biophys Acta 1406:291-298.

Lacor PN, Buniel MC, Chang L, Fernandez SJ, Gong Y, Viola KL, Lambert MP, Velasco PT, Bigio EH, Finch CE, Krafft GA, Klein WL (2004) Synaptic targeting by Alzheimer's-related amyloid beta oligomers. J Neurosci 24:10191-10200.

Lacor PN, Buniel MC, Furlow PW, Clemente AS, Velasco PT, Wood M, Viola KL, Klein WL (2007) Abeta oligomer-induced aberrations in synapse composition, shape, and density provide a molecular basis for loss of connectivity in Alzheimer's disease. J Neurosci 27:796-807.

LaFerla FM, Green KN (2012) Animal models of Alzheimer disease. Cold Spring Harb Perspect Med 2.

Laganowsky A, Liu C, Sawaya MR, Whitelegge JP, Park J, Zhao M, Pensalfini A, Soriaga AB, Landau M, Teng PK, Cascio D, Glabe C, Eisenberg D (2012) Atomic view of a toxic amyloid small oligomer. Science 335:1228-1231.

Lai A, Gibson A, Hopkins CR, Trowbridge IS (1998) Signal-dependent trafficking of beta-amyloid precursor protein-transferrin receptor chimeras in madin-darby canine kidney cells. J Biol Chem 273:3732-3739.

Lai A, Sisodia SS, Trowbridge IS (1995) Characterization of sorting signals in the beta-amyloid precursor protein cytoplasmic domain. J Biol Chem 270:3565-3573.

Lambert MP, Barlow AK, Chromy BA, Edwards C, Freed R, Liosatos M, Morgan TE, Rozovsky I, Trommer B, Viola KL, Wals P, Zhang C, Finch CE, Krafft GA, Klein WL (1998) Diffusible, nonfibrillar ligands derived from Abeta1-42 are potent central nervous system neurotoxins. Proc Natl Acad Sci U S A 95:6448-6453.

Lambert MP, Viola KL, Chromy BA, Chang L, Morgan TE, Yu J, Venton DL, Krafft GA, Finch CE, Klein WL (2001) Vaccination with soluble Abeta oligomers generates toxicity-neutralizing antibodies. J Neurochem 79:595-605.

Lammich S, Kojro E, Postina R, Gilbert S, Pfeiffer R, Jasionowski M, Haass C, Fahrenholz F (1999) Constitutive and regulated alpha-secretase cleavage of Alzheimer's amyloid precursor protein by a disintegrin metalloprotease. Proc Natl Acad Sci U S A 96:3922-3927.

Lanz TA, Wood KM, Richter KE, Nolan CE, Becker SL, Pozdnyakov N, Martin BA, Du P, Oborski CE, Wood DE, Brown TM, Finley JE, Sokolowski SA, Hicks CD, Coffman KJ, Geoghegan KF, Brodney MA, Liston D, Tate B (2010) Pharmacodynamics and pharmacokinetics of the gamma-secretase inhibitor PF-3084014. J Pharmacol Exp Ther 334:269-277.

Lasagna-Reeves CA, Glabe CG, Kayed R (2011) Amyloid-beta annular protofibrils evade fibrillar fate in Alzheimer disease brain. J Biol Chem 286:22122-22130.

Lashuel HA, Hartley D, Petre BM, Walz T, Lansbury PT, Jr. (2002a) Neurodegenerative disease: amyloid pores from pathogenic mutations. Nature 418:291.

Lashuel HA, Hartley D, Petre BM, Walz T, Lansbury PT, Jr. (2002b) Neurodegenerative disease: amyloid pores from pathogenic mutations. Nature 418:291.

Lashuel HA, Lansbury PT, Jr. (2006) Are amyloid diseases caused by protein aggregates that mimic bacterial pore-forming toxins? Q Rev Biophys 39:167-201.

LaVoie MJ, Fraering PC, Ostaszewski BL, Ye W, Kimberly WT, Wolfe MS, Selkoe DJ (2003) Assembly of the gamma-secretase complex involves early formation of an intermediate subcomplex of Aph-1 and nicastrin. J Biol Chem 278:37213-37222.

Lazarov O, Peterson LD, Peterson DA, Sisodia SS (2006) Expression of a familial Alzheimer's disease-linked presenilin-1 variant enhances perforant pathway lesion-induced neuronal loss in the entorhinal cortex. J Neurosci 26:429-434.

Lee MS, Kao SC, Lemere CA, Xia W, Tseng HC, Zhou Y, Neve R, Ahlijanian MK, Tsai LH (2003) APP processing is regulated by cytoplasmic phosphorylation. J Cell Biol 163:83-95.

Lee VM, Balin BJ, Otvos L, Jr., Trojanowski JQ (1991) A68: a major subunit of paired helical filaments and derivatized forms of normal Tau. Science 251:675-678.

Leissring MA, Murphy MP, Mead TR, Akbari Y, Sugarman MC, Jannatipour M, Anliker B, Muller U, Saftig P, De SB, Wolfe MS, Golde TE, LaFerla FM (2002) A physiologic signaling role for the gamma -secretase-derived intracellular fragment of APP. Proc Natl Acad Sci U S A 99:4697-4702.

Lemere CA (2009) Developing novel immunogens for a safe and effective Alzheimer's disease vaccine. Prog Brain Res 175:83-93.

Lemmon MA, Flanagan JM, Treutlein HR, Zhang J, Engelman DM (1992) Sequence specificity in the dimerization of transmembrane alpha-helices. Biochemistry 31:12719-12725.

Lesne S, Koh MT, Kotilinek L, Kayed R, Glabe CG, Yang A, Gallagher M, Ashe KH (2006) A specific amyloid-beta protein assembly in the brain impairs memory. Nature 440:352-357.

Levy E, Carman MD, Fernandez-Madrid IJ, Power MD, Lieberburg I, van Duinen SG, Bots GT, Luyendijk W, Frangione B (1990) Mutation of the Alzheimer's disease amyloid gene in hereditary cerebral hemorrhage, Dutch type. Science 248:1124-1126.

Lewis J, Dickson DW, Lin WL, Chisholm L, Corral A, Jones G, Yen SH, Sahara N, Skipper L, Yager D, Eckman C, Hardy J, Hutton M, McGowan E (2001) Enhanced neurofibrillary degeneration in transgenic mice expressing mutant tau and APP. Science 293:1487-1491.

Li E, Wimley WC, Hristova K (2012) Transmembrane helix dimerization: beyond the search for sequence motifs. Biochim Biophys Acta 1818:183-193.

Li H, Wang B, Wang Z, Guo Q, Tabuchi K, Hammer RE, Sudhof TC, Zheng H (2010) Soluble amyloid precursor protein (APP) regulates transthyretin and Klotho gene expression without rescuing the essential function of APP. Proc Natl Acad Sci U S A 107:17362-17367.

Li S, Hong S, Shepardson NE, Walsh DM, Shankar GM, Selkoe D (2009) Soluble oligomers of amyloid Beta protein facilitate hippocampal long-term depression by disrupting neuronal glutamate uptake. Neuron 62:788-801.

Li SC, Deber CM (1994) A measure of helical propensity for amino acids in membrane environments. Nat Struct Biol 1:558.

Libeu CA, Descamps O, Zhang Q, John V, Bredesen DE (2012) Altering APP proteolysis: increasing sAPPalpha production by targeting dimerization of the APP ectodomain. PLoS One 7:e40027.

Lichtenthaler SF (2012) Cell biology. Sheddase gets guidance. Science 335:179-180.

Lindwall G, Cole RD (1984) Phosphorylation affects the ability of tau protein to promote microtubule assembly. J Biol Chem 259:5301-5305.

Lipton SA (2004) Paradigm shift in NMDA receptor antagonist drug development: molecular mechanism of uncompetitive inhibition by memantine in the treatment of Alzheimer's disease and other neurologic disorders. J Alzheimers Dis 6:S61-S74.

Liu Q, Zerbinatti CV, Zhang J, Hoe HS, Wang B, Cole SL, Herz J, Muglia L, Bu G (2007) Amyloid precursor protein regulates brain apolipoprotein E and cholesterol metabolism through lipoprotein receptor LRP1. Neuron 56:66-78.

Liu SJ, Zhang JY, Li HL, Fang ZY, Wang Q, Deng HM, Gong CX, Grundke-Iqbal I, Iqbal K, Wang JZ (2004) Tau becomes a more favorable substrate for GSK-3 when it is prephosphorylated by PKA in rat brain. J Biol Chem 279:50078-50088.

Liu W, Crocker E, Constantinescu SN, Smith SO (2005a) Helix packing and orientation in the transmembrane dimer of gp55-P of the spleen focus forming virus. Biophys J 89:1194-1202.

Liu W, Crocker E, Zhang W, Elliott JI, Luy B, Li H, Aimoto S, Smith SO (2005b) Structural role of glycine in amyloid fibrils formed from transmembrane alpha-helices. Biochemistry 44:3591-3597.

Liu Y, Peterson DA, Schubert D (1998) Amyloid beta peptide alters intracellular vesicle trafficking and cholesterol homeostasis. Proc Natl Acad Sci U S A 95:13266-13271.

Liu Y, Schubert D (1997) Cytotoxic amyloid peptides inhibit cellular 3-(4,5-dimethylthiazol-2-yl)-2,5-diphenyltetrazolium bromide (MTT) reduction by enhancing MTT formazan exocytosis. J Neurochem 69:2285-2293.

Lorent K, Overbergh L, Moechars D, De SB, Van LF, Van den Berghe H (1995) Expression in mouse embryos and in adult mouse brain of three members of the amyloid precursor protein family, of the alpha-2-macroglobulin receptor/low density lipoprotein receptor-related protein and of its ligands apolipoprotein E, lipoprotein lipase, alpha-2-macroglobulin and the 40,000 molecular weight receptor-associated protein. Neuroscience 65:1009-1025.

Lourenco FC, Galvan V, Fombonne J, Corset V, Llambi F, Muller U, Bredesen DE, Mehlen P (2009) Netrin-1 interacts with amyloid precursor protein and regulates amyloid-beta production. Cell Death Differ 16:655-663.

Lu DC, Shaked GM, Masliah E, Bredesen DE, Koo EH (2003) Amyloid beta protein toxicity mediated by the formation of amyloid-beta protein precursor complexes. Ann Neurol 54:781-789.

Lu JX, Qiang W, Yau WM, Schwieters CD, Meredith SC, Tycko R (2013) Molecular structure of beta-amyloid fibrils in Alzheimer's disease brain tissue. Cell 154:1257-1268.

Lu P, Bai XC, Ma D, Xie T, Yan C, Sun L, Yang G, Zhao Y, Zhou R, Scheres SH, Shi Y (2014) Three-dimensional structure of human gamma-secretase. Nature 512:166-170.

Luhrs T, Ritter C, Adrian M, Riek-Loher D, Bohrmann B, Dobeli H, Schubert D, Riek R (2005) 3D structure of Alzheimer's amyloid-beta(1-42) fibrils. Proc Natl Acad Sci U S A 102:17342-17347.

Ma B, Nussinov R (2011) Polymorphic triple beta-sheet structures contribute to amide hydrogen/deuterium (H/D) exchange protection in the Alzheimer amyloid beta42 peptide. J Biol Chem 286:34244-34253.

Ma QH, Bagnard D, Xiao ZC, Dawe GS (2008) A TAG on to the neurogenic functions of APP. Cell Adh Migr 2:2-8.

MacKenzie KR, Engelman DM (1998) Structure-based prediction of the stability of transmembrane helix-helix interactions: the sequence dependence of glycophorin A dimerization. Proc Natl Acad Sci U S A 95:3583-3590.

MacKenzie KR, Prestegard JH, Engelman DM (1997) A transmembrane helix dimer: structure and implications. Science 276:131-133.

Mandelkow EM, Mandelkow E (1998) Tau in Alzheimer's disease. Trends Cell Biol 8:425-427.

Mastrangelo P, Mathews PM, Chishti MA, Schmidt SD, Gu Y, Yang J, Mazzella MJ, Coomaraswamy J, Horne P, Strome B, Pelly H, Levesque G, Ebeling C, Jiang Y, Nixon RA, Rozmahel R, Fraser PE, St George-Hyslop P, Carlson GA, Westaway D (2005) Dissociated phenotypes in presenilin transgenic mice define functionally distinct gamma-secretases. Proc Natl Acad Sci U S A 102:8972-8977.

Masuda Y, Uemura S, Nakanishi A, Ohashi R, Takegoshi K, Shimizu T, Shirasawa T, Irie K (2008) Verification of the C-terminal intramolecular beta-sheet in Abeta42 aggregates using solid-state NMR: implications for potent neurotoxicity through the formation of radicals. Bioorg Med Chem Lett 18:3206-3210.

Matrone C, Barbagallo AP, La Rosa LR, Florenzano F, Ciotti MT, Mercanti D, Chao MV, Calissano P, D'Adamio L (2011) APP is phosphorylated by TrkA and regulates NGF/TrkA signaling. J Neurosci 31:11756-11761.

Matsumura N, Takami M, Okochi M, Wada-Kakuda S, Fujiwara H, Tagami S, Funamoto S, Ihara Y, Morishima-Kawashima M (2014) gamma-Secretase associated with lipid rafts: multiple interactive pathways in the stepwise processing of beta-carboxyl-terminal fragment. J Biol Chem 289:5109-5121.

Matsumura S, et al. (2011) Two distinct amyloid beta-protein (Abeta) assembly pathways leading to oligomers and fibrils identified by combined fluorescence correlation spectroscopy, morphology, and toxicity analyses. J Biol Chem 286:11555-11562.

Mattson MP (1997) Cellular actions of beta-amyloid precursor protein and its soluble and fibrillogenic derivatives. Physiol Rev 77:1081-1132.

Mattson MP, Cheng B, Culwell AR, Esch FS, Lieberburg I, Rydel RE (1993) Evidence for excitoprotective and intraneuronal calcium-regulating roles for secreted forms of the beta-amyloid precursor protein. Neuron 10:243-254.

Mayer SC, et al. (2008) Discovery of begacestat, a Notch-1-sparing gamma-secretase inhibitor for the treatment of Alzheimer's disease. J Med Chem 51:7348-7351.

Mayeux R, Stern Y (2012) Epidemiology of Alzheimer disease. Cold Spring Harb Perspect Med 2.

McClain MS, Iwamoto H, Cao P, Vinion-Dubiel AD, Li Y, Szabo G, Shao Z, Cover TL (2003) Essential role of a GXXXG motif for membrane channel formation by Helicobacter pylori vacuolating toxin. J Biol Chem 278:12101-12108.

McDonald RJ, Craig LA, Hong NS (2010) The etiology of age-related dementia is more complicated than we think. Behav Brain Res 14:3-11.

McGowan E, Pickford F, Kim J, Onstead L, Eriksen J, Yu C, Skipper L, Murphy MP, Beard J, Das P, Jansen K, Delucia M, Lin WL, Dolios G, Wang R, Eckman CB, Dickson DW, Hutton M, Hardy J, Golde T (2005) Abeta42 is essential for parenchymal and vascular amyloid deposition in mice. Neuron 47:191-199.

McKee AC, Kowall NW, Schumacher JS, Beal MF (1998) The neurotoxicity of amyloid beta protein in aged primates. Amyloid 5:1-9.

Meziane H, Dodart JC, Mathis C, Little S, Clemens J, Paul SM, Ungerer A (1998) Memory-enhancing effects of secreted forms of the beta-amyloid precursor protein in normal and amnestic mice. Proc Natl Acad Sci U S A 95:12683-12688.

Midthune B, Tyan SH, Walsh JJ, Sarsoza F, Eggert S, Hof PR, Dickstein DL, Koo EH (2012) Deletion of the amyloid precursor-like protein 2 (APLP2) does not affect hippocampal neuron morphology or function. Mol Cell Neurosci 49:448-455.

Miller CC, McLoughlin DM, Lau KF, Tennant ME, Rogelj B (2006) The X11 proteins, Abeta production and Alzheimer's disease. Trends Neurosci 29:280-285.

Milton NG (2001) Phosphorylation of amyloid-beta at the serine 26 residue by human cdc2 kinase. Neuroreport 12:3839-3844.

Milton NG (2005) Phosphorylated amyloid-beta: the toxic intermediate in alzheimer's disease neurodegeneration. Subcell Biochem 38:381-402.

Minopoli G, de CP, Bonetti A, Faraonio R, Zambrano N, Russo T (2001) The beta-amyloid precursor protein functions as a cytosolic anchoring site that prevents Fe65 nuclear translocation. J Biol Chem 276:6545-6550.

Miravalle L, Calero M, Takao M, Roher AE, Ghetti B, Vidal R (2005) Amino-terminally truncated Abeta peptide species are the main component of cotton wool plaques. Biochemistry 44:10810-10821.

Mohamed NV, Herrou T, Plouffe V, Piperno N, Leclerc N (2013) Spreading of tau pathology in Alzheimer's disease by cell-to-cell transmission. Eur J Neurosci 37:1939-1948.

Morales-Corraliza J, Mazzella MJ, Berger JD, Diaz NS, Choi JH, Levy E, Matsuoka Y, Planel E, Mathews PM (2009) In vivo turnover of tau and APP metabolites in the brains of wild-type and Tg2576 mice: greater stability of sAPP in the beta-amyloid depositing mice. PLoS One 4:e7134.

Morgado I, Wieligmann K, Bereza M, Ronicke R, Meinhardt K, Annamalai K, Baumann M, Wacker J, Hortschansky P, Malesevic M, Parthier C, Mawrin C, Schiene-Fischer C, Reymann KG, Stubbs MT, Balbach J, Gorlach M, Horn U, Fandrich M (2012) Molecular basis of beta-amyloid oligomer recognition with a conformational antibody fragment. Proc Natl Acad Sci U S A 109:12503-12508.

Mori H, Ishii K, Tomiyama T, Furiya Y, Sahara N, Asano S, Endo N, Shirasawa T, Takio K (1994) Racemization: its biological significance on neuropathogenesis of Alzheimer's disease. Tohoku J Exp Med 174:251-262.

Morimoto A, Irie K, Murakami K, Masuda Y, Ohigashi H, Nagao M, Fukuda H, Shimizu T, Shirasawa T (2004) Analysis of the secondary structure of beta-amyloid (Abeta42) fibrils by systematic proline replacement. J Biol Chem 279:52781-52788.

Mortimer JA, van Duijn CM, Chandra V, Fratiglioni L, Graves AB, Heyman A, Jorm AF, Kokmen E, Kondo K, Rocca WA, . (1991) Head trauma as a risk factor for Alzheimer's

disease: a collaborative re-analysis of case-control studies. EURODEM Risk Factors Research Group. Int J Epidemiol 20 Suppl 2:S28-S35.

Mosher KI, Wyss-Coray T (2014) Microglial dysfunction in brain aging and Alzheimer's disease. Biochem Pharmacol 88:594-604.

Mott RT, Hulette CM (2005) Neuropathology of Alzheimer's disease. Neuroimaging Clin N Am 15:755-65, ix.

Mucke L, Masliah E, Johnson WB, Ruppe MD, Alford M, Rockenstein EM, Forss-Petter S, Pietropaolo M, Mallory M, Abraham CR (1994) Synaptotrophic effects of human amyloid beta protein precursors in the cortex of transgenic mice. Brain Res 666:151-167.

Mucke L, Masliah E, Yu GQ, Mallory M, Rockenstein EM, Tatsuno G, Hu K, Kholodenko D, Johnson-Wood K, McConlogue L (2000) High-level neuronal expression of abeta 1-42 in wild-type human amyloid protein precursor transgenic mice: synaptotoxicity without plaque formation. J Neurosci 20:4050-4058.

Muller T, Concannon CG, Ward MW, Walsh CM, Tirniceriu AL, Tribl F, Kogel D, Prehn JH, Egensperger R (2007) Modulation of gene expression and cytoskeletal dynamics by the amyloid precursor protein intracellular domain (AICD). Mol Biol Cell 18:201-210.

Muller T, Meyer HE, Egensperger R, Marcus K (2008) The amyloid precursor protein intracellular domain (AICD) as modulator of gene expression, apoptosis, and cytoskeletal dynamics-relevance for Alzheimer's disease. Prog Neurobiol 85:393-406.

Multhaup G, Mechler H, Masters CL (1995) Characterization of the high affinity heparin binding site of the Alzheimer's disease beta A4 amyloid precursor protein (APP) and its enhancement by zinc(II). J Mol Recognit 8:247-257.

Multhaup G, Schlicksupp A, Hesse L, Beher D, Ruppert T, Masters CL, Beyreuther K (1996) The amyloid precursor protein of Alzheimer's disease in the reduction of copper(II) to copper(I). Science 271:1406-1409.

Munter LM, Botev A, Richter L, Hildebrand PW, Althoff V, Weise C, Kaden D, Multhaup G (2010) Aberrant amyloid precursor protein (APP) processing in hereditary forms of Alzheimer disease caused by APP familial Alzheimer disease mutations can be rescued by mutations in the APP GxxxG motif. J Biol Chem 285:21636-21643.

Munter LM, Voigt P, Harmeier A, Kaden D, Gottschalk KE, Weise C, Pipkorn R, Schaefer M, Langosch D, Multhaup G (2007) GxxxG motifs within the amyloid precursor protein transmembrane sequence are critical for the etiology of Abeta42. EMBO J 26:1702-1712.

Myers A, et al. (2000) Susceptibility locus for Alzheimer's disease on chromosome 10. Science 290:2304-2305.

Nadezhdin KD, Bocharova OV, Bocharov EV, Arseniev AS (2012) Dimeric structure of transmembrane domain of amyloid precursor protein in micellar environment. FEBS Lett 586:1687-1692.

Nikolaev A, McLaughlin T, O'Leary DD, Tessier-Lavigne M (2009) APP binds DR6 to trigger axon pruning and neuron death via distinct caspases. Nature 457:981-989.

Nilsberth C, Westlind-Danielsson A, Eckman CB, Condron MM, Axelman K, Forsell C, Stenh C, Luthman J, Teplow DB, Younkin SG, Naslund J, Lannfelt L (2001) The 'Arctic' APP mutation (E693G) causes Alzheimer's disease by enhanced Abeta protofibril formation. Nat Neurosci 4:887-893.

Nimmrich V, Grimm C, Draguhn A, Barghorn S, Lehmann A, Schoemaker H, Hillen H, Gross G, Ebert U, Bruehl C (2008) Amyloid beta oligomers (A beta(1-42) globulomer) suppress spontaneous synaptic activity by inhibition of P/Q-type calcium currents. J Neurosci 28:788-797.

Ninomiya H, Roch JM, Sundsmo MP, Otero DA, Saitoh T (1993) Amino acid sequence RERMS represents the active domain of amyloid beta/A4 protein precursor that promotes fibroblast growth. J Cell Biol 121:879-886.

Nishitsuji K, Tomiyama T, Ishibashi K, Ito K, Teraoka R, Lambert MP, Klein WL, Mori H (2009) The E693Delta mutation in amyloid precursor protein increases intracellular accumulation of amyloid beta oligomers and causes endoplasmic reticulum stress-induced apoptosis in cultured cells. Am J Pathol 174:957-969.

Nixon RA, Cataldo AM (2006) Lysosomal system pathways: genes to neurodegeneration in Alzheimer's disease. J Alzheimers Dis 9:277-289.

Noguchi A, et al. (2009) Isolation and characterization of patient-derived, toxic, high mass amyloid beta-protein (Abeta) assembly from Alzheimer disease brains. J Biol Chem 284:32895-32905.

Nomura S, Umeda T, Tomiyama T, Mori H (2013) The E693Delta (Osaka) mutation in amyloid precursor protein potentiates cholesterol-mediated intracellular amyloid beta toxicity via its impaired cholesterol efflux. J Neurosci Res 91:1541-1550.

O'Nuallain B, Freir DB, Nicoll AJ, Risse E, Ferguson N, Herron CE, Collinge J, Walsh DM (2010) Amyloid beta-protein dimers rapidly form stable synaptotoxic protofibrils. J Neurosci 30:14411-14419.

Octave JN (1995) The amyloid peptide and its precursor in Alzheimer's disease. Rev Neurosci 6:287-316.

Oishi M, Nairn AC, Czernik AJ, Lim GS, Isohara T, Gandy SE, Greengard P, Suzuki T (1997) The cytoplasmic domain of Alzheimer's amyloid precursor protein is phosphorylated at Thr654, Ser655, and Thr668 in adult rat brain and cultured cells. Mol Med 3:111-123.

Olofsson A, Sauer-Eriksson AE, Ohman A (2006) The solvent protection of alzheimer amyloid-beta-(1-42) fibrils as determined by solution NMR spectroscopy. J Biol Chem 281:477-483.

Olson MI, Shaw CM (1969) Presenile dementia and Alzheimer's disease in mongolism. Brain 92:147-156.

Osenkowski P, Li H, Ye W, Li D, Aeschbach L, Fraering PC, Wolfe MS, Selkoe DJ, Li H (2009) Cryoelectron microscopy structure of purified gamma-secretase at 12 A resolution. J Mol Biol 385:642-652.

Osterfield M, Egelund R, Young LM, Flanagan JG (2008) Interaction of amyloid precursor protein with contactins and NgCAM in the retinotectal system. Development 135:1189-1199.

Paravastu AK, Leapman RD, Yau WM, Tycko R (2008) Molecular structural basis for polymorphism in Alzheimer's beta-amyloid fibrils. Proc Natl Acad Sci U S A 105:18349-18354.

Pardossi-Piquard R, Petit A, Kawarai T, Sunyach C, Alves da CC, Vincent B, Ring S, D'Adamio L, Shen J, Muller U, St George HP, Checler F (2005) Presenilin-dependent transcriptional control of the Abeta-degrading enzyme neprilysin by intracellular domains of betaAPP and APLP. Neuron 46:541-554.

Park JH, Gimbel DA, GrandPre T, Lee JK, Kim JE, Li W, Lee DH, Strittmatter SM (2006) Alzheimer precursor protein interaction with the Nogo-66 receptor reduces amyloid-beta plaque deposition. J Neurosci 26:1386-1395.

Park SA, Shaked GM, Bredesen DE, Koo EH (2009) Mechanism of cytotoxicity mediated by the C31 fragment of the amyloid precursor protein. Biochem Biophys Res Commun 388:450-455.

Perez RG, Soriano S, Hayes JD, Ostaszewski B, Xia W, Selkoe DJ, Chen X, Stokin GB, Koo EH (1999) Mutagenesis identifies new signals for beta-amyloid precursor protein endocytosis, turnover, and the generation of secreted fragments, including Abeta42. J Biol Chem 274:18851-18856.

Petkova AT, Leapman RD, Guo Z, Yau WM, Mattson MP, Tycko R (2005) Self-propagating, molecular-level polymorphism in Alzheimer's beta-amyloid fibrils. Science 307:262-265.

Pierrot N, Tyteca D, D'auria L, Dewachter I, Gailly P, Hendrickx A, Tasiaux B, Haylani LE, Muls N, N'Kuli F, Laquerriere A, Demoulin JB, Campion D, Brion JP, Courtoy PJ, Kienlen-Campard P, Octave JN (2013) Amyloid precursor protein controls cholesterol turnover needed for neuronal activity. EMBO Mol Med 5:608-625.

Pietrzik CU, Yoon IS, Jaeger S, Busse T, Weggen S, Koo EH (2004) FE65 constitutes the functional link between the low-density lipoprotein receptor-related protein and the amyloid precursor protein. J Neurosci 24:4259-4265.

Pike CJ, Burdick D, Walencewicz AJ, Glabe CG, Cotman CW (1993) Neurodegeneration induced by beta-amyloid peptides in vitro: the role of peptide assembly state. J Neurosci 13:1676-1687.

Pike CJ, Cummings BJ, Cotman CW (1992) beta-Amyloid induces neuritic dystrophy in vitro: similarities with Alzheimer pathology. Neuroreport 3:769-772.

Pike CJ, Cummings BJ, Cotman CW (1995) Early association of reactive astrocytes with senile plaques in Alzheimer's disease. Exp Neurol 132:172-179.

Portelius E, Andreasson U, Ringman JM, Buerger K, Daborg J, Buchhave P, Hansson O, Harmsen A, Gustavsson MK, Hanse E, Galasko D, Hampel H, Blennow K, Zetterberg H (2010) Distinct cerebrospinal fluid amyloid beta peptide signatures in sporadic and PSEN1 A431E-associated familial Alzheimer's disease. Mol Neurodegener 5:2.

Postina R, Schroeder A, Dewachter I, Bohl J, Schmitt U, Kojro E, Prinzen C, Endres K, Hiemke C, Blessing M, Flamez P, Dequenne A, Godaux E, Van LF, Fahrenholz F (2004) A disintegrin-metalloproteinase prevents amyloid plaque formation and hippocampal defects in an Alzheimer disease mouse model. J Clin Invest 113:1456-1464.

Qi-Takahara Y, Morishima-Kawashima M, Tanimura Y, Dolios G, Hirotani N, Horikoshi Y, Kametani F, Maeda M, Saido TC, Wang R, Ihara Y (2005) Longer forms of amyloid beta protein: implications for the mechanism of intramembrane cleavage by gamma-secretase. J Neurosci 25:436-445.

Querfurth HW, LaFerla FM (2010) Alzheimer's disease. N Engl J Med 362:329-344.

Radzimanowski J, Ravaud S, Schott A, Strahl S, Sinning I (2010) Cloning, recombinant production, crystallization and preliminary X-ray diffraction analysis of SDF2-like protein from Arabidopsis thaliana. Acta Crystallogr Sect F Struct Biol Cryst Commun 66:12-14.

Radzimanowski J, Simon B, Sattler M, Beyreuther K, Sinning I, Wild K (2008) Structure of the intracellular domain of the amyloid precursor protein in complex with Fe65-PTB2. EMBO Rep 9:1134-1140.

Ramelot TA, Gentile LN, Nicholson LK (2000) Transient structure of the amyloid precursor protein cytoplasmic tail indicates preordering of structure for binding to cytosolic factors. Biochemistry 39:2714-2725.

Ramelot TA, Nicholson LK (2001) Phosphorylation-induced structural changes in the amyloid precursor protein cytoplasmic tail detected by NMR. J Mol Biol 307:871-884.

Reed MN, Hofmeister JJ, Jungbauer L, Welzel AT, Yu C, Sherman MA, Lesne S, LaDu MJ, Walsh DM, Ashe KH, Cleary JP (2011) Cognitive effects of cell-derived and synthetically derived Abeta oligomers. Neurobiol Aging 32:1784-1794.

Ren Z, Schenk D, Basi GS, Shapiro IP (2007) Amyloid beta-protein precursor juxtamembrane domain regulates specificity of gamma-secretase-dependent cleavages. J Biol Chem 282:35350-35360.

Rezaei-Ghaleh N, Amininasab M, Giller K, Kumar S, Stundl A, Schneider A, Becker S, Walter J, Zweckstetter M (2014) Turn plasticity distinguishes different modes of amyloid-beta aggregation. J Am Chem Soc 136:4913-4919.

Richter L, Munter LM, Ness J, Hildebrand PW, Dasari M, Unterreitmeier S, Bulic B, Beyermann M, Gust R, Reif B, Weggen S, Langosch D, Multhaup G (2010) Amyloid beta 42 peptide (Abeta42)-lowering compounds directly bind to Abeta and interfere with amyloid precursor protein (APP) transmembrane dimerization. Proc Natl Acad Sci U S A 107:14597-14602.

Ring S, Weyer SW, Kilian SB, Waldron E, Pietrzik CU, Filippov MA, Herms J, Buchholz C, Eckman CB, Korte M, Wolfer DP, Muller UC (2007) The secreted beta-amyloid precursor protein ectodomain APPs alpha is sufficient to rescue the anatomical, behavioral, and electrophysiological abnormalities of APP-deficient mice. J Neurosci 27:7817-7826.

Roch JM, Masliah E, Roch-Levecq AC, Sundsmo MP, Otero DA, Veinbergs I, Saitoh T (1994) Increase of synaptic density and memory retention by a peptide representing the trophic domain of the amyloid beta/A4 protein precursor. Proc Natl Acad Sci U S A 91:7450-7454.

Rohe M, Carlo AS, Breyhan H, Sporbert A, Militz D, Schmidt V, Wozny C, Harmeier A, Erdmann B, Bales KR, Wolf S, Kempermann G, Paul SM, Schmitz D, Bayer TA, Willnow TE, Andersen OM (2008) Sortilin-related receptor with A-type repeats (SORLA) affects the amyloid precursor protein-dependent stimulation of ERK signaling and adult neurogenesis. J Biol Chem 283:14826-14834.

Roher AE, Lowenson JD, Clarke S, Woods AS, Cotter RJ, Gowing E, Ball MJ (1993) beta-Amyloid-(1-42) is a major component of cerebrovascular amyloid deposits: implications for the pathology of Alzheimer disease. Proc Natl Acad Sci U S A 90:10836-10840.

Rossjohn J, Cappai R, Feil SC, Henry A, McKinstry WJ, Galatis D, Hesse L, Multhaup G, Beyreuther K, Masters CL, Parker MW (1999) Crystal structure of the N-terminal, growth factor-like domain of Alzheimer amyloid precursor protein. Nat Struct Biol 6:327-331.

Roychaudhuri R, Yang M, Hoshi MM, Teplow DB (2009) Amyloid beta-protein assembly and Alzheimer disease. J Biol Chem 284:4749-4753.

Russ WP, Engelman DM (2000) The GxxxG motif: a framework for transmembrane helix-helix association. J Mol Biol 296:911-919.

Saido TC, Iwatsubo T, Mann DM, Shimada H, Ihara Y, Kawashima S (1995) Dominant and differential deposition of distinct beta-amyloid peptide species, A beta N3(pE), in senile plaques. Neuron 14:457-466.

Saido TC, Yamao-Harigaya W, Iwatsubo T, Kawashima S (1996) Amino- and carboxyl-terminal heterogeneity of beta-amyloid peptides deposited in human brain. Neurosci Lett 215:173-176.

Saito T, Takaki Y, Iwata N, Trojanowski J, Saido TC (2003) Alzheimer's disease, neuropeptides, neuropeptidase, and amyloid-beta peptide metabolism. Sci Aging Knowledge Environ 2003:E1.

Saito Y, Sano Y, Vassar R, Gandy S, Nakaya T, Yamamoto T, Suzuki T (2008) X11 proteins regulate the translocation of amyloid beta-protein precursor (APP) into detergent-resistant membrane and suppress the amyloidogenic cleavage of APP by beta-site-cleaving enzyme in brain. J Biol Chem 283:35763-35771.

Salloway S, Sperling R, Brashear HR (2014) Phase 3 trials of solanezumab and bapineuzumab for Alzheimer's disease. N Engl J Med 370:1460.

Sanders DW, Kaufman SK, DeVos SL, Sharma AM, Mirbaha H, Li A, Barker SJ, Foley AC, Thorpe JR, Serpell LC, Miller TM, Grinberg LT, Seeley WW, Diamond MI (2014) Distinct tau prion strains propagate in cells and mice and define different tauopathies. Neuron 82:1271-1288.

Sato T, Diehl TS, Narayanan S, Funamoto S, Ihara Y, De SB, Steiner H, Haass C, Wolfe MS (2007) Active gamma-secretase complexes contain only one of each component. J Biol Chem 282:33985-33993.

Sato T, Kienlen-Campard P, Ahmed M, Liu W, Li H, Elliott JI, Aimoto S, Constantinescu SN, Octave JN, Smith SO (2006) Inhibitors of amyloid toxicity based on beta-sheet packing of Abeta40 and Abeta42. Biochemistry 45:5503-5516.

Sato T, Tang TC, Reubins G, Fei JZ, Fujimoto T, Kienlen-Campard P, Constantinescu SN, Octave JN, Aimoto S, Smith SO (2009) A helix-to-coil transition at the epsilon-cut site in the

transmembrane dimer of the amyloid precursor protein is required for proteolysis. Proc Natl Acad Sci U S A 106:1421-1426.

Schenk D, et al. (1999) Immunization with amyloid-beta attenuates Alzheimer-disease-like pathology in the PDAPP mouse. Nature 400:173-177.

Schettini G, Govoni S, Racchi M, Rodriguez G (2010) Phosphorylation of APP-CTF-AICD domains and interaction with adaptor proteins: signal transduction and/or transcriptional role--relevance for Alzheimer pathology. J Neurochem 115:1299-1308.

Scheuermann S, Hambsch B, Hesse L, Stumm J, Schmidt C, Beher D, Bayer TA, Beyreuther K, Multhaup G (2001) Homodimerization of amyloid precursor protein and its implication in the amyloidogenic pathway of Alzheimer's disease. J Biol Chem 276:33923-33929.

Scheuner D, et al. (1996) Secreted amyloid beta-protein similar to that in the senile plaques of Alzheimer's disease is increased in vivo by the presenilin 1 and 2 and APP mutations linked to familial Alzheimer's disease. Nat Med 2:864-870.

Schilling S, Lauber T, Schaupp M, Manhart S, Scheel E, Bohm G, Demuth HU (2006) On the seeding and oligomerization of pGlu-amyloid peptides (in vitro). Biochemistry 45:12393-12399.

Schlessinger J (2002) Ligand-induced, receptor-mediated dimerization and activation of EGF receptor. Cell 110:669-672.

Schmidt V, Sporbert A, Rohe M, Reimer T, Rehm A, Andersen OM, Willnow TE (2007) SorLA/LR11 regulates processing of amyloid precursor protein via interaction with adaptors GGA and PACS-1. J Biol Chem 282:32956-32964.

Schnabel J (2011) Amyloid: little proteins, big clues. Nature 475:S12-S14.

Senes A, Gerstein M, Engelman DM (2000) Statistical analysis of amino acid patterns in transmembrane helices: the GxxxG motif occurs frequently and in association with beta-branched residues at neighboring positions. J Mol Biol 296:921-936.

Senes A, Ubarretxena-Belandia I, Engelman DM (2001) The Calpha ---H...O hydrogen bond: a determinant of stability and specificity in transmembrane helix interactions. Proc Natl Acad Sci U S A 98:9056-9061.

Sergeant N, Bombois S, Ghestem A, Drobecq H, Kostanjevecki V, Missiaen C, Wattez A, David JP, Vanmechelen E, Sergheraert C, Delacourte A (2003) Truncated beta-amyloid peptide species in pre-clinical Alzheimer's disease as new targets for the vaccination approach. J Neurochem 85:1581-1591.

Sergeant N, Delacourte A, Buee L (2005) Tau protein as a differential biomarker of tauopathies. Biochim Biophys Acta 1739:179-197.

Serrano-Pozo A, William CM, Ferrer I, Uro-Coste E, Delisle MB, Maurage CA, Hock C, Nitsch RM, Masliah E, Growdon JH, Frosch MP, Hyman BT (2010) Beneficial effect of human anti-amyloid-beta active immunization on neurite morphology and tau pathology. Brain 133:1312-1327.

Shafrir Y, Durell S, Arispe N, Guy HR (2010) Models of membrane-bound Alzheimer's Abeta peptide assemblies. Proteins 78:3473-3487.

Shah S, Lee SF, Tabuchi K, Hao YH, Yu C, LaPlant Q, Ball H, Dann CE, III, Sudhof T, Yu G (2005) Nicastrin functions as a gamma-secretase-substrate receptor. Cell 122:435-447.

Shankar GM, Leissring MA, Adame A, Sun X, Spooner E, Masliah E, Selkoe DJ, Lemere CA, Walsh DM (2009) Biochemical and immunohistochemical analysis of an Alzheimer's disease mouse model reveals the presence of multiple cerebral Abeta assembly forms throughout life. Neurobiol Dis 36:293-302.

Shapiro L, Doyle JP, Hensley P, Colman DR, Hendrickson WA (1996) Crystal structure of the extracellular domain from P0, the major structural protein of peripheral nerve myelin. Neuron 17:435-449.

Shariati SA, De SB (2013) Redundancy and divergence in the amyloid precursor protein family. FEBS Lett 587:2036-2045.

Shimizu T, Watanabe A, Ogawara M, Mori H, Shirasawa T (2000) Isoaspartate formation and neurodegeneration in Alzheimer's disease. Arch Biochem Biophys 381:225-234.

Simons M, Keller P, De SB, Beyreuther K, Dotti CG, Simons K (1998) Cholesterol depletion inhibits the generation of beta-amyloid in hippocampal neurons. Proc Natl Acad Sci U S A 95:6460-6464.

Sisodia SS (1992) Beta-amyloid precursor protein cleavage by a membrane-bound protease. Proc Natl Acad Sci U S A 89:6075-6079.

Sisodia SS, Koo EH, Hoffman PN, Perry G, Price DL (1993) Identification and transport of full-length amyloid precursor proteins in rat peripheral nervous system. J Neurosci 13:3136-3142.

Small DH, Nurcombe V, Reed G, Clarris H, Moir R, Beyreuther K, Masters CL (1994) A heparin-binding domain in the amyloid protein precursor of Alzheimer's disease is involved in the regulation of neurite outgrowth. J Neurosci 14:2117-2127.

Small SA, Gandy S (2006) Sorting through the cell biology of Alzheimer's disease: intracellular pathways to pathogenesis. Neuron 52:15-31.

Smith SO, Bormann BJ (1995) Determination of helix-helix interactions in membranes by rotational resonance NMR. Proc Natl Acad Sci U S A 92:488-491.

Smith SO, Song D, Shekar S, Groesbeek M, Ziliox M, Aimoto S (2001a) Structure of the transmembrane dimer interface of glycophorin A in membrane bilayers. Biochemistry 40:6553-6558.

Smith SO, Song D, Shekar S, Groesbeek M, Ziliox M, Aimoto S (2001b) Structure of the transmembrane dimer interface of glycophorin A in membrane bilayers. Biochemistry 40:6553-6558.

Smith-Swintosky VL, Pettigrew LC, Craddock SD, Culwell AR, Rydel RE, Mattson MP (1994) Secreted forms of beta-amyloid precursor protein protect against ischemic brain injury. J Neurochem 63:781-784.

So PP, Khodr CE, Chen CD, Abraham CR (2013) Comparable dimerization found in wildtype and familial Alzheimer's disease amyloid precursor protein mutants. Am J Neurodegener Dis 2:15-28.

Soba P, Eggert S, Wagner K, Zentgraf H, Siehl K, Kreger S, Lower A, Langer A, Merdes G, Paro R, Masters CL, Muller U, Kins S, Beyreuther K (2005) Homo- and heterodimerization of APP family members promotes intercellular adhesion. EMBO J 24:3624-3634.

Solans A, Estivill X, de La LS (2000) A new aspartyl protease on 21q22.3, BACE2, is highly similar to Alzheimer's amyloid precursor protein beta-secretase. Cytogenet Cell Genet 89:177-184.

Song Y, Hustedt EJ, Brandon S, Sanders CR (2013) Competition between homodimerization and cholesterol binding to the C99 domain of the amyloid precursor protein. Biochemistry 52:5051-5064.

Spasic D, Annaert W (2008) Building gamma-secretase: the bits and pieces. J Cell Sci 121:413-420.

Stancu IC, Ris L, Vasconcelos B, Marinangeli C, Goeminne L, Laporte V, Haylani LE, Couturier J, Schakman O, Gailly P, Pierrot N, Kienlen-Campard P, Octave JN, Dewachter I (2014a) Tauopathy contributes to synaptic and cognitive deficits in a murine model for Alzheimer's disease. FASEB J 28:2620-2631.

Stancu IC, Vasconcelos B, Ris L, Wang P, Villers A, Peeraer E, Buist A, Terwel D, Baatsen P, Oyelami T, Pierrot N, Casteels C, Bormans G, Kienlen-Campard P, Octave JN, Moechars D, Dewachter I (2015) Templated misfolding of Tau by prion-like seeding along neuronal

connections impairs neuronal network function and associated behavioral outcomes in Tau transgenic mice. Acta Neuropathol 129:875-894.

Stancu IC, Vasconcelos B, Terwel D, Dewachter I (2014b) Models of beta-amyloid induced Tau-pathology: the long and "folded" road to understand the mechanism. Mol Neurodegener 9:51.

Stangl M, Schneider D (2015) Functional competition within a membrane: Lipid recognition vs. transmembrane helix oligomerization. Biochim Biophys Acta 1848:1886-1896.

Steiner H (2008) The catalytic core of gamma-secretase: presenilin revisited. Curr Alzheimer Res 5:147-157.

Stelzer W, Langosch D (2012) Sequence-dependent backbone dynamics of a viral fusogen transmembrane helix. Protein Sci 21:1097-1102.

Storey E, Beyreuther K, Masters CL (1996) Alzheimer's disease amyloid precursor protein on the surface of cortical neurons in primary culture co-localizes with adhesion patch components. Brain Res 735:217-231.

Strittmatter WJ, Weisgraber KH, Huang DY, Dong LM, Salvesen GS, Pericak-Vance M, Schmechel D, Saunders AM, Goldgaber D, Roses AD (1993) Binding of human apolipoprotein E to synthetic amyloid beta peptide: isoform-specific effects and implications for late-onset Alzheimer disease. Proc Natl Acad Sci U S A 90:8098-8102.

Stroud JC, Liu C, Teng PK, Eisenberg D (2012) Toxic fibrillar oligomers of amyloid-beta have cross-beta structure. Proc Natl Acad Sci U S A 109:7717-7722.

Struhl G, Adachi A (2000) Requirements for presenilin-dependent cleavage of notch and other transmembrane proteins. Mol Cell 6:625-636.

Sumioka A, Nagaishi S, Yoshida T, Lin A, Miura M, Suzuki T (2005) Role of 14-3-3gamma in FE65-dependent gene transactivation mediated by the amyloid beta-protein precursor cytoplasmic fragment. J Biol Chem 280:42364-42374.

Supnet C, Bezprozvanny I (2010) The dysregulation of intracellular calcium in Alzheimer disease. Cell Calcium 47:183-189.

Suzuki T, Nakaya T (2008) Regulation of amyloid beta-protein precursor by phosphorylation and protein interactions. J Biol Chem 283:29633-29637.

Szodorai A, Kuan YH, Hunzelmann S, Engel U, Sakane A, Sasaki T, Takai Y, Kirsch J, Muller U, Beyreuther K, Brady S, Morfini G, Kins S (2009) APP anterograde transport requires Rab3A GTPase activity for assembly of the transport vesicle. J Neurosci 29:14534-14544.

Takami M, Nagashima Y, Sano Y, Ishihara S, Morishima-Kawashima M, Funamoto S, Ihara Y (2009) gamma-Secretase: successive tripeptide and tetrapeptide release from the transmembrane domain of beta-carboxyl terminal fragment. J Neurosci 29:13042-13052.

Takasugi N, Tomita T, Hayashi I, Tsuruoka M, Niimura M, Takahashi Y, Thinakaran G, Iwatsubo T (2003) The role of presenilin cofactors in the gamma-secretase complex. Nature 422:438-441.

Tang TC, Hu Y, Kienlen-Campard P, El HL, Decock M, Van HJ, Fu Z, Octave JN, Constantinescu SN, Smith SO (2014) Conformational changes induced by the A21G Flemish mutation in the amyloid precursor protein lead to increased Abeta production. Structure 22:387-396.

Tanzi RE, Bertram L (2005) Twenty years of the Alzheimer's disease amyloid hypothesis: a genetic perspective. Cell 120:545-555.

Taylor CJ, Ireland DR, Ballagh I, Bourne K, Marechal NM, Turner PR, Bilkey DK, Tate WP, Abraham WC (2008) Endogenous secreted amyloid precursor protein-alpha regulates hippocampal NMDA receptor function, long-term potentiation and spatial memory. Neurobiol Dis 31:250-260.

Teese MG, Langosch D (2015) Role of GxxxG Motifs in Transmembrane Domain Interactions. Biochemistry 54:5125-5135.

Tekirian TL, Saido TC, Markesbery WR, Russell MJ, Wekstein DR, Patel E, Geddes JW (1998) N-terminal heterogeneity of parenchymal and cerebrovascular Abeta deposits. J Neuropathol Exp Neurol 57:76-94.

Telese F, Bruni P, Donizetti A, Gianni D, D'Ambrosio C, Scaloni A, Zambrano N, Rosenfeld MG, Russo T (2005) Transcription regulation by the adaptor protein Fe65 and the nucleosome assembly factor SET. EMBO Rep 6:77-82.

Terry RD, Masliah E, Salmon DP, Butters N, DeTeresa R, Hill R, Hansen LA, Katzman R (1991) Physical basis of cognitive alterations in Alzheimer's disease: synapse loss is the major correlate of cognitive impairment. Ann Neurol 30:572-580.

Thal DR, Rub U, Orantes M, Braak H (2002) Phases of A beta-deposition in the human brain and its relevance for the development of AD. Neurology 58:1791-1800.

Thinakaran G, Borchelt DR, Lee MK, Slunt HH, Spitzer L, Kim G, Ratovitsky T, Davenport F, Nordstedt C, Seeger M, Hardy J, Levey AI, Gandy SE, Jenkins NA, Copeland NG, Price DL, Sisodia SS (1996) Endoproteolysis of presenilin 1 and accumulation of processed derivatives in vivo. Neuron 17:181-190.

Thinakaran G, Koo EH (2008) Amyloid precursor protein trafficking, processing, and function. J Biol Chem 283:29615-29619.

Tian Y, Bassit B, Chau D, Li YM (2010) An APP inhibitory domain containing the Flemish mutation residue modulates gamma-secretase activity for Abeta production. Nat Struct Mol Biol 17:151-158.

Tomita T (2009) Secretase inhibitors and modulators for Alzheimer's disease treatment. Expert Rev Neurother 9:661-679.

Tomiyama T, Asano S, Furiya Y, Shirasawa T, Endo N, Mori H (1994) Racemization of Asp23 residue affects the aggregation properties of Alzheimer amyloid beta protein analogues. J Biol Chem 269:10205-10208.

Tomiyama T, Nagata T, Shimada H, Teraoka R, Fukushima A, Kanemitsu H, Takuma H, Kuwano R, Imagawa M, Ataka S, Wada Y, Yoshioka E, Nishizaki T, Watanabe Y, Mori H (2008) A new amyloid beta variant favoring oligomerization in Alzheimer's-type dementia. Ann Neurol 63:377-387.

Tong G, Wang JS, Sverdlov O, Huang SP, Slemmon R, Croop R, Castaneda L, Gu H, Wong O, Li H, Berman RM, Smith C, Albright CF, Dockens RC (2012) Multicenter, randomized, double-blind, placebo-controlled, single-ascending dose study of the oral gamma-secretase inhibitor BMS-708163 (Avagacestat): tolerability profile, pharmacokinetic parameters, and pharmacodynamic markers. Clin Ther 34:654-667.

Torok M, Milton S, Kayed R, Wu P, McIntire T, Glabe CG, Langen R (2002) Structural and dynamic features of Alzheimer's Abeta peptide in amyloid fibrils studied by site-directed spin labeling. J Biol Chem 277:40810-40815.

Turner PR, O'Connor K, Tate WP, Abraham WC (2003) Roles of amyloid precursor protein and its fragments in regulating neural activity, plasticity and memory. Prog Neurobiol 70:1-32.

Tyan SH, Koo EH (2015) New tricks from an old dog: Another synaptotoxic fragment from APP. Cell Res 25:1185-1186.

Tycko R (2006) Characterization of amyloid structures at the molecular level by solid state nuclear magnetic resonance spectroscopy. Methods Enzymol 413:103-122.

Tycko R (2015) Amyloid polymorphism: structural basis and neurobiological relevance. Neuron 86:632-645.

Uhlik MT, Temple B, Bencharit S, Kimple AJ, Siderovski DP, Johnson GL (2005) Structural and evolutionary division of phosphotyrosine binding (PTB) domains. J Mol Biol 345:1-20.

Unterreitmeier S, Fuchs A, Schaffler T, Heym RG, Frishman D, Langosch D (2007) Phenylalanine promotes interaction of transmembrane domains via GxxxG motifs. J Mol Biol 374:705-718.

Urbanc B, Cruz L, Yun S, Buldyrev SV, Bitan G, Teplow DB, Stanley HE (2004) In silico study of amyloid beta-protein folding and oligomerization. Proc Natl Acad Sci U S A 101:17345-17350.

van Duijn CM, Hendriks L, Cruts M, Hardy JA, Hofman A, Van BC (1991) Amyloid precursor protein gene mutation in early-onset Alzheimer's disease. Lancet 337:978.

Van BC, Haan J, Bakker E, Hardy JA, Van HW, Wehnert A, Vegter-Van der Vlis M, Roos RA (1990) Amyloid beta protein precursor gene and hereditary cerebral hemorrhage with amyloidosis (Dutch). Science 248:1120-1122.

Vassar R, et al. (1999) Beta-secretase cleavage of Alzheimer's amyloid precursor protein by the transmembrane aspartic protease BACE. Science 286:735-741.

Vellas B, Black R, Thal LJ, Fox NC, Daniels M, McLennan G, Tompkins C, Leibman C, Pomfret M, Grundman M (2009) Long-term follow-up of patients immunized with AN1792: reduced functional decline in antibody responders. Curr Alzheimer Res 6:144-151.

Villemagne VL, Burnham S, Bourgeat P, Brown B, Ellis KA, Salvado O, Szoeke C, Macaulay SL, Martins R, Maruff P, Ames D, Rowe CC, Masters CL (2013) Amyloid beta deposition, neurodegeneration, and cognitive decline in sporadic Alzheimer's disease: a prospective cohort study. Lancet Neurol 12:357-367.

von Rotz RC, Kohli BM, Bosset J, Meier M, Suzuki T, Nitsch RM, Konietzko U (2004) The APP intracellular domain forms nuclear multiprotein complexes and regulates the transcription of its own precursor. J Cell Sci 117:4435-4448.

Wahrle S, Das P, Nyborg AC, McLendon C, Shoji M, Kawarabayashi T, Younkin LH, Younkin SG, Golde TE (2002) Cholesterol-dependent gamma-secretase activity in buoyant cholesterol-rich membrane microdomains. Neurobiol Dis 9:11-23.

Walsh DM, Hartley DM, Kusumoto Y, Fezoui Y, Condron MM, Lomakin A, Benedek GB, Selkoe DJ, Teplow DB (1999) Amyloid beta-protein fibrillogenesis. Structure and biological activity of protofibrillar intermediates. J Biol Chem 274:25945-25952.

Walsh DM, Klyubin I, Fadeeva JV, Cullen WK, Anwyl R, Wolfe MS, Rowan MJ, Selkoe DJ (2002) Naturally secreted oligomers of amyloid beta protein potently inhibit hippocampal long-term potentiation in vivo. Nature 416:535-539.

Walsh DM, Lomakin A, Benedek GB, Condron MM, Teplow DB (1997) Amyloid beta-protein fibrillogenesis. Detection of a protofibrillar intermediate. J Biol Chem 272:22364-22372.

Walsh DM, Minogue AM, Sala FC, Fadeeva JV, Wasco W, Selkoe DJ (2007) The APP family of proteins: similarities and differences. Biochem Soc Trans 35:416-420.

Walter J, Fluhrer R, Hartung B, Willem M, Kaether C, Capell A, Lammich S, Multhaup G, Haass C (2001) Phosphorylation regulates intracellular trafficking of beta-secretase. J Biol Chem 276:14634-14641.

Wang J, Dickson DW, Trojanowski JQ, Lee VM (1999) The levels of soluble versus insoluble brain Abeta distinguish Alzheimer's disease from normal and pathologic aging. Exp Neurol 158:328-337.

Wang JZ, Wu Q, Smith A, Grundke-Iqbal I, Iqbal K (1998) Tau is phosphorylated by GSK-3 at several sites found in Alzheimer disease and its biological activity markedly inhibited only after it is prephosphorylated by A-kinase. FEBS Lett 436:28-34.

Wang Q, Rowan MJ, Anwyl R (2004) Beta-amyloid-mediated inhibition of NMDA receptor-dependent long-term potentiation induction involves activation of microglia and stimulation of inducible nitric oxide synthase and superoxide. J Neurosci 24:6049-6056.

Wang R, Meschia JF, Cotter RJ, Sisodia SS (1991) Secretion of the beta/A4 amyloid precursor protein. Identification of a cleavage site in cultured mammalian cells. J Biol Chem 266:16960-16964.

Wang Y, Ha Y (2004) The X-ray structure of an antiparallel dimer of the human amyloid precursor protein E2 domain. Mol Cell 15:343-353.

Wang Y, Zhang M, Moon C, Hu Q, Wang B, Martin G, Sun Z, Wang H (2009) The APP-interacting protein FE65 is required for hippocampus-dependent learning and long-term potentiation. Learn Mem 16:537-544.

Wasco W, Gurubhagavatula S, Paradis MD, Romano DM, Sisodia SS, Hyman BT, Neve RL, Tanzi RE (1993) Isolation and characterization of APLP2 encoding a homologue of the Alzheimer's associated amyloid beta protein precursor. Nat Genet 5:95-100.

Watanabe N, Tomita T, Sato C, Kitamura T, Morohashi Y, Iwatsubo T (2005) Pen-2 is incorporated into the gamma-secretase complex through binding to transmembrane domain 4 of presenilin 1. J Biol Chem 280:41967-41975.

Westerman MA, Cooper-Blacketer D, Mariash A, Kotilinek L, Kawarabayashi T, Younkin LH, Carlson GA, Younkin SG, Ashe KH (2002) The relationship between Abeta and memory in the Tg2576 mouse model of Alzheimer's disease. J Neurosci 22:1858-1867.

Weyer SW, Klevanski M, Delekate A, Voikar V, Aydin D, Hick M, Filippov M, Drost N, Schaller KL, Saar M, Vogt MA, Gass P, Samanta A, Jaschke A, Korte M, Wolfer DP, Caldwell JH, Muller UC (2011) APP and APLP2 are essential at PNS and CNS synapses for transmission, spatial learning and LTP. EMBO J 30:2266-2280.

Wilhelmus MM, Boelens WC, Otte-Holler I, Kamps B, Kusters B, Maat-Schieman ML, de Waal RM, Verbeek MM (2006) Small heat shock protein HspB8: its distribution in Alzheimer's disease brains and its inhibition of amyloid-beta protein aggregation and cerebrovascular amyloid-beta toxicity. Acta Neuropathol 111:139-149.

Willem M, et al. (2015) eta-Secretase processing of APP inhibits neuronal activity in the hippocampus. Nature 526:443-447.

Williams AD, Shivaprasad S, Wetzel R (2006) Alanine scanning mutagenesis of Abeta(1-40) amyloid fibril stability. J Mol Biol 357:1283-1294.

Winkler E, Julius A, Steiner H, Langosch D (2015) Homodimerization Protects the Amyloid Precursor Protein C99 Fragment from Cleavage by gamma-Secretase. Biochemistry 54:6149-6152.

Wisniewski T, Ghiso J, Frangione B (1991) Peptides homologous to the amyloid protein of Alzheimer's disease containing a glutamine for glutamic acid substitution have accelerated amyloid fibril formation. Biochem Biophys Res Commun 179:1247-1254.

Wolfe MS, Kopan R (2004) Intramembrane proteolysis: theme and variations. Science 305:1119-1123.

Wu HY, Hudry E, Hashimoto T, Kuchibhotla K, Rozkalne A, Fan Z, Spires-Jones T, Xie H, Arbel-Ornath M, Grosskreutz CL, Bacskai BJ, Hyman BT (2010) Amyloid beta induces the morphological neurodegenerative triad of spine loss, dendritic simplification, and neuritic dystrophies through calcineurin activation. J Neurosci 30:2636-2649.

Yamada K, Holth JK, Liao F, Stewart FR, Mahan TE, Jiang H, Cirrito JR, Patel TK, Hochgrafe K, Mandelkow EM, Holtzman DM (2014) Neuronal activity regulates extracellular tau in vivo. J Exp Med 211:387-393.

Yan R, Munzner JB, Shuck ME, Bienkowski MJ (2001) BACE2 functions as an alternative alpha-secretase in cells. J Biol Chem 276:34019-34027.

Yao J, Irwin RW, Zhao L, Nilsen J, Hamilton RT, Brinton RD (2009) Mitochondrial bioenergetic deficit precedes Alzheimer's pathology in female mouse model of Alzheimer's disease. Proc Natl Acad Sci U S A 106:14670-14675.

Young-Pearse TL, Bai J, Chang R, Zheng JB, LoTurco JJ, Selkoe DJ (2007) A critical function for beta-amyloid precursor protein in neuronal migration revealed by in utero RNA interference. J Neurosci 27:14459-14469.

Young-Pearse TL, Chen AC, Chang R, Marquez C, Selkoe DJ (2008) Secreted APP regulates the function of full-length APP in neurite outgrowth through interaction with integrin beta1. Neural Dev 3:15.

Yu JT, Chang RC, Tan L (2009) Calcium dysregulation in Alzheimer's disease: from mechanisms to therapeutic opportunities. Prog Neurobiol 89:240-255.

Zhang H, Ma Q, Zhang YW, Xu H (2012) Proteolytic processing of Alzheimer's beta-amyloid precursor protein. J Neurochem 120 Suppl 1:9-21.

Zhang SQ, Kulp DW, Schramm CA, Mravic M, Samish I, DeGrado WF (2015) The membrane- and soluble-protein helix-helix interactome: similar geometry via different interactions. Structure 23:527-541.

Zhang YW, Wang R, Liu Q, Zhang H, Liao FF, Xu H (2007) Presenilin/gamma-secretase-dependent processing of beta-amyloid precursor protein regulates EGF receptor expression. Proc Natl Acad Sci U S A 104:10613-10618.

Zheng H, Jiang M, Trumbauer ME, Sirinathsinghji DJ, Hopkins R, Smith DW, Heavens RP, Dawson GR, Boyce S, Conner MW, Stevens KA, Slunt HH, Sisoda SS, Chen HY, Van der Ploeg LH (1995) beta-Amyloid precursor protein-deficient mice show reactive gliosis and decreased locomotor activity. Cell 81:525-531.

ANNEX 1: List of scientific papers

1. **Conformational Changes Induced by the A21G Flemish Mutation in the Amyloid Precursor Protein Lead to Increased Aβ Production**

   Tzu-Chun Tang, Yi Hu, Pascal Kienlen-Campard, Laetitia El Haylani, **Marie Decock**, Joanne Van Hees, Ziao Fu, Jean-Noel Octave, Stefan N. Constantinescu, and Steven O. Smith

   Published in Structure. 2014 Mar 4;22(3):387-96.

2. **Analysis by a highly sensitive split luciferase assay of the regions involved in APP dimerization and its impact on processing.**

   Marie Decock, Laetitia El Haylani, Serena Stanga, Ilse Dewachter, Jean-Noël Octave, Steven O. Smith, Stefan N. Constantinescu, Pascal Kienlen-Campard

   Published in FEBS Open Bio. 2015 Sep 6;5:763-73.

3. **Glycines from the APP GXXXG/GXXXA transmembrane motifs promote formation of pathogenic Aβ oligomers in cells**

   Marie Decock, Serena Stanga, Jean Noël Octave, Ilse Dewachter, Steven O. Smith, Stefan N. Constantinescu, Pascal Kienlen-Campard

   Submitted in Frontiers in Aging Neuroscience. 2016 Feb 22.

4. **β-Sheet Structure within the Extracellular Domain of C99 Regulates Processing**

   Yi Hu, Pascal Kienlen-Campard, Tzu-Chun Tang, Xiaoshu Pan, **Marie Decock**, Joanne Van Hees, Ziao Fu, Jean-Noel Octave, Stefan N. Constantinescu and Steven O. Smith

   To be submitted in 2016.

ANNEX 2: Collaboration paper

ANNEX 2

Structure
Article

Conformational Changes Induced by the A21G Flemish Mutation in the Amyloid Precursor Protein Lead to Increased Aβ Production

Tzu-Chun Tang,[1] Yi Hu,[1] Pascal Kienlen-Campard,[2] Laetitia El Haylani,[2] Marie Decock,[2] Joanne Van Hees,[3] Ziao Fu,[1] Jean-Noel Octave,[2] Stefan N. Constantinescu,[3] and Steven O. Smith[1,*]
[1]Department of Biochemistry and Cell Biology, Stony Brook University, Stony Brook, NY 11794-5215, USA
[2]Institute of Neuroscience, Université catholique de Louvain, Brussels 1200, Belgium
[3]Ludwig Institute for Cancer Research and de Duve Institute, Université catholique de Louvain, Brussels 1200, Belgium
*Correspondence: steven.o.smith@stonybrook.edu
http://dx.doi.org/10.1016/j.str.2013.12.012

SUMMARY

Proteolysis of the β C-terminal fragment (β-CTF) of the amyloid precursor protein generates the Aβ peptides associated with Alzheimer's disease. Familial mutations in the β-CTF, such as the A21G Flemish mutation, can increase Aβ secretion. We establish how the Flemish mutation alters the structure of C55, the first 55 residues of the β-CTF, using FTIR and solid-state NMR spectroscopy. We show that the A21G mutation reduces β sheet structure of C55 from Leu17 to Ala21, an inhibitory region near the site of the mutation, and increases α-helical structure from Gly25 to Gly29, in a region near the membrane surface and thought to interact with cholesterol. Cholesterol also increases Aβ peptide secretion, and we show that the incorporation of cholesterol into model membranes enhances the structural changes induced by the Flemish mutant, suggesting a common link between familial mutations and the cellular environment.

INTRODUCTION

The amyloid precursor protein (APP) is an integral membrane protein with a single transmembrane (TM) domain that is expressed in a wide number of different cell types, including neurons (Selkoe, 2004). Processing of APP occurs by the sequential action of several proteases. Both α- and β-secretase first cleave between the extracellular and the TM domains of APP to generate an N-terminal soluble fragment (soluble αAPP or soluble βAPP) and a membrane-anchored C-terminal fragment (α- or β-CTF). The γ-secretase complex cleaves the CTFs within their TM domains. The cleavage of the β-CTF generates predominantly the Aβ40 peptide, but both shorter and longer Aβ peptides are also produced. The major longer peptide generated, Aβ42, has a higher propensity to form aggregates than the shorter isoforms and is the most toxic peptide generated by γ-cleavage (Burdick et al., 1992).

Three clusters of familial Alzheimer's disease (AD) mutations in APP are located close to the α-, β-, and γ-cleavage sites, respectively. Specific mutations within these clusters influence the proteolytic processing of APP to favor increased Aβ42 production over the shorter Aβ peptides or to favor an increase in the total production of Aβ peptides. The substrate numbering is based on the APP695 isoform of APP. Asp597 corresponds to the first residue (i.e., Asp1) of the β-CTF (Figure 1A).

A fourth cluster is located a few residues below the α-secretase cleavage site at K16-L17. This cluster is comprised of the A21G (Flemish), E22Q (Dutch), E22G (Arctic), E22K (Italian), and D23N (Iowa) mutations (Grabowski et al., 2001; Hendriks et al., 1992; Kamino et al., 1992; Levy et al., 1990), which have very different effects on APP processing (De Jonghe et al., 1998) and Aβ peptide aggregation (Betts et al., 2008). The A21G mutation appears to increase Aβ production by approximately 2- to 4-fold, but not via a change in α-secretase cleavage (De Jonghe et al., 1998; Tian et al., 2010). In contrast, mutations at E22 and D23 do not markedly change the level of total secreted Aβ peptides (De Jonghe et al., 1998; Tian et al., 2010) but rather increase the rate of fibril formation after the Aβ peptides are generated by proteolysis. To understand the diversity of effects within this central cluster of mutations midway between the β- and γ-cleavage sites, we focus here on the A21G Flemish mutation and address how the removal of a single methyl group can have such a dramatic influence on Aβ production.

Several residues surrounding the A21G mutation have been found to influence APP processing, although they are not associated with early-onset AD. Yi and colleagues (Tian et al., 2010) found that the L17-V18-F19-F20-A21 sequence is part of an inhibitory motif that modulates γ-secretase processing. Upon deletion of this motif, the catalytic efficiency of γ-secretase increases 25-fold compared to the full-length β-CTF. They suggested that the A21G mutation might disrupt the inhibitory effect of this region, implying that the interaction between APP and γ-secretase is altered upon mutation. In contrast, mutations in the G25-S26-N27-K28 region, which is a few residues C-terminal to position 21, induce the opposite effect. Ren et al. (2007) found that mutations at Ser26 and Lys28 reduce secreted Aβ40 and Aβ42 without a corresponding loss of the APP intracellular domain cleavage product. Golde and colleagues (Kukar et al., 2011) found that the K28A and K28Q mutations shift the major cleavage site to the position of Gly33 from Val40. These results suggest that the precise nature and location of the border region

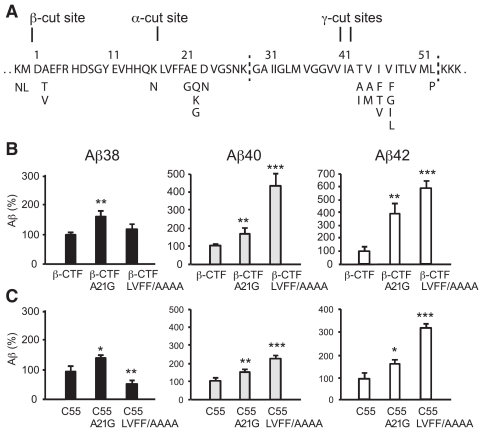

Figure 1. Increase of Aβ Secretion in the A21G and LVFF to AAAA Mutations

(A) Sequence of the extracellular and TM regions of the β-CTF. The β-CTF is produced by β-secretase cleavage of APP. The first 28 amino acids form the extracellular region of the β-CTF and contain the α-secretase cleavage site. The TM domain (denoted by vertical dashed lines) contains the site of γ-secretase cleavage. Both the extracellular and TM regions contain sites of familial AD mutations, shown as the single-letter amino acids below the sequence.

(B) Comparison of the levels of Aβ38, Aβ40, and Aβ42 produced by γ-secretase cleavage of the WT β-CTF, A21G, and LVFF to AAAA mutants.

(C) Comparison of the levels of Aβ38, Aβ40, and Aβ42 produced by γ-secretase cleavage of WT C55 and the corresponding A21G and LVFF to AAAA mutants.

Statistical significance was evaluated by one-way ANOVA followed by Dunnett's post hoc test. Values are the means ± SE, $n > 5$; *$p < 0.05$; **$p < 0.01$; ***$p < 0.001$, compared with control. See also Figure S1.

between the extracellular and TM domains can exert a substantial effect on the position of γ-cleavage within the TM domain.

The structure of the nonmutated, 99-residue β-CTF (also referred to as C99) was determined in detergent micelles by solution nuclear magnetic resonance (NMR) spectroscopy (Beel et al., 2008). Helical structure was observed in the L17-V18-F19-F20 (or LVFF) sequence, the hydrophobic TM domain, and in the last ~10 residues of the cytoplasmic sequence. The LVFF region is of particular interest because of its possible role as an inhibitory motif (Tian et al., 2010) and as a key element in amyloid plaque formation by the Aβ peptides (Inouye et al., 2010). An open question is whether structural changes are induced in the β-CTF upon the A21G mutation.

The A21G mutation may also influence the ability of the β-CTF to associate as TM homodimers. Glycines are abundant in TM helices of membrane proteins and the GxxxG sequence is well known to be a dimerization motif (Lemmon et al., 1992). The TM region of APP is unusual in containing three consecutive GxxxG motifs. The A21G mutation generates a fourth consecutive upstream motif, which raises the possibility that the mutation influences TM helix dimerization. Several studies have targeted these GxxxG sequences and found that mutations alter processing of the β-CTF (Kienlen-Campard et al., 2008; Munter et al., 2007).

In addition, a cholesterol-binding site was identified in the juxtamembrane (JM) region of the β-CTF between the extracellular and TM domains (Barrett et al., 2012). As with the A21G mutation, the presence of cholesterol and cholesterol-rich domains were linked to γ-secretase activity and the level of secreted Aβ (Beel et al., 2008). NMR measurements show that residues that appear sensitive to cholesterol binding include Phe20, Glu22, and Gly33. Phe20 is the last residue in the LVFF sequence. Glu22 is part of the cluster of familial mutations described above. Gly33 is part of the third GxxxG motif that has been implicated in mediating TM helix dimerization of the β-CTF. Depletion of cholesterol inhibits γ-secretase and Aβ secretion, while addition of cholesterol enhances γ-secretase activity (Simons et al., 1998; Wahrle et al., 2002).

In this study, we focus on the structural changes arising from the A21G mutation and compare the changes with those caused by an increase in membrane cholesterol. We first measure how the A21G and surrounding mutations influence processing of APP and the β-CTF, and confirm that the A21G mutation increases secreted Aβ by γ-secretase cleavage. Fourier transform infrared (FTIR) and NMR measurements are made on C55, corresponding to the first 55 residues of the β-CTF, which includes the extracellular sequence, TM domain, and a cluster of intracellular positive charges. The measurements are carried out in model membrane bilayers in which we can modulate the amount of cholesterol. These studies address the structure of C55, the structural changes induced by the A21G mutation, and whether the presence of cholesterol in membrane bilayers acts synergistically with the A21G mutation.

RESULTS

A21G and LVFF-to-Alanine Mutations Both Lead to an Increase in Aβ Production

We first confirm that the A21G mutation results in an increase in Aβ production and then address whether mutations within the upstream LVFF sequence result in comparable changes in processing. Measurements were made using C55 and the β-CTF expressed in Chinese hamster ovary (CHO) cells. Measurements on full-length APP are shown in Figure S1 available online.

Secreted Aβ peptides (Aβ38, Aβ40, and Aβ42) were measured after transfection by multiplex electrochemiluminescence (ECLIA) assays. Proteolysis of the wild-type (WT) β-CTF results predominantly in the Aβ40 peptide (85%), with smaller amounts of Aβ38 (10%) and Aβ42 (5%). Figure 1B shows the level of secreted Aβ peptides produced by γ-secretase cleavage as a percentage relative to WT. Both the A21G mutation and the LVFF to AAAA mutation increase total Aβ production. The A21G mutation results in a 1.7-fold increase in Aβ40. A larger increase (4.5-fold) is observed in Aβ40 for the LVFF to AAAA mutation. There is a striking increase (4-fold) in Aβ42 produced relative to WT in the A21G mutant. In contrast to the increase of Aβ40 and Aβ42 with the A21G and LVFF/AAAA mutations, the level of Aβ38 increases for the A21G but not LVFF/AAAA mutation.

We further compared the influence of the A21G and LVFF to AAAA mutations using C55. Several shorter versions of the β-CTF have previously been shown to function as γ-secretase

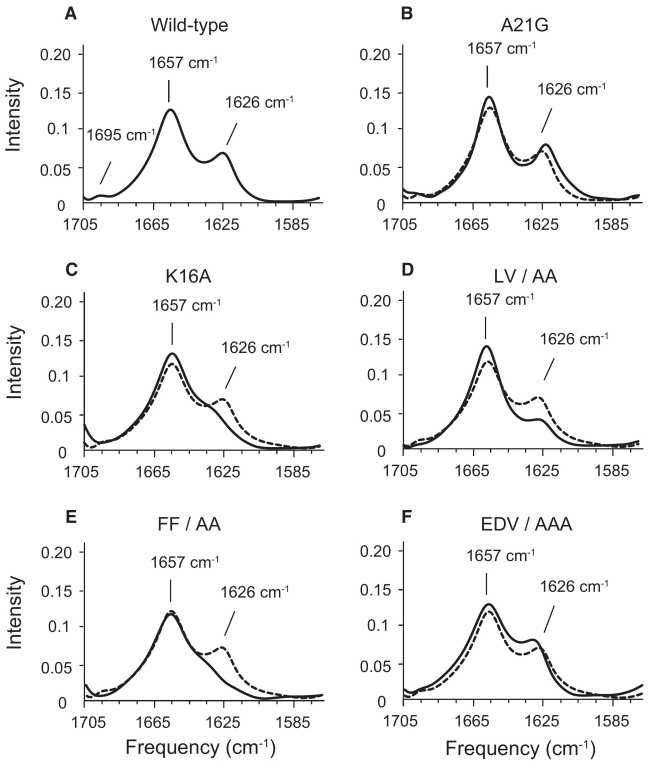

Figure 2. FTIR Spectroscopy of WT C55 and Mutants

Comparison of FTIR spectra of WT C55 (A) reconstituted into DMPC:DMPG bilayers with spectra of the C55 protein containing the A21G mutation (B) and alanine mutations at K16 (C), L17-V18 (D), F19-F20 (E), and E22-D23-V24 (F). For comparison, FTIR spectra of unlabeled WT C55 are presented in dashed lines in (B)–(F). See also Figures S2 and S3.

substrates (Funamoto et al., 2004; Yin et al., 2007). C55 is the C-terminal truncated version of C99 and includes the extracellular and TM regions of the protein. In our structural studies, we used C55 rather than the full-length C99 protein to allow selective incorporation of ^{13}C probes for structural studies. In Figure 1C, we show that both the A21G and the LVFF to AAAA mutations increase Aβ secretion. The changes in Aβ secretion using C55 are similar to those using the full β-CTF, supporting its use as a model γ-secretase substrate.

The LVFF Sequence Is Predominantly β Sheet in Membrane Bilayers

The processing results show that the extracellular A21G mutation strongly promotes Aβ production with both C55 and C99. To address whether there are structural differences between WT C55 and C55 with extracellular mutations, we measured the global secondary structure of C55 reconstituted into model membrane bilayers using FTIR spectroscopy.

The amide I vibration (1,600–1,700 cm^{-1}) is a sensitive marker of secondary structure. Figure 2A presents the amide I region of WT C55 in dimyristoyl-phosphocholine:dimyristoyl-phosphoglycerol (DMPC:DMPG) bilayers. The FTIR spectrum exhibits both an intense band at 1,657 cm^{-1} corresponding to α-helical structure and a weaker band at 1,626 cm^{-1} corresponding to β strand or β sheet structure. Comparison of the FTIR spectrum of C55 with that of a TM peptide having a truncated extracellular domain (Sato et al., 2009) argues that the 1,626 cm^{-1} band arises from the extracellular region of C55 (Figure S2). To determine which residues are responsible for the 1,626 cm^{-1} band, we mutated the KLVFF and EDV sequences that bracket A21. Mutations of K16 and F19-F20 reduce the 1,626 cm^{-1} intensity consistent with a disruption or reduction of the β strand secondary structure (Figure 2). In contrast, the mutation of the E22-D23-V24 sequence does not strongly influence the 1,626 cm^{-1} intensity. These results argue that the extracellular region upstream of A21 folds into β-structure. Comparable results are obtained from FTIR studies on the full-length β-CTF in the WT, A21G, and LVFF mutant (Figure 3).

Integration of the 1,626 cm^{-1} peak suggests the β sheet structure is formed by approximately six to eight residues, suggesting that several additional residues may be involved in β sheet formation. The small 1,695 cm^{-1} resonance observed for WT C55 is often associated with antiparallel β sheet (Paul et al., 2004), and the loss of this peak upon mutation of the LVFF sequence suggests that this region adopts an antiparallel β sheet fold. One possibility is that the KLVFFAE sequence forms antiparallel β sheet through intermolecular interactions. Additional experiments are in progress to test this possibility, as well as the alternative that residues in the region N-terminal to KLVFF fold back and form β sheet through intramolecular interactions.

Earlier solution NMR studies of the full β-CTF and shorter fragments show helical structure of the LVFF sequence (Beel et al., 2008; Nadezhdin et al., 2012). Our observation of β-structure within the LVFF sequence argues that this region adopts a different secondary structure in membrane bilayers than in detergent/lipid mixtures and detergent micelles (Beel et al., 2008; Nadezhdin et al., 2012). To test whether detergent interactions induce helical secondary structure, we compared FTIR spectra of C55 in membrane bilayers, detergent micelles, and

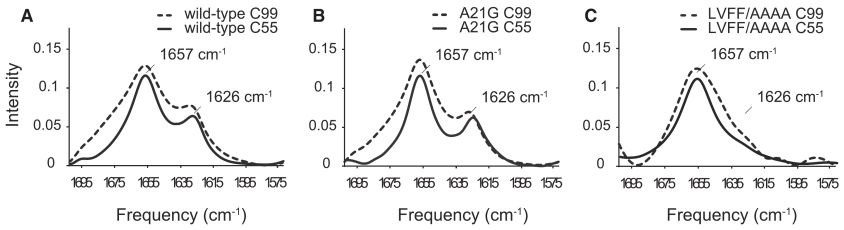

Figure 3. Comparison of C55 and C99 in DMPC:DMPG Bilayers

(A) Both C55 (solid line) and C99 (dashed line) exhibit resonances characteristic of α-helix (1,657 cm^{-1}) and β sheet (1,626 cm^{-1}). The C-terminal 44 residues of C99 are thought to be unstructured and consequently contribute to an overall broadening of the amide I resonance.

(B) The A21G mutation does not significantly influence the FTIR spectra of C55 and C99.

(C) In contrast to the A21G mutation, the LVFF to AAAA mutation removes the 1,626 cm^{-1} β sheet resonance. The disruption of the 1,626 cm^{-1} resonance in both C55 and C99 by the LVFF to AAAA mutation is consistent with this region folding into β sheet secondary structure, which is in disagreement with the solution NMR structures (Barrett et al., 2012; Beel et al., 2008; Nadezhdin et al., 2012) using detergent systems.

bicelles that have been titrated from bilayer-like structures (q = 2.0) to isotropic detergent-like structures (q = 0.2; Figure S3). Both the titration of bicelles toward a more detergent-like environment or direct comparisons of C55 in bilayers and detergent micelles show a loss of β sheet structure characterized by the 1,626 cm^{-1} amide I vibration with added detergent.

The A21G Mutation Influences the β Sheet Structure in Membrane Bilayers

The A21G mutation has only a slight influence on the position of the 1,626 cm^{-1} band observed in the FTIR spectrum of C55 (Figure 2B). To further explore whether there are local changes in structure, we compared FTIR spectra of WT and A21G C55 peptides containing specific ^{13}C labels at backbone C = O positions within the LVFF sequence. The ^{13}C = O labels shift the amide vibration to lower frequencies. The frequency and intensity of the shifted resonances are sensitive to whether the ^{13}C = O labeled sites fall within parallel or antiparallel β sheet structure (Paul et al., 2004; Petty and Decatur, 2005). We selected F19 and F20 for labeling since mutations at these positions have a large influence on the 1,626 cm^{-1} resonance. For WT C55 (Figures 4A and 4C), the incorporation of ^{13}C leads to splitting of the 1,626 cm^{-1} band into two components at 1,608 cm^{-1} and 1,630 cm^{-1}. These shifts are similar to those described for the KLVFFAED octapeptide (Figure S4), which forms fibrils with β strands in an antiparallel orientation (Balbach et al., 2000). In contrast, ^{13}C labeling does not cause the β sheet peak to split in the A21G mutant (Figures 4B and 4D), suggesting that the antiparallel structure observed at positions F19 and F20 has been disrupted or altered. Previous studies have shown that the extent of splitting and intensity is dependent on the position of the ^{13}C = O label. For example, Axelsen and colleagues (Paul et al., 2004) found that C = O groups at the edge of β sheet and not involved in hydrogen bonds had higher frequencies and reduced intensity compared to hydrogen-bonded C = O groups within β sheet. As a result, we conclude that A21 is at the edge of the β sheet structure formed (in part) by the LVFF sequence and attribute the weak intensity at ~1,610 cm^{-1} in the A21G mutant to the ^{13}C = O carbonyls of F19 and F20.

The A21G Mutation Increases the Helical Character of the $G^{25}SNKG^{29}$ Sequence

Solid-state NMR is complementary to FTIR spectroscopy and allows us to probe local structure. Figure 5 presents the results from two-dimensional (2D) magic angle spinning NMR spectra of C55 obtained with dipolar assisted rotational resonance (DARR). Figures 5A–5D show selected rows from the 2D spectra corresponding to the ^{13}C = O resonances of F19, F20, G29, and A30. Comparison of the WT C55 (black) and A21G (red) spectra illustrates that the A21G mutation induces distinct changes in chemical shift at some positions, but not others.

Figures 5E and 5F and Table S1 summarize the chemical shifts of selected Cα and C = O resonances between L17 and I31. The chemical shifts are plotted as differences from the average residue chemical shifts. Deviations to lower chemical shift values correspond to β sheet secondary structure. Deviations to higher chemical shift values correspond to α-helical secondary structure. For WT C55, the Cα and C = O resonances between L17 and A21 all exhibit negative deviations corresponding to β strand or sheet structure. The observation of β-structure is consistent with the FTIR results but contrasts with solution NMR structures previously determined of this region (Beel et al., 2008; Nadezhdin et al., 2012). Mutation to A21G results in less negative deviations of both the Cα and C = O chemical shifts for residues F19–A21, suggesting that there is a reduction in β-structure. G29 and A30 both exhibit positive deviations consistent with the helical TM domain beginning at K28. Mutation to A21G does not alter these latter chemical shifts. The two residues probed between the LVFF region and the TM domain—V24 and G25—exhibit negative shifts in WT C55 and positive shifts in the A21G mutant, suggesting a shift in local secondary structure to α-helix.

The conclusion that the region between G25 and G29 increases in helical structure in the A21G mutant is supported by DARR NMR measurements between these two residues. Figure 6A presents DARR NMR spectra of the WT (black) and A21G C55 (red) peptides ^{13}C labeled at G25 and G29. The distance between the ^{13}C = O and $^{13}C\alpha$ carbons is ~5.3 Å, which is within the ~6 Å DARR distance range when this region is α-helical. However, this distance is considerably longer (~12–13 Å) in an extended conformation. Comparison of the two spectra

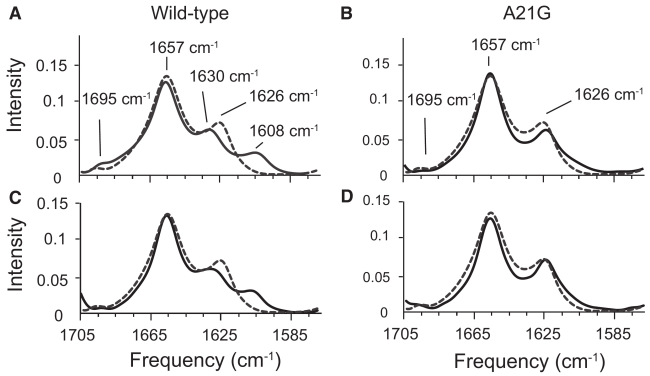

Figure 4. Influence of $^{13}C = O$ Labeling on the Amide I Vibration of WT and A21G C55

FTIR spectra are shown of WT C55 (A and C) and the A21G mutant (B and D) containing $^{13}C = O$ labels at F19 (A and B) and F20 (C and D). Spectra of unlabeled WT C55 are shown in dashed lines in (A)–(D) for comparison. The incorporation of $^{13}C = O$ labels at F19 and F20 only influences the 1,626 cm^{-1} band of WT C55. The C55 peptides were reconstituted in DMPC:DMPG bilayers. See also Figure S4.

shows the appearance of the cross peak (arrow) correlating the G25 $^{13}C = O$ and G29 $^{13}C\alpha$ resonances in the A21G mutant. The appearance of the G25 $^{13}C = O$ to G29 $^{13}C\alpha$ cross peak is consistent with the stretch of amino acids between these residues folding into helical structure in the A21G mutant.

The Familial E22Q and D23N Mutations Do Not Markedly Influence the Extracellular β Sheet Structure

For comparison to A21, we studied the adjacent two positions (E22 and D23), which are also sites of familial AD mutations, using FTIR and magic angle spinning (MAS) NMR. In FTIR measurements of C55 containing either the E22Q or D23N mutations (Figures S5C and S5D), the incorporation of $^{13}C = O$ at F19 leads to a splitting of the 1,626 cm^{-1} band as in WT C55. In MAS NMR measurements (Figures S5G and S5H), $^{13}C = O$ labeling at F19, V24, and G25 in E22Q or D23N C55 also yields spectra similar to WT C55, and not the large chemical shift changes observed in the A21G mutant.

These observations highlight the critical position of A21. Mutation of the LVFF sequence just N-terminal to A21 can decrease the β sheet structure in the extracellular domain and decrease Aβ secretion. In contrast, mutations just C-terminal to A21 do not significantly influence C55 structure or Aβ processing. These studies agree with previous results showing that A21G exhibits distinct phenotypes from familial mutations at E22 and D23 (De Jonghe et al., 1998; Tian et al., 2010). To further test the idea that the influence of the A21G mutation is similar to that of mutations in the LVFF sequence rather than in the ED sequence, we measured Aβ secretion in a series of A21 mutants. In Figure 7, we show that extension of the LVFF sequence with an A21F substitution reduces Aβ40 and Aβ42 secretion, whereas extension of the E22-D23 sequence with an A21E substitution increases Aβ secretion similar to the observation in the A21G mutant.

Dimerization of WT and A21G C55 Is Mediated by a GxxxG Interface

In soluble proteins, glycines serve as both helix and β sheet breakers. However, in TM helices, glycines mediate helix dimerization (Lemmon et al., 1992). The TM region of APP is unusual in containing three consecutive GxxxG motifs. The A21G mutation generates a fourth consecutive GxxxG motif. The observation that the helical secondary structure increases in the region between G25 and G29 in the A21G mutant raises the possibility that the helical $G^{25}xxxG^{29}$ motif stabilizes a TM dimer of C55.

The dimer structure of the TM domain of APP has been reported in both detergent micelles (Nadezhdin et al., 2012) and membrane bilayers (Sato et al., 2009). In DMPC:DMPG bilayers, the TM domain dimerizes via the $G^{29}xxxG^{33}xxxG^{37}$ interface (Sato et al., 2009). In contrast, the $G^{38}xxxA^{42}$ sequence mediates dimerization in dodecylphosphocholine micelles (Nadezhdin et al., 2012). Two-dimensional DARR NMR experiments were designed to test if either of these dimer interfaces exists in WT C55 or in the A21G mutant. These experiments involve co-mixing of two different peptides where cross peaks in the 2D spectra are only observed between heterodimers. Specifically, ^{13}C labels were selectively incorporated at G33 and A42 in two different C55 peptides (peptide 1 contains G33 $^{13}C = O$ and A42 $^{13}C\beta$, and peptide 2 contains G33 $^{13}C\alpha$ and A42 $^{13}C = O$). In the heterodimer, the G33 residues are closely packed if the $G^{33}xxxG^{37}$ motif mediates dimerization, whereas the A42 residues are in close proximity if the $G^{38}xxxA^{42}$ motif mediates dimerization.

The two WT C55 (or the two ^{13}C-labeled A21G C55) peptides were reconstituted into 1-palmitoyl-2-oleoyl-phosphocholine:1-palmitoyl-2-oleoyl-phosphoserine (POPC:POPS) membranes in equimolar amounts. Figure 8 presents the DARR NMR spectrum of WT C55 (black) overlaid with the spectrum of the A21G mutant (red). In both the WT and A21G C55 peptides, interpeptide cross peaks are observed between G33 ($^{13}C\alpha$) and G33 ($^{13}C = O$) (red box), but not between A42 ($^{13}C\beta$) and A42 ($^{13}C = O$) (blue box). No intensity was observed at this position in DARR NMR spectra of the single peptides containing the G33 $^{13}C = O$ and A42 $^{13}C\beta$ labels alone or the G33 $^{13}C\alpha$ and A42 $^{13}C = O$ labels alone, and the cross peak was reduced with the addition of unlabeled peptide (data not shown). The cross peak was only observed when the two peptides were mixed.

It is possible to relate the intensity of the cross peaks to the proportion of the peptide associating as dimers if one assumes that the packing interactions within the dimer structure are the same for WT C55 and the A21G mutant. In Figure 8A, the cross peak intensity increases ~1.5-fold (relative to the spinning side band at ~26 ppm), suggesting that the K_d decreases for the A21G mutant of C55 compared to the WT sequence. Since

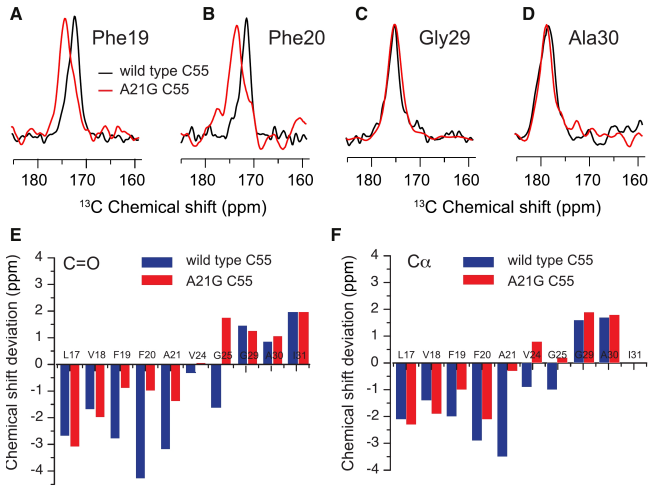

Figure 5. Comparison of ^{13}C NMR Chemical Shifts between WT and A21G C55

(A–D) Overlap of the carbonyl region of WT C55 (black) and the A21G mutant (red) labeled with U-^{13}C F19 (A), U-^{13}C F20 (B), U-^{13}C G29 (C), and U-^{13}C A30 (D). The A21G mutation leads to higher chemical shift values in the ^{13}C = O carbonyl resonances of the adjacent F19 and F20 residues, but not G29 and A30. Spectra correspond to rows taken through the Cα diagonal resonance.

(E and F) Carbonyl (E) and Cα (F) carbon chemical shifts are plotted relative to their average values obtained from the Biological Magnetic Resonance Bank database (http://www.bmrb.wisc.edu/ref_info/statful.htm).

See also Table S1.

dimerization is occurring within the membrane bilayer, it is possible to define a K_d in terms of the concentration of C55 (relative to the amount of lipid) that yields equal amounts of monomer and dimer (Song et al., 2013). If we assume that the cross peak intensity for dimer corresponds to that for C55 in cholesterol-containing membranes (Figures 8B and 8C), we can estimate a K_d of ~2 mol% on the basis of the cross peak intensities observed in Figure 8A. However, it is important to note that we cannot yet rule out that the increase in cross peak intensity results in a change in the dimer interface rather than a change in affinity. In either case, changes in the G33-G33 cross peak intensity show that a change within the structure of the extracellular domain of C55 can be transmitted down to the TM domain in the absence of the γ-secretase complex.

Cholesterol-Rich Bilayers Increase the Helicity of the TM Domain of WT C55

Both familial mutations and environmental factors influence Aβ generation by γ-secretase. For example, a higher concentration of serum cholesterol has been statistically observed as a risk factor for AD (Kivipelto et al., 2001). Hypercholesterolemia leads to an increase in Aβ deposition and intraneuronal accumulation of toxic Aβ oligomers in transgenic mice (Umeda et al., 2012). NMR studies reveal that cholesterol interacts with the β-CTF at the JM boundary between the extracellular and TM domains in micelles or detergent/lipid mixtures (Barrett et al., 2012). On the basis of our observations in the A21G mutant, we investigated the possibility that cholesterol may influence the structure of the extracellular region of the β-CTF and enhance the structural changes induced by the A21G mutation.

To test the influence of cholesterol on the structure of the LVFF sequence, FTIR spectra are presented in Figure S6 of C55 ^{13}C-labeled at F19. We observe a splitting of the 1,626 cm^{-1} band as for the WT peptide in bilayers without cholesterol, arguing that cholesterol does not influence the LVFF antiparallel β sheet structure. In contrast, the addition of cholesterol to POPC:POPS bilayers results in a 2.2 ppm downfield shift of the NMR ^{13}C = O resonance of G25, although without influencing the carbonyl chemical shifts of F20 or G33, resonances observed to be sensitive to cholesterol in detergent (Beel et al., 2008). This observation is consistent with a shift to more helical structure in the region of G25.

The increase in helical secondary structure in the region between G25 and G29 is supported by intrahelical DARR NMR measurements. Figure 6B presents the DARR spectra of WT C55 reconstituted in POPC:POPS (blue) and in POPC:POPS:cholesterol (red) using the same ^{13}C labeling scheme as described above. In Figure 6B, the cross peak between G25 ^{13}C = O and G29 ^{13}Cα is only observed in WT C55 upon the addition of cholesterol. The appearance of the G25-G29 cross peak in the A21G mutant or upon the addition of cholesterol in WT C55 indicates that both conditions induce TM helical structure of the C55 peptide.

The observation that both the A21G mutant and cholesterol addition result in a G25-G29 cross peak raises the question as to whether these two different mechanisms can act synergistically. Figure 6C presents 2D DARR NMR spectra of the WT (blue) and A21G C55 (red) peptide in POPC:POPS:cholesterol bilayers using the same ^{13}C labeling scheme as above. The intensity of the cross peak of the A21G mutant is ~1.5-fold higher in the cholesterol containing membranes consistent with a synergistic effect.

We next investigated whether cholesterol influences the monomer-dimer equilibrium of the WT or A21G C55 peptides. Figure 8B presents a comparison of the interhelical G33-G33 dimer cross peak upon the incorporation of cholesterol into POPC:POPS membranes. Rows highlighting the interhelical G33 (^{13}Cα)-G33 (^{13}C = O) cross peak at 46.2 ppm are shown for WT C55 (black) reconstituted into POPC:POPS:cholesterol bilayers and for the A21G mutant (red) reconstituted into POPC:POPS:cholesterol bilayers. The cross peak intensity for WT C55 with cholesterol is approximately the same as that for the A21G peptide without cholesterol in POPC:POPS membranes, suggesting that the monomer-dimer equilibrium is approximately the same. When the A21G mutant is incorporated into POPC:POPS:cholesterol

Conformational Changes Induced by A21G

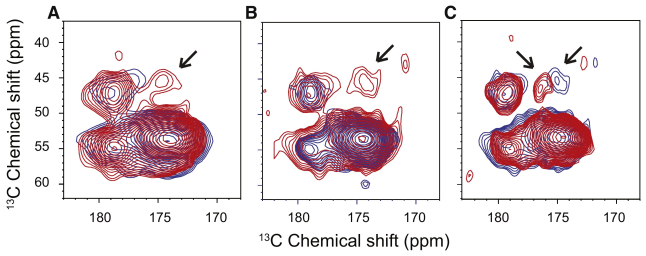

Figure 6. The ^{13}C DARR NMR Measurements between G25 and G29 in WT and A21G C55

Regions of the 2D DARR NMR spectra are shown corresponding to C = O to Cα crosspeaks.

(A) WT (blue) and A21G (red) C55 containing ^{13}C-labels at G25 (^{13}C = O) and G29 (^{13}Cα) were reconstituted into DMPC:DMPG bilayers. An interresidue cross peak (arrow) between these ^{13}C sites is only observed for the A21G mutant and corresponds to the formation of helical secondary structure.

(B) DARR NMR measurements on WT C55 in POPC:POPS (blue) and WT C55 in POPC:POPS:cholesterol (red) using the same G25 (^{13}C = O) and G29 (^{13}Cα) labeled peptide as in (A).

(C) DARR NMR measurements on WT C55 (blue) and A21G C55 (red) peptide in POPC:POPS:cholesterol bilayers. Upon addition of cholesterol, the cross peak is observed for both the WT and mutant peptides. The spectra are scaled to the strong 1,2-^{13}C L17 cross peak at 173 ppm corresponding to directly bonded carbons, which is not expected to change intensity in these spectra.

See also Figure S6.

membranes (red), the cross peak intensity increases ~2-fold, consistent with a synergistic effect of A21G and cholesterol. Figure 8C illustrates the influence of cholesterol on the G33-G33 cross peak intensity as cholesterol is increased in POPC:POPS bilayers from 0 to 30 mol%. As discussed for the A21G mutation, the increase in cross peak intensity may be due to a change in conformation rather than affinity. However, both A21G and cholesterol appear to have the same influence on TM interactions.

DISCUSSION

The Structure of APP near the Region of A21G Regulates Processing

The A21G mutation has a strong influence on intramembranous processing by the γ-secretase complex. We address how the loss of a single methyl group alters the structure of the extracellular region and TM domain using FTIR and NMR spectroscopy, and we propose how these changes are linked to processing of the β-CTF. FTIR and NMR measurements of C55 in bilayers provide evidence that β strand secondary structure is adopted in the extracellular region of the β-CTF and that the A21G mutation influences the upstream LVFF sequence (particularly F19 and F20) and the downstream GSNKG sequence, with a small effect on TM dimerization. These data emphasize the ability of glycine to destabilize β sheet structure (Minor and Kim, 1994) and to stabilize TM dimers through GxxxG motifs (Lemmon et al., 1992).

The Flemish mutation was first described by Hendriks et al. (1992) and later was shown to increase Aβ production by ~2-fold (De Jonghe et al., 1998). Yi and colleagues (Tian et al., 2010) found that the extracellular LVFFAED sequence was inhibitory to the activity of γ-secretase. They observed that deletion of this sequence resulted in a 10-fold increase in secreted Aβ40. To more directly test the role of the LVFF sequence in regulating Aβ secretion, we substituted the LVFF sequence with four alanine residues and found that the mutation increases Aβ secretion (Aβ40 and Aβ42) ~4.5-fold, considerably less than the increase observed when the sequence is deleted, but much greater than the ~1.7 fold increase due to the A21G mutation (Figure 1).

Our studies suggest that A21 is at the edge of the β sheet fold in the extracellular domain of the β-CTF. The FTIR measurements reveal only modest changes in the 1,626 cm^{-1} band upon mutation of A21 to glycine. In contrast, the A21G mutation results in large changes in the chemical shifts at F19, F20, and G25, consistent with unraveling of the β sheet structure at the end of the LVFF sequence and the formation of helical secondary structure in the GSNKG sequence. Strikingly, mutation of A21, but not the adjacent E22 and D23 residues, induces structural changes in the LVFF and GSNKG sequences and an increase in Aβ. A21 appears to be at a breakpoint between a well-defined β strand and the TM helix; extension of the LVFF sequence with an A21F substitution reduces Aβ secretion, whereas extension of the E22-D23 sequence with an A21E substitution increases Aβ secretion (Figure 7).

The WT and A21G C55 Dimerize through the GxxxG and Not the GxxxA Interface

The observation that the A21G mutation introduces an additional GxxxG motif into the β-CTF and that the G^{25}xxxG^{29} sequence becomes more helical suggests that the A21G mutation influences TM dimerization. Mutation of the consecutive G^{29}xxxG^{33}xxxG^{37} motifs supports the idea that TM dimerization influences processing (Kienlen-Campard et al., 2008; Munter et al., 2007). Recently, the dimer structure of residues Q15–K53 was determined in detergent micelles (Nadezhdin et al., 2012). Surprisingly, the dimer interface in their NMR structure was formed from the G^{38}xxxA^{42} sequence rather than G^{33}xxxG^{37}.

Above we show unambiguously that the A21G dimer is mediated by the G^{33}xxxG^{37} interface. The strong G33 Cα and G33 C = O cross peak can only be explained by a well-defined dimer structure. The observation that the A21G mutation has only a small influence on the G33-G33 cross peak intensity implies that the large influence of the mutation on processing is associated with the structural changes in the extracellular domain rather than with dimerization. These results support the conclusions of Tian et al. (2010) that the LVFFAED sequence is inhibitory.

The A21G Mutation and Cholesterol Act Synergistically

Many cellular factors appear to influence the overall level of secreted Aβ peptides and the Aβ42/Aβ40 ratio, including the

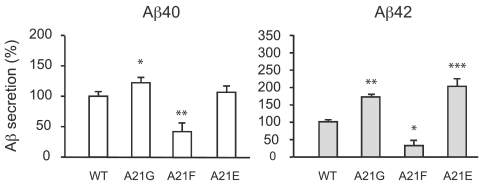

Figure 7. Influence of β-CTF Processing upon Substitution of Ala21 with Aromatic and Charged Residues

The A21F mutation reduces Aβ40 and Aβ42 production. This mutation replaces A21 with a hydrophobic phenylalanine identical to the last residue in the upstream LVFF sequence; A21E increases both Aβ40 and Aβ42 secretion. The A21E mutation replaces A21 with a residue identical to the downstream Glu22. Values are the means ± SE, n > 5; *p < 0.05; **p < 0.01; ***p < 0.001, compared with control. See also Figure S5.

presence of cholesterol (Beel et al., 2008; Simons et al., 1998; Wahrle et al., 2002). Upon the addition of cholesterol to model membranes, we observe an increase in α-helical secondary structure, and in the A21G mutant, a shift of the monomer-dimer equilibrium toward dimer or reorientation of the dimer interface to strengthen the G33-G33 contact. It is known that cholesterol increases the thickness of the bilayer, and we infer that this induces an increase in the helical structure between G25 and G29, in a fashion similar to that of A21G. In neuronal axons, the concentration of cholesterol is estimated to be ~15% (Calderon et al., 1995). These results suggest that dimerization is facilitated by the $G^{25}xxxG^{29}$ interface in A21G and that cholesterol helps stabilize this interface. Together, our studies and recent studies by Sanders and coworkers (Song et al., 2013) indicate that dimerization of the WT TM sequence of APP is weak but can be modulated by protein concentration, mutation, and the membrane environment.

The results on the A21G mutation and added cholesterol point to a simple model in which structural changes in the extracellular sequence (LVFFAEDVGSNK) lead to a reduction of inhibitory interactions and influence dimerization. The nature of the inhibitory interactions may originate with interactions between the LVFF sequence and γ-secretase (Tian et al., 2010) or with the membrane surface (Beel et al., 2008). The convergence of results reveals that both mutational and environmental factors can induce conformational changes in γ-secretase substrates that have implications in AD.

EXPERIMENTAL PROCEDURES

Materials

The ^{13}C-amino acids were obtained from Cambridge Isotope Laboratories. Detergents were obtained from Sigma-Aldrich and lipids from Avanti Polar Lipids. Human APP-specific antibody (WO-2) was obtained from Millipore. All cell culture reagents were from Invitrogen. The plasmids used to express human APP695 or β-CTF in eukaryotic cells have been previously described (Kienlen-Campard et al., 2008). The different mutants were generated by site-directed mutagenesis according to manufacturer's instructions (QuickChange, Stratagene).

Cell Cultures and Transfection

CHO cells were cultured in F12 medium supplemented with 10% fetal bovine serum and antibiotics at 37°C and 5% CO_2 and transfected 24 hours after seeding as previously described (Kienlen-Campard et al., 2008). Western blotting was performed on cell lysates (10 μg protein). Membranes were incubated at 4°C overnight with human APP-specific WO-2 monoclonal antibody (1:2,000), washed and incubated with 1:10,000 secondary anti-mouse antibody conjugated to horseradish peroxidase, followed by enhanced chemiluminescence revelation (Amersham). Aβ production was monitored in the culture media 48 hours after transfection (Kienlen-Campard et al., 2008). Briefly, samples were cleared by centrifugation (12,000 *g*, 3 min, 4°C). Aβ38/Aβ40/Aβ42 and soluble APPα/β were quantified in 25 μl of cellular medium by multiplex ECLIA assay according to the manufacturer's instructions (MesoScale Discovery).

Peptide Synthesis, Purification, and Reconstitution of C55 into Bicelles

C55 peptides (Asp1-Lys55) corresponding to the TM and JM regions of APP were synthesized by solid-phase methods (Keck Facility, Yale University). The purity was confirmed with MALDI-TOF mass spectrometry and analytical reverse-phase high-pressure liquid chromatography. For reconstitution into bicelles, the C55 peptides were refolded with 16 mM dihexoylphosphocholine (DHPC). The fractions containing purified protein were collected on the basis of the absorbance at 280 nm. The peptide-to-lipid ratio was 1:50 in bicelles with different q values (0.25, 0.35, 1.0, and 2.0) by adding proper amounts of lipids in the protein stock solutions. The samples of peptides reconstituted into bicelles were prepared by several cool-and-thaw cycles until the samples appeared clear.

Protein Overexpression and Purification

The C55 sequence was subcloned into a pET21a vector and expressed with an N-terminal methionine and a C-terminal linker plus His-tag (KLAAALEHHHHHH). The C55 protein was purified using a Nickel nitrilotriacetic acid column. Cell pellets were washed three times with the 35 ml of lysis buffer until the washed solution became clear. The pellets were then dissolved in 35 ml of urea/SDS buffer (20 mM Tris, 150 mM NaCl, 8 M urea, 0.2% SDS, pH 7.8) and mixed overnight at room temperature. The resulting solution was centrifuged at 25,000 *g* for 20 min. The supernatants were pooled with the pre-equilibrium Nickel beads and mixed for 2 hours at room temperature. The beads were then washed with urea/SDS buffer, and the proteins were eluted with 250 mM imidazole in Tris-buffered saline solution (pH 7.8) containing octyl-β-D-glucoside. The eluted fractions were collected and checked by SDS-PAGE. The protein purity was further confirmed with mass spectroscopy.

Reconstitution of C55 into Bicelles

The C55 peptides were eluted from the Ni column and refolded with 16 mM DHPC (Avanti lipids) in the elution buffer as described above. The fractions containing purified protein were collected on the basis of the absorbance at 260–280 nm. The peptide-to-lipid ratio was 1:50 in bicelles with different q values (0.25, 0.35, 1.0, and 2.0) by adding proper amounts of lipids in the protein stock solutions. The samples of peptides reconstituted into bicelles were prepared as described (Lu et al., 2012) by several cool-and-thaw cycles until the samples appeared clear.

Reconstitution of C55 into Membrane Bilayers

The C55 peptides were cosolubilized with lipid and octyl-β-glucoside in hexafluoroisopropanol. The peptide:lipid molar ratio was 1:50 and the molar ratios between lipids were as follows: DMPC:DMPG, 10:3; POPC:POPS,10:3; or POPC:POPS:cholesterol, 10:3:5.6. The solution was incubated for 3 hours at 30°C, after which the solvent was removed under a stream of argon gas and then under vacuum overnight. Then 2-(N-morpholino)ethanesulfonic acid (MES) buffer (5 mM MES, 50 mM NaCl, pH 6.2) was added to the solid from the previous step and gently mixed at 30°C for 6 hours. The octyl-β-glucoside was removed by dialysis (Smith et al., 2002). DMPC and POPC are representative lipids with saturated and unsaturated fatty acyl chains, respectively, while the DMPG and POPS headgroups introduce an overall negative membrane charge similar to that in cellular plasma membranes. DMPC can be titrated with DHPC to convert from membrane bilayers to isotropic (detergent-like) bicelles. POPC is abundant in plasma membranes and exhibits a continuous transition from a liquid disordered state to liquid ordered state

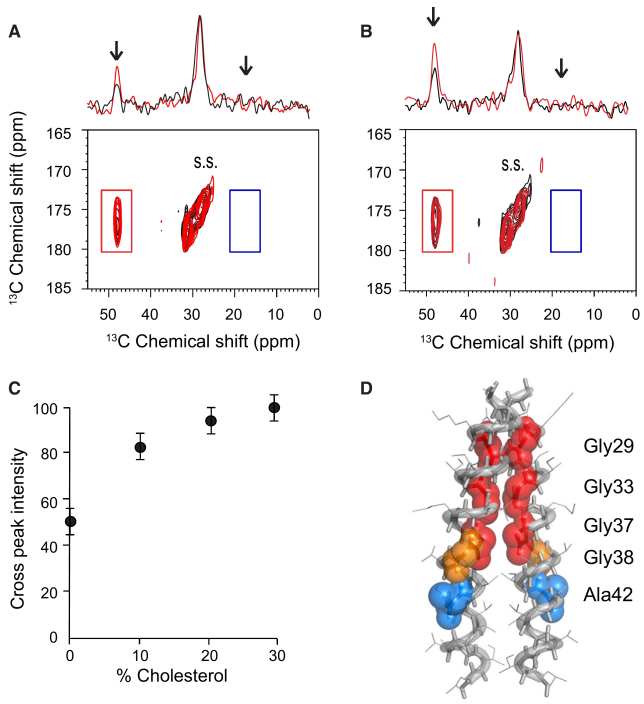

Figure 8. Interhelical ^{13}C DARR NMR Measurements of WT and A21G C55 Reconstituted into POPC:POPS Bilayers

Two WT C55 or two A21G C55 peptides were mixed in equal molar amounts to establish the dimer interface, either G^{29}xxxG^{33}xxxG^{37} or G^{38}xxxA^{42}.

(A) 1D and 2D DARR NMR spectra of WT C55 (black) and A21G C55 (red) are overlapped. Only cross peaks resulting from G33 on different peptides (i.e., G33 Cα to G33 C = O) are observed. Cross peaks are not observed between A42 on different peptides (i.e., A42 Cβ to A42 C = O, blue box).

(B) 1D and 2D DARR NMR spectra of WT C55 (black) and A21G C55 (red) are overlapped in POPC:POPS membranes with 30 mol% cholesterol. Rows are shown through the G33 C = O diagonal resonance. The resonance at ~26 ppm is a spinning side band and serves as an internal control for comparing relative intensity changes between spectra.

(C) Influence of the G33 Cα to G33 C = O cross peak intensity on cholesterol content for A21G C55. The content of the cholesterol in POPC:POPS membranes was varied from 0%–30%. Error bars reflect the noise level of the measurements.

(D) Molecular model of the C55 TM dimer mediated by the G^{29}xxxG^{33}xxxG^{37} interface (red). A42 (blue) is oriented away from the interface.

with the addition of cholesterol (London, 2005). In our studies, only small differences were observed in the FTIR and NMR spectra between C55 reconstituted into POPC:POPS or DMPC:DMPG bilayers. The only marked differences were observed upon titration of cholesterol into the POPC:POPS membranes.

FTIR Spectroscopy

Polarized attenuated total reflection (ATR) FTIR spectra were obtained on a Bruker IFS 66V/S spectrometer. ATR-FTIR spectroscopy was used to characterize the global secondary structure and the orientation of the TM domain of C55 in bilayers. The WT and A21G C55 peptides reconstituted in bilayers were layered on a germanium plate and bulk water removed by a slow flow of nitrogen gas. Similar dichroic ratios of the 1,657 cm^{-1} band of 3.2–3.3 are observed for both peptides regardless of the lipid mixture used in these studies. The high dichroic ratio is consistent with an orientation of the TM α-helix of ~20° relative to the bilayer normal and indicates that both peptides can be reconstituted into bilayers by detergent dialysis.

Solid-State NMR Spectroscopy

NMR experiments were performed at a ^{13}C frequency of 125 MHz on a Bruker AVANCE spectrometer. The MAS spinning rate was set to 9–11 kHz (±5 Hz). The ramped amplitude cross polarization contact time was 2 ms. Two-pulse phase-modulated decoupling was used during the evolution and acquisition periods with a radiofrequency field strength of 80 kHz. Internuclear ^{13}C…^{13}C distance constraints were obtained from 2D DARR NMR experiments (Takegoshi et al., 2001) using a mixing time of 600 ms. The sample temperature was maintained at 198 K (±2 K). The ^{13}C chemical shifts are referenced to external 4,4-dimethyl-4-silapentane-1-sulfonic acid.

SUPPLEMENTAL INFORMATION

Supplemental Information includes six figures and one table and can be found with this article online at http://dx.doi.org/10.1016/j.str.2013.12.012.

ACKNOWLEDGMENTS

This work was supported by grants from the National Institutes of Health (RO1-AG027317 to S.O.S.), the Interuniversity Attraction Poles Programme-Belgian State-Belgian Science Policy (IAP P7/16 to J.-N.O. and P.K.-C. and PAI 7/43-DDUV38B5 to S.N.C.), and the Alzheimer Research Foundation (SAO-FRMA to P.K.-C.) and by support from the Salus Sanguinis, Fondation contre le cancer, ARC Program ARC 06/11-336 of the Université catholique de Louvain, FRS-FNRS Belgium (to S.N.C.).

Received: September 30, 2013
Revised: December 11, 2013
Accepted: December 12, 2013
Published: January 23, 2014

REFERENCES

Balbach, J.J., Ishii, Y., Antzutkin, O.N., Leapman, R.D., Rizzo, N.W., Dyda, F., Reed, J., and Tycko, R. (2000). Amyloid fibril formation by A beta 16-22, a seven-residue fragment of the Alzheimer's β-amyloid peptide, and structural characterization by solid state NMR. Biochemistry *39*, 13748–13759.

Barrett, P.J., Song, Y., Van Horn, W.D., Hustedt, E.J., Schafer, J.M., Hadziselimovic, A., Beel, A.J., and Sanders, C.R. (2012). The amyloid

precursor protein has a flexible transmembrane domain and binds cholesterol. Science *336*, 1168–1171.

Beel, A.J., Mobley, C.K., Kim, H.J., Tian, F., Hadziselimovic, A., Jap, B., Prestegard, J.H., and Sanders, C.R. (2008). Structural studies of the transmembrane C-terminal domain of the amyloid precursor protein (APP): does APP function as a cholesterol sensor? Biochemistry *47*, 9428–9446.

Betts, V., Leissring, M.A., Dolios, G., Wang, R., Selkoe, D.J., and Walsh, D.M. (2008). Aggregation and catabolism of disease-associated intra-Abeta mutations: reduced proteolysis of AbetaA21G by neprilysin. Neurobiol. Dis. *31*, 442–450.

Burdick, D., Soreghan, B., Kwon, M., Kosmoski, J., Knauer, M., Henschen, A., Yates, J., Cotman, C., and Glabe, C. (1992). Assembly and aggregation properties of synthetic Alzheimer's A4/β amyloid peptide analogs. J. Biol. Chem. *267*, 546–554.

Calderon, R.O., Attema, B., and DeVries, G.H. (1995). Lipid composition of neuronal cell bodies and neurites from cultured dorsal root ganglia. J. Neurochem. *64*, 424–429.

De Jonghe, C., Zehr, C., Yager, D., Prada, C.M., Younkin, S., Hendriks, L., Van Broeckhoven, C., and Eckman, C.B. (1998). Flemish and Dutch mutations in amyloid β precursor protein have different effects on amyloid β secretion. Neurobiol. Dis. *5*, 281–286.

Funamoto, S., Morishima-Kawashima, M., Tanimura, Y., Hirotani, N., Saido, T.C., and Ihara, Y. (2004). Truncated carboxyl-terminal fragments of β-amyloid precursor protein are processed to amyloid β-proteins 40 and 42. Biochemistry *43*, 13532–13540.

Grabowski, T.J., Cho, H.S., Vonsattel, J.P., Rebeck, G.W., and Greenberg, S.M. (2001). Novel amyloid precursor protein mutation in an Iowa family with dementia and severe cerebral amyloid angiopathy. Ann. Neurol. *49*, 697–705.

Hendriks, L., van Duijn, C.M., Cras, P., Cruts, M., Van Hul, W., van Harskamp, F., Warren, A., McInnis, M.G., Antonarakis, S.E., Martin, J.J., et al. (1992). Presenile dementia and cerebral haemorrhage linked to a mutation at codon 692 of the β-amyloid precursor protein gene. Nat. Genet. *1*, 218–221.

Inouye, H., Gleason, K.A., Zhang, D., Decatur, S.M., and Kirschner, D.A. (2010). Differential effects of Phe19 and Phe20 on fibril formation by amyloidogenic peptide A β 16-22 (Ac-KLVFFAE-NH2). Proteins *78*, 2306–2321.

Kamino, K., Orr, H.T., Payami, H., Wijsman, E.M., Alonso, M.E., Pulst, S.M., Anderson, L., O'dahl, S., Nemens, E., White, J.A., et al. (1992). Linkage and mutational analysis of familial Alzheimer disease kindreds for the APP gene region. Am. J. Hum. Genet. *51*, 998–1014.

Kienlen-Campard, P., Tasiaux, B., Van Hees, J., Li, M., Huysseune, S., Sato, T., Fei, J.Z., Aimoto, S., Courtoy, P.J., Smith, S.O., et al. (2008). Amyloidogenic processing but not amyloid precursor protein (APP) intracellular C-terminal domain production requires a precisely oriented APP dimer assembled by transmembrane GXXXG motifs. J. Biol. Chem. *283*, 7733–7744.

Kivipelto, M., Helkala, E.L., Laakso, M.P., Hänninen, T., Hallikainen, M., Alhainen, K., Soininen, H., Tuomilehto, J., and Nissinen, A. (2001). Midlife vascular risk factors and Alzheimer's disease in later life: longitudinal, population based study. BMJ *322*, 1447–1451.

Kukar, T.L., Ladd, T.B., Robertson, P., Pintchovski, S.A., Moore, B., Bann, M.A., Ren, Z., Jansen-West, K., Malphrus, K., Eggert, S., et al. (2011). Lysine 624 of the amyloid precursor protein (APP) is a critical determinant of amyloid β peptide length: support for a sequential model of γ-secretase intramembrane proteolysis and regulation by the amyloid β precursor protein (APP) juxtamembrane region. J. Biol. Chem. *286*, 39804–39812.

Lemmon, M.A., Flanagan, J.M., Treutlein, H.R., Zhang, J., and Engelman, D.M. (1992). Sequence specificity in the dimerization of transmembrane α-helices. Biochemistry *31*, 12719–12725.

Levy, E., Carman, M.D., Fernandez-Madrid, I.J., Power, M.D., Lieberburg, I., van Duinen, S.G., Bots, G.T., Luyendijk, W., and Frangione, B. (1990). Mutation of the Alzheimer's disease amyloid gene in hereditary cerebral hemorrhage, Dutch type. Science *248*, 1124–1126.

London, E. (2005). How principles of domain formation in model membranes may explain ambiguities concerning lipid raft formation in cells. Biochim. Biophys. Acta *1746*, 203–220.

Lu, Z., Van Horn, W.D., Chen, J., Mathew, S., Zent, R., and Sanders, C.R. (2012). Bicelles at low concentrations. Mol. Pharmacol. *9*, 752–761.

Minor, D.L., Jr., and Kim, P.S. (1994). Measurement of the β-sheet-forming propensities of amino acids. Nature *367*, 660–663.

Munter, L.M., Voigt, P., Harmeier, A., Kaden, D., Gottschalk, K.E., Weise, C., Pipkorn, R., Schaefer, M., Langosch, D., and Multhaup, G. (2007). GxxxG motifs within the amyloid precursor protein transmembrane sequence are critical for the etiology of Abeta42. EMBO J. *26*, 1702–1712.

Nadezhdin, K.D., Bocharova, O.V., Bocharov, E.V., and Arseniev, A.S. (2012). Dimeric structure of transmembrane domain of amyloid precursor protein in micellar environment. FEBS Lett. *586*, 1687–1692.

Paul, C., Wang, J.P., Wimley, W.C., Hochstrasser, R.M., and Axelsen, P.H. (2004). Vibrational coupling, isotopic editing, and β-sheet structure in a membrane-bound polypeptide. J. Am. Chem. Soc. *126*, 5843–5850.

Petty, S.A., and Decatur, S.M. (2005). Experimental evidence for the reorganization of β-strands within aggregates of the Abeta(16-22) peptide. J. Am. Chem. Soc. *127*, 13488–13489.

Ren, Z., Schenk, D., Basi, G.S., and Shapiro, I.P. (2007). Amyloid β-protein precursor juxtamembrane domain regulates specificity of γ-secretase-dependent cleavages. J. Biol. Chem. *282*, 35350–35360.

Sato, T., Tang, T.C., Reubins, G., Fei, J.Z., Fujimoto, T., Kienlen-Campard, P., Constantinescu, S.N., Octave, J.N., Aimoto, S., and Smith, S.O. (2009). A helix-to-coil transition at the ε-cut site in the transmembrane dimer of the amyloid precursor protein is required for proteolysis. Proc. Natl. Acad. Sci. USA *106*, 1421–1426.

Selkoe, D.J.; American College of Physicians; American Physiological Society (2004). Alzheimer disease: mechanistic understanding predicts novel therapies. Ann. Intern. Med. *140*, 627–638.

Simons, M., Keller, P., De Strooper, B., Beyreuther, K., Dotti, C.G., and Simons, K. (1998). Cholesterol depletion inhibits the generation of β-amyloid in hippocampal neurons. Proc. Natl. Acad. Sci. USA *95*, 6460–6464.

Smith, S.O., Eilers, M., Song, D., Crocker, E., Ying, W.W., Groesbeek, M., Metz, G., Ziliox, M., and Aimoto, S. (2002). Implications of threonine hydrogen bonding in the glycophorin A transmembrane helix dimer. Biophys. J. *82*, 2476–2486.

Song, Y., Hustedt, E.J., Brandon, S., and Sanders, C.R. (2013). Competition between homodimerization and cholesterol binding to the C99 domain of the amyloid precursor protein. Biochemistry *52*, 5051–5064.

Takegoshi, K., Nakamura, S., and Terao, T. (2001). ^{13}C-^{1}H dipolar-assisted rotational resonance in magic-angle spinning NMR. Chem. Phys. Lett. *344*, 631–637.

Tian, Y., Bassit, B., Chau, D.M., and Li, Y.M. (2010). An APP inhibitory domain containing the Flemish mutation residue modulates γ-secretase activity for Abeta production. Nat. Struct. Mol. Biol. *17*, 151–158.

Umeda, T., Tomiyama, T., Kitajima, E., Idomoto, T., Nomura, S., Lambert, M.P., Klein, W.L., and Mori, H. (2012). Hypercholesterolemia accelerates intraneuronal accumulation of Aβ oligomers resulting in memory impairment in Alzheimer's disease model mice. Life Sci. *91*, 1169–1176.

Wahrle, S., Das, P., Nyborg, A.C., McLendon, C., Shoji, M., Kawarabayashi, T., Younkin, L.H., Younkin, S.G., and Golde, T.E. (2002). Cholesterol-dependent γ-secretase activity in buoyant cholesterol-rich membrane microdomains. Neurobiol. Dis. *9*, 11–23.

Yin, Y.I., Bassit, B., Zhu, L., Yang, X., Wang, C., and Li, Y.M. (2007). γ-Secretase substrate concentration modulates the Abeta42/Abeta40 ratio: implications for Alzheimer disease. J. Biol. Chem. *282*, 23639–23644.